[redacted]

CR-66358

STUDY OF THE INFLUENCE OF SIZE OF A MANNED LIFTING BODY ENTRY VEHICLE ON RESEARCH POTENTIAL AND COST

FINAL REPORT

Part VII. Selected Entry Vehicle Design

N70-76678
(ACCESSION NUMBER)
(THRU)
246
(PAGES)
(CODE)
CR-66358
(NASA CR OR TMX OR AD NUMBER)
(CATEGORY)
FACILITY FORM 602

Declassified by authority of NASA
Classification Change Notices No. 325
Dated 8/31/70

[redacted]

CLASSIFICATION CHANGED
UNCLASSIFIED
To
By authority of NASA TD-70428 Date 8/10/70

Prepared by

MARTIN MARIETTA

for

NATIONAL AERONAUTICS AND SPACE ADMINISTRATION

U. S. Government Agencies and Contractors Only

[redacted]

C67-4817

[redacted]

92

CR-66358

STUDY OF THE INFLUENCE OF SIZE OF A MANNED LIFTING BODY ENTRY VEHICLE ON RESEARCH POTENTIAL AND COST

FINAL REPORT

Part VII. Selected Entry Vehicle Design

May 1967

Distribution of this report is provided in the interest of information exchange. Responsibility for the contents resides in the author or organization that prepared it.

[redacted]

UNCLASSIFIED

[redacted]

Prepared Under Contract No. NAS 1-6209 by

MARTIN MARIETTA CORPORATION

Baltimore, Maryland 21203

for

NATIONAL AERONAUTICS AND SPACE ADMINISTRATION

[redacted]

U. S. Government Agencies and Contractors Only

PRECEDING PAGE BLANK NOT FILMED.

FOREWORD

This document is a part of the final report on a "Study of the Influence of Size of a Manned Lifting Body Entry Vehicle on Research Potential and Cost," conducted by the Martin Marietta Corporation, Baltimore Division, for the National Aeronautics and Space Administration, Langley Research Center, under Contract NAS 1-6209 dated April 1966. The final report is presented in eight parts:

I.	Summary	CR-66352
II.	Research Program Experiments	CR-66353
III.	Flight Performance	CR-66354
IV.	Candidate Entry Vehicle Designs	CR-66355
V.	Systems Integration	CR-66356
VI.	Research Vehicle Size Selection and Program Definition	CR-66357
VII.	Selected Entry Vehicle Design	CR-66358
VIII.	Alternative Approaches	CR-66359

The study was managed at Martin Marietta by:

Robert L. Lohman--Study Manager

Rudolph C. Haefeli--Assistant Study Manager

The principal contributors to the study were James McCown, Robert Schwab, Ray Sorrell and James Vaeth; Mr. Louis Sheldahl also made a major contribution to the study as Study Manager during the first quarter.

DECLASSIFIED

DECLASSIFIED

ABSTRACT (Total Study)

This study presents data—based upon a developed logic, task definitions, vehicle criteria, system analyses and design, and concepts of operation and implementation—with which the usefulness and cost of an entry flight research program can be evaluated.

The study defines 52 specific research tasks of value in developing operational lifting body systems, primarily for near-earth missions. Parametric design and performance data are evolved within a matrix of 5 vehicle sizes (with 1, 2, 4, 6 and 8 men) and 4 boosters (GLV, Titan III–2, Titan III–5 and Saturn IB) for all flight phases, from launch to landing. The design studies include vehicle arrangements, weight, aerodynamic heating and subsystem details. Systems integration analyses yield both design data, subsystem tradeoffs, and development and operations plans; and they lead, in turn, to cost effectiveness analyses which become the primary basis for vehicle and program selection.

A 25-foot long, 3-man vehicle weighing 12,342 pounds is selected for a research program of 9 manned (plus 2 unmanned) flights. This vehicle performs the maximum number of tasks and affords the highest research value per unit cost and the lowest cost per unit of payload in orbit; the estimated program cost is $1 billion. A detailed preliminary design of this vehicle is accomplished, including layout drawings and descriptions of each subsystem to identify available hardware as well as future options. Modifications for secondary research objectives—rendezvous and docking and supercircular entry—are considered.

The study also includes a brief examination of 2 smaller unmanned vehicles as alternate approaches to reduce cost.

DECLASSIFIED

DECLASSIFIED

CONTENTS

		Page
	FOREWORD	iii
	SUMMARY	vii
I.	INTRODUCTION	1
II.	VEHICLE DESIGN AND ARRANGEMENT	3
	A. Design Approach	3
	B. Geometry and Arrangement	5
III.	WEIGHT AND BALANCE STUDIES	15
	A. Subsystem Weight Breakdown	15
	B. Balance and Ballast Studies	26
	C. Test Equipment	27
	D. Booster Adapter Subsystems	27
	E. Mass Properties	29
	F. Total D/3 Vehicle Weights	29
IV.	SUBSYSTEM DEFINITION STUDIES	31
	A. Heat Shield	31
	B. Structure	49
	C. Landing and Emergency Recovery	57
	D. Crew Station	77
	E. Navigation and Guidance	106
	F. Electronic Flight Control Subsystem	126
	G. Flight Control Actuation	139
	H. Propulsion and Ordnance	150
	I. Communication Subsystem	162
	J. Instrumentation and Data Handling Subsystem	177
	K. Electrical Power	196
	L. Environmental Control and Life Support	201
	M. Malfunction Detection and Alarm Subsystem	205
V.	CAPABILITY FOR SECONDARY OBJECTIVES	211
	A. Supercircular Entry Velocity Module	211
	B. Rendezvous and Docking Experiment Modification	220
	C. Landing Engine Experiment	234
	D. Summary of Weight Modifications	240
	REFERENCES	245

DECLASSIFIED

PRECEDING PAGE BLANK NOT FILMED.

[redacted]

SUMMARY

This part presents the detail preliminary design of the entry vehicle selected as the most cost effective research tool under NASA Contract NAS 1-6209 entitled "Study of the Influence of Size of a Manned Lifting Body Entry Vehicle on Research Potential and Cost." The design study conducted on the selected research vehicle (designated D/3) is a further expansion and definition of the parametric vehicle design studies reported in Part IV.

The D/3 vehicle, a 25-foot (7.62 m) HL-10 modified with a "D" canopy, is designed specifically for conducting research on entry from near-earth orbits as described in Parts II through VI. In addition to this primary objective, the D/3 vehicle has been evaluated for two secondary research objectives, namely, to investigate: (1) the peculiar problems associated with rendezvous and docking of a lifting body entry vehicle, and (2) the necessary heat shield, control and propulsion modification of the vehicle associated with supercircular entry velocities.

The design philosophy of the D/3 vehicle is to provide a versatile entry research vehicle based on existing subsystem technology. Through this approach, a reliable test platform can be achieved for evaluating new and potentially improved subsystems for future operational systems.

This part provides a detailed description of the D/3 vehicle, including layout drawings, detail weights statements, and a description of each of the subsystem designs. The subsystem design descriptions identify existing hardware available for the application as well as potential problem areas. Essentially all of the subsystems are within projected 1969 technology. However, continued analyses and simulations are recommended.

Two of the potential problems are associated with the separated flow region in front of the lower flaps when they are deflected downward. The flow can result in a structural dynamic problem if unsteady separation (hypersonic buzz) occurs at the time of maximum abort hinge moments. It can also result in a heating problem if the turbulent separated flow reattachment heating approaches three times the stagnation heating. Although both of these problems may be avoided by angle of attack limitations, specific tests are needed to define the problem areas and to provide bases for design criteria for the HL-10.

The weight of the D/3 entry vehicle is 12 342 pounds (5598.3 kg). The adapter, which includes the deorbit/abort propulsion, weighs 1963 pounds (890.4 kg), giving a total launch weight of 14 305 pounds (6488.7 kg). A resource capability of 75 cubic feet (2.12 m^3) is available for conducting the primary research task.

The D/3 entry vehicle design is developed for launch by a Titan III booster with five-segment solids. Both a Titan III and a Saturn IB can be used as boosters to accomplish the secondary research objectives.

[redacted]

The subsystem approaches chosen for the D/3 design are: (1) conventional aluminum skin, frame, and stringer structure, (2) a refurbishable, all-ablative heat shield, (3) hydraulic flight control actuation, (4) wheel, tire, and brush skid landing gear, with air-oil strut for energy absorption, (5) hydrogen peroxide reaction control and landing assist propulsion, (6) silver-zinc batteries for electrical power, (7) direct vision for landing, (8) a conventional platform-type inertial system and dual horizon scanner for the primary navigation and guidance, backed by a simple PRIME-type guidance system using strapdown inertial sensors, (9) a fly-by-wire electronic flight control system, (10) a Gemini approach to communication and tracking and an Apollo telemetry system, and (11) a combination of Gemini and Apollo equipment for the environmental control system.

I. INTRODUCTION

This part of the final report on a "Study of the Influence of Size of a Manned Lifting Body Entry Vehicle on Research Potential and Cost" (NASA 1-6209) deals with the detail preliminary design of the selected D/3 vehicle. The D/3 vehicle is 25 feet (7.62 m) long and carries a three-man crew on a research mission (the vehicle is sized for a maximum crew of six). The D/3 configuration of the HL-10 is one of five candidate vehicle designs reported in Part IV. It was selected during the earlier study phase as the most cost-effective vehicle size and crew size for conducting entry research related to return from near-earth orbits.

The depth of design on the D/3 vehicle has been extended beyond that generated for the cost-effectiveness task to provide the most realistic basis possible, within the scope of the study, for determining: (1) the adequacy of available components and technology, (2) the development and test programs required, (3) the development schedule, (4) the optimum research flight program plan, and (5) the detailed project cost. The results of this extended study depth are also reported in Parts V and VI.

The general design criteria for the D/3 are presented in detail in Part IV where these same criteria were the basis for the parametric design phase from which the D/3 vehicle was selected. The criteria result in conservative designs which provide margins even under the extreme conditions which may be encountered on research flights. Only the principal criteria, plus special criteria associated with the greater design depth, are repeated in the present document. Part IV also contains many of the subsystem tradeoff studies, analysis techniques and performance evaluations which led to the D/3 design approach; these activities were necessary to meet the intent of the contract Statement of Work to make maximum use of available technology.

This document presents detailed information on the internal arrangements of the D/3 entry vehicle configuration and the launch vehicle adapter. These arrangements have been derived partly from a simple, full-scale crew station mockup which was developed and used for seat positioning, instrument panel arrangements, and control locations as well as for visibility studies and crew mobility investigations.

Detailed weight and balance analyses are also presented. They are based on the identification of specific available hardware components for use in the D/3 vehicle. These equipment identifications make use of pertinent data provided by potential subsystem suppliers.

Specifications--including functional and performance requirements, reliability goals, reuse criteria, etc.--were provided to the following subsystem suppliers, whose responses have been considered for incorporation in the D/3 preliminary design:

(1) Deorbit/abort propulsion

(a) Aerojet-General Corporation
(b) Thiokol Chemical Corporation

(2) Reaction control and landing assist propulsion

(a) Walter Kidde and Company, Inc.
(b) Bell Aerosystems Company

(3) Navigation and guidance

(a) Autonetics Division, North American Aviation, Inc.
(b) Honeywell, Inc.
(c) TRW Systems
(d) United Aircraft, Corporate Systems Center
(e) Raytheon Company, Space and Information Systems Division
(f) A. C. Electronics

(4) Electronic flight control system

(a) Sperry Phoenix Company
(b) Honeywell, Inc.
(c) Autonetics Division, North American Aviation, Inc.

(5) Flight control surface actuation

(a) Pesco Products Division, Borg-Warner Corporation
(b) Moog Inc.
(c) Hydraulic Research and Manufacturing Company

(6) Instrumentation and data management

(a) TRW Systems
(b) Lockheed Missiles and Space Company
(c) Radiation, Inc.
(d) Leach Corporation
(e) Space Craft, Inc.

The most significant portions of the information supplied by these organizations are included in this document.

In addition to detailed descriptions of each selected subsystem, this part also contains information on some of the alternate subsystem components. The latter, although in an earlier developmental stage, potentially offer significant benefits for future operational lifting body systems in the form of higher performance, higher reliability, less weight or lower cost. These alternate subsystems are prime candidates for testing in the proposed research flight program (Parts II and VI).

Finally, conceptual designs for modification of the D/3 entry vehicle and for special modules required to accomplish secondary research objectives are presented. As defined by the contract Statement of Work, the secondary objectives include: (1) orbital experiments involving rendezvous and docking typical of a logistics support and rescue vehicle, and (2) supercircular entry velocity research. A typical landing engine installation, proposed for a research experiment and possible application in future all-weather operations, is also described in this document.

II. VEHICLE DESIGN AND ARRANGEMENT

The selected size entry vehicle which evolved from the parametric entry vehicle design phase (Part IV) is designated D/3 (fig. 1). The design of this vehicle is based upon the philosophy of providing a versatile entry research vehicle utilizing existing subsystem technology.

A. DESIGN APPROACH

The design approach will provide a reliable test platform for new and improved subsystems without the restrictions that might be imposed by the use of new, untried systems in the basic vehicle. A conservative approach is also reflected in the design of heat shield, structure, control system and emergency abort system.

The basic all-ablative heat shield is sized to protect the vehicle for the total heating conditions associated with flight to the toe of the footprint and for all-turbulent heating over the surface of the vehicle. In all except the most extreme flights, the total heating will be only about 60 percent of this design value. Laminar to turbulent transition is not expected to occur over much of the surface of the vehicle, except on the research flights that try to force transition. These factors, along with the normal safety factors used in the design, provide considerable conservatism in the heat shield.

The structure and control actuation system are designed for the most severe environments that can result from an abort anywhere along a booster ascent trajectory with insertion at an altitude of 80 nautical miles (148.17 km). Recovery from these aborts can result in a 6-g pull-up condition and maximum dynamic pressure of 1200 pounds per square foot (575 MN/m^2). For normal flight conditions, the largest pull-up load factor is about 2 g, with a dynamic pressure of 400 pounds per square foot (191.7 MN/m^2). These abort conditions represent limit design loads on the vehicle. By designing for these conditions, considerable margin is built into the vehicle for normal research operation.

The emergency abort approach includes complete recovery by parachute of the entire vehicle with the crew on board. Sufficient abort propulsion system thrust and velocity impulse is provided to allow escape at anytime, from the pad and throughout the flight. This system is retained for deorbit purposes as a redundant capability. Vehicle recovery is accomplished by a ring sail parachute system that will allow safe sink velocities and attitudes for either water or ground landing.

The entry vehicle subsystems are designed for five orbits, while the basic research mission is three orbits. Subsystems whose single failures could require immediate entry for crew safety are provided with sufficient backup and redundancy to allow completion of one orbit plus entry. This approach contributes to both crew safety and research mission success.

The D vehicle is of sufficient size for a six-man crew. The basic D/3 vehicle, as configured for the research mission, with three crewmen, has considerable flexibility in crew station arrangement. This provides the second crewman with sufficient panel

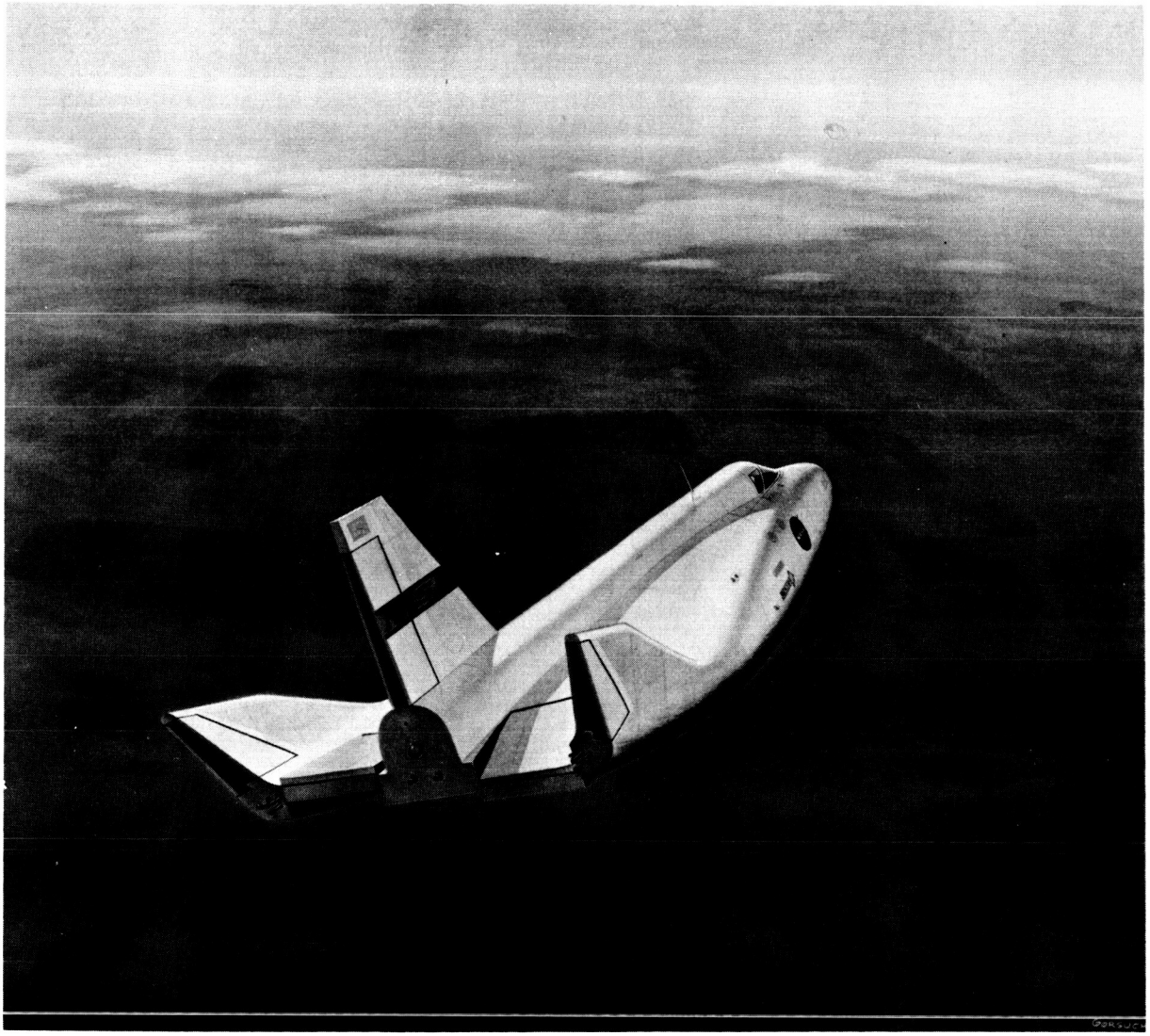

FIGURE 1. CONCEPT OF HL-10 D/3 VEHICLE

space to conduct entry research experiments on alternative guidance, navigation and flight control systems. Sufficient room is also available so that an indirect vision system could be evaluated for both space viewing and landing.

Another form of flexibility built into the vehicle is the extra thickness allowed for the heat shield. This permits the simple adaptation of radiative and alternative ablative heat shield experiments as well as different forms of active and passive structural cooling. This space also allows for the application of a thicker heat shield for the higher velocity entry experiments of the secondary objectives.

The D/3 vehicle is designed for internal access for most of the subsystems. External access is provided for the remainder. The basic vehicle and subsystems are designed to be reusable with only functional checkout and evaluation between flights. The ablative heat shield is simply refurbished by removal of the fasteners. The basic pressure and heating sensors are built in the heat shield at the time of fabrication. By proper advance planning of the research flights, the best arrangement of the sensors for each flight can be simply achieved.

The D/3 vehicle could be modified with the addition of a tunnel in the base area and three crew seats to provide a six-man logistics ferry or rescue vehicle for future mission applications.

B. GEOMETRY AND ARRANGEMENT

The D/3 vehicle is 25 feet (7.62 m) in length from the apex of the nose to the base of the body. As resolved in the conjunctive studies, this vehicle also incorporates the conical windshield and canopy extension which is a slight modification of Langley Research Center's canopy "D".

The three-man research crew was determined to be optimum for the research program, as described in Part VI. The D-size vehicle was determined to be the minimum for accommodating a crew of six 95-percentile men. As a research vehicle, the space which would have been occupied by the additional crew members is reserved for installation of research equipment.

The volume available for research equipment in the selected D/3 vehicle is 56.2 cubic feet (1.59 m^3) in the forebody and 18.6 cubic feet (0.53 m^3) in the afterbody. An additional volume of 27 cubic feet (0.76 m^3) is left unoccupied in the rear of the afterbody because of depth limitations and because each additional pound of weight at this location requires the addition of an equal amount of ballast in the nose.

1. Compartmentation

Physical subsystem integration, crew mobility, accessibility and fabrication complexity are sensitive to the arrangement itself and the compartmentation dictated by the arrangement. Design studies were performed in this phase to optimize the arrangement. The result is shown in figure 2. A significant feature which evolved from these design studies--as shown in the final arrangement--is that each major section (division of vehicle) resolved into a relatively self-contained entity.

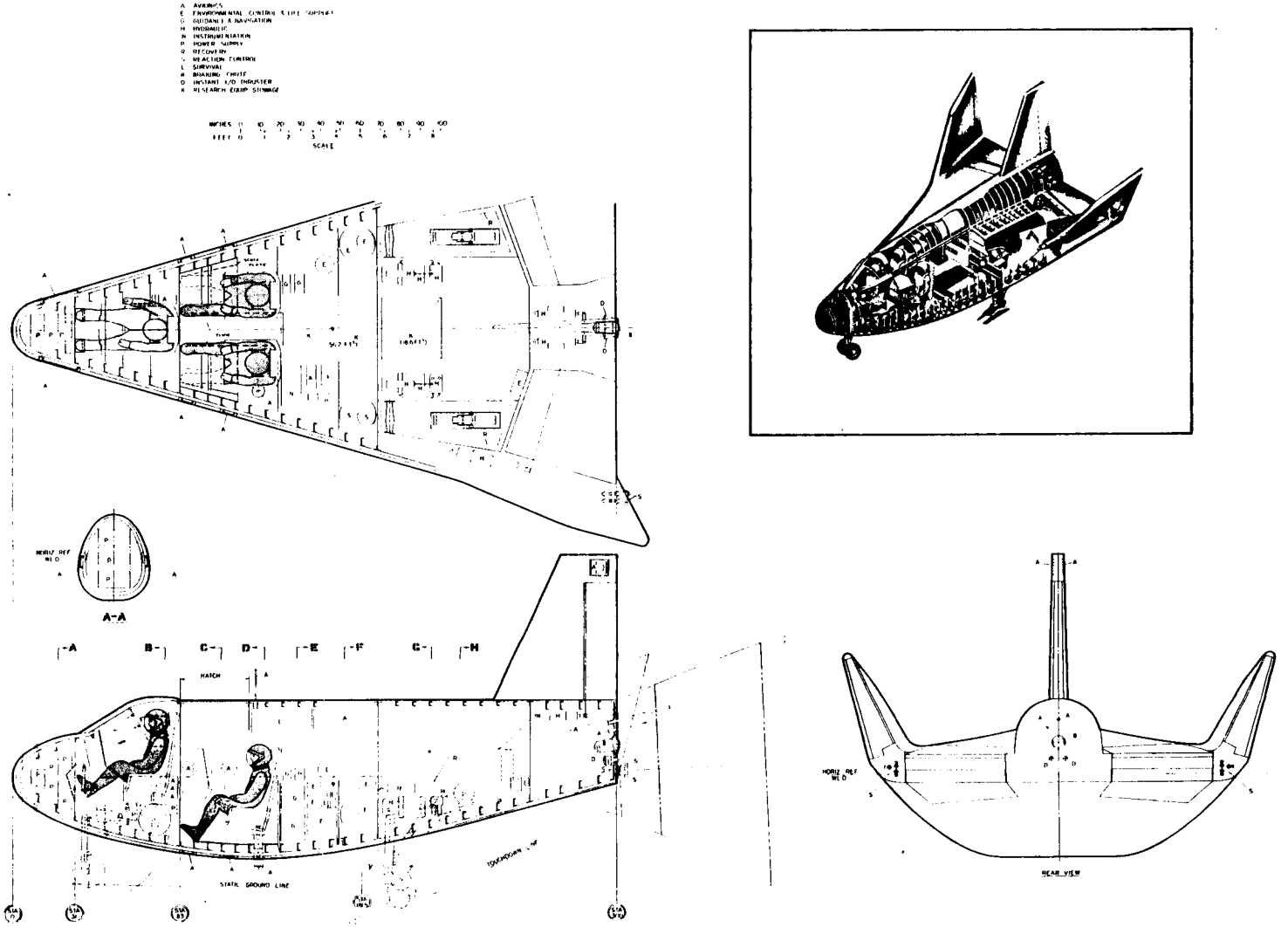

FIGURE 2. INBOARD PROFILE

[redacted]

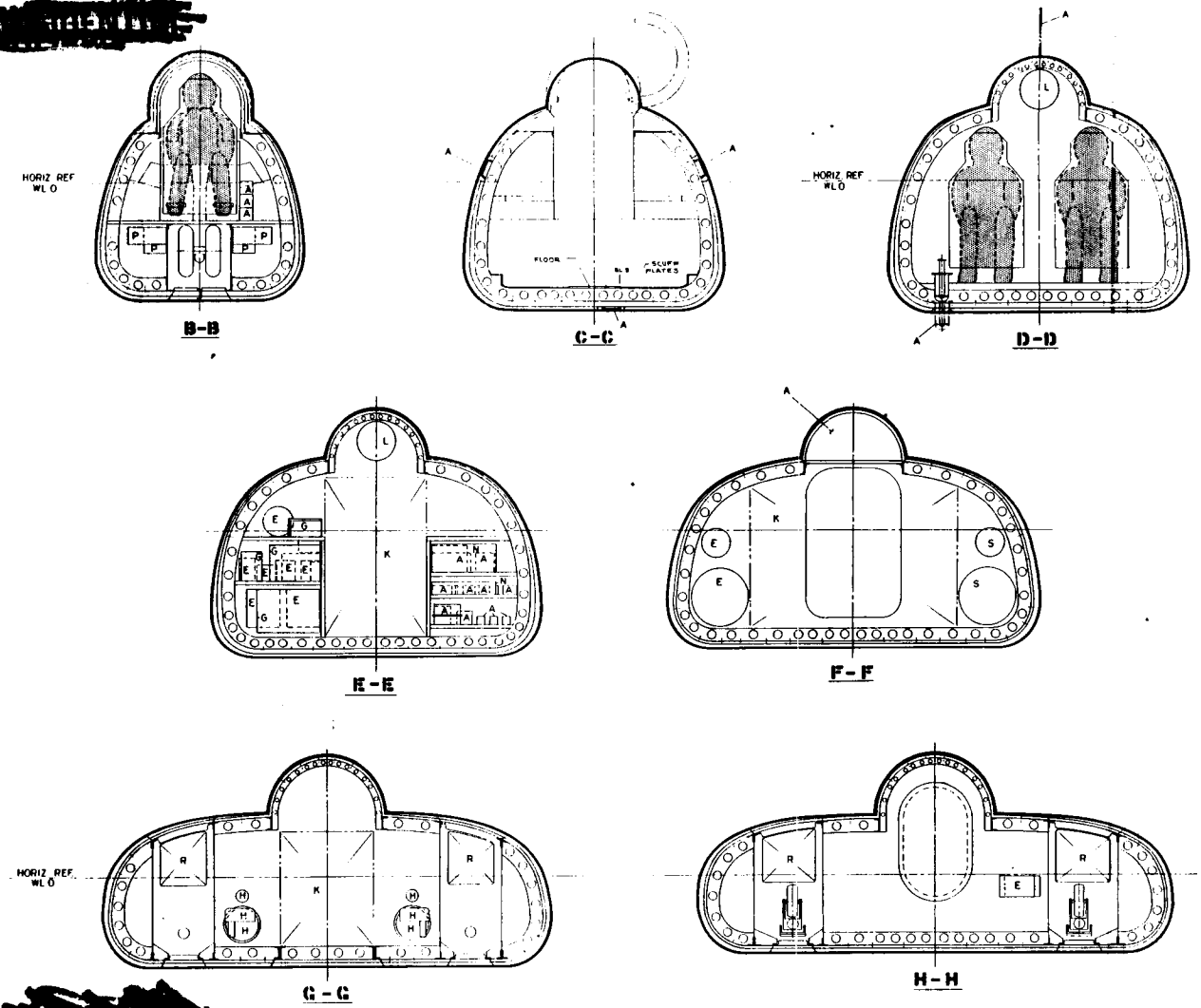

FIGURE 2. --CONCLUDED

[redacted]

For descriptive purposes the vehicle compartmentation and the major sections are identified as follows (fig. 3):

Section	Station	Length, cm
Nose cap	0 to 31	78.75
Forebody*	31 to 181.5	382.3
	31 to 83	132
Afterbody	181.5 to 257	191.8
Body extension	257 to 300	109.2
Tip fin assemblies		
Control surfaces		

* The pilot's compartment is included in the forebody.

2. Nose Cap

The nose cap is a separable section which is fastened in place at the forward pressure bulkhead (Station 31). This entire section may be removed for refurbishment. It is designed to be replaceable and permits installation of different heat shield arrangements for research purposes on subsequent vehicles.

The main electrical power supply batteries are mounted off the forward pressure bulkhead (Station 31), and the nose cap is a glove which fits over this array.

3. Forebody Arrangement

The forebody contains the crew, display panels, functional subsystems, and a reserved space for research equipment.

(1) This section is the only area in which it is mandatory to pressurize and thermally control for crew occupancy. The other sections of the vehicle either are inherently isolated or can be isolated--reducing the load on the environmental control and life support system, minimizing leakage, and alleviating malfunction hazards.

(2) Design studies, including a full-scale mockup, were utilized to determine the crew arrangement. The arrangement which afforded the best results is shown. The pilot is located in the forward location, where the most direct visibility is available, and the other two crew members are directly behind the pilot, seated side by side. This arrangement is the most compatible for cooperative task sharing and crew mobility.

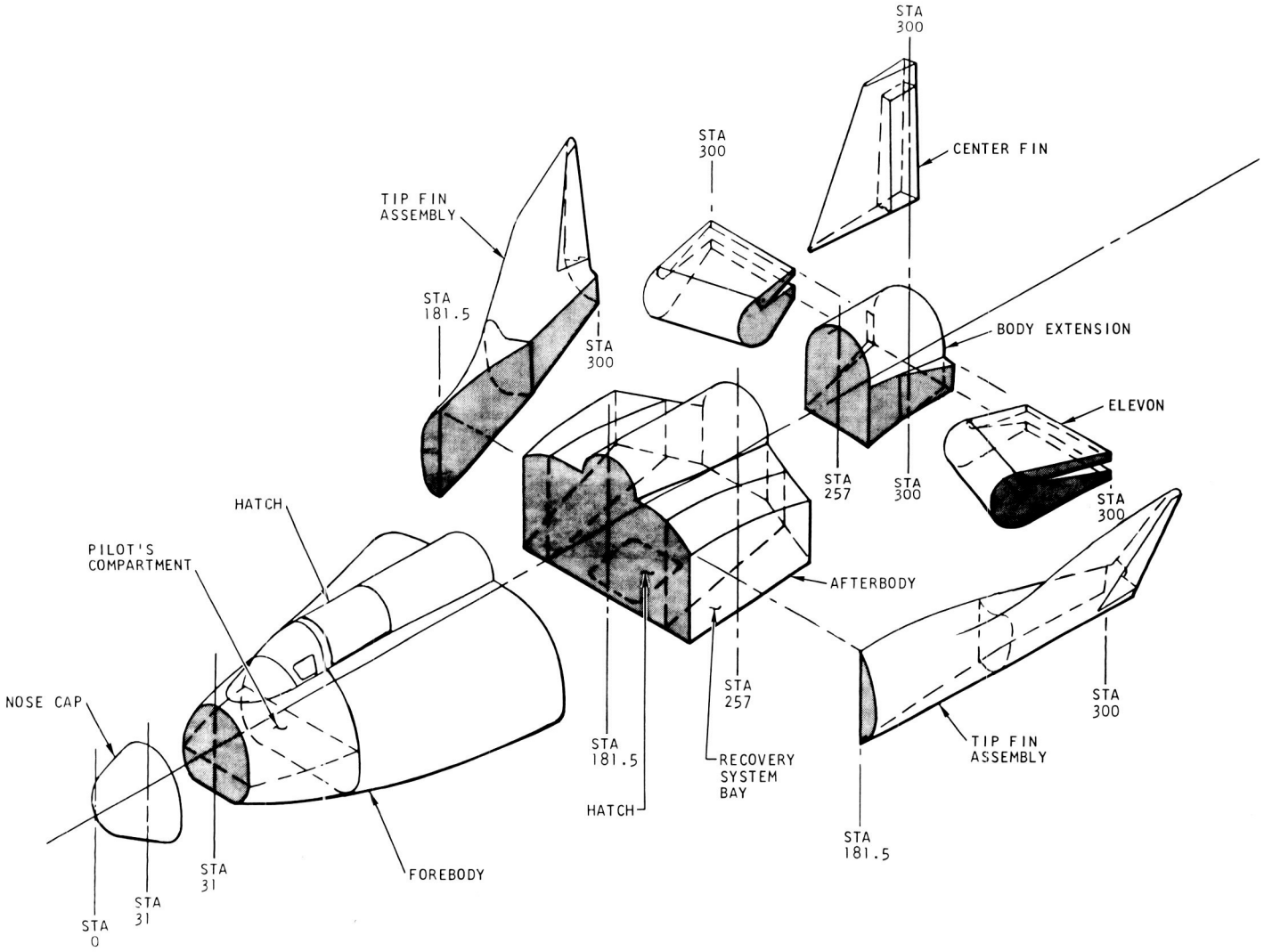

FIGURE 3. MAJOR SECTIONS OF HL-10 D/3 VEHICLE

ER 14471-7

(3) Standard cockpit display panels are provided for the pilot, that is, forward panel and side consoles. Display panels are provided on the rear side of the pilot's bulkhead for the two crew members with the crew members on the right side acting as copilot.

(4) Ingress and egress is through a single overhead hatch located between the two crew members. The two seats are spaced so that the hinged pilot seat can rotate backward between the aft seats. The pilot enters first and leaves last.

This arrangement is an improvement over that shown in the five-vehicle parametric phase. The jettisonable windshield (canopy) is eliminated, along with its attendant sealing and leakage problems. Also, the complexity of having a jettisonable heat shield cover mounted onto a jettisonable section is eliminated, along with the related sequencing problems. A small increment of internal space is gained by these eliminations.

(5) The subsystem components are arranged in rack assemblies just behind the two crew members. Avionics and instrumentation components are on the left side while guidance and environmental control components are on the right side.

The components are arranged on three shelves on each side, and all components are accessible for maintenance and checkout from the center aisle between the crew members. Each of the shelves may be removed for bench checkout or to replace components for research objectives on subsequent missions.

The shelves incorporate cold plating for equipment thermal control.

(6) Supply tankage is located in the corners at the aft end of the forebody behind the equipment racks off the main gear bulkhead (Station 181.5).

(7) Crew survival equipment is located in the canopy extension (overhead) immediately adjacent to the hatch.

(8) The remainder of the forebody is reserved for research equipment. This space is roughly "T" shaped, having an available volume of 52.6 cubic feet (1.59 cm^3), and it straddles the center of gravity so that variations in weight on the different missions will not affect the vehicle balance. This space is located within the vehicle where the maximum useful height is available, permitting larger size pieces of equipment.

(9) The D/3 vehicle and crew seating are not designed for ejection seats. An ejection seat and ejection hatch may be incorporated at the pilot's location with some moderate modification. However, the side-by-side arrangement of the additional crew members is incompatible with ejection seats from both structural and space availability viewpoints. If more than one ejection seat is desired, tandem crew seating will have to be incorporated

4. Afterbody Arrangement

The afterbody has three parallel structural torque boxes; the outer bays contain the recovery subsystems, while the central area contains the hydraulic systems and a reserved space for research equipment. The center bay is pressurized. The outer bays are not pressurized.

(1) A pair of vertical beams along each side, between the main gear bulkhead (Station 181.5) and rear bulkhead (Station 257), separates the afterbody into three bays. The outer bays (or main gear wells) enclose the main gear in the lower halves and the vehicle emergency recovery parachute canisters in the upper halves. Structural panels in the lower surface of the unpressurized bays are sheared and then hinged open for main gear extension. In an emergency, the upper surface is sheared instead, and the chute canister (which is an integral part of the panel) is pivoted about a fulcrum for deployment of the chutes.

(2) An access hatch in the lower surface is provided for access to the central area. Modular hydraulic system units are located adjacent to the opening for ease of servicing and maintenance. The space immediately above the hatch is assigned to research equipment installation (18.6 ft^3, 0.53 cm^3) where it is readily accessible for checkout and maintenance.

5. Body Extension

The body extension is the fixed structural portion of the vehicle between the elevons from the rear bulkhead (Station 257) to the base of the vehicle (Station 300). It has flat sides and bottom with a rounded crown which blends in with the canopy extension.

(1) Structurally, this section includes a fitting along the crown for attachment of the center fin and rudder actuators and fittings along the sides for the inboard elevon hinges. These fittings run the length of the body extension, transferring the loads from the interface separation points (Station 300) into the main body of the vehicle.

(2) A shielded and insulated solid bulkhead closes off the back end at the interface separation plane. This bulkhead supports two extendable antennas, the recovery drogue chute and the landing assist (instant L/D) thrustors.

(3) Three of four adapter attachments pass through the interface bulkhead, as noted above. The fourth attachment is by a strut which passes through the bottom of the body extension and attaches at the rear bulkhead (Station 257). This strut is covered by a nonstructural fairing. It is separated and jettisoned when the forward adapter section is jettisoned. The hole in the bottom of the vehicle is filled with a plug which is automatically driven into position by spring force when the strut is jettisoned.

6. Tip Fin Assemblies

The tip fins, body-to-fin fillet areas, and afterbody side panels are included in an integral structural unit, called tip fin assemblies. The assembly runs from Station 181.5 to the aftermost tip of the fin. It is attached to the afterbody along the length of the outboard main gear beams and at the two main bulkheads. This assembly also end-plates the outboard end of the elevons.

(1) The outboard elevon hinge, elevon actuators and tip-fin flap actuators are embedded within this section.

(2) The attitude control reaction thrustor arrays are located at the rear face of the lower end of this section (Station 300).

7. Entry Vehicle Fabrication

The design of the HL-10(D/3) entry vehicle is particularly compatible with the objectives of a research program from a fabrication standpoint. The several sections of the vehicle (fig. 3) can each be fabricated independently and then assembled into the whole integrated unit. The whole unit can then be broken down into the major sections and conveniently shipped to destination.

This type of "prefab" construction inherently incorporates the flexibility and growth potential desired for a research program. Each or any of the various sections can be custom built or altered for various mission objectives as the program continues; special sections could be furnished to replace standard sections and even newly designed sections of slightly different shapes, (e.g., new nose shape) may be interchanged at any desired point.

While this program does not warrant the expense and effort of interchangeability, the design of the D/3 vehicle is such that interchangeability could readily be attained should this vehicle be employed in a future operational system.

8. Adapter

The adapter is essentially a truncated conical transition section between the D/3 entry vehicle and launch vehicle (booster). The design of the adapter for a Titan is shown in figure 4.

(1) The adapter is approximately 6 feet (188 cm) long and 10 feet (305 cm) in diameter at the larger aft end. The half cone angle is a nominal 27.5°. The interface is oblong-shaped, 57.48 inches (146 cm) high and 42.7 inches (108.5 cm) wide. The adapter shape is faired in from end to end

(2) The adapter is set at a 2.5° angle relative to the D/3 horizontal reference line for launch and ascent considerations. This angular change is integral within the adapter.

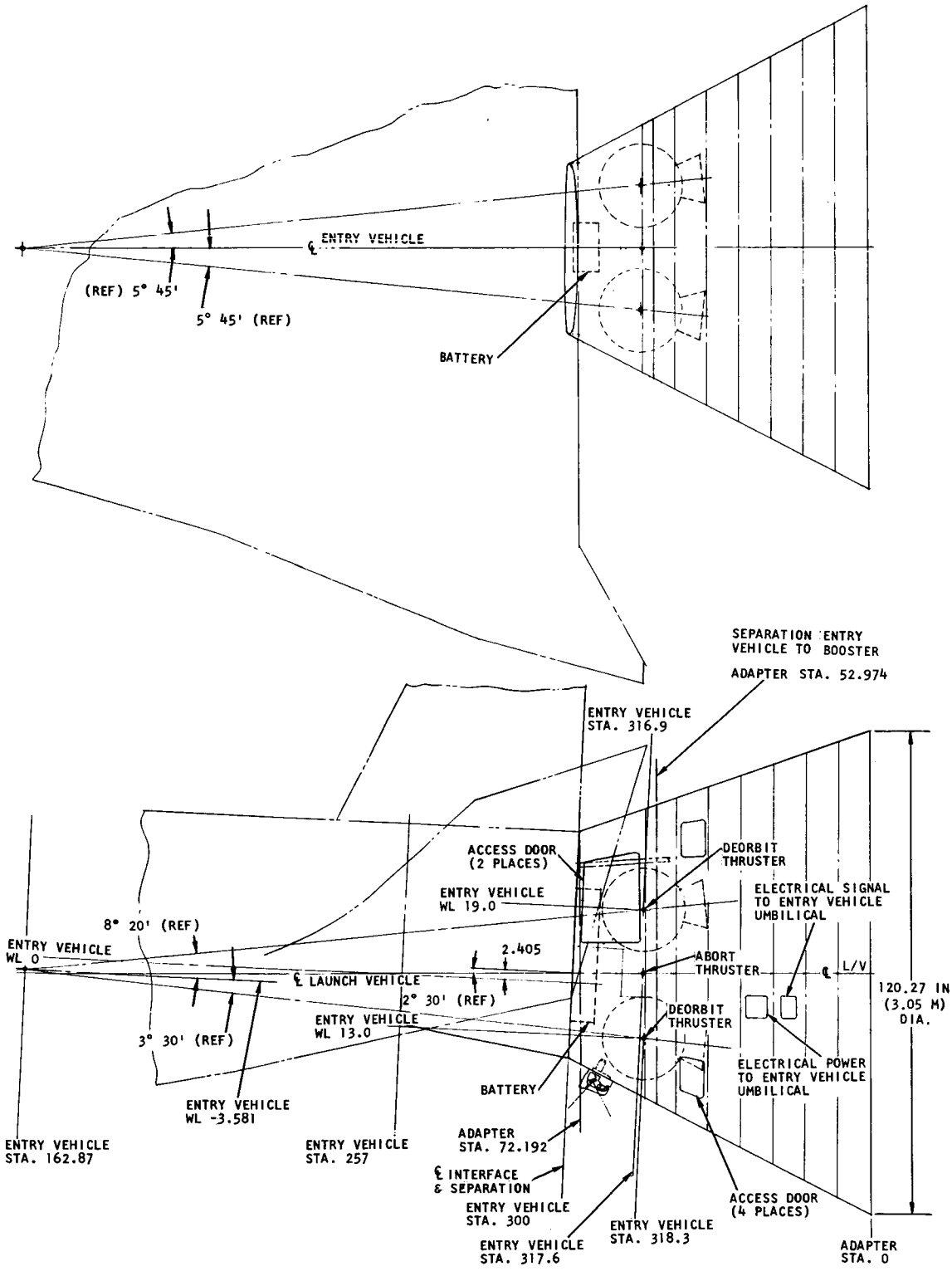

FIGURE 4. TITAN III ADAPTER SECTION

(3) The adapter is fabricated in one piece and rigidly fastened to the bolting ring on the Titan. A linear-shaped charge shears and separates the smaller forward section, 21 inches (53.3 cm) in length, from the remainder in both normal and emergency modes. The larger section remains with the booster.

(4) The forward adapter section contains an array of four spherical solid rocket motors which furnish impulse for deorbit and/or abort operations. These motors are arranged so that their thrust lines converge at the design center of gravity of the combined entry vehicle and forward adapter at motor burnout.

(5) Four batteries, which supply electrical power during ascent and orbital phases, are installed inside the forward adapter section. A pair of horizon sensors is located externally at the lower portion of this section.

(6) The forward adapter section is jettisoned after deorbit (or abort) with the solid rocket motors, batteries, and horizon sensors attached; the separation plane is at the entry vehicle interface (Station 300). None of these items is jettisoned separately at any time.

(7) Umbilical connectors are located in the aft adapter section, and access panels are placed to permit addition of pyrotechnic devices at the latest possible moment in countdown.

III. WEIGHT AND BALANCE STUDIES

This section presents the detail weight breakdown on the D/3 configuration as designated for the primary near-earth orbit entry research mission. This design phase has resulted in no significant weight changes in the weight data shown for the five vehicles in Part IV. However, because of the increased depth of study on the D/3 vehicle, the detail weight of Part IV and this part are not necessarily the same. The basic methodology for the weights development is shown in Part IV along with the criteria used for vehicle design.

The overall accuracy of the weight data is considered to be good for the following reasons:

(1) Martin Marietta has made detail designs of lifting bodies, particularly in the medium lift-to-drag range, for the last five years.

(2) Experience and information are available from two Air Force/Martin Marietta hardware programs, namely, the PRIME and the PILOT, which are currently in production. The actual weight of the PRIME is 35 pounds (3.9%) below the incentive contract weight of 890 pounds. The weight of PILOT, of which one vehicle is almost completely built, is 116 pounds (1.1%) above the incentive contract weight of 10 929 pounds.

(3) System components are primarily of current state-of-the-art status, having been developed for Gemini, Apollo, PRIME, PILOT, the X-15, etc.

(4) Structure and heat shield, which represent 44 percent of the entry vehicle weight, probably present the greatest problem from a weight accuracy standpoint. Here again Martin Marietta experience in aircraft structure and Martin Marietta technology experience in heat shield development should tend to minimize inaccuracies. The structural weight is broken down in detail and based on a combination of analytical and statistical data. Recent data gained from the first flight of the PRIME indicate that the structure and heat shield concept functioned properly; however, this particular flight did not approach any extreme (design limit) conditions.

A. SUBSYSTEM WEIGHT BREAKDOWN

1. Entry Vehicle Structural Derivation

The D/3 structural weights are based on the design studies reported in Part IV and this section. A structural layout for the D/3 vehicle is shown in fig. 17.

Body structures derivation. - The body structural derivation is summarized below:

	lbM	kg
Shell	(531)	(241)
Includes skin, stringers and frames in all areas except outboard fin torque box and tunnel area aft of pressure bulkhead		
379 ft^2 at 1.25 lbM/ft^2 x 1.12	531	
35.2 m^2 at 6.10 kg/m^2 x 1.12		241
Outboard fin torque box	(341)	(155)
Starts at Station 181 outboard of wheel well and includes all structure under outer fin panels		
Side shell Station 173 to aft pressure bulkhead		
29.3 ft^2 at 1.5 lbM/ft^2 x 2	88	
2.72 m^2 at 7.32 kg/m^2 x 2		40
Bulkheads (5/side) in side panel		
3.3 ft^2 at 3.0 lbM/ft^2 x 10	99	
0.306 m^2 at 14.64 kg/m^2 x 10		45
Shell under outboard fin panels		
38.5 ft^2 at 2.0 lbM/ft^2 x 2	154	
3.57 m^2 at 9.76 kg/m^2 x 2		70
Tunnel area aft of pressure bulkhead	(108)	(49)
36.0 ft^2 at 3.0 lbM/ft^2	108	
3.34 m^2 at 14.64 kg/m^2		49
Bulkheads and special frames	(355)	(161)
Bulkhead Station 31		
10.2 ft^2 at 1.75 lbM/ft^2	18	
0.95 m^2 at 8.54 kg/m^2		8
Frame Station 83		
20.0 ft at 3.2 lbM/ft x 1.41	90	
6.1 m at 4.75 kg/m x 1.41		41

	lbM	kg
Frame Station 181		
27.0 ft at 4.1 lbM/ft x 1.41	155	
8.23 m at 6.1 kg/m x 1.41		70
Aft pressure bulkhead		
30.6 ft^2 at 2.5 lbM/ft^2 x 1.2	92	
2.84 m^2 at 12.2 kg/m^2 x 1.2		42
Beams	(188)	(85)
Outboard main gear		
20.0 ft^2 at 1.5 lbM/ft^2 x 2	60	
1.86 m^2 at 7.32 kg/m^2 x 2		27
Inboard main gear		
20.0 ft^2 at 1.5 lbM/ft^2 x 2	60	
1.86 m^2 at 7.32 kg/m^2 x 2		27
Nose gear		
17.0 ft^2 at 2.0 lbM/ft^2 x 2	68	
1.58 m^2 at 9.76 kg/m^2 x 2		31
Longerons	(50)	(23)
Estimate	50	23
Canopy	(97)	(44)
Estimate based on PILOT	97	44
Hatches and doors	(287)	(130)
Entrance hatch, including coaming		
7.1 ft^2 at 13.6 lbM/ft^2 (ref. Gemini)	97	
0.66 m^2 at 66.4 kg/m^2		44
Main gear doors		
5.0 ft^2 at 5.0 lbM/ft^2 x 2	50	
0.46 m^2 at 24.41 kg/m^2 x 2		23

	lbM	kg
Nose gear doors		
5.7 ft^2 at 5.0 lbM/ft^2 (ref. PILOT)	28	
0.53 m^2 at 24.41 kg/m^2		12
Emergency chute doors		
6.2 ft^2 at 5.0 lbM/ft^2 x 2	62	
0.58 m^2 at 24.41 kg/m^2 x 2		28
Miscellaneous small doors, coaming, etc.		
Estimate	50	23
Tail supports and elevon cove area	(70)	(32)
Estimate (ref. PILOT)	70	32
Flooring	(60)	(27)
Estimate	60	27
Miscellaneous	(150)	(68)
Estimate	150	68
Total body structure	2237	1015

Tail structure derivation. - The tail structure weight has been derived by using the PILOT structure as a base and modifying this data as necessary. The HL-10 surfaces are considerably thicker in cross-section even after allowing for heat shield covering. This benefit is offset to a minor extent in that the HL-10 is constructed of titanium whereas aluminum was used for the PILOT structure.

Surface	HL-10 flat plate area		PILOT (ref.) unit weight		HL-10 unit weight		HL-10 weight	
	ft^2	m^2	lbM/ft^2	kg/m^2	lbM/ft^2	kg/m^2	lbM	kg
Elevon--Lower (2)	33	3.06	2.5	12.2	4.0	19.5	132	60
--Upper (2)	20	1.86	2.8	13.7	2.5	12.2	50	23
Fins --Outer (2)	31.4	2.92	6.5	31.7	6.0	29.3	188	85
--Center (2)	15.7	1.46	3.6	17.6	4.0	19.5	63	29
Flaps --Outer fin (4)	16.2	1.50	--	--	2.5	12.2	40	18
--Center fin (2)	12.5	1.16	--	--	2.0	9.8	25	11
Total	128.8	11.96			3.4 (av)	18.9 (av)	498	226

Structure weight summary. - The total weights of the D/3 body and tail structure are shown below:

	lbM	kg
Body structure	2237	1015
Tail structure	498	226
Total	2735	1241

2. Heat Shield

The heat shield weight for the D/3 vehicle is based on an all-ablative heat shield design sized for all-turbulent flow. This weight, along with weight for all of the detail heat shield design developed for the D/3 vehicle, is summarized in the following tabulation, based on the detail studies reported in Part IV:

	Heating condition	lbM	kg
All-ablative	Laminar	2420	1097.9
	Turbulent	2710*	1230.3*
Ablative-radiative (max. use radiative)	Laminar	2150	975.2
	Turbulent	2450	1111.0
Ablative-radiative (min. weight)	Laminar	2080	943.4
	Turbulent	2370	1075.0
Ablative-radiative (max. use radiative) with abort protection	Laminar	2180	988.8
	Turbulent	2500	1135.0
Ablative-radiative (min. weight) with abort protection	Laminar	2110	957.1
	Turbulent	2430	1106.0

* Used for weights summary of D/3 vehicle.

3. Crew and Furnishings

A summary of the weight for the crew and furnishings is shown below:

	lbM		kg	
Crew (3) 80 percentile		540		244.9
Pressure suits (3)		75		34.0
Seats including torso restraints (3)		105		47.6
Survival kit		78		35.4
Seawater desalt kit (1)	1.4		0.6	
Rations--4 days	24.0		10.9	
Drinking water	12.0		5.5	

Radio and batteries	20.5		9.3	
Three-man raft	12.0		5.5	
Miscellaneous	8.1		3.6	
Personal hygiene		3		1.4
Relief provisions		2		0.9
Biomedical sensors		6		2.7
Food and containers		6		2.7
Maps, manual and case		6		2.7
Repair kit		2		0.9
Water*		--		--
Total		823		373.2

*Water for crew consumption is included in the environmental system weight total.

4. Display Panels

A summary of the display panel instrument weights is presented below:

	lbM	kg
Instruments	(100.5)	(45.2)
Flight director	6.5	2.9
Altimeter	4.2	1.9
Mach meter	3.0	1.4
Energy management display	10.0	4.5
Velocity, range and altitude error	3.0	1.4
h command indicator	9.1	4.1
α command indicator	9.1	4.1
Control surface indicators (4)	4.0	1.8
Roll rate error indicator	1.5	0.7
Roll error indicator	1.5	0.7
Heading error indicator	1.5	0.7
LV performance indicator	12.0	5.4
Clock and elapsed time indicators (3)	6.9	3.1
Accelerometer	1.5	0.7
Electric voltage level	0.5	0.2
Electric current drain	0.5	0.2
Malfunction warning panel	3.0	1.4
Hydraulic system pressure gages (2)	2.0	0.9
Propellant temperature gage	1.0	0.5
Propellant pressure gage	1.0	0.5
Propellant quantity gage	4.0	1.8
Motor case temperature gage	0.5	0.2
Suit and cabin pressure gage	1.4	0.6
Suit and cabin CO_2 gage	1.4	0.6
Suit and cabin temperature gage	1.0	0.5
O_2 quantity gage	2.0	0.9

	lbM	kg
H_2O quantity gage	2.0	0.9
Glycol quantity gage	2.0	0.9
O_2 storage temperature gage	1.0	0.5
O_2 storage pressure gage	1.4	0.6
Steam temperature gage	2.0	0.9
Controls	(29.9)	(13.7)
Landing chute lever	1.0	0.5
Abort lever	1.0	0.5
Recovery chute lever	1.0	0.5
Guidance computer panel	8.4	3.8
Side stick controllers (2)	4.5	2.0
Switches (70)	14.0	6.4
Lights (36)	(3.6)	(1.6)
Panels	(36.0)	(16.3)
Circuitry	(36.0)	(16.3)
Total	206.0	93.1

5. Electrical Power System

The electrical system in the entry vehicle provides only that power required during re-entry for all systems except the surface controls. That portion of the electrical power system required for launch and orbiting time is now included in the adapter to reduce the entry vehicle weight and to allow more volume for test equipment.

The weight breakdown for the entry vehicle portion is shown below:

	lbM	kg
Batteries (2)	124	56.2
Wiring, relays, switches, etc.	230	104.3
Total	354	160.5

6. Environmental System

A summary of the environmental control and life support system weights is presented below:

	lbM	kg
Fixed system	(269.9)	(122.4)
Atmosphere control system	80.4	36.5
O_2 supply and pressure system	8.2	3.7
Water supply system	1.0	0.5
Thermal control system	52.5	23.8
Cold plates	40.0	18.1
Ducts, clamps, etc.	30.0	13.6
Instrumentation sensors	10.8	4.9
Glycol	10.0	4.5
Umbilical, etc.	12.0	5.4
Supports and miscellaneous	25.0	11.4
Expendables	(156.6)	(71.0)
Oxygen--cryogenic	23.8	10.8
Oxygen--7000 psi (48.5 MN/m^2)	18.8	8.5
Water	110.0	49.9
L_1OH and CO_2	4.0	1.8
Tanks	(71.8)	(32.6)
Oxygen--cryogenic	16.6	7.5
Oxygen--7000 psi (48.5 MN/m^2)	37.6	17.1
Water	17.6	8.0
Total	498.3	226.0

7. Guidance, Navigation and Communications

A summary of the entry vehicle guidance, navigation and communication weights is presented below:

	lbM	kg
Guidance and navigation	(263.0)	(119.3)
Primary inertial platform and digital computer	127.0	57.5
Backup guidance	39.0	17.7
Dual horizon scanners	26.0	11.8
Flight control system	22.0	10.0
Air data sensors	5.0	2.3
Wiring and supports at 20%	44.0	20.0
Communications	(240.0)	(108.9)
Audio center	7.9	3.6
hf transceiver	6.3	2.9
vhf recovery beacon	2.5	1.1
vhf voice communication including coax switch and hybrid	18.5	8.4
vhf satellite communication	20.0	9.1
vhf command receiver including hybrids	21.4	9.7

	lbM		kg	
Telemetry transmission (S-band)		14.1		6.4
Exciters (3)	4.8		2.2	
Coax switches (2)	4.0		1.8	
Triplexer	3.0		1.4	
Isolators (3)	2.3		1.0	
Radar beacon tracking (C-band)		15.6		7.1
Transponders (2)	8.6		3.9	
Coax switches (2)	4.0		1.8	
Power divider	1.5		0.7	
Phase shifter	1.5		0.7	
Radar beacon tracking (K_a band)		4.5		2.0
Transponder	4.5		2.0	
Antennas		89.2		40.5
hf transceiver	6.7		3.0	
vhf recovery including filter (2)	1.8		0.8	
vhf voice including window and diplexer	18.2		8.3	
vhf satellite (flush)	44.0		20.0	
uhf command including window (2)	9.2		4.2	
S-band including window (3)	5.1		2.3	
C-band including window (3)	3.6		1.6	
K_a-band including window	0.6		0.3	
Wiring and supports		40.0		18.1
Total		503.0		228.2

8. Instrumentation

A summary of the instrumentation system weights is presented below:

	lbM	kg
Tape recorder		
Leach Apollo recorder with 2 transports	66	29.9
Remote multiplexers		
16 at 3.5 lbM (1.6 kg) each	56	25.4
Central encoder and power supply		
6 at 6.0 lbM (2.7 kg) each	36	16.3
Sensors and signal conditioning weight		
2000 at 0.16 lbM (0.0725 kg) each	320	145.2
Wiring		
25 lbM (11.3 kg) + 2000 at 0.03 lbM (0.0136 kg) each	85	38.6
Installation weight		
10%	62	28.1
Total	625	283.5

9. Reaction Control and Landing Assist Systems

A summary of the entry vehicle reaction control and landing assist system is shown below:

	lbM	kg
Engines	(45.0)	(20.4)
Roll and pitch (4)	11.2	5.1
Yaw (2)	6.4	2.9
Landing assist (2)	17.0	7.7
Supports	10.4	4.7
Propellant system	(67.0)	(30.4)
Tank (450 psi)	26.5	12.0
Plumbing, fittings, valves, etc.	20.0	9.1
Supports	20.5	9.3
Pressure system	(29.0)	(13.1)
Nitrogen	5.6	2.5
Tanks	10.2	4.6
Plumbing, fittings, valves, etc.	8.2	3.7
Supports	5.0	2.3
Electrical provisions	(10.7)	(4.9)
Propellant (peroxide)	(198.4)	(90.0)
Usable	180.4	81.8
Trapped and unusable	18.0	8.2
Total	350.1	158.8

10. Surface Control Actuation

The control surface actuation system consists of the hydraulic system, electrical bias surface actuators and a separate electrical power system. A summary of the weight breakdown for this system is shown below.

	lbM	kg
Hydraulic system	(420)	(190.5)
Pump-motor-reservoir (dry) (2)	92	41.7
Accumulators, 60 in.^{3} (2)	14	6.4
Filter units (2)	20	9.1
Plumbing	30	13.6
Hydraulic fluid	22	10.0
Supports and miscellaneous	32	14.5
Actuators--Elevons (2)	90	40.8
--Rudders (2)	50	22.7
--Elevon flaps (2) (electrical)	34	15.4
--Tip fin flaps (4) (electrical)	36	16.3

	lbM	kg
Electrical power system	(526)	(238.6)
Batteries (7)	434	196.9
Reverse current relays (7)	21	9.5
Motor contactors (2)	8	3.6
Circuitry	63	28.6
Total	946	429.1

11. Landing Gear and Braking Chute

The primary recovery system of the D/3 vehicle consists of a wheel and tire on the nose gear, a touchdown wheel in a skid for the main gear and a braking chute to minimize landing runout. A summary of the system weight breakdown is shown below:

	Main Gear		Nose Gear		Chute	
	lbM	kg	lbM	kg	lbM	kg
Landing Gear						
Wheels, tires and tubes	--		29.4	13.3		
Skids	117.2	53.2	--	--		
Skid positioner	17.8	8.1	--	--		
Torque arm assembly	17.8	8.1	--	--		
Piston assembly	74.4	33.7	32.0	14.5		
Cylinder and trunnion assembly	73.6	33.4	23.2	10.5		
Lower bearing and seal assembly	5.4	2.4	5.1	2.3		
Drag strut assembly	31.2	14.2	15.7	7.1		
Metering pin assembly	3.8	1.7	1.7	0.8		
Stand pipe and orifice plate	7.8	3.5	2.5	1.1		
Miscellaneous bolts	6.0	2.7	8.8	4.0		
Oleo trunnion caps	5.2	2.4	2.6	1.2		
Drag strut trunnion caps	5.2	2.4	2.6	1.2		
Gear actuator	17.8	8.1	8.9	4.0		
Door mechanism link	10.0	4.5	10.0	4.5		
Braking Chute						
Main chute					3.0	1.4
Pilot chute					0.8	0.4
Chute risers					3.0	1.4
Chute bag					1.3	0.6
System controls					4.0	1.8
External fittings					7.0	3.2
Total item	393.2	178.4	142.5	64.5	19.1	8.8
Total					554.8	251.7

12. Emergency Chutes

Emergency recovery of the D/3 vehicle is accomplished with four clover-leaf parachutes in the event that a horizontal ground landing cannot be achieved. A summary of the emergency chute recovery system weights is shown below:

	lbM	kg
Pilot chute mortar guns (2)	20	9.1
Pilot chutes (2)	24	10.9
Pilot chute bridles (2)	16	6.8
Main chutes (4)	440	200.0
Main chute risers (4)	33	15.0
Main chute bags (2)	30	13.6
Vehicle harness (1)	20	9.1
Chute disconnects (2)	12	5.4
Chute canister and actuator (2)	60	27.2
Controls, sequence and power	23	10.4
Total	678	307.5

B. BALANCE AND BALLAST STUDIES

Ballast weight is necessary in order to keep the entry vehicle c.g. at or forward of 53 percent of the entry vehicle length.

As noted in the balance calculations below, the D/3 vehicle without any test equipment requires a total of 220 pounds (100 kg) of ballast. Since the centroid of the test equipment compartment is located at 57.3 percent of entry vehicle length, the effect of loading in test equipment is minimal. If the maximum amount of test equipment permitted with the wing loading of 55.1 pounds per square foot (269 kg/m^2) is located evenly through the compartment, the weight of additional ballast required would be +88 pounds (+40 kg).

	Weight		c.g.,
	lb	kg	% of length
Structure	2735	1241	60.4
Heat shield	2710	1229	57.0
Crew and provisions	823	373	33.7
Display panels	206	93	18.3
Electrical system	354	161	41.0
Environment system	498	226	53.5
Guidance, navigation and communication	503	228	50.4
Instrumentation	625	283	47.8
Reaction control and landing assist	350	159	68.0
Surface controls	946	429	42.6
Landing gear	555	252	59.3

	Weight		
	lb	kg	c.g., % of length
Emergency chutes	678	307	71.6
Ballast	220	100	3.3
Total	11 203	5081	53.0
Maximum test equipment	1 051	477	57.3
Additional ballast	88	40	3.3
Total	12 342	5598	53.0

C. TEST EQUIPMENT

The test equipment weight noted on the chart of 1051 pounds (477 kg) represents the maximum permissible allowed within the restraint of a maximum wing loading of 55.1 pounds per square foot (269 kg/m^2) permitted for the D/3 vehicle. This is based on the current weight estimates for the other components and systems of the D/3 vehicle. This weight would therefore tend to fluctuate some during the start of hardware program. The volume available for this test equipment is 74.8 cubic feet (2.12 m^3) and, based on the allowable experiment weight, results in an average overall density of 14.3 pounds per cubic foot (69.8 kg/m^2).

It is interesting to note that on a seven flight testing program there is currently one flight with a test load of 1030 pounds (467 kg). The next highest is 585 pounds (265 kg). The above indicates that the test equipment allowance does not appear to be critical.

D. BOOSTER ADAPTER SUBSYSTEMS

1. Adapter Structure

A weight of 510 pounds (231 kg) for the D-size vehicle adapter, derived in the parametric vehicle design studies, is considered adequate since the total spacecraft weights are comparable.

2. Deorbit-Abort Propulsion

A summary of the deorbit/abort propulsion system weights is presented in the following tabulation:

	lbM	kg
Abort engines		
Spherical solids (mass fraction = 0.9) (2)	452	205.0
Deorbit engines		
Spherical solids (mass fraction = 0.9) (2)	516	234.1
Installation		
Estimated at 10%	97	44.0
Total	1065	483.1

Box beams incorporated and included in the adapter structure permit a lower estimate for installation weight than was used in the five vehicle design studies.

3. Electrical System--Adapter

All electrical power to the entry vehicle--except for surface control actuation during launch, ascent and orbiting period--are included in the adapter.

	lbM	kg
Batteries		
LR-100 (4)	248	112.5
Circuitry and supports		
Estimated	40	18.1
Total	288	130.6

4. Miscellaneous

A 100-pound (45.4 kg) weight is allowed for miscellaneous items. This provides for a number of minor items, such as umbilicals, other than electrical, that will be added in the detailed design of the adapter.

E. MASS PROPERTIES

The mass properties developed for the D/3 entry vehicle are tabulated below:

Weight	12 342 lb	(489 kg)
Center of gravity (distance from nose)	13.25 ft	(4.04 m)
I_y	17 940 slug-ft^2	(24 308 kg-m^2)
I_z	21 865 slug-ft^2	(29 627 kg-m^2)
I_R	5080 slug-ft^2	(6883 kg-m^2)
Principal axis, nose up	1.3°	(0.0226 rad)

F. TOTAL D/3 VEHICLE WEIGHTS

The total D/3 vehicle weights are summarized below:

TABLE 1

D/3 Vehicle Weight

	lbM	kg
Entry vehicle	(12 342)	(5598)
Structure	2 735	1241
Heat shield	2 710	1229
Crew and provisions (3)	823	373
Display panels	206	93
Electrical system	354	161
Environmental system	498	226
Guidance, navigation and communications	503	228
Instrumentation	625	283
Reaction control and landing assist	350	159
Surface controls	946	429
Landing gear	555	252
Emergency chutes	678	307
Ballast	308	140
Test equipment	1 051	477
Adapter	(1 963)	(890)
Structure	510	231
Deorbit-abort propulsion	1 065	483
Electrical	288	131
Miscellaneous	100	45
Launch weight	14 305	6488

(This page unclassified)

PRECEDING PAGE BLANK NOT FILMED

[redacted]

IV. SUBSYSTEM DEFINITION STUDIES

This section presents a review of the subsystem studies conducted for the selected D/3 vehicle. The D/3 vehicle subsystems design and components are based on the utilization of existing technology and are conservatively sized to provide a versatile entry research test platform.

This study effort is a detailed extension for one vehicle of the parametric design studies conducted for the five vehicles and reported in Part IV. The subsystem studies defined in this document are based on the design criteria reported in section II of Part IV.

As a result of the Part IV parametric vehicle design studies, design specifications were prepared on the following subsystems and submitted to potential suppliers for detail component definition, subsystem cost comparisons, and comments on the design approach:

(1) Deorbit and abort propulsion

(2) Reaction control and landing assist

(3) Guidance and navigation

(4) Electronic flight control

(5) Instrumentation data management

(6) Flight control actuation.

Most of the suppliers who were approached made replies to the request. Details on the suppliers' responses are shown in the appropriate subsystem section.

Also shown in this section are the effects on subsystem design of the secondary flight research objectives.

A. HEAT SHIELD

As a result of the design and tradeoff studies conducted during the parametric entry vehicle design phase of the study (Part IV), an all-ablative heat shield was chosen for the D/3 entry research vehicle. These studies included a comparison of six different entry trajectories that represented the bounds of the entry heating environment. They were made to determine the most severe condition on each of 238 points over the vehicle surface (table 2). The complete heat shield design environment and criteria are presented in section II of Part IV. The tradeoff studies compared radiative versus ablative heat shields for each of these areas to determine the total heat shield weight for six different design combinations and for both laminar and turbulent heating (table 3 and fig. 5). The radiative and ablative materials utilized in the studies are summarized in table 4. A more complete definition of the materials is shown in Part IV.

[redacted]

TABLE 2

DESIGN TRAJECTORY HEATING SUMMARY

Design* trajectory	Total heat, Btu/ft^2 (MJ/m^2)	Maximum heat rate, Btu/ft^2/sec (kW/m^2)	Time, sec	Angle of attack, deg	Bank angle, deg
1	136 000 (1543)	128 (1452)	2750	27	0
2	117 000 (1328)	145 (1645)	2100	27	±45
3	77 000 (874)	196 (2224)	1340	27	±75
4	68 000 (771)	99 (1123)	1700	52	0
5	58 000 (658)	110 (1248)	1300	52	±45
6	40 000 (454)	145 (1646)	800	52	±75

* Design trajectories defined in Part IV.

TABLE 3

SUMMARY OF TOTAL HEAT SHIELD WEIGHTS FOR TRADEOFFS*

	Heating condition	lb	kg
All-ablative	Laminar	2420	1098
	Turbulent	2710	1230
Ablative-radiative (max. use radiative)	Laminar	2150	975
	Turbulent	2450	1111
Ablative-radiative (min. weight combination)	Laminar	2080	943
	Turbulent	2370	1075
Ablative-radiative (max. use radiative) with abort protection	Laminar	2180	989
	Turbulent	2500	1135
Ablative-radiative (min. weight combination) with abort protection	Laminar	2110	957
	Turbulent	2430	1106

* Detail tradeoff data in Part IV.

TABLE 4

SUMMARY OF HEAT SHIELD MATERIALS

	Density, lb/in.^{3}	Density, gm/cc	Emissivity	Design heating rate limit, Btu/ft^2/sec	Design heating rate limit, MW/m^2/sec
Radiative					
Beryllium	0.066	1.85	0.75	2.7	30.67
Superalloy	0.29	8.03	0.80	15	170.5
Columbium	0.31	8.58	0.80	30	341.0
Tantalum	0.60	16.62	0.80	54	61[illegible].0
Ablative					
MA 25S	0.0165	0.457	0.72	0.5	50.6
ESA 3560HF	0.1736	0.482	0.80	125	1420.0
ESA 5500	0.0318	0.881	0.90	157	1782.0
Silica phenolic	0.03935	1.091	0.85	None	

Presented in this section of the report is a review of further studies to investigate: (1) the effects of initial entry angle (γ_i) on heat shield weights, (2) separated flow heating rates, (3) heat shield research experiments, and (4) detail heat shield design studies.

1. Initial Entry Angle

A study was made to determine the sensitivity of the ablative heat shield weight to changes in the initial entry angle. All-ablative heat shield weights (normalized with respect to weights for HL-10 design conditions) are presented in figure 6 as a function of initial entry angle for several variations of heat shield design parameters. Total heat shield weight curves are presented for an 800° F (700° K) ablator backface temperature with and without safety factors. Curves are also included for a restricted footprint where the heat design conditions are limited to the maximum crossrange flight and for a 600° F (558° K) ablator backface temperature.

The effect of increasing the initial entry angle is generally to reduce the total heating and heating time, with attendant decreases in the total heat shield weights for all conditions studied. For example, increasing the initial entry angle from -1.5° to -2.5° results in a 10 percent reduction in heat shield weight. However, the reduction in heat shield weight with increasing entry angles (γ_i) becomes a tradeoff with the increasing propulsion weights required to achieve the higher γ_i.

[redacted]

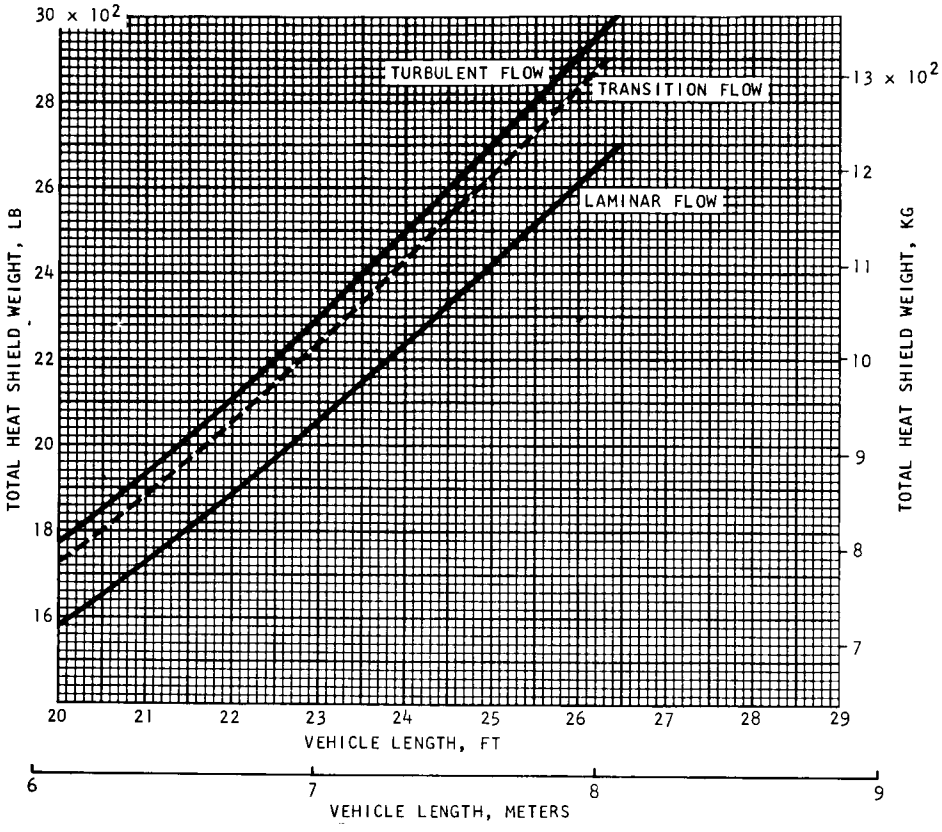

FIGURE 5. HL-10 HEAT SHIELD WEIGHTS FOR ALL ABLATIVE DESIGN

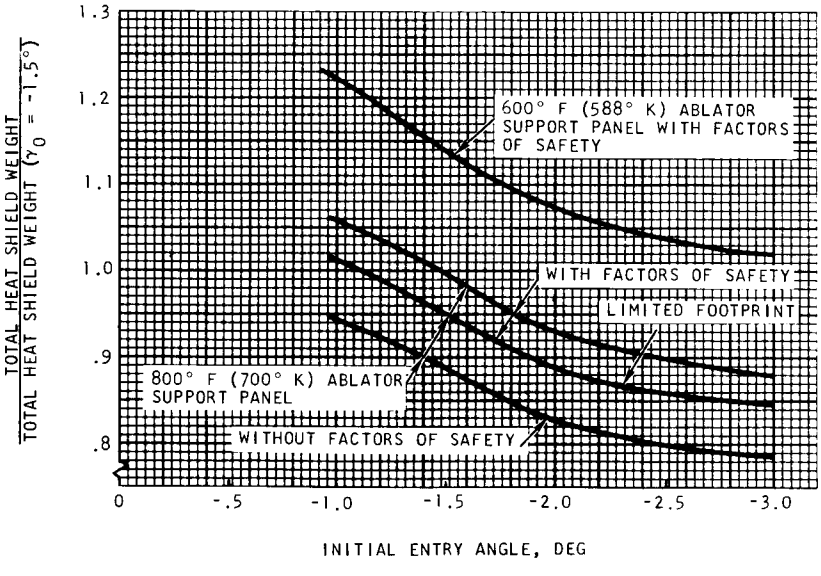

FIGURE 6. EFFECTS OF INITIAL ENTRY ANGLE ON HEAT SHIELD WEIGHT

[redacted]

2. Heat Shield Research Experiments

One of the primary experiments on the entry research vehicle program is the evaluation of new ablative materials and alternative heat shield approaches, such as radiative, transpiration cooling and various structural cooling techniques. An air gap of about 1/2 inch was provided between the insulation and the structure to provide extra space for the testing of these concepts. A typical rigid ablative and radiative experimental panel arrangement is shown in figures 7 and 8.

The NASA 602 elastomeric silicon, low-density nylon phenolic, and low-density silica phenolic are typical of alternative ablator systems which it may be desirable to flight test. An analysis was made to determine the required thicknesses of these ablators for a location on the bottom surface of the vehicle, which has a maximum total heating

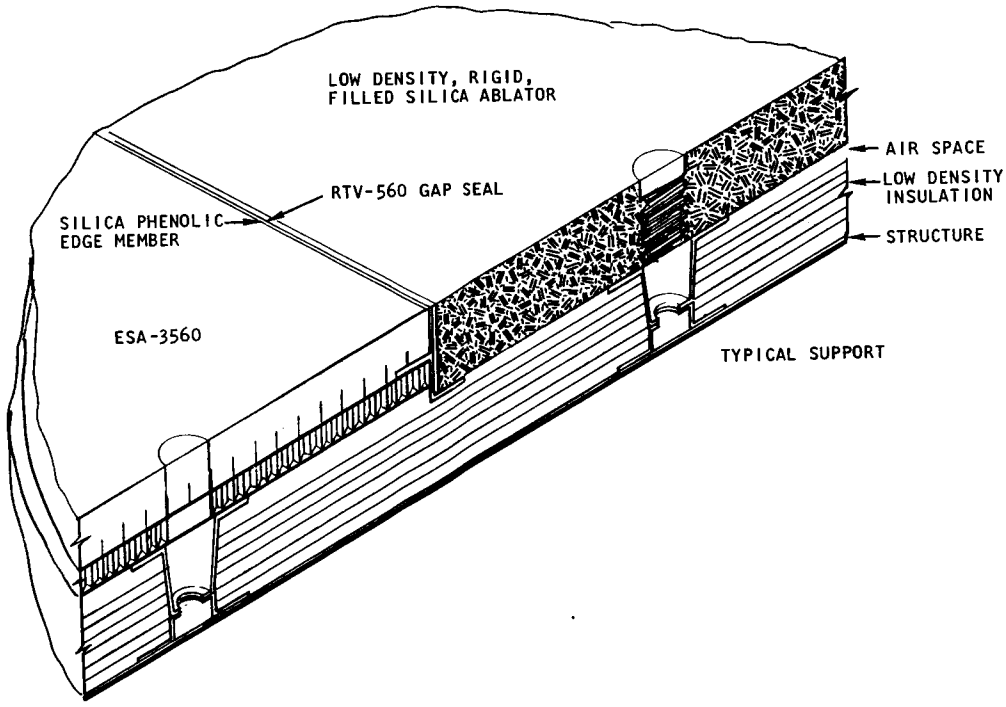

FIGURE 7. TYPICAL ABLATOR EXPERIMENT INSTALLATION

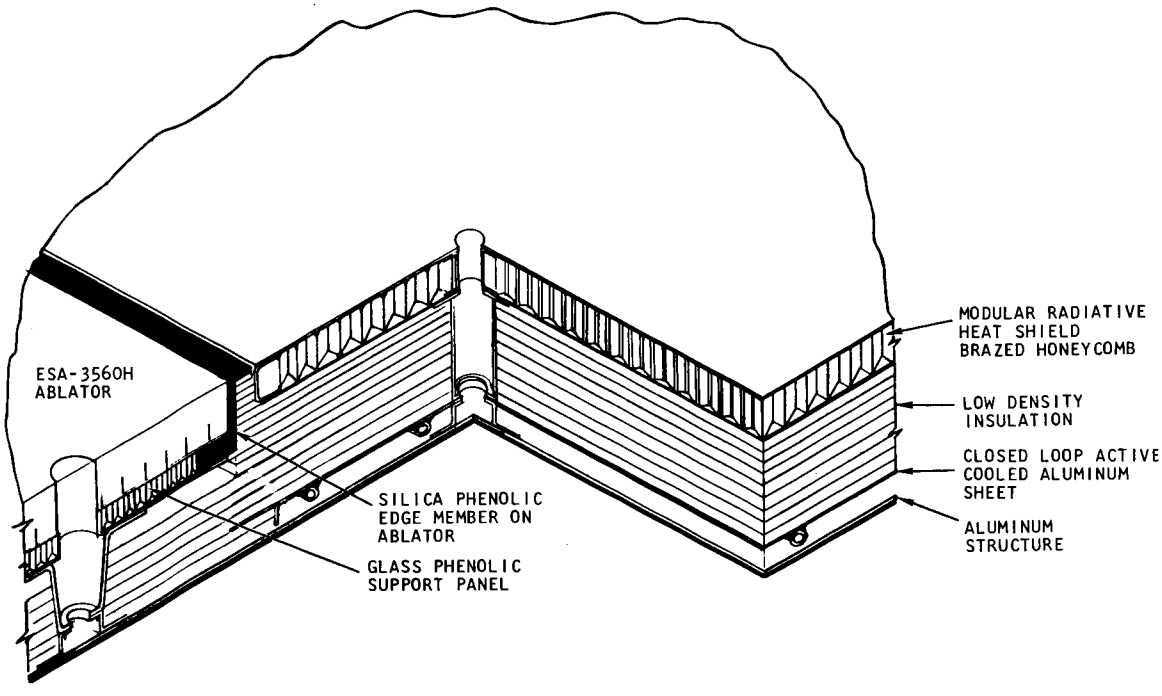

FIGURE 8. RADIATIVE PANEL--ACTIVE COOLING EXPERIMENT

of 27 000 Btu/ft^2 (306 MJ/m^2). The required thickness for a 800° F (700° K) ablator backface temperature is listed in table 5 along with the corresponding thickness of ESA 3560HF ablator.

TABLE 5

ABLATOR EXPERIMENT REQUIREMENTS

Ablator	Required thickness, in.	Required thickness, cm	Weight, lb	Weight, kg
ESA 3560HF	1.14	2.9	2.85	1.09
NASA 602	0.94	2.385	3.45	1.56
Low-density nylon phenolic	0.91	2.31	2.73	1.238
Low-density silica phenolic	1.91	4.85	10.80	4.89

The NASA 602 ablator is a nonstructural ablator and requires a support panel similar to the ESA 3560HF. The low-density nylon phenolic and the low-density silica phenolic are rigid ablators and may be developed so that they can be structurally supported by fiber glass edge members as shown in figure 7.

The radiative panel experiments will consist of evaluating panel material and structural design concepts. The experiments will also utilize either an active or passive structural cooling concept. For normal operation, the cooling concept tubing and plumbing system will be built into the structure (fig. 8). However, for the experimental program, which will handle various cooling concepts, the cooling panel can be attached to the ablator heat shield attachment point and the plumbing can be routed to a common header for entry into the structural pressure shell (fig. 8). Some of the particular materials and concepts of interest are listed in table 4.

Transpiration cooling panels, while not studied in detail, can be handled in a manner similar to the radiative panel experiments.

One special problem that occurs in a radiative-ablative vehicle heat shield approach is the edge joint between the radiative panel and the ablative panels. The hotter radiative panel offers a direct heat short into the lower temperature substrate panel of the ablator. This must be prevented through the utilization of specially designed joints to eliminate this undesirable heat flow.

Another problem could occur if ablative heat shield materials were to undergo surface recession at the interface. This would result in adverse flow conditions and undesirable heating. The silicon oxide forming ablators do not undergo significant surface recession until the surface temperature exceeds about 3100° F, which is also the maximum temperature estimated for tantalum radiative heat shields. Therefore, as long as ESA 3560 or similar elastomeric silicon ablators are utilized, interface mismatch should not become a problem.

5. Heat Shield Design

The all-ablative refurbishable heat shield concept selected for the D/3 vehicle has been studied extensively by Martin Marietta on NASA Contract NAS 1-5253 and reported in NASA CR-638, -639 and -640. The basic heat shield concept and some of the fabrication details are shown in figure 9. A 20- by 36-inch panel was fabricated to demonstrate the feasibility of the concept (figs. 10, 11 and 12). This panel was made of the materials and concept shown in figure 9, utilizing the ESA 3560HF ablator material.

The ablative heat shield material coverages determined for the D/3 vehicle are shown in figure 13. The ablators utilized are: (1) ESA 5500 for the nose, front leading edge areas; and flaps; (2) ESA 3560HF for the windward surface of the body and outboard fins, and (3) MA 255 for the leeward surfaces of the vehicle. The details of an access panel, showing the edge members and fasteners for panel removal, are shown in figure 14. Lower flap heat shield details are shown in figure 15.

The calculated ablator and insulation thickness at 238 points over the surface of the vehicle are summarized in table 6. Also summarized in this table are the effective local to stagnation heating rate ratios and the safety factor utilized for the vehicle design. The location of the 238 points over the vehicle surface is shown in figure 16.

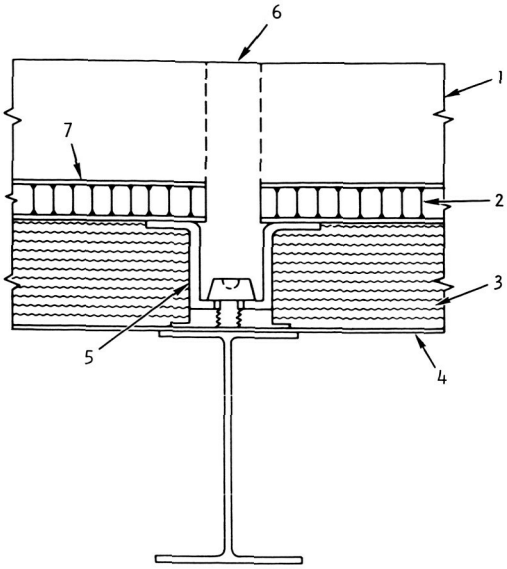

1	ABLATOR:	THICKNESS DETERMINED BY LOCAL HEAT INPUT: MARTIN ESA-3560HF, MA-25S AND ESA-5500.
2	SUBSTRATE:	REINFORCED PHENOLIC SANDWICH PANEL; FACINGS--2-PLY, 181-A-1100 GLASS FABRIC; CORE--6 LB/CU FT HRP 3/16-IN. CELL; RESIN--CTL 91 LD PHENOLIC; BOND CORE-TO-FACE, HT-424 ADHESIVE; MAXIMUM TEMPERATURE--800° F.
3	INSULATION:	MULTILAYER MICROQUARTZ (6.21 LB/CU FT); 5 LAYERS OF 0.0005 ALUMINUM FOIL/IN.; COMPOSITE DENSITY--6.5 LB/CU FT.
4	STRUCTURE:	2219-T6 ALUMINUM-WELDED-SKIN. FRAME-STRINGER MAXIMUM TEMPERATURE--200° F INCLUDING AFTERHEAT EFFECTS
5	STAND-OFF:	SUBSTRATE PANEL ATTACHMENT. GLASS REINFORCED PHENOLIC HAT 0.060-IN. WALL THICKNESS.
6	ABLATOR SUPPORT PLUG:	NONREMOVABLE SUPPORT PLUG INSTALLED AFTER PANEL IS BOLTED TO VEHICLE. BONDED FOR ESA ABLATORS, SCREW THREADS FOR RIGID ABLATORS.
7	ABLATOR BOND:	ABLATOR BONDED TO SUBSTRATE PANEL HT-424. ADHESIVE USED TO BOND HONEYCOMB MATRIX FOR ESA ABLATORS AND CARBON PHENOLIC ABLATORS.

FIGURE 9. REFURBISHABLE ABLATIVE HEAT SHIELD COMPOSITE CONCEPT

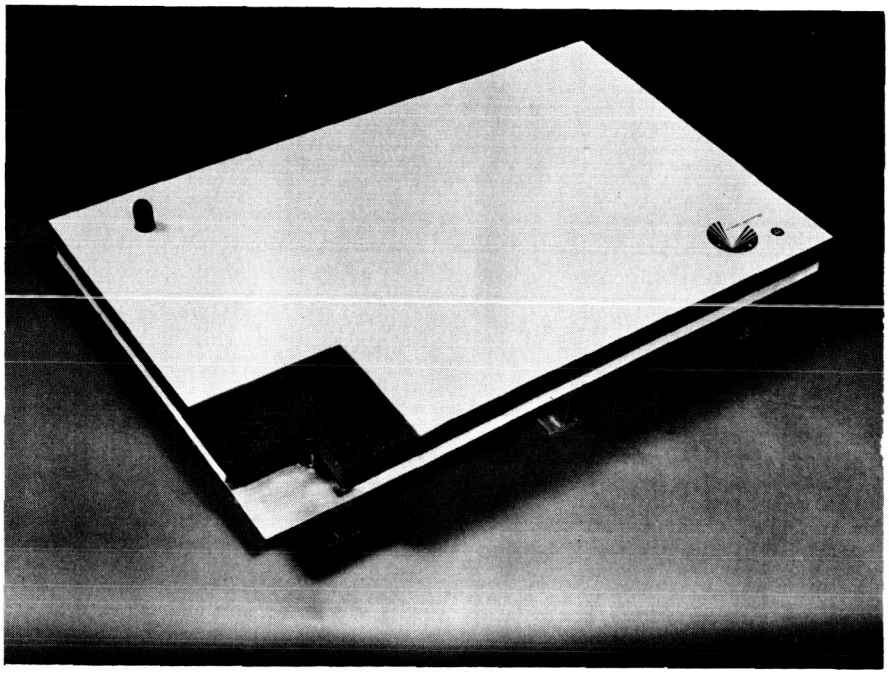

FIGURE 10. REFURBISHABLE HEAT SHIELD DEMONSTRATION PANEL

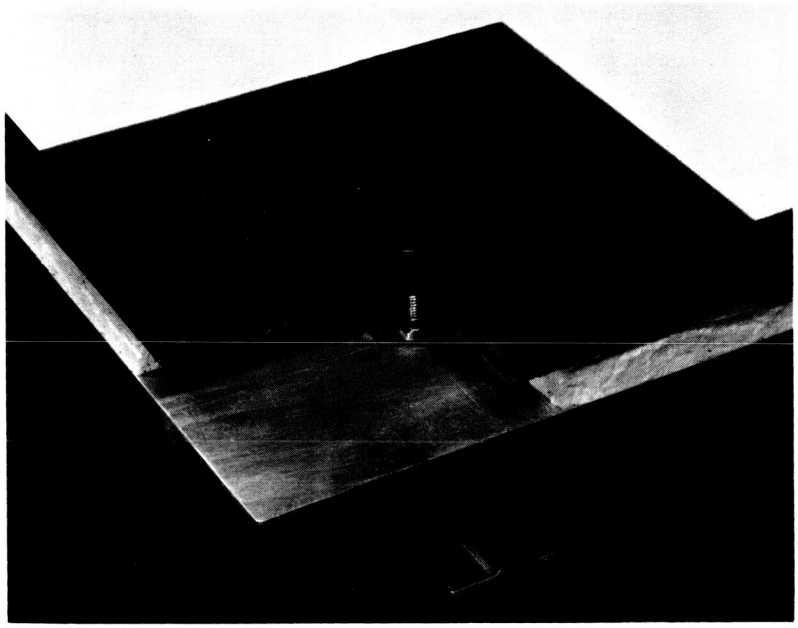

FIGURE 11. PANEL ATTACHMENT DETAIL

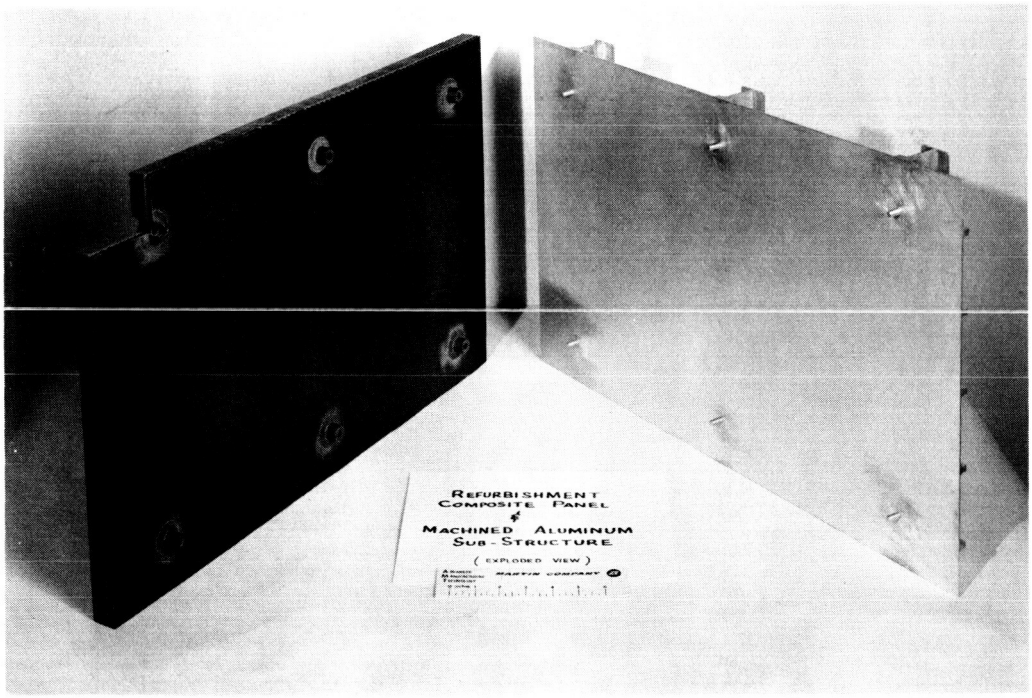

FIGURE 12. INTERIOR OF PANEL ATTACHMENT DETAIL

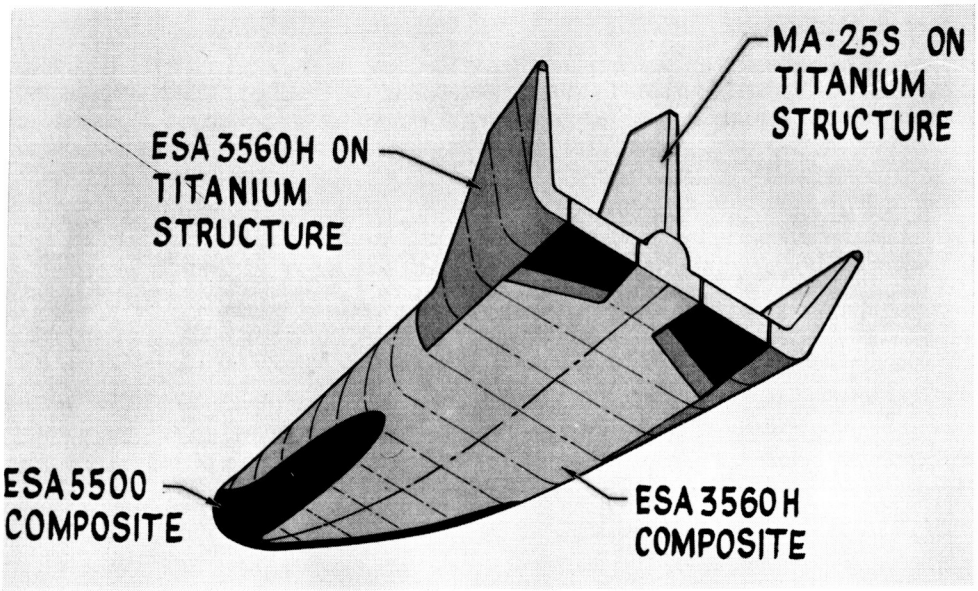

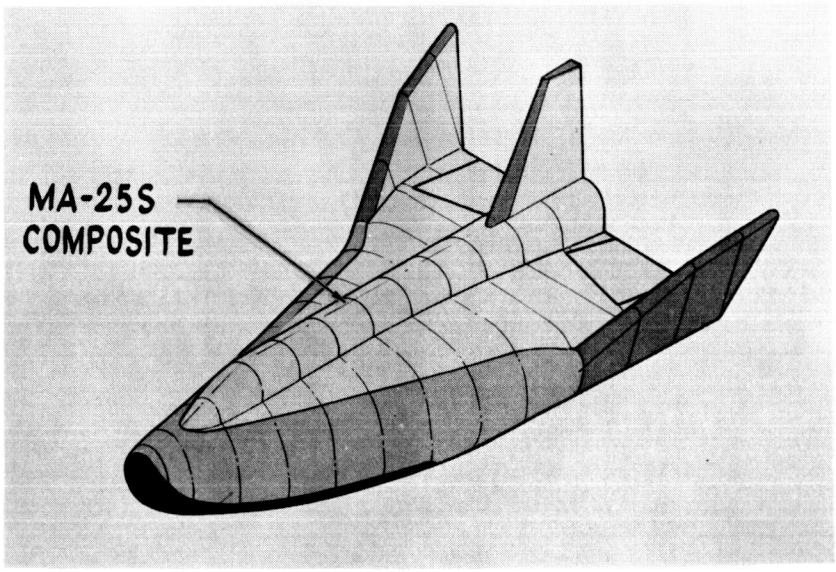

FIGURE 13. ABLATIVE MATERIAL COVERAGE ON D/3 VEHICLE

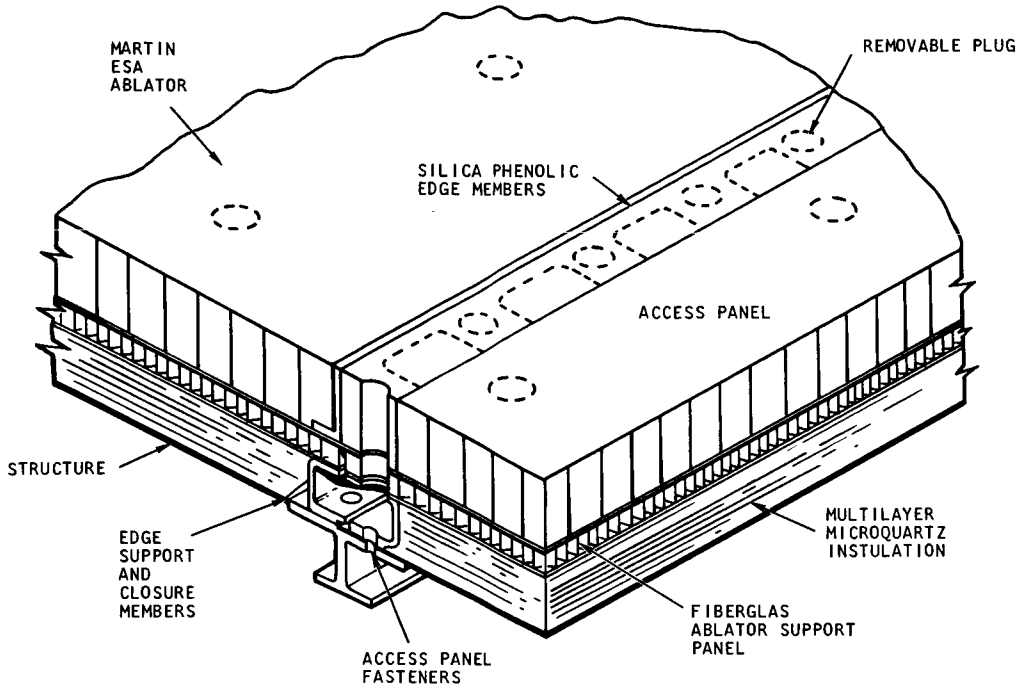

FIGURE 14. ACCESS PANEL DETAILS

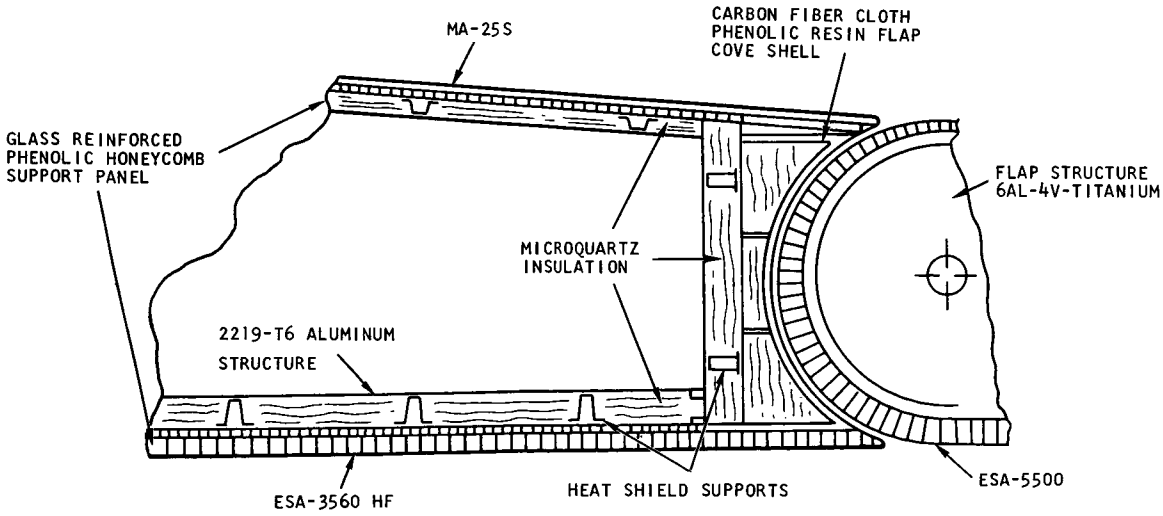

FIGURE 15. HEAT SHIELD DETAILS IN FLAP COVE AREA

TABLE 6

HEAT SHIELD DESIGN COMPUTER PROGRAM

Summary of Ablator and Insulation Thickness, Heating Ratios and Safety Factor on D/3 Vehicle (location of points shown in fig. 16).

All-ablative heat shield, turbulent flow, and microquartz insulation.

HL-10 Geometry

Element number	Area, ft^2	X/L	Y/L	Z/L	Area/L^2	Area, m^2
1	0.219E 00	0.255E-02	0.210E-01	0.297E-01	0.351E-03	0.204E-01
2	0.269E 00	0.797E-02	0.210E-01	0.246E-01	0.431E-03	0.250E-01
3	0.289E 00	0.133E-01	0.210E-01	0.206E-01	0.462E-03	0.268E-01
4	0.261E 00	0.178E-01	0.210E-01	0.153E-01	0.418E-03	0.243E-01
5	0.175E 00	0.205E-01	0.210E-01	0.105E-01	0.280E-03	0.162E-01
6	0.254E 00	0.223E-01	0.210E-01	0.531E-02	0.407E-03	0.236E-01
7	0.232E 00	0.234E-01	0.210E-01	-0.787E-03	0.371E-03	0.215E-01
8	0.306E 00	0.229E-01	0.210E-01	-0.752E-02	0.490E-03	0.284E-01
9	0.197E 00	0.212E-01	0.210E-01	-0.135E-01	0.315E-03	0.183E-01
10	0.146E 00	0.192E-01	0.210E-01	-0.172E-01	0.235E-03	0.136E-01
11	0.198E 00	0.166E-01	0.210E-01	-0.203E-01	0.317E-03	0.184E-01
12	0.199E 00	0.129E-01	0.210E-01	-0.233E-01	0.318E-03	0.184E-01
13	0.234E 00	0.846E-02	0.210E-01	-0.255E-01	0.374E-03	0.217E-01
14	0.255E 00	0.295E-02	0.210E-01	-0.269E-01	0.408E-03	0.237E-01
15	0.311E 00	0.570E-02	0.624E-01	-0.602E-01	0.498E-03	0.289E-01
16	0.408E 00	0.179E-01	0.624E-01	0.554E-01	0.653E-03	0.379E-01
17	0.426E 00	0.299E-01	0.624E-01	0.454E-01	0.682E-03	0.396E-01
18	0.367E 00	0.391E-01	0.624E-01	0.330E-01	0.587E-03	0.341E-01
19	0.258E 00	0.448E-01	0.624E-01	0.232E-01	0.413E-03	0.240E-01
20	0.388E 00	0.492E-01	0.624E-01	0.116E-01	0.621E-03	0.360E-01
21	0.343E 00	0.521E-01	0.624E-01	-0.187E-02	0.549E-03	0.318E-01
22	0.512E 00	0.527E-01	0.624E-01	-0.176E-01	0.820E-03	0.476E-01
23	0.329E 00	0.506E-01	0.624E-01	-0.326E-01	0.526E-03	0.305E-01
24	0.255E 00	0.455E-01	0.624E-01	-0.426E-01	0.409E-03	0.238E-01
25	0.316E 00	0.409E-01	0.624E-01	-0.497E-01	0.505E-03	0.294E-01
26	0.354E 00	0.321E-01	0.624E-01	-0.567E-01	0.566E-03	0.328E-01
27	0.393E 00	0.207E-01	0.624E-01	-0.640E-01	0.629E-03	0.365E-01
28	0.414E 00	0.713E-02	0.624E-01	-0.643E-01	0.663E-03	0.385E-01
29	0.539E 00	0.729E-02	0.110E 00	0.755E-01	0.862E-03	0.500E-01
30	0.605E 00	0.202E-01	0.110E 00	0.676E-01	0.968E-03	0.562E-01
31	0.705E 00	0.342E-01	0.110E 00	0.534E-01	0.127E-02	0.739E-01
32	0.520E 00	0.465E-01	0.110E 00	0.390E-01	0.847E-03	0.492E-01
33	0.386E 00	0.525E-01	0.110E 00	0.275E-01	0.618E-03	0.359E-01
34	0.642E 00	0.552E-01	0.110E 00	0.137E-01	0.102E-02	0.596E-01
35	0.545E 00	0.632E-01	0.110E 00	-0.246E-02	0.873E-03	0.507E-01
36	0.916E 00	0.666E-01	0.110E 00	-0.229E-01	0.146E-02	0.851E-01
37	0.593E 00	0.673E-01	0.110E 00	-0.439E-01	0.950E-03	0.551E-01
38	0.455E 00	0.640E-01	0.110E 00	-0.577E-01	0.728E-03	0.423E-01
39	0.511E 00	0.570E-01	0.110E 00	-0.684E-01	0.818E-03	0.475E-01
40	0.647E 00	0.451E-01	0.110E 00	-0.777E-01	0.103E-02	0.601E-01
41	0.602E 00	0.285E-01	0.110E 00	-0.803E-01	0.110E-02	0.643E-01
42	0.702E 00	0.964E-02	0.110E 00	-0.846E-01	0.112E-02	0.652E-01
43	0.439E 00	0.104E-01	0.152E 00	0.883E-01	0.703E-03	0.408E-01
44	0.206E 00	0.254E-01	0.152E 00	0.746E-01	0.633E-03	0.368E-01
45	0.435E 00	0.388E-01	0.152E 00	0.574E-01	0.697E-03	0.405E-01
46	0.294E 00	0.523E-01	0.152E 00	0.432E-01	0.471E-03	0.273E-01
47	0.229E 00	0.595E-01	0.152E 00	0.312E-01	0.356E-03	0.213E-01
48	0.397E 00	0.662E-01	0.152E 00	0.157E-01	0.635E-03	0.369E-01
49	0.236E 00	0.726E-01	0.152E 00	-0.275E-02	0.539E-03	0.312E-01
50	0.591E 00	0.775E-01	0.152E 00	-0.258E-01	0.946E-03	0.549E-01
51	0.397E 00	0.801E-01	0.152E 00	-0.527E-01	0.636E-03	0.369E-01
52	0.291E 00	0.772E-01	0.152E 00	-0.701E-01	0.466E-03	0.270E-01
53	0.302E 00	0.693E-01	0.152E 00	-0.827E-01	0.483E-03	0.280E-01
54	0.399E 00	0.549E-01	0.152E 00	-0.929E-01	0.639E-03	0.371E-01
55	0.438E 00	0.341E-01	0.152E 00	-0.980E-01	0.701E-03	0.407E-01
56	0.429E 00	0.113E-01	0.152E 00	-0.986E-01	0.687E-03	0.398E-01
57	0.785E 00	0.139E-01	0.185E 00	0.995E-01	0.125E-02	0.726E-01
58	0.765E 00	0.343E-01	0.185E 00	0.779E-01	0.122E-02	0.711E-01
59	0.366E 00	0.463E-01	0.185E 00	0.583E-01	0.586E-03	0.340E-01
60	0.392E 00	0.570E-01	0.185E 00	0.467E-01	0.628E-03	0.364E-01
61	0.331E 00	0.655E-01	0.185E 00	0.343E-01	0.530E-03	0.307E-01
62	0.569E 00	0.735E-01	0.185E 00	0.175E-01	0.910E-03	0.528E-01
63	0.477E 00	0.809E-01	0.185E 00	-0.275E-02	0.763E-03	0.442E-01
64	0.868E 00	0.864E-01	0.185E 00	-0.299E-01	0.138E-02	0.806E-01
65	0.565E 00	0.892E-01	0.185E 00	-0.592E-01	0.904E-03	0.525E-01
66	0.413E 00	0.863E-01	0.185E 00	-0.786E-01	0.661E-03	0.384E-01
67	0.405E 00	0.775E-01	0.185E 00	-0.922E-01	0.649E-03	0.377E-01
68	0.569E 00	0.613E-01	0.185E 00	-0.102E 00	0.910E-03	0.528E-01
69	0.642E 00	0.375E-01	0.185E 00	-0.107E 00	0.102E-02	0.596E-01
70	0.601E 00	0.123E-01	0.185E 00	-0.107E 00	0.961E-03	0.558E-01
71	0.117E 01	0.175E-01	0.227E 00	0.108E 00	0.188E-02	0.109E 00
72	0.112E 01	0.419E-01	0.227E 00	0.797E-01	0.180E-02	0.104E 00
73	0.277E 00	0.529E-01	0.227E 00	0.593E-01	0.444E-03	0.258E-01
74	0.500E 00	0.628E-01	0.227E 00	0.509E-01	0.800E-03	0.464E-01
75	0.438E 00	0.728E-01	0.227E 00	0.380E-01	0.702E-03	0.407E-01
76	0.778E 00	0.827E-01	0.227E 00	0.195E-01	0.124E-02	0.723E-01
77	0.647E 00	0.917E-01	0.227E 00	-0.314E-02	0.103E-02	0.601E-01
78	0.120E 01	0.979E-01	0.227E 00	-0.340E-01	0.192E-02	0.112E 00
79	0.724E 00	0.100E 00	0.227E 00	-0.662E-01	0.112E-02	0.654E-01
80	0.594E 00	0.969E-01	0.227E 00	-0.874E-01	0.950E-03	0.551E-01
81	0.523E 00	0.858E-01	0.227E 00	-0.102E 00	0.837E-03	0.486E-01
82	0.775E 00	0.679E-01	0.227E 00	-0.112E 00	0.124E-02	0.720E-01
83	0.827E 00	0.409E-01	0.227E 00	-0.117E 00	0.132E-02	0.763E-01
84	0.764E 00	0.132E-01	0.227E 00	-0.117E 00	0.122E-02	0.710E-01
85	0.248E 01	0.196E-01	0.291E 00	0.111E 00	0.396E-02	0.230E 00
86	0.152E 01	0.439E-01	0.291E 00	0.830E-01	0.259E-02	0.150E 00
87	0.377E 00	0.564E-01	0.291E 00	0.657E-01	0.140E-02	0.815E-01
88	0.120E 01	0.715E-01	0.291E 00	0.571E-01	0.160E-02	0.929E-01
89	0.944E 00	0.842E-01	0.291E 00	0.439E-01	0.151E-02	0.877E-01
90	0.171E 01	0.973E-01	0.291E 00	0.227E-01	0.275E-02	0.159E 00
91	0.139E 01	0.109E 00	0.291E 00	-0.393E-02	0.222E-02	0.128E 00
92	0.260E 01	0.116E 00	0.291E 00	-0.403E-01	0.416E-02	0.241E 00
93	0.148E 01	0.118E 00	0.291E 00	-0.791E-01	0.238E-02	0.138E 00
94	0.119E 01	0.112E 00	0.291E 00	-0.101E 00	0.189E-02	0.110E 00
95	0.106E 01	0.988E-01	0.291E 00	-0.116E 00	0.170E-02	0.982E-01
96	0.161E 01	0.751E-01	0.291E 00	-0.124E 00	0.259E-02	0.150E 00
97	0.152E 01	0.444E-01	0.291E 00	-0.125E 00	0.259E-02	0.150E 00
98	0.151E 01	0.144E-01	0.291E 00	-0.125E 00	0.241E-02	0.140E 00
99	0.243E 01	0.194E-01	0.375E 00	0.112E 00	0.389E-02	0.226E 00
100	0.124E 01	0.424E-01	0.375E 00	0.988E-01	0.198E-02	0.115E 00
101	0.221E 01	0.655E-01	0.375E 00	0.700E-01	0.354E-02	0.205E 00
102	0.131E 01	0.944E-01	0.375E 00	0.544E-01	0.210E-02	0.122E 00
103	0.112E 01	0.109E 00	0.375E 00	0.377E-01	0.180E-02	0.104E 00
104	0.180E 01	0.123E 00	0.375E 00	0.141E-01	0.289E-02	0.168E 00
105	0.234E 01	0.134E 00	0.375E 00	-0.220E-01	0.375E-02	0.218E 00
106	0.254E 01	0.140E 00	0.375E 00	-0.662E-01	0.407E-02	0.236E 00
107	0.191E 01	0.132E 00	0.375E 00	-0.102E 00	0.306E-02	0.177E 00
108	0.950E 00	0.117E 00	0.375E 00	-0.121E 00	0.152E-02	0.882E-01
109	0.772E 00	0.103E 00	0.375E 00	-0.128E 00	0.123E-02	0.717E-01
110	0.167E 01	0.809E-01	0.375E 00	-0.131E 00	0.268E-02	0.155E 00
111	0.168E 01	0.489E-01	0.375E 00	-0.131E 00	0.269E-02	0.156E 00
112	0.172E 01	0.164E-01	0.375E 00	-0.131E 00	0.276E-02	0.160E 00
113	0.232E 01	0.192E-01	0.458E 00	0.113E 00	0.372E-02	0.216E 00
114	0.130E 01	0.423E-01	0.458E 00	0.903E-01	0.208E-02	0.121E 00
115	0.322E 01	0.756E-01	0.458E 00	0.692E-01	0.515E-02	0.299E 00
116	0.163E 01	0.117E 00	0.458E 00	0.504E-01	0.261E-02	0.152E 00

TABLE 6.--Continued

HEAT SHIELD DESIGN COMPUTER PROGRAM

Element number	Area, ft^2	X/L	Y/L	Z/L	Area/L^2	Area, m^2
117	0.127E 01	0.136E 00	0.458E 00	0.309E-01	0.204E-02	0.118E 00
118	0.160E 01	0.149E 00	0.458E 00	0.728E-02	0.256E-02	0.149E 00
119	0.313E 01	0.160E 00	0.458E 00	-0.351E-01	0.501E-02	0.291E 00
120	0.183E 01	0.165E 00	0.458E 00	-0.808E-01	0.293E-02	0.170E 00
121	0.199E 01	0.152E 00	0.458E 00	-0.111E 00	0.318E-02	0.184E 00
122	0.157E 01	0.124E 00	0.458E 00	-0.127E 00	0.252E-02	0.146E 00
123	0.522E 00	0.104E 00	0.458E 00	-0.130E 00	0.835E-03	0.485E-01
124	0.160E 01	0.843E-01	0.458E 00	-0.130E 00	0.257E-02	0.149E 00
125	0.168E 01	0.526E-01	0.458E 00	-0.130E 00	0.270E-02	0.156E 00
126	0.189E 01	0.182E-01	0.458E 00	-0.130E 00	0.302E-02	0.175E 00
127	0.232E 01	0.192E-01	0.541E 00	0.113E 00	0.372E-02	0.216E 00
128	0.142E 01	0.427E-01	0.541E 00	0.892E-01	0.227E-02	0.132E 00
129	0.344E 01	0.793E-01	0.541E 00	0.696E-01	0.550E-02	0.319E 00
130	0.181E 01	0.127E 00	0.541E 00	0.549E-01	0.290E-02	0.168E 00
131	0.143E 01	0.151E 00	0.541E 00	0.371E-01	0.230E-02	0.133E 00
132	0.155E 01	0.168E 00	0.541E 00	0.150E-01	0.248E-02	0.144E 00
133	0.309E 01	0.182E 00	0.541E 00	-0.252E-01	0.495E-02	0.287E 00
134	0.147E 01	0.189E 00	0.541E 00	-0.668E-01	0.236E-02	0.137E 00
135	0.217E 01	0.177E 00	0.541E 00	-0.978E-01	0.348E-02	0.202E 00
136	0.228E 01	0.144E 00	0.541E 00	-0.118E 00	0.364E-02	0.211E 00
137	0.846E 00	0.114E 00	0.541E 00	-0.121E 00	0.135E-02	0.786E-01
138	0.168E 01	0.908E-01	0.541E 00	-0.121E 00	0.269E-02	0.156E 00
139	0.184E 01	0.571E-01	0.541E 00	-0.121E 00	0.295E-02	0.171E 00
140	0.207E 01	0.197E-01	0.541E 00	-0.121E 00	0.331E-02	0.192E 00
141	0.235E 01	0.192E-01	0.625E 00	0.113E 00	0.376E-02	0.218E 00
142	0.169E 01	0.433E-01	0.625E 00	0.869E-01	0.271E-02	0.157E 00
143	0.349E 01	0.811E-01	0.625E 00	0.680E-01	0.559E-02	0.325E 00
144	0.211E 01	0.133E 00	0.625E 00	0.583E-01	0.338E-02	0.196E 00
145	0.176E 01	0.165E 00	0.625E 00	0.430E-01	0.281E-02	0.163E 00
146	0.153E 01	0.188E 00	0.625E 00	0.226E-01	0.244E-02	0.142E 00
147	0.307E 01	0.205E 00	0.625E 00	-0.155E-01	0.491E-02	0.285E 00
148	0.124E 01	0.213E 00	0.625E 00	-0.538E-01	0.198E-02	0.115E 00
149	0.239E 01	0.200E 00	0.625E 00	-0.835E-01	0.382E-02	0.222E 00
150	0.232E 01	0.166E 00	0.625E 00	-0.104E 00	0.371E-02	0.215E 00
151	0.136E 01	0.131E 00	0.625E 00	-0.106E 00	0.219E-02	0.127E 00
152	0.189E 01	0.101E 00	0.625E 00	-0.106E 00	0.303E-02	0.176E 00
153	0.209E 01	0.640E-01	0.625E 00	-0.106E 00	0.335E-02	0.194E 00
154	0.238E 01	0.222E-01	0.625E 00	-0.106E 00	0.380E-02	0.221E 00
155	0.232E 01	0.192E-01	0.708E 00	0.113E 00	0.372E-02	0.216E 00
156	0.199E 01	0.439E-01	0.708E 00	0.839E-01	0.318E-02	0.184E 00
157	0.324E 01	0.806E-01	0.708E 00	0.645E-01	0.519E-02	0.301E 00
158	0.249E 01	0.135E 00	0.708E 00	0.595E-01	0.398E-02	0.231E 00
159	0.224E 01	0.178E 00	0.708E 00	0.478E-01	0.359E-02	0.208E 00
160	0.153E 01	0.209E 00	0.708E 00	0.307E-01	0.246E-02	0.142E 00
161	0.310E 01	0.229E 00	0.708E 00	-0.511E-02	0.496E-02	0.288E 00
162	0.102E 01	0.238E 00	0.708E 00	-0.408E-01	0.164E-02	0.956E-01
163	0.188E 01	0.227E 00	0.708E 00	-0.651E-01	0.300E-02	0.174E 00
164	0.220E 01	0.197E 00	0.708E 00	-0.842E-01	0.352E-02	0.204E 00
165	0.227E 01	0.155E 00	0.708E 00	-0.883E-01	0.364E-02	0.211E 00
166	0.210E 01	0.114E 00	0.708E 00	-0.883E-01	0.336E-02	0.195E 00
167	0.236E 01	0.729E-01	0.708E 00	-0.883E-01	0.378E-02	0.219E 00
168	0.271E 01	0.253E-01	0.708E 00	-0.883E-01	0.433E-02	0.251E 00
169	0.132E 01	0.192E-01	0.773E 00	0.113E 00	0.211E-02	0.122E 00
170	0.128E 01	0.447E-01	0.773E 00	0.814E-01	0.205E-02	0.119E 00
171	0.162E 01	0.784E-01	0.773E 00	0.606E-01	0.260E-02	0.150E 00
172	0.163E 01	0.133E 00	0.773E 00	0.582E-01	0.261E-02	0.151E 00
173	0.156E 01	0.186E 00	0.773E 00	0.504E-01	0.250E-02	0.145E 00
174	0.915E 00	0.225E 00	0.773E 00	0.371E-01	0.146E-02	0.850E-01
175	0.170E 01	0.247E 00	0.773E 00	0.236E-02	0.273E-02	0.158E 00
176	0.521E 00	0.254E 00	0.773E 00	-0.328E-01	0.835E-03	0.484E-01
177	0.795E 00	0.244E 00	0.773E 00	-0.524E-01	0.127E-02	0.739E-01
178	0.815E 00	0.223E 00	0.773E 00	-0.669E-01	0.130E-02	0.758E-01
179	0.191E 01	0.179E 00	0.773E 00	-0.702E-01	0.306E-02	0.178E 00
180	0.135E 01	0.127E 00	0.773E 00	-0.702E-01	0.216E-02	0.125E 00
181	0.153E 01	0.812E-01	0.773E 00	-0.702E-01	0.245E-02	0.142E 00
182	0.176E 01	0.283E-01	0.773E 00	-0.704E-01	0.282E-02	0.163E 00
183	0.137E 00	0.196E-02	0.815E 00	0.142E 00	0.219E-03	0.127E-01
184	0.459E 00	0.462E-02	0.815E 00	0.131E 00	0.735E-03	0.427E-01
185	0.854E 00	0.219E-01	0.815E 00	0.111E 00	0.136E-02	0.794E-01
186	0.107E 01	0.454E-01	0.815E 00	0.794E-01	0.171E-02	0.994E-01
187	0.120E 01	0.791E-01	0.815E 00	0.565E-01	0.193E-02	0.112E 00
188	0.122E 01	0.133E 00	0.815E 00	0.557E-01	0.195E-02	0.113E 00
189	0.134E 01	0.189E 00	0.815E 00	0.517E-01	0.215E-02	0.125E 00
190	0.743E 00	0.234E 00	0.815E 00	0.439E-01	0.119E-02	0.691E-01
191	0.390E 00	0.253E 00	0.815E 00	0.467E-01	0.624E-03	0.362E-01
192	0.146E 01	0.266E 00	0.815E 00	0.425E-01	0.233E-02	0.135E 00
193	0.134E 01	0.271E 00	0.815E 00	0.600E-02	0.215E-02	0.125E 00
194	0.591E 00	0.262E 00	0.815E 00	-0.304E-01	0.946E-03	0.549E-01
195	0.497E 00	0.249E 00	0.815E 00	-0.495E-01	0.795E-03	0.461E-01
196	0.372E 00	0.233E 00	0.815E 00	-0.579E-01	0.596E-03	0.346E-01
197	0.152E 01	0.191E 00	0.815E 00	-0.590E-01	0.244E-02	0.141E 00
198	0.107E 01	0.134E 00	0.815E 00	-0.590E-01	0.172E-02	0.999E-01
199	0.117E 01	0.848E-01	0.815E 00	-0.590E-01	0.187E-02	0.108E 00
200	0.134E 01	0.295E-01	0.815E 00	-0.592E-01	0.214E-02	0.124E 00
201	0.441E 00	0.196E-02	0.875E 00	0.240E 00	0.706E-03	0.410E-01
202	0.642E 01	0.649E-02	0.875E 00	0.179E 00	0.102E-01	0.596E 00
203	0.177E 01	0.238E-01	0.875E 00	0.110E 00	0.284E-02	0.165E 00
204	0.293E 01	0.464E-01	0.875E 00	0.755E-01	0.468E-02	0.272E 00
205	0.293E 01	0.820E-01	0.875E 00	0.489E-01	0.469E-02	0.272E 00
206	0.269E 01	0.135E 00	0.875E 00	0.489E-01	0.431E-02	0.250E 00
207	0.331E 01	0.192E 00	0.875E 00	0.481E-01	0.530E-02	0.308E 00
208	0.186E 01	0.241E 00	0.875E 00	0.464E-01	0.297E-02	0.172E 00
209	0.398E 01	0.275E 00	0.875E 00	0.793E-01	0.637E-02	0.369E 00
210	0.152E 01	0.301E 00	0.875E 00	0.111E 00	0.243E-02	0.141E 00
211	0.218E 01	0.307E 00	0.875E 00	0.891E-01	0.349E-02	0.202E 00
212	0.310E 01	0.296E 00	0.875E 00	0.410E-01	0.496E-02	0.288E 00
213	0.112E 01	0.287E 00	0.875E 00	0.255E-02	0.179E-02	0.104E 00
214	0.199E 01	0.274E 00	0.875E 00	-0.229E-01	0.318E-02	0.184E 00
215	0.104E 01	0.254E 00	0.875E 00	-0.414E-01	0.167E-02	0.973E-01
216	0.107E 01	0.235E 00	0.875E 00	-0.450E-01	0.172E-02	0.998E-01
217	0.348E 01	0.193E 00	0.875E 00	-0.454E-01	0.557E-02	0.323E 00
218	0.541E 01	0.111E 00	0.875E 00	-0.454E-01	0.865E-02	0.502E 00
219	0.330E 01	0.305E-01	0.875E 00	-0.454E-01	0.528E-02	0.306E 00
220	0.377E 00	0.364E-02	0.958E 00	0.320E 00	0.604E-03	0.350E-01
221	0.105E 02	0.102E-01	0.958E 00	0.218E 00	0.169E-01	0.982E 00
222	0.151E 01	0.258E-01	0.958E 00	0.109E 00	0.242E-02	0.140E 00
223	0.341E 01	0.477E-01	0.958E 00	0.707E-01	0.545E-02	0.317E 00
224	0.278E 01	0.835E-01	0.958E 00	0.392E-01	0.445E-02	0.258E 00
225	0.267E 01	0.135E 00	0.958E 00	0.392E-01	0.427E-02	0.248E 00
226	0.328E 01	0.192E 00	0.958E 00	0.392E-01	0.526E-02	0.305E 00
227	0.217E 01	0.245E 00	0.958E 00	0.392E-01	0.348E-02	0.202E 00
228	0.723E 01	0.295E 00	0.958E 00	0.102E 00	0.115E-01	0.672E 00
229	0.932E 00	0.332E 00	0.958E 00	0.163E 00	0.149E-02	0.866E-01
230	0.226E 01	0.336E 00	0.958E 00	0.140E 00	0.362E-02	0.210E 00
231	0.440E 01	0.321E 00	0.958E 00	0.788E-01	0.705E-02	0.409E 00
232	0.147E 01	0.300E 00	0.958E 00	0.246E-01	0.235E-02	0.137E 00
233	0.231E 01	0.290E 00	0.958E 00	-0.611E-02	0.370E-02	0.214E 00
234	0.148E 01	0.261E 00	0.958E 00	-0.223E-01	0.237E-02	0.137E 00
235	0.127E 01	0.236E 00	0.958E 00	-0.234E-01	0.203E-02	0.118E 00
236	0.339E 01	0.192E 00	0.958E 00	-0.234E-01	0.542E-02	0.315E 00
237	0.530E 01	0.112E 00	0.958E 00	-0.234E-01	0.849E-02	0.492E 00
238	0.339E 01	0.314E-01	0.958E 00	-0.234E-01	0.542E-02	0.315E 00

TABLE 6.--Continued

HEAT SHIELD DESIGN COMPUTER PROGRAM

Heat Shield Output in English Units

Element number	Trajectory[1]	$FQ(Q_L/Q_S)$[2]	FQ	Insulation[3] thickness, inch	Ablator thickness, inch	Weight, pound
1	1	0.2224E 00	0.1150E 01	0.1730E 01	0.1404E 01	0.1167E 01
2	1	0.3893E 00	0.1150E 01	0.1999E 01	0.1723E 01	0.1667E 01
3	1	0.4449E 00	0.1150E 01	0.1939E 01	0.1795E 01	0.1848E 01
4	1	0.4904E 00	0.1150E 01	0.1968E 01	0.1847E 01	0.1711E 01
5	1	0.5117E 00	0.1150E 01	0.1981E 01	0.1871E 01	0.1159E 01
6	1	0.5339E 00	0.1150E 01	0.1994E 01	0.1894E 01	0.1698E 01
7	1	0.5617E 00	0.1150E 01	0.2009E 01	0.1921E 01	0.1560E 01
8	1	0.6118E 00	0.1150E 01	0.2035E 01	0.1967E 01	0.2111E 01
9	1A	0.6674E 00	0.1150E 01	0.2061E 01	0.2014E 01	0.2222E 01
10	1A	0.7509E 00	0.1150E 01	0.2097E 01	0.2077E 01	0.1634E 01
11	1A	0.8343E 00	0.1150E 01	0.2128E 01	0.2134E 01	0.2236E 01
12	1A	0.9455E 00	0.1150E 01	0.2166E 01	0.2202E 01	0.2242E 01
13	1A	0.1023E 01	0.1150E 01	0.2182E 01	0.2244E 01	0.2692E 01
14	1A	0.1040E 01	0.1150E 01	0.2187E 01	0.2253E 01	0.2960E 01
15	1	0.7859E-01	0.1250E 01	0.1416E 01	0.7941E 00	0.1148E 01
16	1	0.8899E-01	0.1150E 01	0.1454E 01	0.8881E 00	0.1584E 01
17	1	0.1390E 00	0.1150E 01	0.1588E 01	0.1124E 01	0.1952E 01
18	1	0.2558E 00	0.1150E 01	0.1772E 01	0.1487E 01	0.2029E 01
19	1	0.3281E 00	0.1150E 01	0.1847E 01	0.1621E 01	0.1528E 01
20	1	0.3949E 00	0.1150E 01	0.1903E 01	0.1731E 01	0.2410E 01
21	1	0.4527E 00	0.1150E 01	0.1944E 01	0.1805E 01	0.2202E 01
22	1	0.4905E 00	0.1150E 01	0.1968E 01	0.1848E 01	0.3354E 01
23	1	0.5005E 00	0.1150E 01	0.1974E 01	0.1859E 01	0.2163E 01
24	1	0.5117E 00	0.1150E 01	0.1981E 01	0.1871E 01	0.1693E 01
25	1	0.5728E 00	0.1150E 01	0.2015E 01	0.1932E 01	0.2148E 01
26	1	0.6007E 00	0.1150E 01	0.2029E 01	0.1957E 01	0.2429E 01
27	1	0.5283E 00	0.1150E 01	0.1991E 01	0.1888E 01	0.2621E 01
28	1	0.5005E 00	0.1150E 01	0.1974E 01	0.1859E 01	0.2728E 01
29	1	0.4232E-01	0.1250E 01	0.1230E 01	0.4150E 00	0.1464E 01
30	1	0.6045E-01	0.1250E 01	0.1337E 01	0.6276E 00	0.1981E 01
31	1	0.8464E-01	0.1250E 01	0.1439E 01	0.8282E 00	0.3022E 01
32	1	0.1001E 00	0.1150E 01	0.1499E 01	0.9294E 00	0.2151E 01
33	1	0.1168E 00	0.1150E 01	0.1536E 01	0.1020E 01	0.1663E 01
34	1	0.1390E 00	0.1150E 01	0.1588E 01	0.1124E 01	0.2938E 01
35	1	0.1557E 00	0.1150E 01	0.1622E 01	0.1191E 01	0.2593E 01
36	1	0.2836E 00	0.1150E 01	0.1803E 01	0.1549E 01	0.5212E 01
37	1	0.4060E 00	0.1150E 01	0.1911E 01	0.1746E 01	0.3711E 01
38	1	0.4894E 00	0.1150E 01	0.1968E 01	0.1847E 01	0.2978E 01
39	1	0.5395E 00	0.1150E 01	0.1997E 01	0.1899E 01	0.3422E 01
40	1	0.5117E 00	0.1150E 01	0.1981E 01	0.1871E 01	0.4278E 01
41	1	0.4449E 00	0.1150E 01	0.1939E 01	0.1795E 01	0.4426E 01
42	1	0.3837E 00	0.1150E 01	0.1894E 01	0.1716E 01	0.4325E 01
43	1	0.2418E-01	0.1250E 01	0.1061E 01	0.1704E 00	0.8228E 00
44	1	0.3627E-01	0.1250E 01	0.1193E 01	0.3231E 00	0.9810E 00
45	1	0.5441E-01	0.1250E 01	0.1305E 01	0.5648E 00	0.1356E 01
46	1	0.6650E-01	0.1250E 01	0.1366E 01	0.6945E 00	0.1008E 01
47	1	0.8464E-01	0.1250E 01	0.1439E 01	0.8282E 00	0.8715E 00
48	1	0.1001E 00	0.1150E 01	0.1499E 01	0.9284E 00	0.1613E 01
49	1	0.1223E 00	0.1150E 01	0.1550E 01	0.1048E 01	0.1473E 01
50	1	0.1501E 00	0.1150E 01	0.1611E 01	0.1170E 01	0.2776E 01
51	1	0.3448E 00	0.1150E 01	0.1842E 01	0.1658E 01	0.2384E 01
52	1	0.5005E 00	0.1150E 01	0.1974E 01	0.1859E 01	0.1916E 01
53	1	0.6173E 00	0.1150E 01	0.2038E 01	0.1972E 01	0.2087E 01
54	1	0.5283E 00	0.1150E 01	0.1991E 01	0.1888E 01	0.2661E 01
55	1	0.3949E 00	0.1150E 01	0.1903E 01	0.1731E 01	0.2719E 01
56	1	0.3226E 00	0.1150E 01	0.1842E 01	0.1622E 01	0.2530E 01
57	1	0.1813E-01	0.1250E 01	0.9748E 00	0.6018E-01	0.1317E 01
58	1	0.4836E-01	0.1250E 01	0.1270E 01	0.4946E 00	0.2239E 01
59	1	0.6045E-01	0.1250E 01	0.1337E 01	0.6276E 00	0.1200E 01
60	1	0.7254E-01	0.1250E 01	0.1392E 01	0.7363E 00	0.1398E 01
61	1	0.8464E-01	0.1250E 01	0.1439E 01	0.8282E 00	0.1258E 01
62	1	0.1056E 00	0.1150E 01	0.1506E 01	0.9606E 00	0.2360E 01

Heat Shield Output in Metric Units

Element number	Trajectory[1]	$FQ(Q_L/Q_S)$[2]	FQ	Insulation thickness, cm	Ablator thickness, cm	Weight, kg
1	1	0.2226E 00	0.1150E 01	0.4404E 01	0.3575E 01	0.5297E 00
2	1	0.3895E 00	0.1150E 01	0.4834E 01	0.4388E 01	0.7564E 00
3	1	0.4452E 00	0.1150E 01	0.4936E 01	0.4571E 01	0.8382E 00
4	1	0.4897E 00	0.1150E 01	0.5009E 01	0.4701E 01	0.7761E 00
5	1	0.5120E 00	0.1150E 01	0.5043E 01	0.4762E 01	0.5257E 00
6	1	0.5343E 00	0.1150E 01	0.5076E 01	0.4821E 01	0.7706E 00
7	1	0.5621E 00	0.1150E 01	0.5115E 01	0.4891E 01	0.7116E 00
8	1	0.6122E 00	0.1150E 01	0.5180E 01	0.5008E 01	0.9576E 00
9	1A	0.6678E 00	0.1150E 01	0.5247E 01	0.5127E 01	0.1008E 01
10	1A	0.7513E 00	0.1150E 01	0.5337E 01	0.5289E 01	0.7503E 00
11	1A	0.8348E 00	0.1150E 01	0.5418E 01	0.5433E 01	0.1013E 01
12	1A	0.9461E 00	0.1150E 01	0.5514E 01	0.5605E 01	0.1016E 01
13	1A	0.1024E 01	0.1150E 01	0.5555E 01	0.5713E 01	0.1221E 01
14	1A	0.1040E 01	0.1150E 01	0.5567E 01	0.5736E 01	0.1343E 01
15	1	0.7864E-01	0.1250E 01	0.3606E 01	0.1995E 01	0.5209E 00
16	1	0.8905E-01	0.1150E 01	0.3701E 01	0.2184E 01	0.7187E 00
17	1	0.1391E 00	0.1150E 01	0.4044E 01	0.2861E 01	0.8858E 00
18	1	0.2560E 00	0.1150E 01	0.4511E 01	0.3767E 01	0.9205E 00
19	1	0.3283E 00	0.1150E 01	0.4702E 01	0.4133E 01	0.6935E 00
20	1	0.3951E 00	0.1150E 01	0.4844E 01	0.4407E 01	0.1093E 01
21	1	0.4530E 00	0.1150E 01	0.4949E 01	0.4595E 01	0.9994E 00
22	1	0.4908E 00	0.1150E 01	0.5011E 01	0.4705E 01	0.1521E 01
23	1	0.5009E 00	0.1150E 01	0.5026E 01	0.4732E 01	0.9814E 00
24	1	0.5120E 00	0.1150E 01	0.5043E 01	0.4762E 01	0.7683E 00
25	1	0.5732E 00	0.1150E 01	0.5130E 01	0.4917E 01	0.9744E 00
26	1	0.6010E 00	0.1150E 01	0.5166E 01	0.4982E 01	0.1101E 01
27	1	0.5287E 00	0.1150E 01	0.5068E 01	0.4806E 01	0.1189E 01
28	1	0.5009E 00	0.1150E 01	0.5026E 01	0.4732E 01	0.1237E 01
29	1	0.4234E-01	0.1250E 01	0.3131E 01	0.1036E 01	0.6642E 00
30	1	0.6049E-01	0.1250E 01	0.3405E 01	0.1597E 01	0.8990E 00
31	1	0.8469E-01	0.1250E 01	0.3663E 01	0.2108E 01	0.1371E 01
32	1	0.1001E 00	0.1150E 01	0.3792E 01	0.2363E 01	0.9759E 00
33	1	0.1168E 00	0.1150E 01	0.3910E 01	0.2597E 01	0.7546E 00
34	1	0.1391E 00	0.1150E 01	0.4044E 01	0.2861E 01	0.1332E 01
35	1	0.1558E 00	0.1150E 01	0.4131E 01	0.3033E 01	0.1176E 01
36	1	0.2838E 00	0.1150E 01	0.4591E 01	0.3943E 01	0.2364E 01
37	1	0.4062E 00	0.1150E 01	0.4866E 01	0.4445E 01	0.1683E 01
38	1	0.4897E 00	0.1150E 01	0.5009E 01	0.4701E 01	0.1351E 01
39	1	0.5398E 00	0.1150E 01	0.5084E 01	0.4835E 01	0.1552E 01
40	1	0.5120E 00	0.1150E 01	0.5043E 01	0.4762E 01	0.1940E 01
41	1	0.4452E 00	0.1150E 01	0.4936E 01	0.4571E 01	0.2007E 01
42	1	0.3840E 00	0.1150E 01	0.4823E 01	0.4368E 01	0.1962E 01
43	1	0.2419E-01	0.1250E 01	0.2702E 01	0.4337E 00	0.3732E 00
44	1	0.3629E-01	0.1250E 01	0.3013E 01	0.8225E 00	0.4451E 00
45	1	0.5444E-01	0.1250E 01	0.3324E 01	0.1437E 01	0.6154E 00
46	1	0.6654E-01	0.1250E 01	0.3478E 01	0.1742E 01	0.4573E 00
47	1	0.8469E-01	0.1250E 01	0.3663E 01	0.2108E 01	0.3953E 00
48	1	0.1001E 00	0.1150E 01	0.3792E 01	0.2363E 01	0.7320E 00
49	1	0.1224E 00	0.1150E 01	0.3946E 01	0.2667E 01	0.6683E 00
50	1	0.1502E 00	0.1150E 01	0.4103E 01	0.2978E 01	0.1259E 01
51	1	0.3450E 00	0.1150E 01	0.4740E 01	0.4221E 01	0.1081E 01
52	1	0.5009E 00	0.1150E 01	0.5026E 01	0.4732E 01	0.8694E 00
53	1	0.6177E 00	0.1150E 01	0.5187E 01	0.5020E 01	0.9468E 00
54	1	0.5287E 00	0.1150E 01	0.5068E 01	0.4806E 01	0.1207E 01
55	1	0.3951E 00	0.1150E 01	0.4844E 01	0.4407E 01	0.1233E 01
56	1	0.3228E 00	0.1150E 01	0.4699E 01	0.4130E 01	0.1147E 01
57	1	0.1814E-01	0.1250E 01	0.2481E 01	0.1735E 00	0.5978E 00
58	1	0.4839E-01	0.1250E 01	0.3233E 01	0.1259E 01	0.1016E 01
59	1	0.6049E-01	0.1250E 01	0.3405E 01	0.1597E 01	0.5444E 00
60	1	0.7259E-01	0.1250E 01	0.3545E 01	0.1874E 01	0.6342E 00
61	1	0.8469E-01	0.1250E 01	0.3663E 01	0.2108E 01	0.5710E 00
62	1	0.1057E 00	0.1150E 01	0.3833E 01	0.2445E 01	0.1070E 01

TABLE 6.--Continued

HEAT SHIELD DESIGN COMPUTER PROGRAM

Element number	Trajectory[1]	$FQ(Q_L/Q_S)$[2]	FQ	Insulation thickness, inch[3]	Ablator thickness, inch	Weight, pound
63	1	0.1112E 00	0.1150E 01	0.1521E 01	0.9912E 00	0.2017E 01
64	1	0.1668E 00	0.1150E 01	0.1543E 01	0.1232E 01	0.4220E 01
65	1	0.4727E 00	0.1150E 01	0.1957E 01	0.1828E 01	0.3666E 01
66	1	0.6118E 00	0.1150E 01	0.2035E 01	0.1967E 01	0.2849E 01
67	1	0.6674E 00	0.1150E 01	0.2061E 01	0.2014E 01	0.4570E 01
68	1	0.4727E 00	0.1150E 01	0.1957E 01	0.1828E 01	0.3693E 01
69	1	0.3337E 00	0.1150E 01	0.1852E 01	0.1640E 01	0.3816E 01
70	1	0.2781E 00	0.1150E 01	0.1797E 01	0.1537E 01	0.3400E 01
71	1B	0.7254E-02	0.1500E 01	0.6936E 00	0.1521E-01	0.1582E 01
72	1	0.3527E-01	0.1250E 01	0.1183E 01	0.3231E 00	0.2797E 01
73	1	0.5441E-01	0.1250E 01	0.1305E 01	0.5649E 00	0.8637E 00
74	1	0.6287E-01	0.1250E 01	0.1349E 01	0.6510E 00	0.1668E 01
75	1	0.7254E-01	0.1250E 01	0.1392E 01	0.7353E 00	0.1561E 01
76	1	0.8464E-01	0.1250E 01	0.1439E 01	0.8282E 00	0.2959E 01
77	1	0.8899E-01	0.1150E 01	0.1434E 01	0.8581E 00	0.2510E 01
78	4	0.5562E 00	0.1150E 01	0.1643E 01	0.1232E 01	0.6031E 01
79	1	0.5951E 00	0.1150E 01	0.2025E 01	0.1952E 01	0.4823E 01
80	1A	0.7063E 00	0.1150E 01	0.2078E 01	0.2044E 01	0.6690E 01
81	1A	0.6585E 00	0.1150E 01	0.2057E 01	0.2007E 01	0.5893E 01
82	1	0.3782E 00	0.1150E 01	0.1890E 01	0.1728E 01	0.4761E 01
83	1	0.2792E 00	0.1150E 01	0.1798E 01	0.1539E 01	0.4687E 01
84	1	0.2614E 00	0.1150E 01	0.1779E 01	0.1500E 01	0.4251E 01
85	1B	0.7254E-02	0.1500E 01	0.6986E 00	0.1521E-01	0.3328E 01
86	1B	0.7254E-02	0.1500E 01	0.6986E 00	0.1521E-01	0.2179E 01
87	1	0.3022E-01	0.1250E 01	0.1128E 01	0.2496E 00	0.1923E 01
88	1	0.4232E-01	0.1250E 01	0.1230E 01	0.4150E 00	0.2719E 01
89	1	0.6045E-01	0.1250E 01	0.1337E 01	0.6276E 00	0.3091E 01
90	1	0.7859E-01	0.1250E 01	0.1416E 01	0.7841E 00	0.6332E 01
91	1	0.8343E-01	0.1150E 01	0.1434E 01	0.8197E 00	0.5242E 01
92	1	0.1279E 00	0.1150E 01	0.1563E 01	0.1074E 01	0.1156E 02
93	1	0.5450E 00	0.1150E 01	0.2000E 01	0.1905E 01	0.9993E 01
94	1A	0.7063E 00	0.1150E 01	0.2078E 01	0.2044E 01	0.1333E 02
95	1	0.5117E 00	0.1150E 01	0.1991E 01	0.1871E 01	0.7062E 01
96	1	0.3170E 00	0.1150E 01	0.1837E 01	0.1613E 01	0.9466E 01
97	1	0.2502E 00	0.1150E 01	0.1765E 01	0.1474E 01	0.8919E 01
98	1	0.2280E 00	0.1150E 01	0.1737E 01	0.1419E 01	0.8079E 01
99	1B	0.7254E-02	0.1500E 01	0.6986E 00	0.1521E-01	0.3265E 01
100	1B	0.7254E-02	0.1500E 01	0.6986E 00	0.1521E-01	0.1667E 01
101	1	0.1450E-01	0.1500E 01	0.9076E 00	0.1521E-01	0.3376E 01
102	1	0.3022E-01	0.1250E 01	0.1128E 01	0.2496E 00	0.2881E 01
103	1	0.4232E-01	0.1250E 01	0.1230E 01	0.4150E 00	0.3068E 01
104	1	0.6892E-01	0.1250E 01	0.1377E 01	0.7038E 00	0.6291E 01
105	1	0.1001E 00	0.1150E 01	0.1499E 01	0.9284E 00	0.9541E 01
106	1	0.2224E 00	0.1150E 01	0.1730E 01	0.1404E 01	0.1352E 02
107	1	0.6007E 00	0.1150E 01	0.2029E 01	0.1957E 01	0.1312E 02
108	1	0.4394E 00	0.1150E 01	0.1935E 01	0.1789E 01	0.6055E 01
109	1	0.3148E 00	0.1150E 01	0.1835E 01	0.1609E 01	0.4519E 01
110	1	0.2614E 00	0.1150E 01	0.1779E 01	0.1500E 01	0.9322E 01
111	1	0.2280E 00	0.1150E 01	0.1737E 01	0.1419E 01	0.9014E 01
112	1	0.2002E 00	0.1150E 01	0.1698E 01	0.1341E 01	0.8884E 01
113	1B	0.7254E-02	0.1500E 01	0.6986E 00	0.1521E-01	0.3119E 01
114	1B	0.7254E-02	0.1500E 01	0.6986E 00	0.1521E-01	0.1750E 01
115	1B	0.7254E-02	0.1500E 01	0.6986E 00	0.1521E-01	0.4322E 01
116	1	0.2418E-01	0.1250E 01	0.1061E 01	0.1704E 00	0.3063E 01
117	1	0.4232E-01	0.1250E 01	0.1230E 01	0.4150E 00	0.3466E 01
118	1	0.6287E-01	0.1250E 01	0.1349E 01	0.6510E 00	0.5357E 01
119	1	0.1001E 00	0.1150E 01	0.1489E 01	0.9284E 00	0.1274E 02
120	1	0.3670E 00	0.1150E 01	0.1881E 01	0.1692E 01	0.1119E 02
121	1	0.3949E 00	0.1150E 01	0.1903E 01	0.1731E 01	0.1235E 02
122	1	0.2947E 00	0.1150E 01	0.1815E 01	0.1572E 01	0.9076E 01
123	1	0.2669E 00	0.1150E 01	0.1785E 01	0.1513E 01	0.2920E 01
124	1	0.2280E 00	0.1150E 01	0.1737E 01	0.1419E 01	0.8595E 01
125	1	0.1891E 00	0.1150E 01	0.1681E 01	0.1307E 01	0.8539E 01
126	1	0.1669E 00	0.1150E 01	0.1643E 01	0.1232E 01	0.9204E 01
127	1B	0.7254E-02	0.1500E 01	0.6986E 00	0.1521E-01	0.3119E 01
128	1B	0.7254E-02	0.1500E 01	0.6986E 00	0.1521E-01	0.1910E 01

Element number	Trajectory[1]	$FQ(Q_L/Q_S)$[2]	FQ	Insulation thickness, cm	Ablator thickness, cm	Weight, kg
63	1	0.1113E 00	0.1150E 01	0.3872E 01	0.2523E 01	0.9151E 00
64	1	0.1669E 00	0.1150E 01	0.4184E 01	0.3138E 01	0.1914E 01
65	1	0.4730E 00	0.1150E 01	0.4983E 01	0.4654E 01	0.1663E 01
66	1	0.6122E 00	0.1150E 01	0.5180E 01	0.5008E 01	0.1292E 01
67	1	0.6678E 00	0.1150E 01	0.5247E 01	0.5127E 01	0.2073E 01
68	1	0.4730E 00	0.1150E 01	0.4983E 01	0.4654E 01	0.1675E 01
69	1	0.3339E 00	0.1150E 01	0.4715E 01	0.4176E 01	0.1731E 01
70	1	0.2782E 00	0.1150E 01	0.4575E 01	0.3913E 01	0.1542E 01
71	1B	0.7259E-02	0.1500E 01	0.1778E 01	0.3872E-01	0.7179E 00
72	1	0.3629E-01	0.1250E 01	0.3013E 01	0.8225E 00	0.1269E 01
73	1	0.5444E-01	0.1250E 01	0.3324E 01	0.1437E 01	0.3918E 00
74	1	0.6291E-01	0.1250E 01	0.3435E 01	0.1657E 01	0.7569E 00
75	1	0.7259E-01	0.1250E 01	0.3545E 01	0.1874E 01	0.7084E 00
76	1	0.8469E-01	0.1250E 01	0.3663E 01	0.2108E 01	0.1342E 01
77	1	0.8905E-01	0.1150E 01	0.3701E 01	0.2184E 01	0.1138E 01
78	4	0.5565E 00	0.1150E 01	0.4194E 01	0.3138E 01	0.2736E 01
79	1	0.5955E 00	0.1150E 01	0.5159E 01	0.4970E 01	0.2188E 01
80	1A	0.7068E 00	0.1150E 01	0.5291E 01	0.5205E 01	0.3034E 01
81	1A	0.6589E 00	0.1150E 01	0.5237E 01	0.5109E 01	0.2672E 01
82	1	0.3784E 00	0.1150E 01	0.4811E 01	0.4348E 01	0.2160E 01
83	1	0.2793E 00	0.1150E 01	0.4579E 01	0.3919E 01	0.2126E 01
84	1	0.2615E 00	0.1150E 01	0.4528E 01	0.3819E 01	0.1928E 01
85	1B	0.7259E-02	0.1500E 01	0.1778E 01	0.3872E-01	0.1509E 01
86	1B	0.7259E-02	0.1500E 01	0.1778E 01	0.3872E-01	0.9886E 00
87	1	0.3024E-01	0.1250E 01	0.2873E 01	0.6355E 00	0.8729E 00
88	1	0.4234E-01	0.1250E 01	0.3131E 01	0.1056E 01	0.1233E 01
89	1	0.6049E-01	0.1250E 01	0.3405E 01	0.1597E 01	0.1402E 01
90	1	0.7864E-01	0.1250E 01	0.3606E 01	0.1995E 01	0.2872E 01
91	1	0.8348E-01	0.1150E 01	0.3652E 01	0.2086E 01	0.2378E 01
92	1	0.1280E 00	0.1150E 01	0.3980E 01	0.2735E 01	0.5245E 01
93	1	0.5454E 00	0.1150E 01	0.5092E 01	0.4849E 01	0.4533E 01
94	1A	0.7068E 00	0.1150E 01	0.5291E 01	0.5205E 01	0.6049E 01
95	1	0.5120E 00	0.1150E 01	0.5043E 01	0.4762E 01	0.3203E 01
96	1	0.3172E 00	0.1150E 01	0.4675E 01	0.4106E 01	0.4294E 01
97	1	0.2504E 00	0.1150E 01	0.4495E 01	0.3753E 01	0.4046E 01
98	1	0.2281E 00	0.1150E 01	0.4423E 01	0.3612E 01	0.3664E 01
99	1B	0.7259E-02	0.1500E 01	0.1778E 01	0.3872E-01	0.1481E 01
100	1B	0.7259E-02	0.1500E 01	0.1778E 01	0.3872E-01	0.7561E 00
101	1	0.1451E-01	0.1500E 01	0.2310E 01	0.3872E-01	0.1531E 01
102	1	0.3024E-01	0.1250E 01	0.2873E 01	0.6355E 00	0.1307E 01
103	1	0.4234E-01	0.1250E 01	0.2131E 01	0.1056E 01	0.1392E 01
104	1	0.6896E-01	0.1250E 01	0.3505E 01	0.1796E 01	0.2854E 01
105	1	0.1001E 00	0.1150E 01	0.3792E 01	0.2363E 01	0.4328E 01
106	1	0.2226E 00	0.1150E 01	0.4404E 01	0.3575E 01	0.6134E 01
107	1	0.6010E 00	0.1150E 01	0.5166E 01	0.4982E 01	0.5952E 01
108	1	0.4396E 00	0.1150E 01	0.4926E 01	0.4553E 01	0.2746E 01
109	1	0.3150E 00	0.1150E 01	0.4671E 01	0.4096E 01	0.2050E 01
110	1	0.2615E 00	0.1150E 01	0.4528E 01	0.3819E 01	0.4228E 01
111	1	0.2281E 00	0.1150E 01	0.4423E 01	0.3612E 01	0.4089E 01
112	1	0.2003E 00	0.1150E 01	0.4323E 01	0.3415E 01	0.4030E 01
113	1B	0.7259E-02	0.1500E 01	0.1778E 01	0.3872E-01	0.1415E 01
114	1B	0.7259E-02	0.1500E 01	0.1778E 01	0.3872E-01	0.7939E 00
115	1B	0.7259E-02	0.1500E 01	0.1778E 01	0.3872E-01	0.1960E 01
116	1	0.2419E-01	0.1250E 01	0.2702E 01	0.4337E 00	0.1389E 01
117	1	0.4234E-01	0.1250E 01	0.3131E 01	0.1056E 01	0.1572E 01
118	1	0.6291E-01	0.1250E 01	0.3435E 01	0.1657E 01	0.2430E 01
119	1	0.1001E 00	0.1150E 01	0.3792E 01	0.2363E 01	0.5780E 01
120	1	0.3673E 00	0.1150E 01	0.4788E 01	0.4307E 01	0.5077E 01
121	1	0.3951E 00	0.1150E 01	0.4844E 01	0.4407E 01	0.5602E 01
122	1	0.2949E 00	0.1150E 01	0.4620E 01	0.4002E 01	0.4117E 01
123	1	0.2671E 00	0.1150E 01	0.4544E 01	0.3851E 01	0.1324E 01
124	1	0.2281E 00	0.1150E 01	0.4423E 01	0.3612E 01	0.3898E 01
125	1	0.1892E 00	0.1150E 01	0.4280E 01	0.3328E 01	0.3873E 01
126	1	0.1669E 00	0.1150E 01	0.4184E 01	0.3138E 01	0.4175E 01
127	1B	0.7259E-02	0.1500E 01	0.1778E 01	0.3872E-01	0.1415E 01
128	1B	0.7259E-02	0.1500E 01	0.1778E 01	0.3872E-01	0.8666E 00

[redacted]

[redacted]

TABLE 6.--Continued

HEAT SHIELD DESIGN COMPUTER PROGRAM

Element number	Trajectory[1]	$FQ(Q_L/Q_S)$[2]	FQ	Insulation[3] thickness, inch	Ablator thickness, inch	Weight, pound
129	1B	0.7254E-02	0.1500E 01	0.6986E 00	0.1521E-01	0.4619E 01
130	1	0.2419E-01	0.1250E 01	0.1061E 01	0.1704E 00	0.3392E 01
131	1	0.4232E-01	0.1250E 01	0.1230E 01	0.4150E 00	0.3910E 01
132	1	0.6045E-01	0.1250E 01	0.1337E 01	0.6276E 00	0.5085E 01
133	1	0.1557E 00	0.1150E 01	0.1622E 01	0.1191E 01	0.1471E 02
134	1	0.2892E 00	0.1150E 01	0.1809E 01	0.1560E 01	0.8458E 01
135	1	0.3114E 00	0.1150E 01	0.1831E 01	0.1603E 01	0.1271E 02
136	1	0.2614E 00	0.1150E 01	0.1779E 01	0.1500E 01	0.1268E 02
137	1	0.2169E 00	0.1150E 01	0.1722E 01	0.1389E 01	0.4460E 01
138	1	0.1835E 00	0.1150E 01	0.1672E 01	0.1289E 01	0.8426E 01
139	1	0.1501E 00	0.1150E 01	0.1611E 01	0.1170E 01	0.8574E 01
140	1	0.1223E 00	0.1150E 01	0.1550E 01	0.1048E 01	0.9077E 01
141	1B	0.7254E-02	0.1500E 01	0.6986E 00	0.1521E-01	0.3158E 01
142	1B	0.7254E-02	0.1500E 01	0.6986E 00	0.1521E-01	0.2279E 01
143	1B	0.7254E-02	0.1500E 01	0.6986E 00	0.1521E-01	0.4693E 01
144	1	0.2419E-01	0.1250E 01	0.1061E 01	0.1704E 00	0.3955E 01
145	1	0.6045E-01	0.1250E 01	0.1337E 01	0.6276E 00	0.5767E 01
146	1	0.7254E-01	0.1250E 01	0.1392E 01	0.7363E 00	0.5449E 01
147	1	0.1446E 00	0.1150E 01	0.1600E 01	0.1147E 01	0.1425E 02
148	1	0.2447E 00	0.1150E 01	0.1759E 01	0.1461E 01	0.6772E 01
149	1	0.2558E 00	0.1150E 01	0.1772E 01	0.1487E 01	0.1322E 02
150	1	0.2391E 00	0.1150E 01	0.1752E 01	0.1447E 01	0.1259E 02
151	1	0.1835E 00	0.1150E 01	0.1672E 01	0.1289E 01	0.6860E 01
152	1	0.1446E 00	0.1150E 01	0.1600E 01	0.1147E 01	0.8792E 01
153	1	0.1168E 00	0.1150E 01	0.1536E 01	0.1020E 01	0.9021E 01
154	1	0.9455E-01	0.1150E 01	0.1472E 01	0.8943E 00	0.9459E 01
155	1B	0.7254E-02	0.1500E 01	0.6986E 00	0.1521E-01	0.3119E 01
156	1B	0.7254E-02	0.1500E 01	0.6986E 00	0.1521E-01	0.2670E 01
157	1B	0.7254E-02	0.1500E 01	0.6986E 00	0.1521E-01	0.4354E 01
158	1B	0.7254E-02	0.1500E 01	0.6986E 00	0.1521E-01	0.3341E 01
159	1	0.4232E-01	0.1250E 01	0.1230E 01	0.4150E 00	0.6097E 01
160	1	0.7254E-01	0.1250E 01	0.1392E 01	0.7363E 00	0.5473E 01
161	1	0.1168E 00	0.1150E 01	0.1536E 01	0.1020E 01	0.1334E 02
162	1	0.2169E 00	0.1150E 01	0.1722E 01	0.1389E 01	0.5424E 01
163	1	0.2447E 00	0.1150E 01	0.1759E 01	0.1461E 01	0.1026E 02
164	1	0.2280E 00	0.1150E 01	0.1737E 01	0.1419E 01	0.1178E 02
165	1	0.1857E 00	0.1150E 01	0.1676E 01	0.1296E 01	0.1146E 02
166	1	0.1557E 00	0.1150E 01	0.1622E 01	0.1191E 01	0.9985E 01
167	1	0.1279E 00	0.1150E 01	0.1563E 01	0.1074E 01	0.1050E 02
168	1	0.1001E 00	0.1150E 01	0.1489E 01	0.9264E 00	0.1101E 02
169	1B	0.7254E-02	0.1500E 01	0.6986E 00	0.1521E-01	0.1776E 01
170	1B	0.7254E-02	0.1500E 01	0.6986E 00	0.1521E-01	0.1724E 01
171	1B	0.7254E-02	0.1500E 01	0.6986E 00	0.1521E-01	0.2180E 01
172	1	0.1450E-01	0.1500E 01	0.9076E 00	0.1521E-01	0.2488E 01
173	1	0.4232E-01	0.1250E 01	0.1230E 01	0.4150E 00	0.4256E 01
174	1	0.1112E 00	0.1150E 01	0.1521E 01	0.9912E 00	0.3867E 01
175	1	0.1557E 00	0.1150E 01	0.1622E 01	0.1191E 01	0.8109E 01
176	1	0.2180E 00	0.1150E 01	0.1724E 01	0.1392E 01	0.2754E 01
177	1	0.2280E 00	0.1150E 01	0.1737E 01	0.1419E 01	0.4256E 01
178	1	0.2336E 00	0.1150E 01	0.1745E 01	0.1433E 01	0.4394E 01
179	1	0.2002E 00	0.1150E 01	0.1698E 01	0.1341E 01	0.9860E 01
180	1	0.1635E 00	0.1150E 01	0.1637E 01	0.1220E 01	0.6525E 01
181	1	0.1334E 00	0.1150E 01	0.1576E 01	0.1099E 01	0.5928E 01
182	1	0.1001E 00	0.1150E 01	0.1489E 01	0.9264E 00	0.7168E 01
183	1B	0.7254E-02	0.1500E 01	0.6986E 00	0.1521E-01	0.1841E 00
184	1B	0.7254E-02	0.1500E 01	0.6986E 00	0.1521E-01	0.6167E 00
185	1B	0.7254E-02	0.1500E 01	0.6986E 00	0.1521E-01	0.1145E 01
186	1B	0.7254E-02	0.1500E 01	0.6986E 00	0.1521E-01	0.1435E 01
187	1B	0.7254E-02	0.1500E 01	0.6986E 00	0.1521E-01	0.1520E 01
188	1B	0.7254E-02	0.1500E 01	0.6986E 00	0.1521E-01	0.1637E 01
189	1	0.1450E-01	0.1500E 01	0.9076E 00	0.1521E-01	0.2052E 01
190	1	0.4836E-01	0.1250E 01	0.1270E 01	0.4946E 00	0.2176E 01
191	1	0.1279E 00	0.1150E 01	0.1563E 01	0.1074E 01	0.1734E 01
192	1	0.1835E 00	0.1150E 01	0.1672E 01	0.1289E 01	0.7316E 01
193	1	0.1835E 00	0.1150E 01	0.1672E 01	0.1289E 01	0.6760E 01
194	1	0.2280E 00	0.1150E 01	0.1737E 01	0.1419E 01	0.3165E 01

Element number	Trajectory[1]	$FQ(Q_L/Q_S)$[2]	FQ	Insulation thickness, cm	Ablator thickness, cm	Weight, kg
129	1B	0.7259E-02	0.1500E 01	0.1775E 01	0.3872E-01	0.2095E 01
130	1	0.2419E-01	0.1250E 01	0.2702E 01	0.4337E 00	0.1539E 01
131	1	0.4234E-01	0.1250E 01	0.3131E 01	0.1056E 01	0.1773E 01
132	1	0.6049E-01	0.1250E 01	0.3405E 01	0.1597E 01	0.2307E 01
133	1	0.1558E 00	0.1150E 01	0.4121E 01	0.3023E 01	0.6675E 01
134	1	0.2894E 00	0.1150E 01	0.4606E 01	0.3973E 01	0.3837E 01
135	1	0.3116E 00	0.1150E 01	0.4662E 01	0.4081E 01	0.5767E 01
136	1	0.2615E 00	0.1150E 01	0.4528E 01	0.3819E 01	0.5753E 01
137	1	0.2170E 00	0.1150E 01	0.4395E 01	0.3536E 01	0.2023E 01
138	1	0.1836E 00	0.1150E 01	0.4257E 01	0.3283E 01	0.3822E 01
139	1	0.1502E 00	0.1150E 01	0.4102E 01	0.2978E 01	0.3935E 01
140	1	0.1224E 00	0.1150E 01	0.3946E 01	0.2667E 01	0.4117E 01
141	1B	0.7259E-02	0.1500E 01	0.1779E 01	0.3872E-01	0.1432E 01
142	1B	0.7259E-02	0.1500E 01	0.1779E 01	0.3872E-01	0.1032E 01
143	1B	0.7259E-02	0.1500E 01	0.1779E 01	0.3872E-01	0.2128E 01
144	1	0.2419E-01	0.1250E 01	0.2702E 01	0.4337E 00	0.1794E 01
145	1	0.6049E-01	0.1250E 01	0.3405E 01	0.1597E 01	0.2616E 01
146	1	0.7259E-01	0.1250E 01	0.3545E 01	0.1874E 01	0.2472E 01
147	1	0.1447E 00	0.1150E 01	0.4074E 01	0.2921E 01	0.6466E 01
148	1	0.2448E 00	0.1150E 01	0.4476E 01	0.3719E 01	0.3071E 01
149	1	0.2560E 00	0.1150E 01	0.4511E 01	0.3787E 01	0.5997E 01
150	1	0.2393E 00	0.1150E 01	0.4469E 01	0.3684E 01	0.5713E 01
151	1	0.1836E 00	0.1150E 01	0.4257E 01	0.3293E 01	0.3111E 01
152	1	0.1447E 00	0.1150E 01	0.4074E 01	0.2921E 01	0.3988E 01
153	1	0.1168E 00	0.1150E 01	0.3910E 01	0.2597E 01	0.4092E 01
154	1	0.9461E-01	0.1150E 01	0.3749E 01	0.2276E 01	0.4291E 01
155	1B	0.7259E-02	0.1500E 01	0.1779E 01	0.3872E-01	0.1415E 01
156	1B	0.7259E-02	0.1500E 01	0.1779E 01	0.3872E-01	0.1211E 01
157	1B	0.7259E-02	0.1500E 01	0.1779E 01	0.3872E-01	0.1975E 01
158	1B	0.7259E-02	0.1500E 01	0.1779E 01	0.3872E-01	0.1515E 01
159	1	0.4234E-01	0.1250E 01	0.3131E 01	0.1056E 01	0.2766E 01
160	1	0.7259E-01	0.1250E 01	0.3545E 01	0.1874E 01	0.2482E 01
161	1	0.1168E 00	0.1150E 01	0.3910E 01	0.2597E 01	0.6052E 01
162	1	0.2170E 00	0.1150E 01	0.4395E 01	0.3536E 01	0.2460E 01
163	1	0.2448E 00	0.1150E 01	0.4477E 01	0.3719E 01	0.4657E 01
164	1	0.2281E 00	0.1150E 01	0.4423E 01	0.3612E 01	0.5347E 01
165	1	0.1858E 00	0.1150E 01	0.4266E 01	0.3301E 01	0.5199E 01
166	1	0.1558E 00	0.1150E 01	0.4131E 01	0.3039E 01	0.4529E 01
167	1	0.1280E 00	0.1150E 01	0.3980E 01	0.2735E 01	0.4766E 01
168	1	0.1001E 00	0.1150E 01	0.3792E 01	0.2363E 01	0.4994E 01
169	1B	0.7259E-02	0.1500E 01	0.1778E 01	0.3872E-01	0.8055E 00
170	1B	0.7259E-02	0.1500E 01	0.1778E 01	0.3872E-01	0.7822E 00
171	1B	0.7259E-02	0.1500E 01	0.1778E 01	0.3872E-01	0.9890E 00
172	1	0.1451E-01	0.1500E 01	0.2310E 01	0.3872E-01	0.1129E 01
173	1	0.4234E-01	0.1250E 01	0.3131E 01	0.1056E 01	0.1930E 01
174	1	0.1113E 00	0.1150E 01	0.2872E 01	0.2523E 01	0.1754E 01
175	1	0.1558E 00	0.1150E 01	0.4131E 01	0.3033E 01	0.3678E 01
176	1	0.2181E 00	0.1150E 01	0.4389E 01	0.3544E 01	0.1249E 01
177	1	0.2281E 00	0.1150E 01	0.4423E 01	0.3612E 01	0.1930E 01
178	1	0.2337E 00	0.1150E 01	0.4442E 01	0.3649E 01	0.1993E 01
179	1	0.2003E 00	0.1150E 01	0.4323E 01	0.3415E 01	0.4472E 01
180	1	0.1636E 00	0.1150E 01	0.4108E 01	0.3107E 01	0.2960E 01
181	1	0.1335E 00	0.1150E 01	0.4012E 01	0.2799E 01	0.3142E 01
182	1	0.1001E 00	0.1150E 01	0.3792E 01	0.2363E 01	0.3251E 01
183	1B	0.7259E-02	0.1500E 01	0.1778E 01	0.3872E-01	0.8351E-01
184	1B	0.7259E-02	0.1500E 01	0.1778E 01	0.3872E-01	0.2797E 00
185	1B	0.7259E-02	0.1500E 01	0.1778E 01	0.3872E-01	0.5201E 00
186	1B	0.7259E-02	0.1500E 01	0.1778E 01	0.3872E-01	0.6511E 00
187	1B	0.7259E-02	0.1500E 01	0.1778E 01	0.3872E-01	0.7349E 00
188	1B	0.7259E-02	0.1500E 01	0.1778E 01	0.3872E-01	0.7429E 00
189	1	0.1451E-01	0.1500E 01	0.2310E 01	0.3872E-01	0.9312E 00
190	1	0.4839E-01	0.1250E 01	0.3233E 01	0.1259E 01	0.9874E 00
191	1	0.1280E 00	0.1150E 01	0.3980E 01	0.2735E 01	0.7868E 00
192	1	0.1836E 00	0.1150E 01	0.4257E 01	0.3283E 01	0.3318E 01
193	1	0.1836E 00	0.1150E 01	0.4257E 01	0.3283E 01	0.3066E 01
194	1	0.2281E 00	0.1150E 01	0.4423E 01	0.3612E 01	0.1435E 01

TABLE 6.--Concluded

HEAT SHIELD DESIGN COMPUTER PROGRAM

Element number	Trajectory[1]	$FQ(Q_L/Q_S)$[2]	FQ	Insulation thickness[3], inch	Ablator thickness inch	Weight, pound
195	1	0.2336E 00	0.1150E 01	0.1745E 01	0.1433E 01	0.2677E 01
196	1	0.2280E 00	0.1150E 01	0.1737E 01	0.1419E 01	0.1993E 01
197	1	0.2002E 00	0.1150E 01	0.1698E 01	0.1341E 01	0.7558E 01
198	1	0.1501E 00	0.1150E 01	0.1611E 01	0.1170E 01	0.5052E 01
199	1	0.1446E 00	0.1150E 01	0.1600E 01	0.1147E 01	0.5425E 01
200	1	0.1001E 00	0.1150E 01	0.1489E 01	0.9284E 00	0.5453E 01
201	1B	0.7254E-02	0.1500E 01	0.6986E 00*	0.1521E-01	0.5926E 00
202	1B	0.7254E-02	0.1500E 01	0.6986E 00*	0.1521E-01	0.8614E 01
203	1B	0.7254E-02	0.1500E 01	0.6986E 00	0.1521E-01	0.2384E 01
204	1B	0.7254E-02	0.1500E 01	0.6986E 00	0.1521E-01	0.2931E 01
205	1B	0.7254E-02	0.1500E 01	0.6986E 00	0.1521E-01	0.3940E 01
206	1B	0.7254E-02	0.1500E 01	0.6986E 00	0.1521E-01	0.3617E 01
207	1B	0.7254E-02	0.1500E 01	0.6986E 00	0.1521E-01	0.4448E 01
208	1B	0.7254E-02	0.1500E 01	0.6986E 00	0.1521E-01	0.2497E 01
209	1	0.8343E-01	0.1150E 01	0.1434E 01*	0.8197E 00	0.1504E 02
210	1	0.4727E 00	0.1150E 01	0.1557E 01*	0.1828E 01	0.9869E 01
211	1	0.2725E 00	0.1150E 01	0.1791E 01*	0.1525E 01	0.1228E 02
212	1	0.2280E 00	0.1150E 01	0.1737E 01	0.1419E 01	0.1658E 02
213	1	0.2336E 00	0.1150E 01	0.1745E 01	0.1433E 01	0.6058E 01
214	1	0.2336E 00	0.1150E 01	0.1745E 01	0.1433E 01	0.1071E 02
215	1	0.2280E 00	0.1150E 01	0.1737E 01	0.1419E 01	0.5606E 01
216	1	0.5784E 00	0.1150E 01	0.2018E 01	0.1937E 01	0.7314E 01
217	1	0.5784E 00	0.1150E 01	0.2018E 01	0.1937E 01	0.2369E 02
218	1	0.1446E 00	0.1150E 01	0.1600E 01	0.1147E 01	0.2508E 02
219	1	0.9455E-01	0.1150E 01	0.1472E 01	0.8943E 00	0.1311E 02
220	1B	0.7254E-02	0.1500E 01	0.6986E 00*	0.1521E-01	0.5068E 00
221	1B	0.7254E-02	0.1500E 01	0.6986E 00*	0.1521E-01	0.1418E 02
222	1B	0.7254E-02	0.1500E 01	0.6986E 00	0.1521E-01	0.2030E 01
223	1B	0.7254E-02	0.1500E 01	0.6986E 00	0.1521E-01	0.4578E 01
224	1B	0.7254E-02	0.1500E 01	0.6986E 00	0.1521E-01	0.3734E 01
225	1B	0.7254E-02	0.1500E 01	0.6986E 00*	0.1521E-01	0.3583E 01
226	1B	0.7254E-02	0.1500E 01	0.6986E 00*	0.1521E-01	0.4410E 01
227	1B	0.7254E-02	0.1500E 01	0.6986E 00	0.1521E-01	0.2922E 01
228	1B	0.7254E-02	0.1500E 01	0.6986E 00*	0.1521E-01	0.9706E 01
229	1	0.1015E-01	0.1500E 01	0.8001E 00*	0.1521E-01	0.1320E 01
230	1	0.9455E-01	0.1150E 01	0.1472E 01*	0.8943E 00	0.9015E 01
231	1	0.3059E 00	0.1150E 01	0.1826E 01	0.1593E 01	0.2559E 02
232	1	0.2224E 00	0.1150E 01	0.1730E 01	0.1404E 01	0.7830E 01
233	1	0.2336E 00	0.1150E 01	0.1745E 01	0.1433E 01	0.1245E 02
234	1	0.2614E 00	0.1150E 01	0.1779E 01	0.1500E 01	0.8256E 01
235	1A	0.6674E 00	0.1150E 01	0.2061E 01	0.2014E 01	0.1432E 02
236	1A	0.6785E 00	0.1150E 01	0.2066E 01	0.2023E 01	0.3820E 02
237	1A	0.7230E 00	0.1150E 01	0.2085E 01	0.2057E 01	0.5970E 02
238	1	0.9789E-01	0.1150E 01	0.1482E 01	0.9150E 00	0.1366E 02

Element number	Trajectory[1]	$FQ(Q_L/Q_S)$[2]	FQ	Insulation thickness cm	Ablator thickness cm	Weight, kg
195	1	0.2337E 00	0.1150E 01	0.4442E 01	0.3649E 01	0.1214E 01
196	1	0.2281E 00	0.1150E 01	0.4423E 01	0.3612E 01	0.9042E 00
197	1	0.2003E 00	0.1150E 01	0.4323E 01	0.3415E 01	0.3564E 01
198	1	0.1502E 00	0.1150E 01	0.4103E 01	0.2978E 01	0.2292E 01
199	1	0.1447E 00	0.1150E 01	0.4074E 01	0.2921E 01	0.2461E 01
200	1	0.1001E 00	0.1150E 01	0.3792E 01	0.2363E 01	0.2474E 01
201	1B	0.7259E-02	0.1500E 01	0.1778E 01*	0.3872E-01	0.2688E 00
202	1B	0.7259E-02	0.1500E 01	0.1778E 01*	0.3872E-01	0.3907E 01
203	1B	0.7259E-02	0.1500E 01	0.1778E 01	0.3872E-01	0.1081E 01
204	1B	0.7259E-02	0.1500E 01	0.1778E 01	0.3872E-01	0.1789E 01
205	1B	0.7259E-02	0.1500E 01	0.1778E 01	0.3872E-01	0.1787E 01
206	1B	0.7259E-02	0.1500E 01	0.1778E 01	0.3872E-01	0.1640E 01
207	1B	0.7259E-02	0.1500E 01	0.1778E 01	0.3872E-01	0.2017E 01
208	1B	0.7259E-02	0.1500E 01	0.1778E 01	0.3872E-01	0.1132E 01
209	1	0.8348E-01	0.1150E 01	0.3652E 01*	0.2086E 01	0.6824E 01
210	1	0.4730E 00	0.1150E 01	0.4983E 01*	0.4654E 01	0.4476E 01
211	1	0.2727E 00	0.1150E 01	0.4560E 01*	0.3893E 01	0.5570E 01
212	1	0.2281E 00	0.1150E 01	0.4423E 01	0.3612E 01	0.7524E 01
213	1	0.2337E 00	0.1150E 01	0.4442E 01	0.3649E 01	0.2748E 01
214	1	0.2337E 00	0.1150E 01	0.4442E 01	0.3649E 01	0.4862E 01
215	1	0.2281E 00	0.1150E 01	0.4423E 01	0.3612E 01	0.2543E 01
216	1	0.5788E 00	0.1150E 01	0.5137E 01	0.4931E 01	0.3317E 01
217	1	0.5788E 00	0.1150E 01	0.5137E 01	0.4931E 01	0.1074E 02
218	1	0.1447E 00	0.1150E 01	0.4074E 01	0.2921E 01	0.1138E 02
219	1	0.9461E-01	0.1150E 01	0.3748E 01	0.2276E 01	0.5950E 01
220	1B	0.7259E-02	0.1500E 01	0.1778E 01*	0.3872E-01	0.2299E 00
221	1B	0.7259E-02	0.1500E 01	0.1778E 01*	0.3872E-01	0.6434E 01
222	1B	0.7259E-02	0.1500E 01	0.1778E 01	0.3872E-01	0.9210E 00
223	1B	0.7259E-02	0.1500E 01	0.1778E 01	0.3872E-01	0.2076E 01
224	1B	0.7259E-02	0.1500E 01	0.1778E 01	0.3872E-01	0.1694E 01
225	1B	0.7259E-02	0.1500E 01	0.1778E 01*	0.3872E-01	0.1625E 01
226	1B	0.7259E-02	0.1500E 01	0.1778E 01*	0.3872E-01	0.2000E 01
227	1B	0.7259E-02	0.1500E 01	0.1778E 01*	0.3872E-01	0.1325E 01
228	1B	0.7259E-02	0.1500E 01	0.1778E 01*	0.3872E-01	0.4402E 01
229	1	0.1016E-01	0.1500E 01	0.2036E 01*	0.3872E-01	0.5991E 00
230	1	0.9461E-01	0.1150E 01	0.3748E 01*	0.2276E 01	0.4089E 01
231	1	0.3061E 00	0.1150E 01	0.4649E 01	0.4057E 01	0.1160E 02
232	1	0.2226E 00	0.1150E 01	0.4404E 01	0.3575E 01	0.3552E 01
233	1	0.2337E 00	0.1150E 01	0.4442E 01	0.3649E 01	0.5649E 01
234	1	0.2615E 00	0.1150E 01	0.4528E 01	0.3819E 01	0.3745E 01
235	1A	0.6678E 00	0.1150E 01	0.5247E 01	0.5127E 01	0.6498E 01
236	1A	0.6790E 00	0.1150E 01	0.5260E 01	0.5150E 01	0.1732E 02
237	1A	0.7239E 00	0.1150E 01	0.5309E 01	0.5237E 01	0.2707E 02
238	1	0.9795E-01	0.1150E 01	0.3774E 01	0.2329E 01	0.6198E 01

Half of total area	0.3460E 03
Half of total heat shield weight	0.1351E 04
Center of gravity	0.1504E 02
Average design q	0.1597E 00

Half of total area	0.3214E 02
Half of total heat shield weight	0.6129E 03
Center of gravity	0.4585E 01
Average design q	0.1598E 00

NOTES: (1) A--Use of ESA 5500 as ablative material
B--Use of MA 255 as ablative material
all other--ESA 3560

(2) FQ--Factor of safety applied to heating rates
Q_L/Q_S--Ratio of local heating rate to stagnation heating rate

(3) *--Insulation and support panel deleted for "hot tail" design

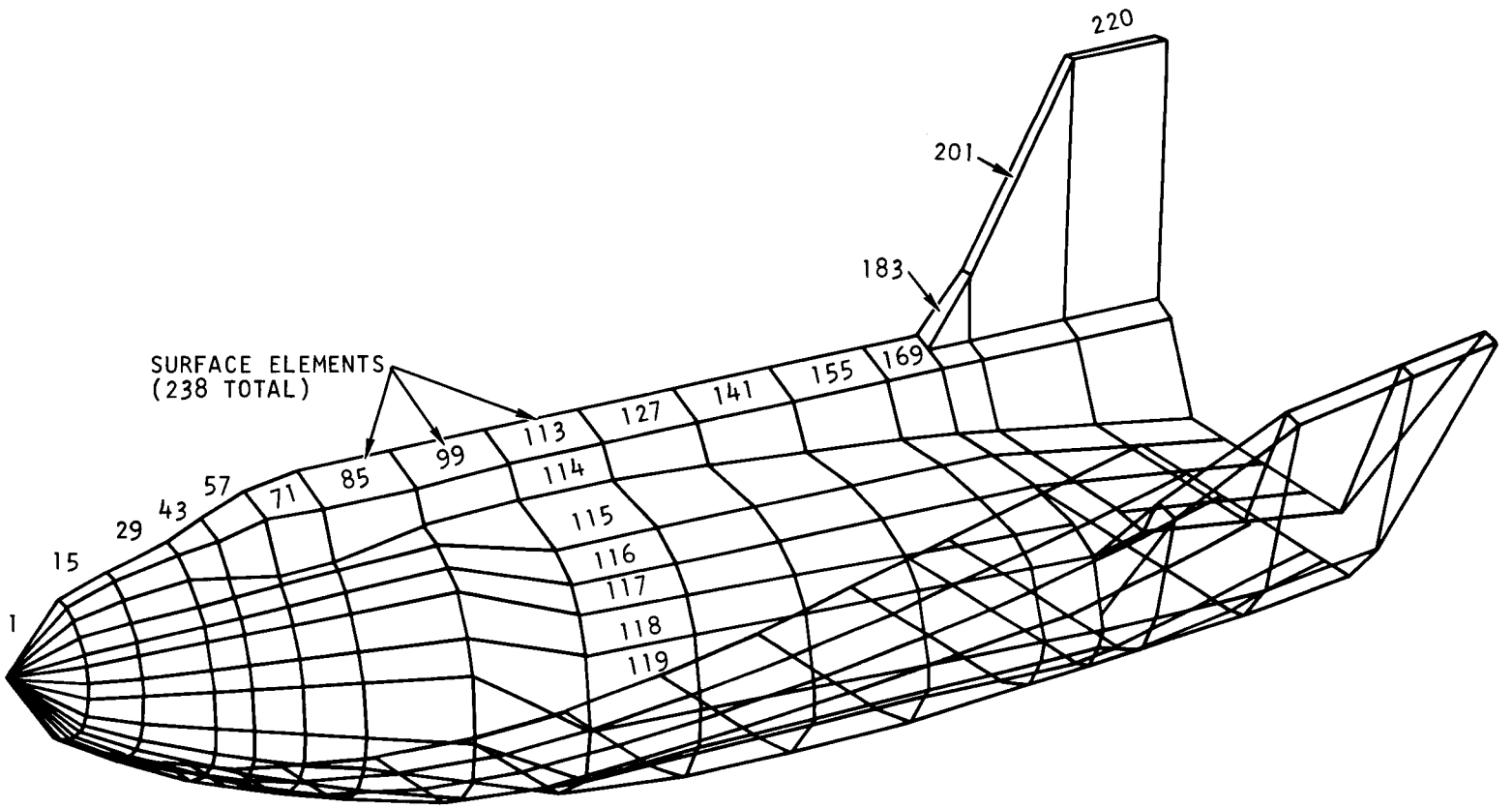

FIGURE 16. HL-10 HEAT SHIELD MODEL

B. STRUCTURE

The basic structural approach for the D/3 vehicle is a buckled-skin concept design utilizing an aluminum frame and longeron structure (fig. 17). Several longerons, bulkheads and beams provide the main paths for distribution of the concentrated loads of booster ascent and landing. The fins and control surfaces are made of 6Al-4V titanium as separate units and then joined to the body structure. By using a buckled-skin design concept, a simple reliable structure can be achieved that is easy to fabricate and relatively free from the complex problems associated with thermal stresses in heated structures. All manufacturing processes required for fabrication of the structure are existing within the current state of the art.

1. Design

The selection of the buckled skin approach is based on structural design and trade-off studies described in Part IV. Also described in Part IV are the detailed design criteria used for the D/3 entry vehicle structural design. A summary of the critical structural loading conditions and margins of safety are shown in table 7.

TABLE 7

SUMMARY OF DESIGN LOADING CONDITIONS AND FACTORS OF SAFETY

	Limit load	Ultimate load	Factor of safety
Internal pressure	5.0 psi (34.5 kN/m^2)	10 psi (68.95 kN/m^2)	2.0
Landing condition (acceleration)			
Vertical	4.0 g	6.0 g	1.5
Horizontal	1.3 g	1.95 g	1.5
Pitch	1.12 rad/sec^2	1.68 rad/sec^2	1.5
* Boost (max. $C_N q\alpha$)			
Axial acceleration	1.7 g	2.55 g	1.5
* Abort pullout	5.65 g	8.5 g	1.5
* First stage burnout	4.3 g	6.46 g	1.5
* Second stage burnout	4.1 g	6.15 g	1.5
* Stage 0 burnout	1.3 g	1.95 g	1.5

* Booster is Titan III-2.

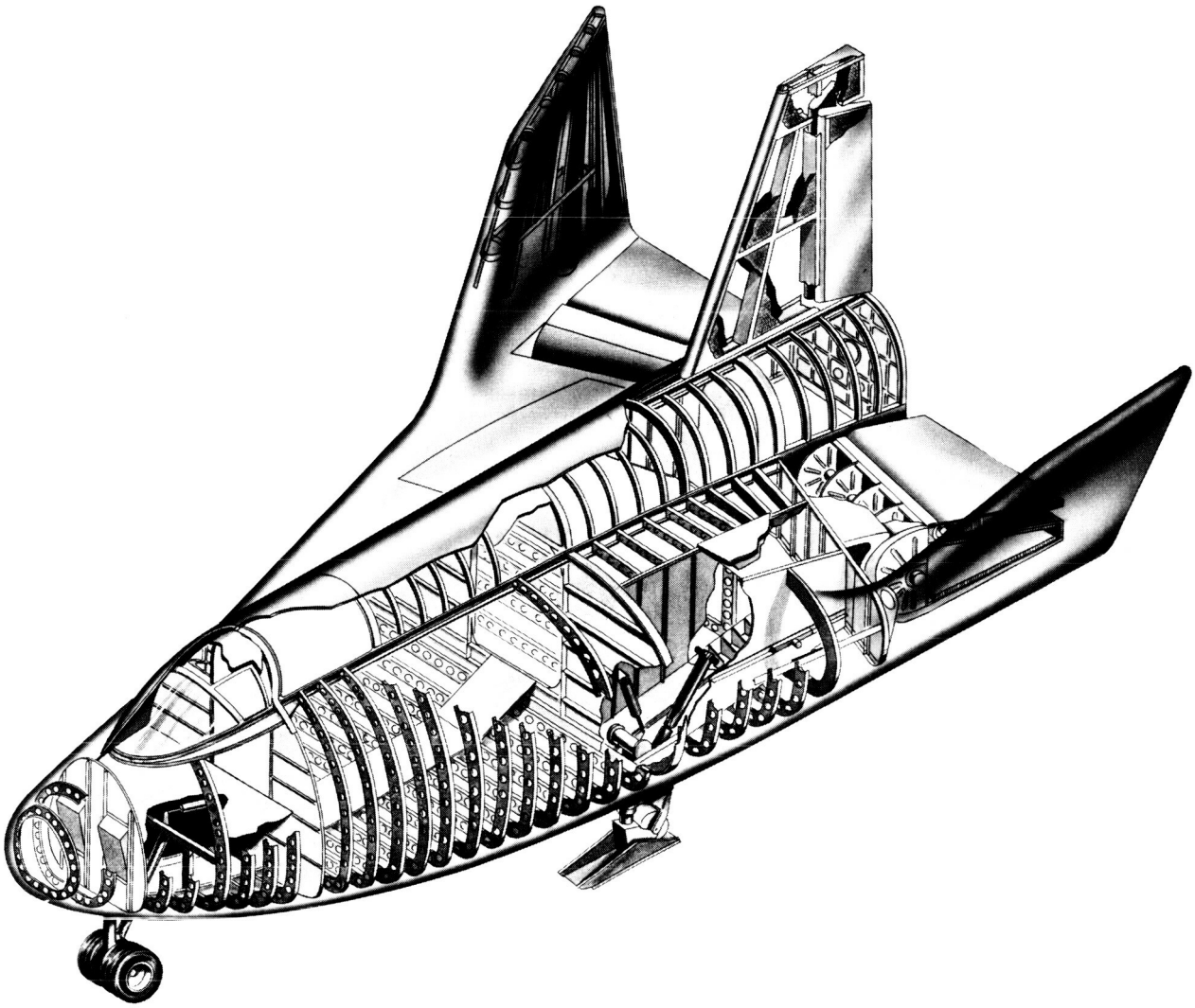

FIGURE 17. D/3 STRUCTURAL CONCEPT

Computized design and tradeoff studies (Part IV) were made to determine critical loading conditions and to select optimum landing gear location and configuration. The two critical overall load design conditions were the ascent and final landing. The abort condition influenced nose, fin and control surface design because of the high dynamic pressures.

For the D/3 vehicle, a wheel nose gear and a combination skid-wheel main gear was selected. The gear configuration minimized landing loads and body structural weight. To provide a full range of potential body structural concepts, six various constructions were evaluated to determine the most efficient concept. The results showed that the buckling-type skin concept was the most efficient. Studies of the tip and center fin structure indicated that a weight savings could be achieved by utilizing an 800° F titanium structure. A summary of the critical structural dimensions determined for the D/3 vehicle is shown in table 8.

TABLE 8

SUMMARY OF CRITICAL STRUCTURAL DIMENSIONS

Body	
Shell (nonweld areas)	0.025 in. (0.063 cm)
Shell (weld areas)	0.060 in. (0.153 cm)
Stringer and longerons	Taper
Frame depth (taper)--top crown	2.5 in. (6.25 cm) minimum
--lower surface	4.0 in. (10.1 cm) maximum
Frame thickness--top crown	0.075 in. (0.191 cm)
--lower surface	0.10 in. (0.254 cm)
Frame spacing--average	11 in. (28 cm)
Center fin	
Honeycomb skin panel--faces	0.010 in. (0.025 cm)
--core depth	0.50 in. (1.27 cm)
Substructure	Varies
Outer fin	
Single skin corrugation panel (average combined skin thickness)	0.050 in. (0.127 cm)

Dynamic design studies were conducted to define minimum stiffenesses for fins, control surface and entry vehicle to booster adapter structure. These studies are presented in detail in Part IV.

2. Structural Description

A structural assembly drawing for the D/3 vehicle is shown in figure 18.

Body structure. - The primary body structure is composed of a welded pressure skin, builtup longeron sections, stringers that act mainly as panel breakers, and lipped "Z" or channel cross-section frames.

[redacted]

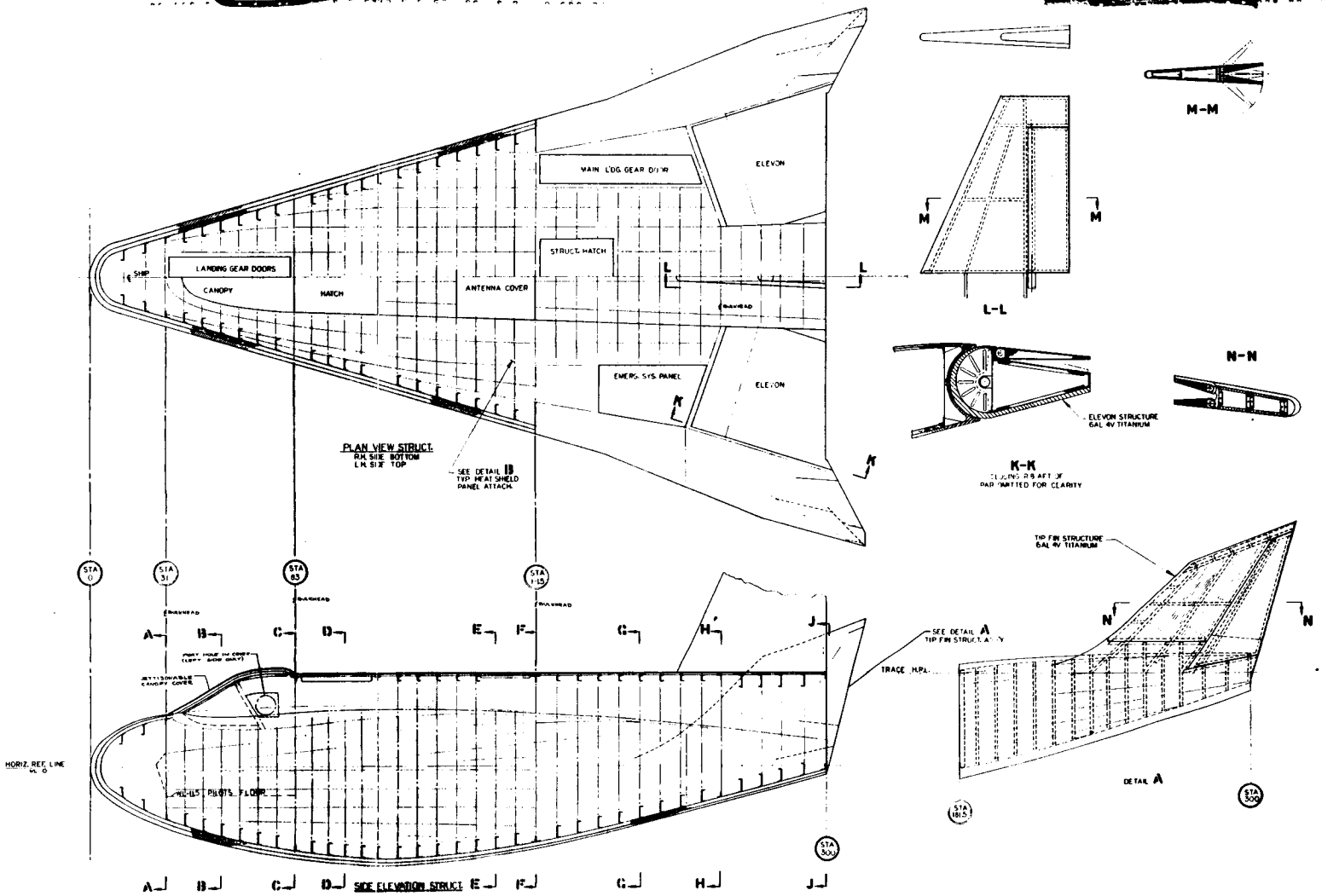

FIGURE 18. D/3 VEHICLE STRUCTURAL LAYOUT

[redacted]

[redacted]

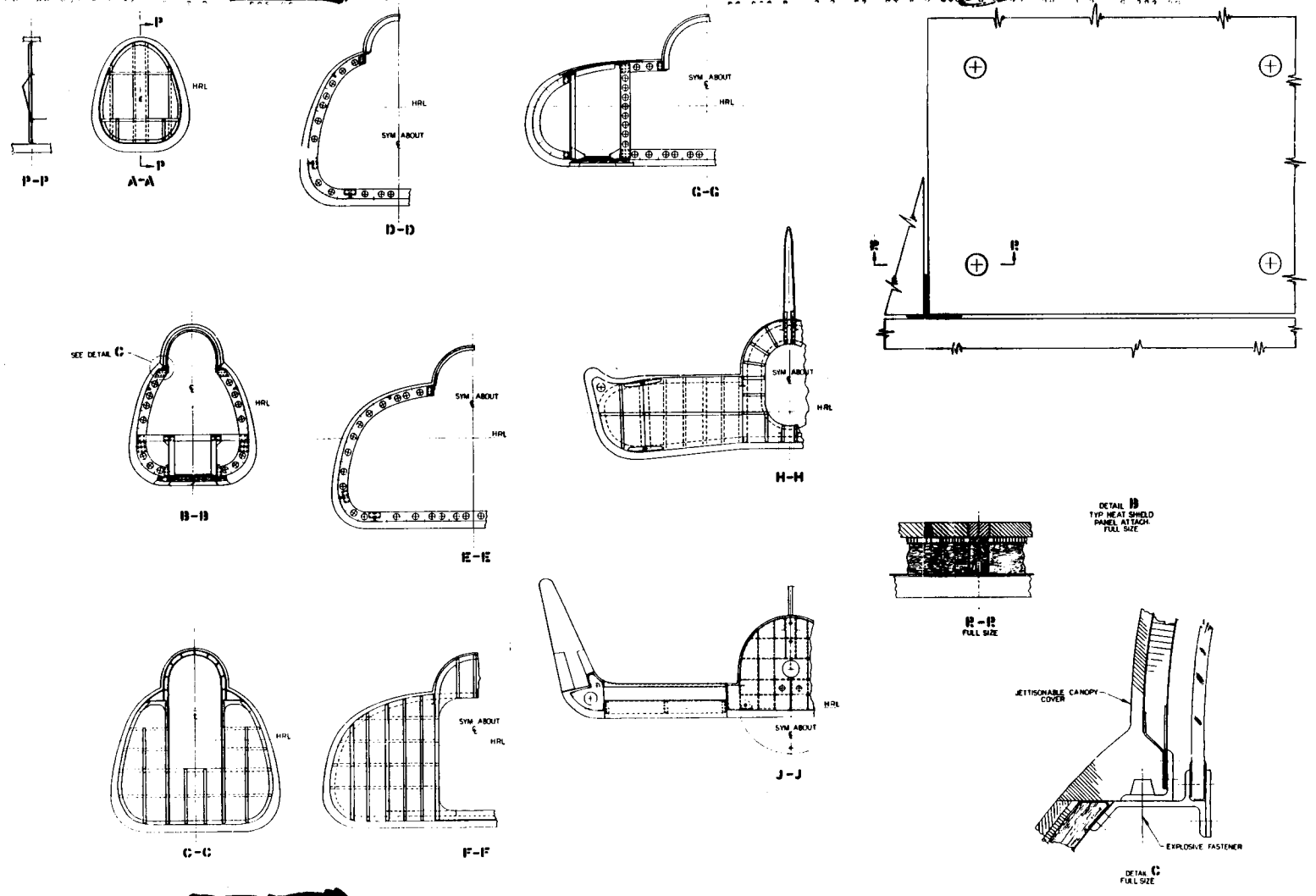

FIGURE 18. --CONCLUDED

[redacted]

There are several pressure and load distribution bulkheads. The main forward pressure bulkhead is located at Station 31 (0.788 m). In addition to resisting pressure loads, it also redistributes the nose gear loads into the body bending members. A load bulkhead is located immediately aft of the pilot station (Station 83, 2.11m). Its main functions are to distribute the nose gear drag strut loads, provide a transition for the jettisonable canopy cover support sill, and act as a closing member for the forward edge of the access hatch.

The aft edge of the access hatch ends at Station 117 (2.97 m). This hatch is essentially a portion of the canopy ridge structure. It will take only net internal and external pressure loads, not overall bending loads. Because of the refurbishable heat shield requirements, the hinging mechanism will be similar to that shown in reference 3.

Between Stations 149 and 181 (3.78 m and 4.60 m), the entire head bump area is occupied by an antenna for communication. This is a structural fiber glass shell.

At Station 181 (4.6 m), a partial bulkhead is provided to redistribute main gear loads and also act as a pressure transition area. From this station, aft to the back canted pressure bulkhead, a pressure beam has been incorporated along butt line 20 (0.508 m). It provides for a nonpressurized section for the main gear well and the emergency chute containers. This design simplifies the sealing requirements.

The doors on the crown for the chutes and the main gear doors are considered nonstructural. In reality, this provides an almost natural shear lag path for the boost loads. To make the outboard crown and lower skins effective would almost be an impossible task, if the doors were structural. In addition, the elevon actuators would also be in this compartment, and to seal them for pressure would result in additional weight penalties.

The main aft pressure bulkhead intersects the body centerline at Station 257 (6.53 m). This bulkhead remains normal to the vehicle centerline in the head bump area, and then cants forward following the elevon hinge line. Frames are spaced at an average of 7 to 8 inches (0.178 m to 0.203 m). The pressure skin is an 0.032-inch (0.81-mm) 2219-T6 skin which is welded together along weld lands. The stringers and frames and longerons are spot welded to the pressure skin.

The body frames vary in depth from the bottom centerline to the top centerline. In the aft body area, where the cross section becomes flattened, the wheel well walls act as the bars to reduce the frame bending moments. Forward of the wheel well pressure beams, the crown longeron members will be used to provide resisting springs to alleviate the pressure moments. In the major hatch areas, secondary crown and bottom beams will be utilized to support hatch pressure loads.

Figure 18 shows the cross-sectional views of the major bulkheads. These are section cuts A-A, C-C, F-F, H-H and J-J. The main cabin pressure seal is at bulkhead J-J. However, as can be seen, the center portion may be removed for a tunnel way during a growth mission. All structure aft of J-J is designed to maintain pressure inboard of butt line 20 (0.507 m). The ascent booster loads are taken by longeron members. Section J-J shows three of the main pickup points. The crown pickup point is backed by two builtup channel section axial members. The boost kick loads will all be redistributed by the bulkhead. The two head bump structure longerons lag the load into the crown skin. The lower pickup point is essentially on the lower surface plane line

and here again the bottom longeron feeds and lags the boost load out into the lower surface. The remaining adapter pickup point is located on the vehicle centerline at the aft cabin pressure bulkhead. This can be seen in figure 19 which shows the adapter-entry vehicle interface points.

The outboard portions of the aft body are utilized as torque boxes and beams for supporting the tip fin structure. The major reaction points for the tip fin are the bulkhead at H-H and F-F. This also provides a logical manufacturing break point. This tip fin reaction structure is conventional aluminum construction with the refurbishable heat shields. This structure is then closed off by a closing rib at which the tip fin spars are attached to the spar pickup points.

Tip and center fin structure.- For the selected design vehicle, a weight tradeoff study was completed to select a minimum weight tail structure. The importance of an efficient tail structure is reflected not only in tail structural weight alone, but more significantly in required ballast weight to provide a given c.g. position. Two structural concepts were evaluated. The first was an 800° F (700° K) titanium thermostructural concept and the second a 200° F (367° K) aluminum thermostructural concept. The results of this structural study showed that by using the titanium thermostructural concept a tail weight savings of 78 pounds (171 kg) could be realized. Considering ballast effects, this weight savings amounted to 139.5 pounds (307 kg). As a result, all tail surfaces utilized the titanium thermostructural concept.

For the center fin, a two-spar bending box was used, with a third spar (leading edge) being used for torsion. An analysis of the critical design loads indicated that minimum material gage set by manufacturing limitations dictated the design. The covers are only used to support local pressure and transfer the pressure loads to the bending spars. This required a stiffness efficient cover, which dictated a honeycomb panel design. The panel depth was kept to a minimum to avoid severe face temperature differences and resulting weight penalty. Using a two spar structure with no cover axial continuity minimizes fin restraint thermally and again will not create thermal weight penalty. Since the fin was minimum gage critical, a check was made to see if stiffness was critical. The estimated fin torsional frequency was 145 cps while the required frequency to prevent flutter was 90 cps. So stiffness was not a structural design restraint. The entire fin structure can be removed by disconnecting the main spar splices in the tunnel area.

The tip fin structure, by virtue of its antisymmetric heating environment, uses a single skin corrugation cover. This will again minimize thermal restraint and resulting thermal stress weight penalties. The main bending spars are attached to bulkheads in the body tip fin support structure. These in turn distribute the loads into the body reaction torque box. The refurbishment is accomplished by removing the windward and leeward surface skins and reapplying the ablative heat shield material. The leeward surface is detached which then makes the windward surface attachments accessible. The leading edge of the tip fin will be replaced after each flight.

Control surfaces.- All control surfaces use titanium material. Generally, all surfaces are full torque boxes and are driven at one end through a torque tube and control surface rib. The center and tip fin surfaces use three hinge points, of which the base hinge is fixed and the other two are unrestrained in the hinge line direction. All control surface actuators are located in the aluminum structural area. In addition, all surfaces incorporate a bearing heat shield segment which is used to block heat during rotation.

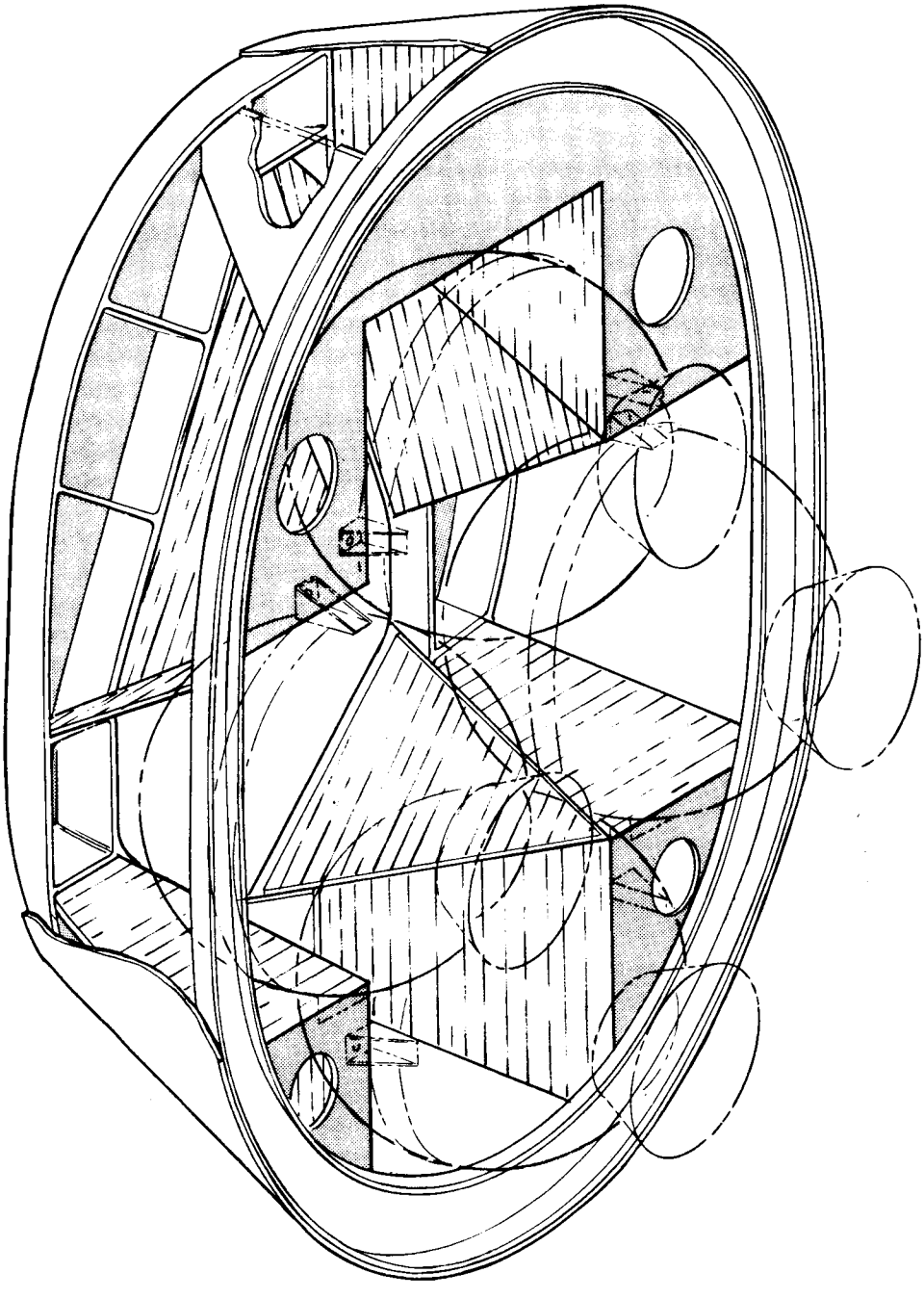

FIGURE 19. ADAPTER STRUCTURE WITH ABORT/DEORBIT ENGINES

Adapter. - The adapter is a conventional skin-stringer-frame aluminum structure. Each end has a load distribution frame or bulkhead. The abort motor loads are taken by an internal web system which then transfers the loads to the entry vehicle-adapter interface pickup points (fig. 19).

C. LANDING AND EMERGENCY RECOVERY

1. Landing System

Based on the results of the parametric vehicle design study phase, the configuration selected for the D/3 vehicle is geometrically that of a conventional tricycle airplane gear (fig. 20). The main gear in this configuration is located aft of and close to the center of gravity of the vehicle. The controlling longitudinal location places the vehicle center of gravity just over or slightly forward of main gear when at the maximum touchdown angle of 25° (0.436 rad) (fig. 21). The optimum longitudinal location of the nose gear and lateral offset of the main gears result in a configuration which provides the vehicle with a roll-over (lateral) stability factor of 0.67 g.

An air-oil shock absorbing system is used for both the main and nose gear. Main gear flotation is provided by wire brush skids with touchdown wheels which result in minimum vehicle pitching at touchdown and maximum drag characteristics during slide out. The nose gear dual co-rotating wheels result in a drag ratio (main gear to nose gear) of approximately 40 to 1, providing good slide-out stability. A braking deceleration chute is provided to reduce slide out to a minimum and to provide additional slide-out stability. The slide-out analyses conducted in the parametric vehicle design study (Part IV) indicate the HL-10 can land on a 150 foot (45.6 m) wide and 10 000 foot (3050 m) long runway in a 20-knot (10.25 m/sec) crosswind by use of aerodynamic rudder control. This landing system was designed in accordance with the following specifications and design criteria:

Military Specifications:

MIL-S-8552--Strut, aircraft shock absorber (air-oil type)

MIL-T-6053--Tests, impact, shock absorber, landing gear, aircraft

MIL-W-5013--Wheel and brake assemblies, aircraft

MIL-A-8862--Airplane strength and rigidity--landplane landing and ground loads

MIL-A-8866--Airplane strength and rigidity--reliability requirements, repeated loads and fatigue

MIL-C-5041--Castings, aircraft pneumatic tire

MIL-T-5014--Tubes, inner, aircraft pneumatic tire

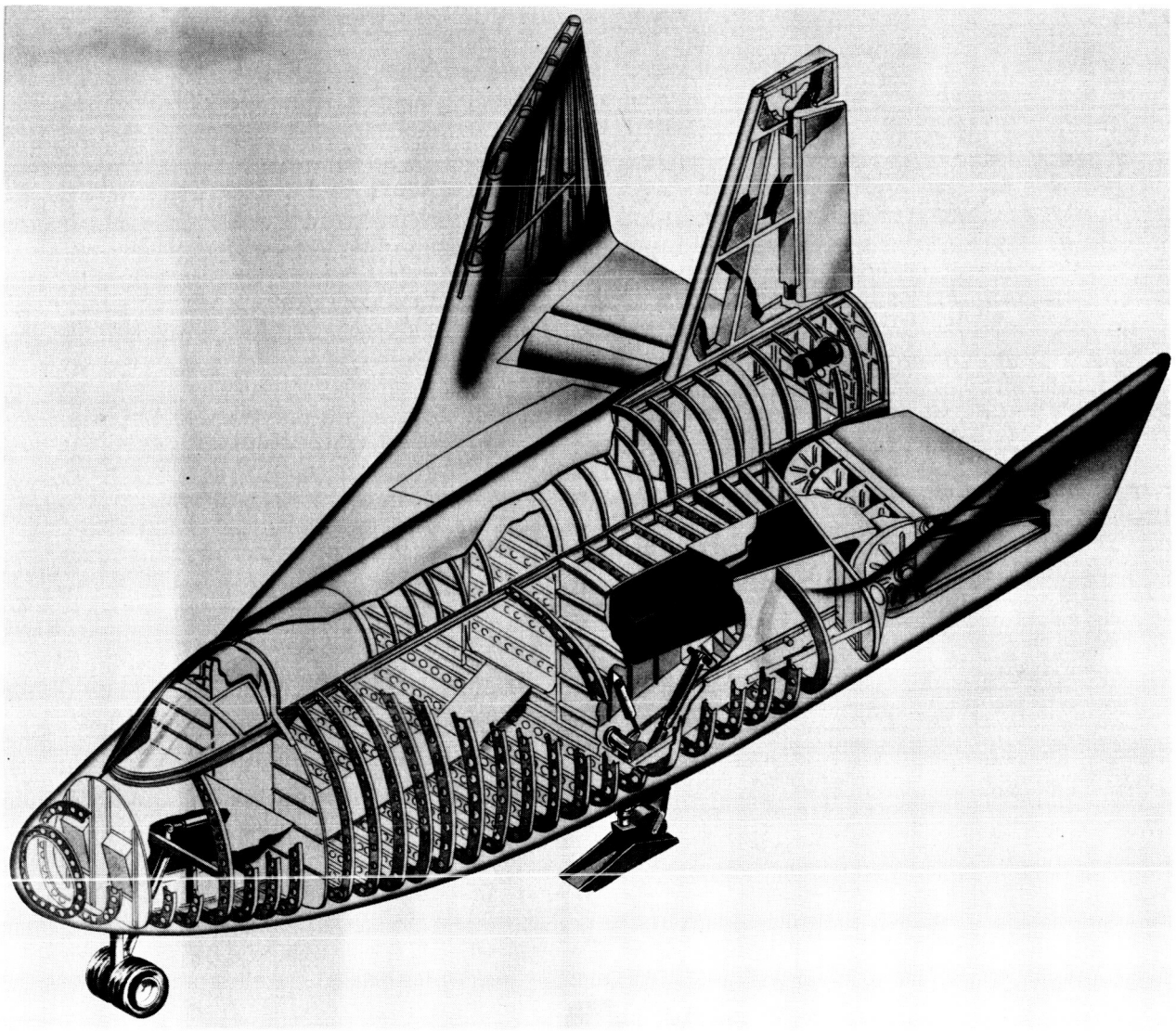

FIGURE 20. CONCEPT OF LANDING AND RECOVERY SYSTEM

MIL-D-9056--Aircraft deceleration parachute system, general requirements for

AFSCM-80--Handbook of instructions for aircraft designers.

Design Criteria:

Horizontal touchdown velocity--200 to 230 knots (102.5 to 117.5 m/sec)

Vertical sink velocity--13 fps (3.96 m/sec)

Maximum vertical load factor--4.0 g

Vehicle angle of attack at touchdown--20 to 25° (0.349 to 0.436 rad)

Maximum design crosswind--20 knots (10.25 m/sec)

Gear extension period--2 sec max.

Gear well temperatures:

Ascent temperature of 125° F maximum for approximately 10 minutes

In-space environment for periods of up to 15 orbits with gear well temperature range of +40° to +100° F

Entry gear well temperature of 200° F maximum for a period of approximately 30 minutes.

Gear shock absorbing stroke for 4-g load factor:

Kinetic energy of vehicle = $1/2\ MV^2$

= 32 300 ft-lb (43 800 J)

Shock strut energy = W x L. F. x S x EFF

= 39 600 S-ft-lb (53 300 J)

$$\text{Stroke} = \frac{KE_V}{E_S} = 0.815 \text{ ft} = 10 \text{ in.} = 0.25 \text{ m}$$

Used stroke = 10 in. (0.25m). Show 11 in. (0.28m) available.

Where:

M = vehicle mass

V = sink velocity at touchdown

W = vehicle weight

S = shock strut stroke

EFF = shock strut efficiency = 80%

L. F. = landing gear load factor.

Nose gear installation. - The nose gear, geometrically located as shown in figure 21, utilizes a relatively simple design concept (fig. 22). The co-rotation feature of the dual wheels inherently provides the required antishimmy characteristics. Centering cams incorporated in the design of the upper and lower bearing installation of the shock strut maintain a centered position of the wheels until some shock strut deflection is realized. Located on the axle socket is the sequence switch, which is the terminal function for deploying the deceleration chute. The gear is held in the stowed position by anchoring the drag strut to the vehicle structure with a bolt and explosive nut. The gear is extended by a pneumatic actuator pressurized by a self-contained pyrotechnic gas generator (fig. 23). Doors supported on goose-neck hinges (necessary due to door thickness) are opened by a fixed-length mechanical link attached to the oleo strut. The gear after extension is held in the down and locked position by a dead-center locked position of the drag strut (fig. 23). Specific component weights as associated with the nose gear installation are shown in table 9.

TABLE 9

D/3 NOSE GEAR WEIGHT

	Weight	
	lbM	kg
Nose gear tires (2 units)	10.8	4.91
Nose gear tire tubes (2 units)	4.2	1.91
Nose wheels (2 units)	14.4	6.56
Piston socket assembly with axle and bearings	20.8	9.46
Cylinder and trunnion assembly	23.2	10.55
Piston and upper bearing	11.2	5.09
Lower bearing--seal collar and centering cam	5.1	2.32
Stand pipe and orifice	2.5	1.14
Metering pin assembly	1.7	0.77
Wheel and miscellaneous bolts	8.8	4.00
Drag strut assembly	15.7	7.14
Oleo trunnion caps	2.6	1.18
Drag strut trunnion caps	2.6	1.18
Gear actuating cylinder assembly	8.9	4.05
Door actuating linkage (at 5 lb each)	10.0	4.54
Weight total assembly	142.5	64.80

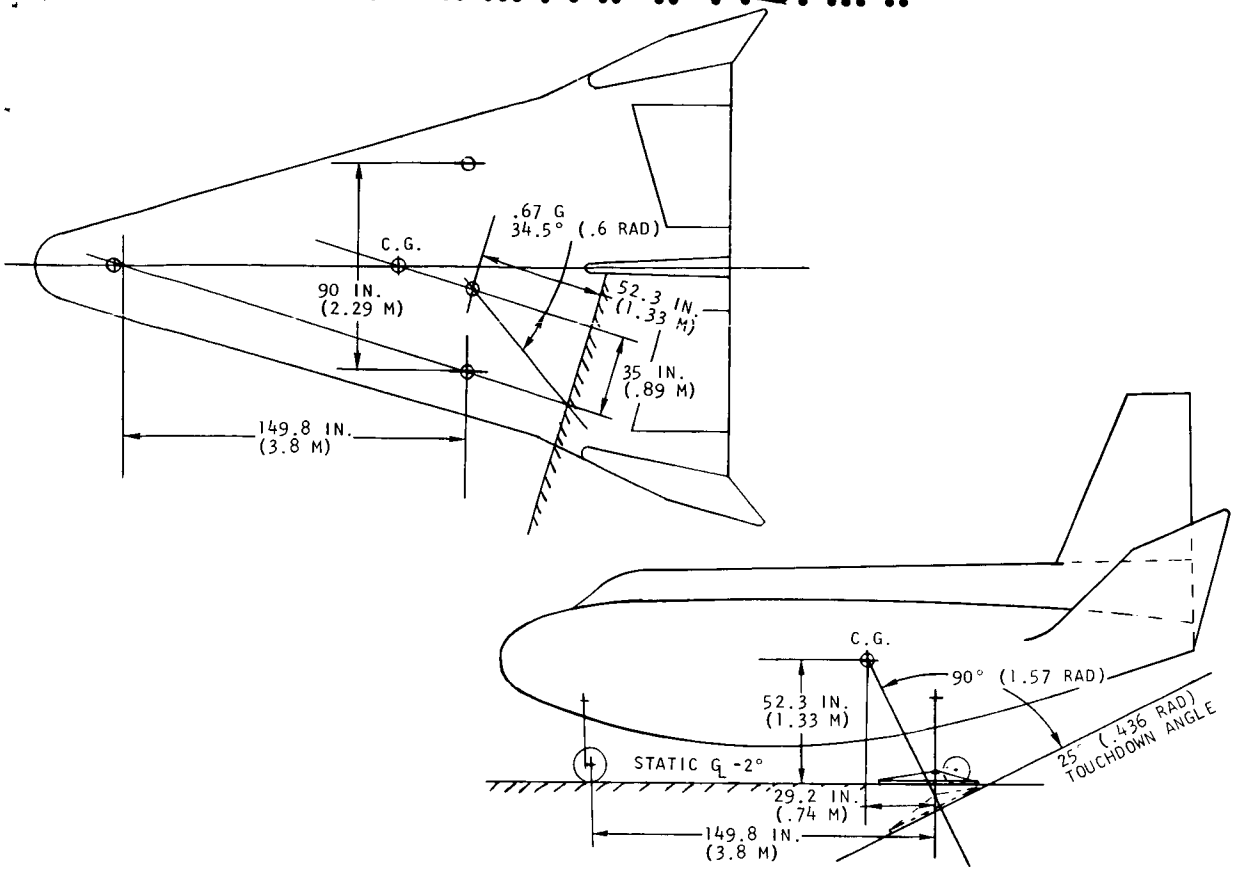

FIGURE 21. D/3 VEHICLE LANDING GEAR LOCATION

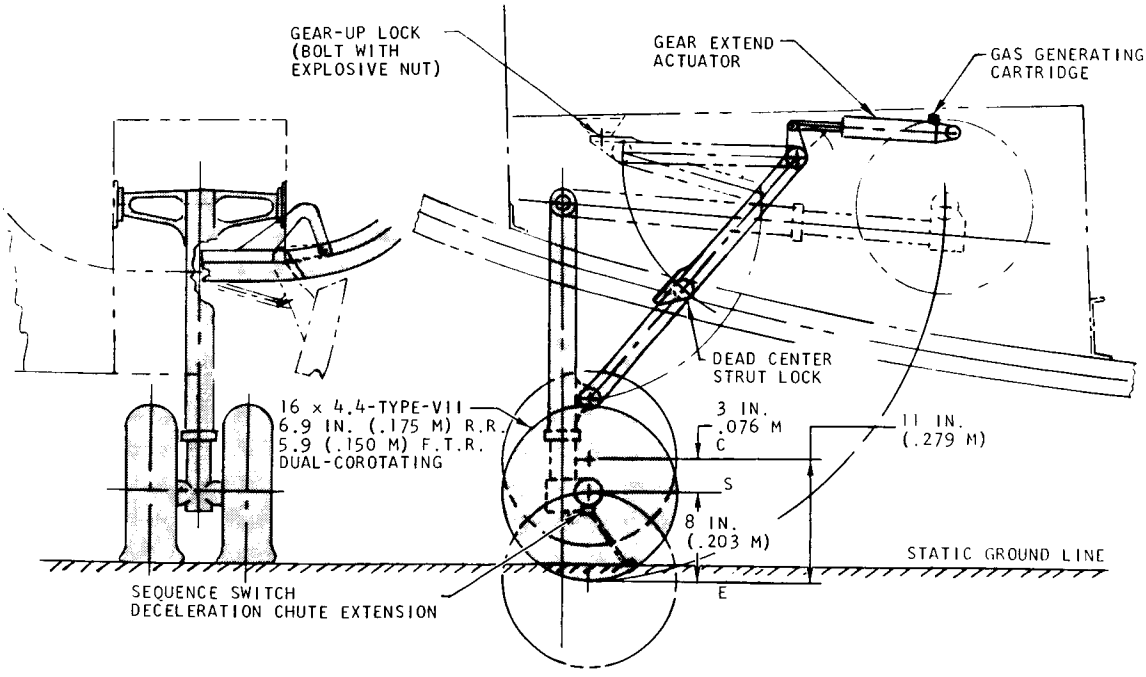

FIGURE 22. NOSE GEAR INSTALLATION

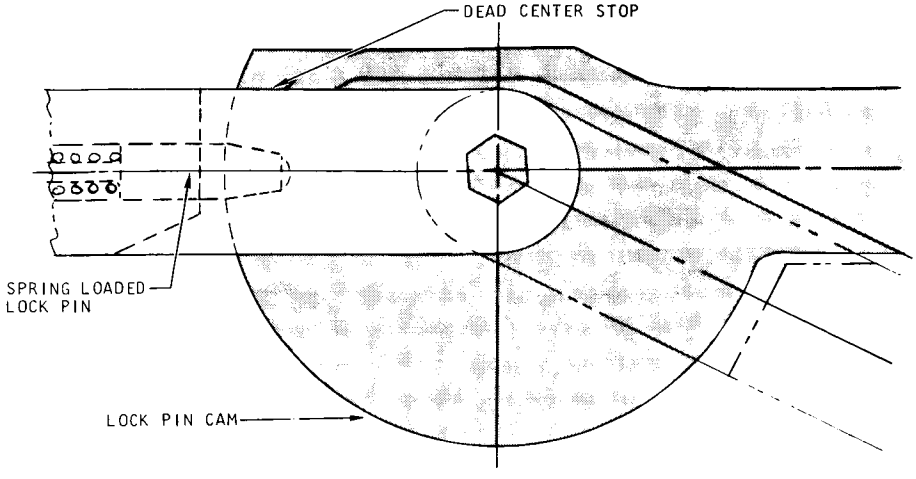

TYPICAL STRUT LOCK
(SCHEMATIC)

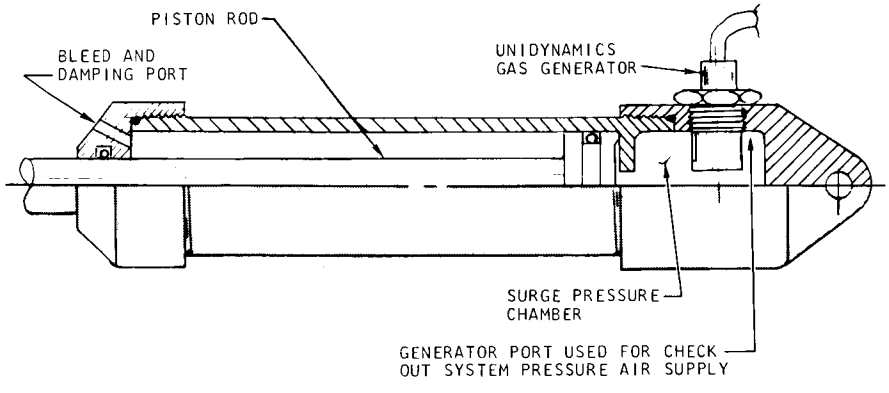

FIGURE 23. TYPICAL GEAR ACTUATOR

Main gear installation. - The main gear incorporates a wire brush skid to provide vehicle flotation (fig. 24). This skid (fig. 25) is a design version of the skid proposed by the Goodyear Tire and Rubber Company for the Dyna-Soar program. Incorporated to function in conjunction with this skid is a touchdown wheel rigidly positioned on the lower extremity of the main gear shock strut. The wheel is geometrically located so that when the vehicle touches down in nose-up attitude the wheels make the only contact with the ground, thereby presenting a low drag, and thus eliminating the pitch condition. With the vehicle in the three-point attitude, the wheel is free of ground contact and the vehicle is supported on the skid. The skid has the high drag characteristics necessary for decelerating the vehicle.

The gear is held in the retracted position by a bolt and explosive nut attached to a lug provided on the drag strut trunnion bar. Gear extension is by actuator incorporating its own self-contained pyrotechnic gas generator (fig. 23). The gear after extension is held in place by dead-center locking of the drag strut (fig. 23). Component weights as associated with the main gear installations are shown in table 10.

TABLE 10

D/3 MAIN GEAR WEIGHT

	Weight	
	lbM	kg
Main gear skid	41.4	18.80
Touchdown wheel	15.0	6.66
Axle assembly (touchdown wheel)	1.4	0.62
Skid bolt	0.8	0.36
Piston assembly	37.2	16.90
Torque arm assembly	8.9	4.04
Skid positioner	8.9	4.04
Cylinder and trunnion assembly	36.8	16.70
Lower bearing and seal assembly	2.7	1.23
Metering pin assembly	1.9	0.84
Stand pipe and orifice plate	3.9	1.23
Miscellaneous bolts	3.0	1.36
Drag strut assembly	15.6	7.10
Oleo trunnion caps	2.6	1.18
Drag strut trunnion caps	2.6	1.18
Gear actuator	8.9	4.04
Main gear door linkage	5.0	2.27
Total weight	196.6	89.05

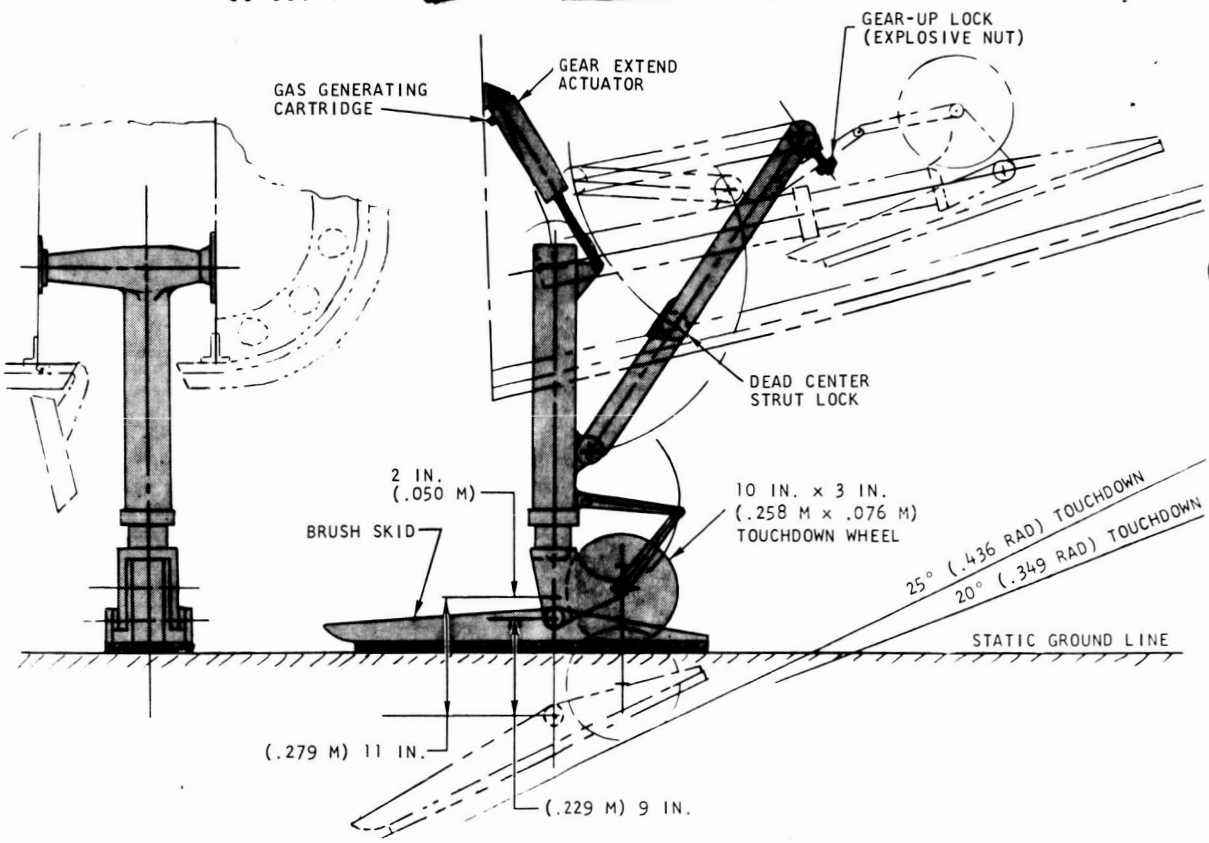

FIGURE 24. MAIN GEAR INSTALLATION

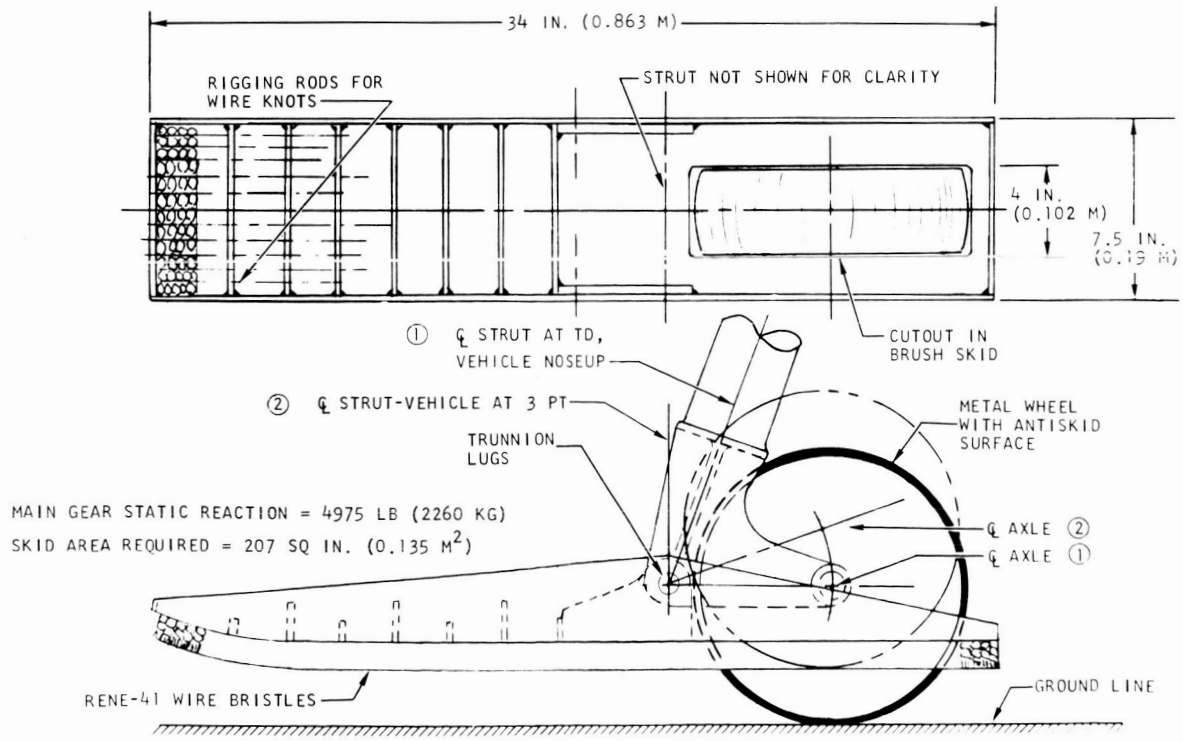

FIGURE 25. WIRE BRUSH SKID WITH TOUCHDOWN WHEEL

Deceleration brake chute. - The braking chute system is provided to shorten the vehicle slide-out distance and to improve vehicle slide-out stability during this period (fig. 26). The system is activated by the pilot just prior to entering the last flare maneuver before landing. The chute system by this activation becomes anchored to the vehicle by a solenoid lock which is incorporated to protect against inadvertent chute ejection. The pilot chute, however, will not be ejected until closure of final sequence switch which is automatically activated by nose gear contact on the runway. Basic characteristics of the chute installation are presented in table 11.

TABLE 11

D/3 BRAKING CHUTE WEIGHT AND STOWAGE VOLUME

Item No.		Weight lbM	Weight kg
1	14 ft diameter (4.26 m) chute	3.0	1.36
2	4.62 ft^2 (0.43 m^2) pilot chute	0.8	0.36
3	Chute risers	3.0	1.36
4	Chute bag	1.3	0.55
5	System controls	4.0	1.82
6	External fittings, etc.	7.0	3.19
	Total weight	19.1	8.64

NOTE: System volume for Items 1 through 4, based on packing density of 40 lb/ft^3.
Stowage volume required $= \frac{8}{40} = 0.2\ ft^3$ (0.056 m^3).

Using 14 ft (4.26 m) diameter chute.

Recovery area (Edwards) at 2300-ft (7000 m) altitude.

Chute drag, $D_c = C_{D_o} S \frac{1}{2} \rho V^2 = 0.094\ V^2$

where

C_{D_o} = chute drag coefficient = 0.55

S = chute area = 154 ft^2 = (14.3 m^2)

ρ = air density = 0.00222

V = vehicle velocity (fps).

ER 14471-7

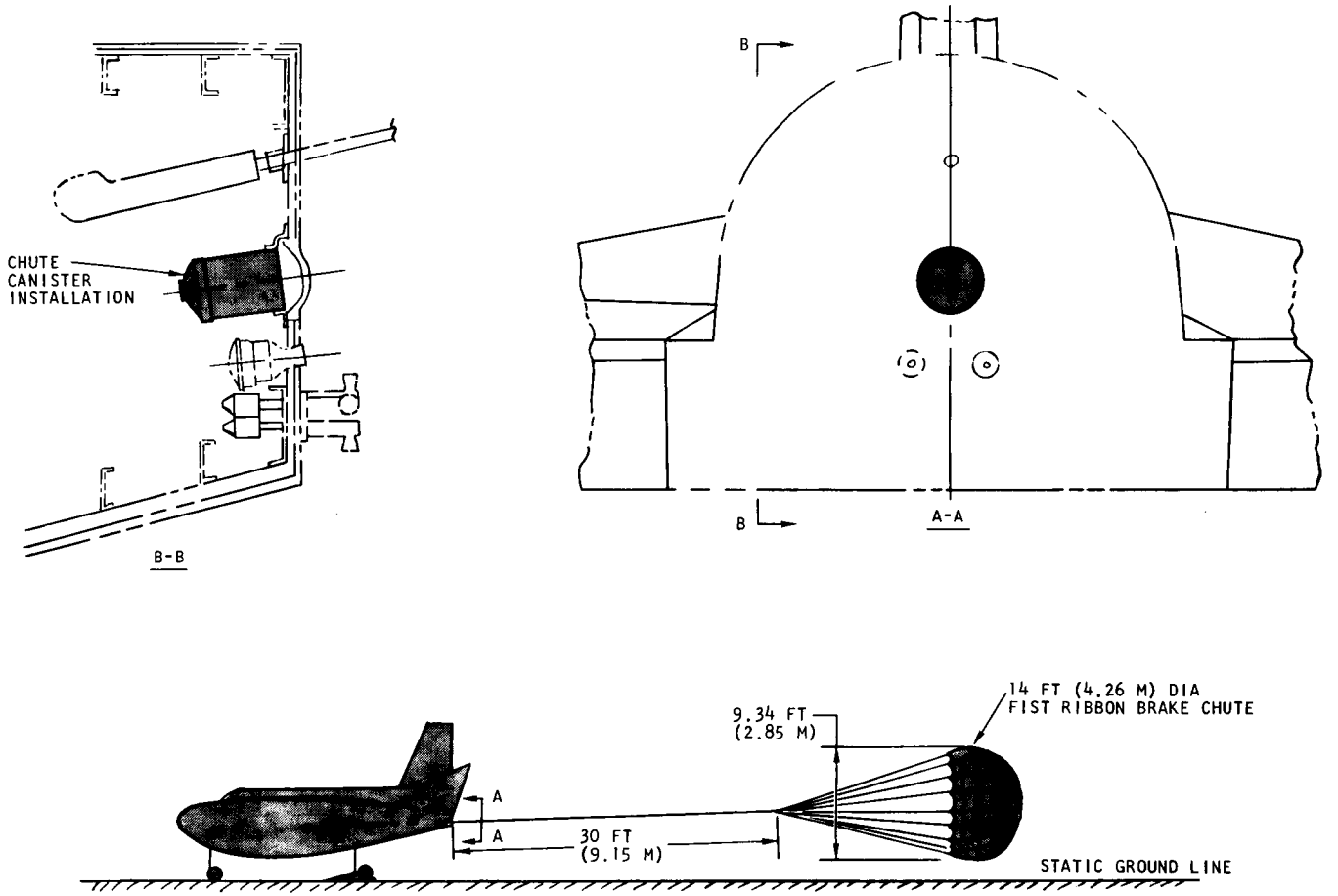

FIGURE 26. BRAKE CHUTE CONFIGURATION

For landing angle of attack =

25° - V = 197 knots = 331 fps (101 m/sec)

D_c = 10 250 lb (45.7 kN) = 0.83 g.

Opening shock = 0.00244 r^2 V^2 = 13 150 lb (58.5 kN) = 1.07 g

20° - V = 226 knots = 380 fps (116 m/sec)

D_c = 13 550 lb (60.3 kN) = 1.1 g.

Opening shock = 0.00244 r^2 V^2 = 17 300 lb (77.0 kN) = 1.4 g.

Pilot chute area required = 0.03 drag chute area

C_p = 4.62 ft^2 (0.43 m^2)

Landing system weight. - Summary weights for the landing system are:

		lb	kg
A	Nose gear weight	142.5	64.8
B	Left main gear weight	196.6	89.1
C	Right main gear weight	196.6	89.1
D	Deceleration brake chute	19.1	8.7
	Total weight	554.8	251.7

Percent of total vehicle weight = $\frac{554.8}{12\ 342}$ = 0.0450 lb.

Landing system performance. - Vehicle performance during slide-out phase was investigated for two general runway conditions consisting of a skid drag coefficient of 0.6, representing lake bed conditions, and a coefficient of 0.4 representing improved runway conditions. Vehicle performance for these conditions together with a 20-knot (10.25 m/sec) crosswind for fixed rudder settings of +20° (0.349 rad), 0° and -20° (0.349 rad) are reflected in figures 27 through 30.

In summary, it can be concluded that the D/3 vehicle can land successfully on an improved runway of limited width under adverse crosswind conditions of 20 knots (10.25 m/sec).

The drag from gear reactions is calculated in the following manner.

For a 14-foot diameter chute at recovery area altitude of 2300 feet (7000 m)

Chute drag, $D_c = C_{D_o} S \frac{1}{2} \rho V^2$

$= 0.094\ V^2$

[redacted]

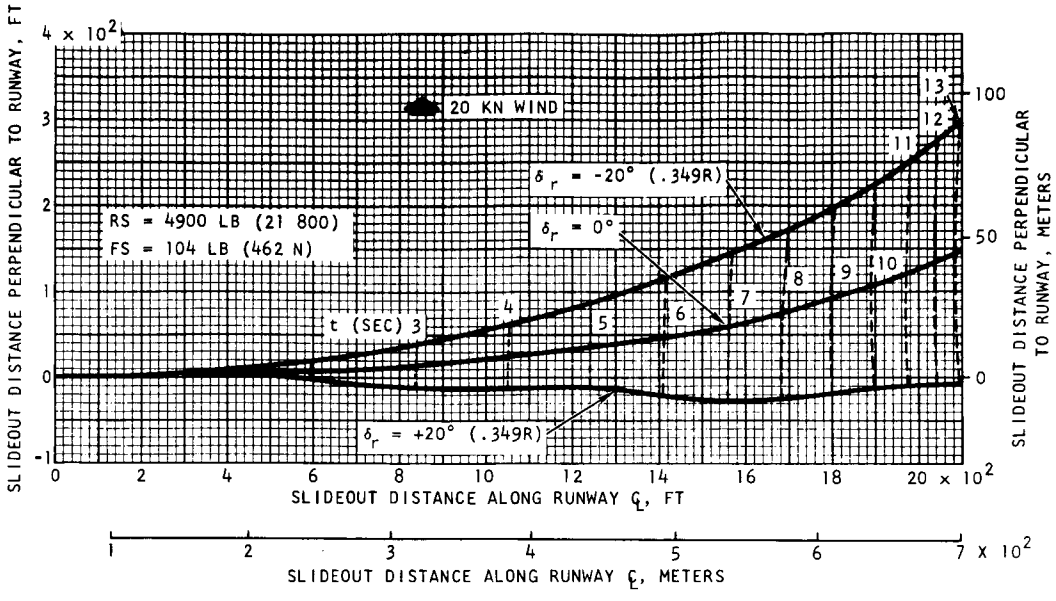

FIGURE 27. SLIDEOUT ON LAKE BED WITH DRAG CHUTE

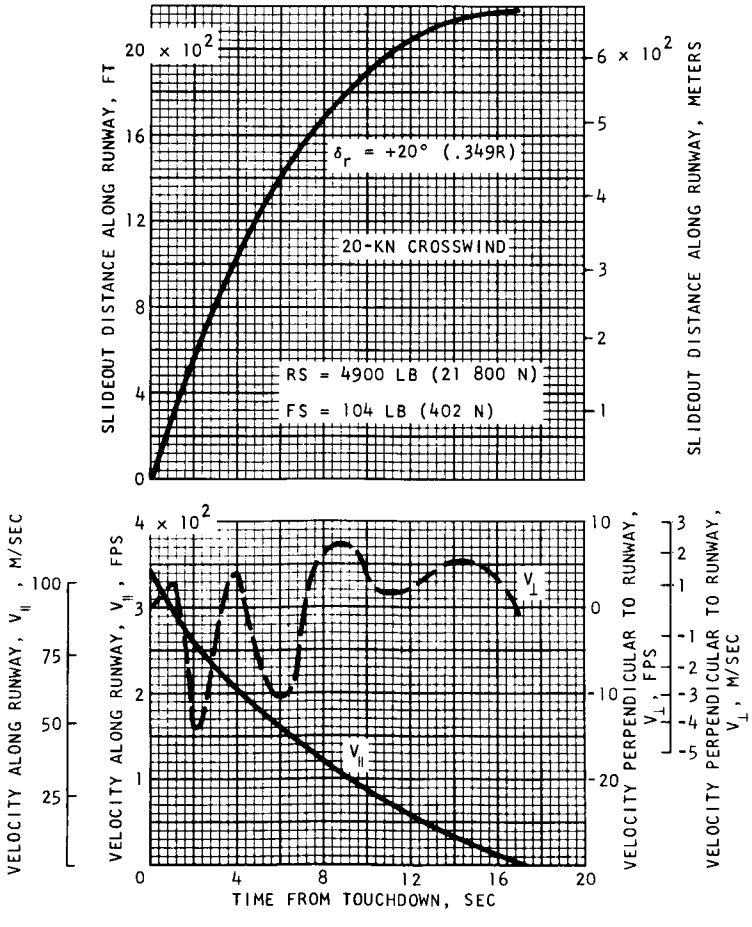

FIGURE 28. SLIDEOUT VELOCITY AND TIME ON LAKE BED WITH DRAG CHUTE

[redacted]

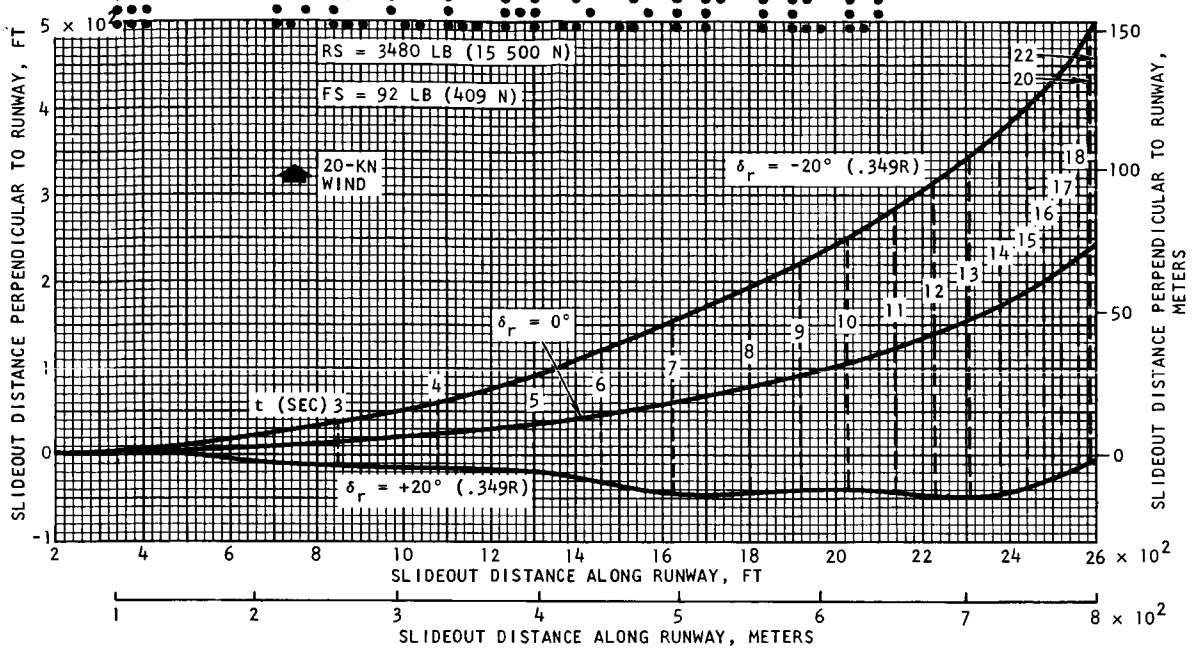

FIGURE 29. SLIDEOUT ON IMPROVED RUNWAY WITH DRAG CHUTE

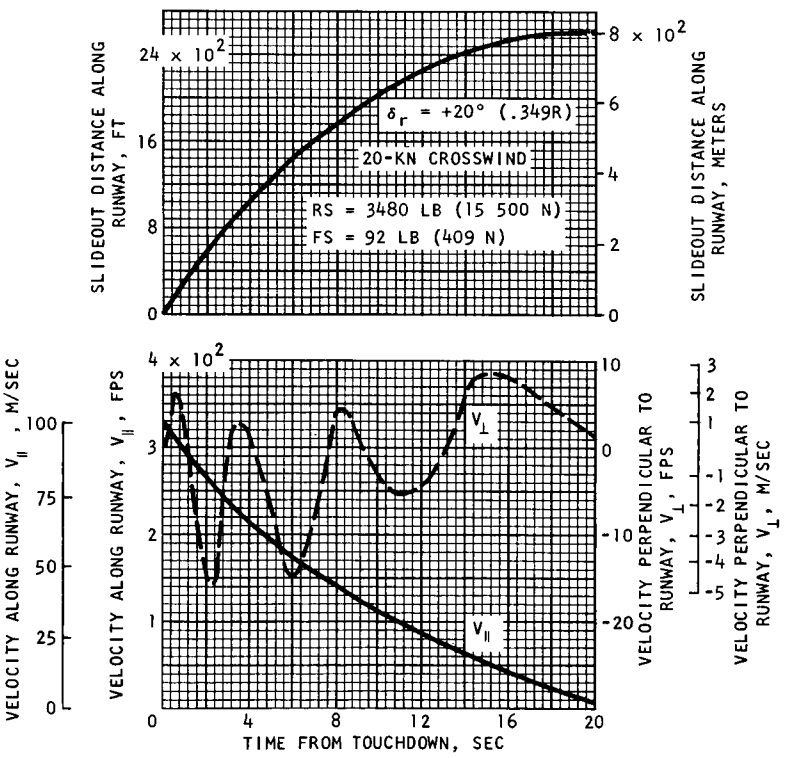

FIGURE 30. SLIDEOUT VELOCITY AND TIME ON IMPROVED RUNWAY WITH DRAG CHUTE

Chute $K_2 V^2$ airspeed = 0.094 V^2 airspeed

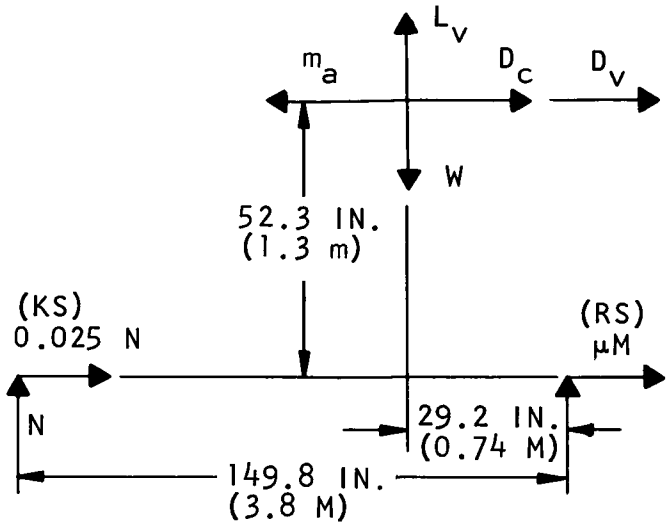

D_c = chute drag	N = nose gear reaction ⊥ runway
D_v = vehicle drag	M = main gear reaction ⊥ runway
W = vehicle weight	μ = skid friction coefficient
L_v = vehicle lift	0.025 = rolling friction coefficient
Ks = nose wheel drag	Rs = rear skid drag

With vehicle attitude of -2° in three-point condition, L = 0.

Solving for N and M

$$\Sigma_H = 0 = m_a - D_c - D_v - 0.025\,N - \mu M = 0$$

$$\Sigma_V = 0 = N + M + L_v - W = 0$$

$$\Sigma M_{c.g.} = 0 = 120.6\,N - 29.2\,M - (0.025\,N + \mu M)\,52.3 = 0$$

M = W - N substituting for M above and using values of μ = 0.6 and 0.4 result in

for μ = 0.6

N = 4160 lb	M = 8182 lb
KS = 104 lb	RS = 4900 lb

for $\mu = 0.4$

N = 3660 lb	M = 8682 lb
KS = 92 lb	RS = 3480 lb

2. Emergency Recovery System

The recovery system will be used as the emergency means of assuring safe crew recovery in the event of an ascent abort or any other emergency requiring flight termination away from a prepared landing site. Since the system will be used only in emergencies, the vehicle structure over each of the chute canisters located in each of the main gear compartments will be cut by pyrotechnic shaped charges as the initial effort in activating the recovery system. Immediately following this event (controlled by a time delay relay), the gas generators in the canister positioning actuators (fig. 23) will be fired, causing the after end of the canisters to protrude above the vehicle surface (fig. 31). Canister positioning geometry is established to align the canister parallel with flight paths for ease of chute package extraction.

The chute packages stowed within the canisters will be sealed and pressure-vented to minimize space exposure effects on the parachute materials. Stowed within each canister are the 20-foot (6.1 m) diameter pilot chute, the pilot chute ejection mortar, and the bag containing two 91.6-foot (28.0 m) diameter ring sail recovery chutes and their suspension lines. The steel cable chute risers and vehicle harness connecting the dual chute installations are imbedded in the vehicle ablative covering.

With the canisters in position, the pilot chutes are ejected by firing of the mortars. These chutes provide the drag necessary to extract the main chute packages. The main chute risers, upon becoming taut, generate a resisting force to the chute package which is being accelerated by the pilot chute. This resisting force breaks the riser tie-down to the chute pack, opens the end of the chute pack, and begins to extract the chute suspension lines, which in turn are followed by the chute canopy.

The chutes are extracted in a reefed condition of approximately 2.5 percent of full chute canopy. The junction point of the two chute risers and the vehicle harness is anchored at this time to a structural point on the vehicle. This location establishes a chute force line directly through the center of gravity of the vehicle, reducing vehicle perturbations to a minimum.

The chutes will remain in the reefed condition and anchored until the vehicle reaches predicted terminal velocity pressure "q" conditions. When this condition is reached, a "q" switch will initiate dereefing and activate the mooring release, allowing the vehicle riser and harness cable to tear through the ablative material to its final anchorage point. This anchorage positions the vehicle in a tail-down, 70° inclination for land or water impact.

The angle of 70° was selected on the basis of data available from tests conducted by NASA-Langley (ref. 4). The 70° penetration in water, at sink velocities well above these provided by this recovery system, will result in relatively low load factors and assure vehicle recovery after water penetration to a right-side-up attitude. For land-based recovery, the vehicle in this attitude will provide the crew with optimum posi-

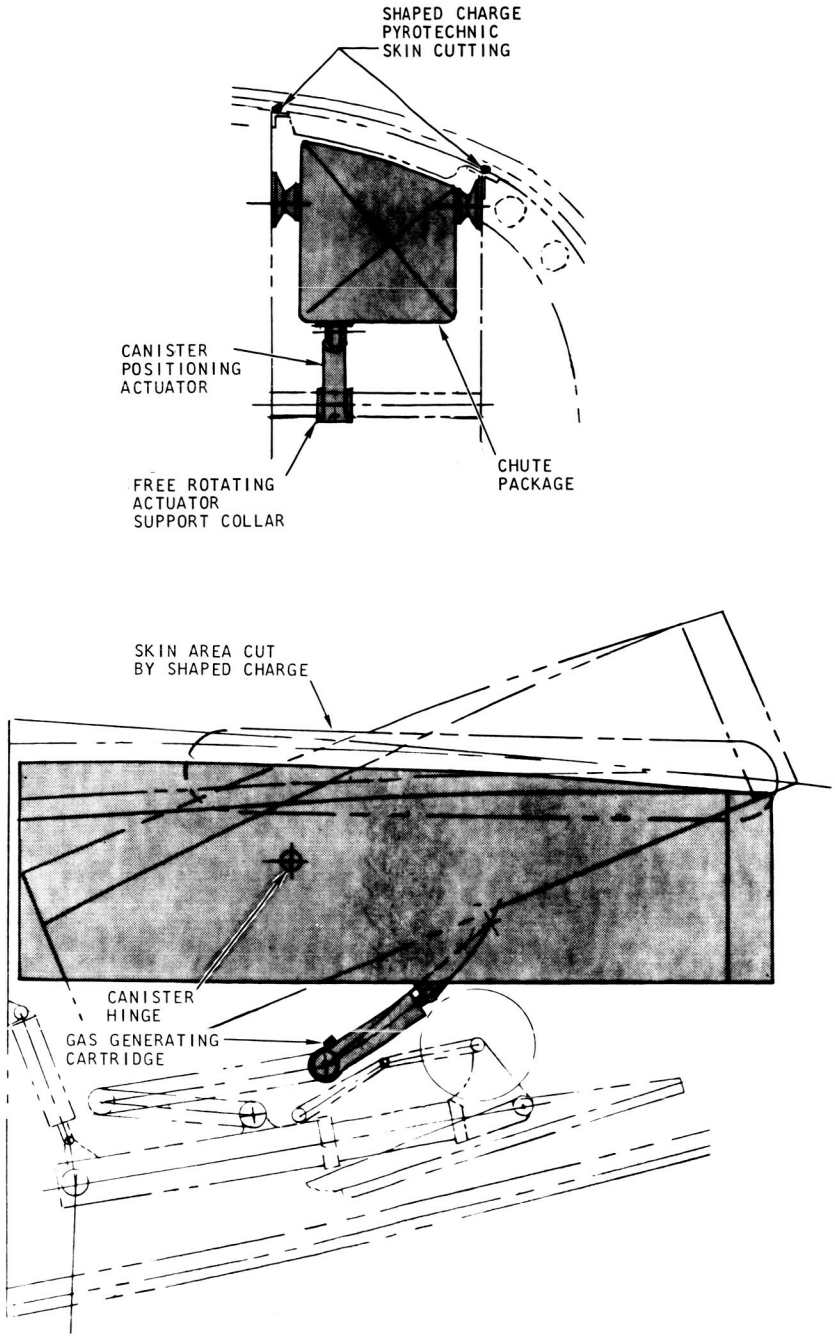

FIGURE 31. RECOVERY CHUTE INSTALLATION

tioning for deceleration and will permit maximum structural deformation for impact energy absorption. With the vehicle in this attitude, the physical attachment point of the riser to the vehicle is considerably forward of the vehicle center of gravity, establishing a geometric force line advantageous for dampening vehicle tendency to pitch at impact. With the vehicle hanging in free suspension, the attitude control system can be used to retain the vehicle in the desired attitude (bottom side windward) for landing in a ground wind drift condition. The recovery chutes release will be activated by the pilot after completion of recovery.

For the pad abort condition, the "q" switch setting will not be exceeded, thereby permitting the chutes to bypass the reefing cycle during the pad abort recovery mode. Preliminary analysis indicates that, even at a minimum pad abort boost altitude of 1500 feet (458m), ample time exists for full chute deployment and vehicle deceleration to the terminal velocity of 25 fps (7.62 m/sec).

Basic computations and schematics are reflected in the following pages and in figures 31, 32 and 33. The recovery system weight is summarized in table 12.

TABLE 12

RECOVERY SYSTEM WEIGHT

	Weight	
	lb	kg
Pilot chute mortar guns (2)	20	9.10
Pilot chutes (2)	24	10.90
Pilot chute bridles (2)	16	6.80
Main chute bags (double compartment) (2)	30	13.63
Main chutes (4)	440	200.00
Main chute risers (4)	33	15.00
Vehicle harness (1)	20	9.10
Chute disconnects (2)	12	5.45
Chute canisters and actuators (2)	60	27.20
Control and sequence and power	23	10.40
System weight	675	307.58

Required main chute area. -

$$V_e^2 = \frac{2W}{\rho C_{D_o} S}$$

ER 14471-7

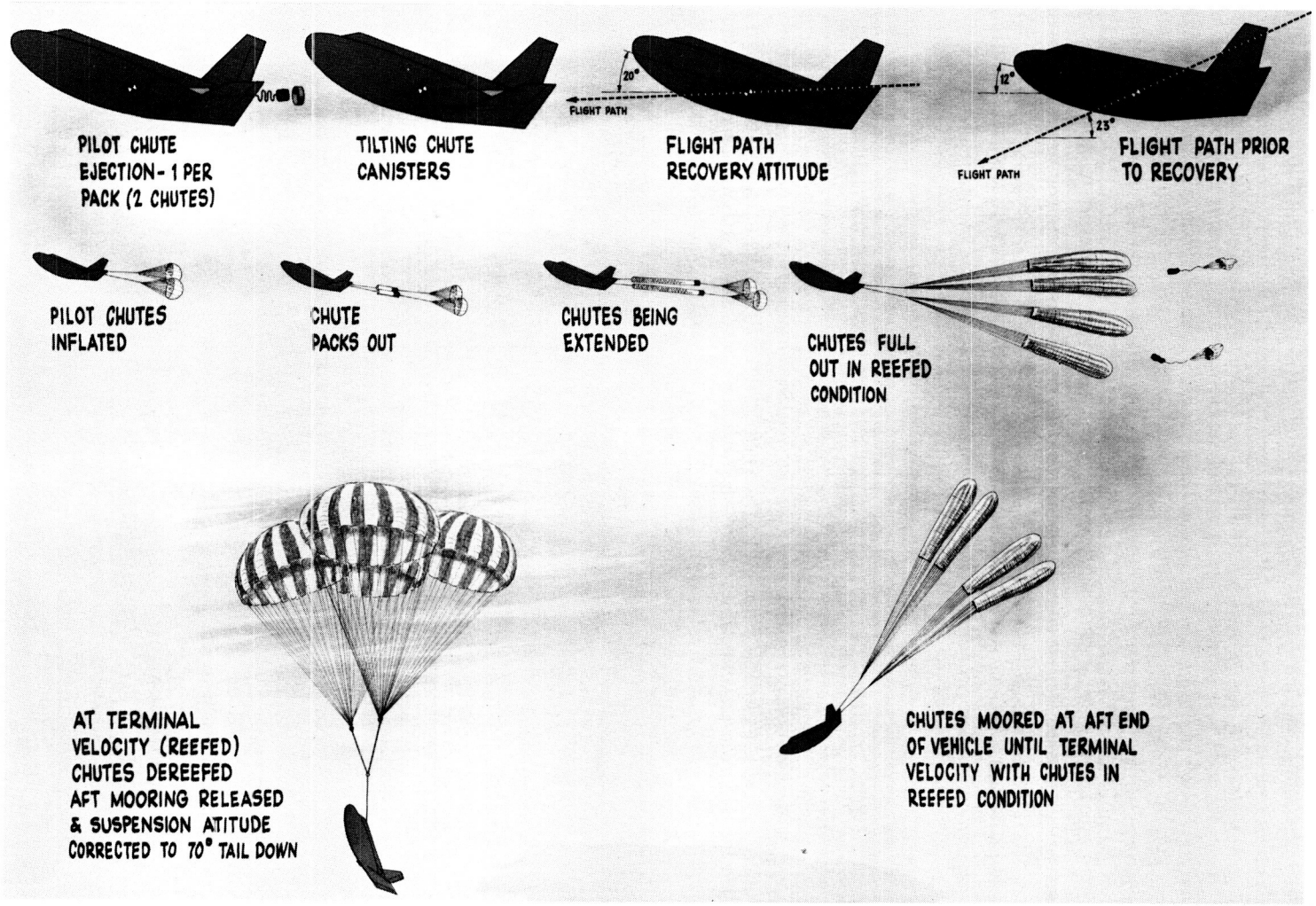

FIGURE 32. RECOVERY SEQUENCE

$$S = \frac{2W}{\rho C_{D_o} V^2}$$

For

V_e = 25 fps (7.02 m/sec)

S = 26 400 ft^2 (2450 m^2)

where

W = vehicle weight

ρ = 0.00222 density at 2300 ft (700 m)

C_{D_o} = chute drag coefficient

S = chute area

V_e = terminal velocity

C_{D_o} = for single chute = 0.78

C_{D_o} = for cluster chutes = 0.78 x 0.865

= 0.675

Using four chute cluster

S/chute = 6600 ft^2 (613 m^2)

Chute dia = 91.6 ft (28.0 m)

Required extraction chute area.- Each extraction chute must supply drag sufficient to extract the package containing two main chutes. Minimum vehicle velocity condition occurs when the system is used in pad abort recovery. Vehicle velocity under this condition is predicted at 135 fps (41.2 m/sec) minimum.

Recommended practice from the parachute handbook (ref. 5) is to use a pilot chute $C_{D_o} S \approx$ to 0.03 main chute $C_{D_o} S$ for velocities to 200 knots. Therefore, since only one pilot chute is used per side.

$$S_p = \frac{0.03 \times 13\,200\ (1226\ m^2) \times 0.675}{0.78}$$

S_p = 342 ft^2 (31.7 m^2)

= 20 ft (6.1 m) diameter.

Pilot chute drag at minimum vehicle velocity - 135 fps (41.2 m/sec) =

$$D_p = 1/2\ \rho\ C_{D_o}\ S\ V^2$$

$$= 5400 \text{ lb } (2450 \text{ kg}).$$

Chute package to be extracted = 503 lb (228 kg); drag to weight ratio = 10.7.

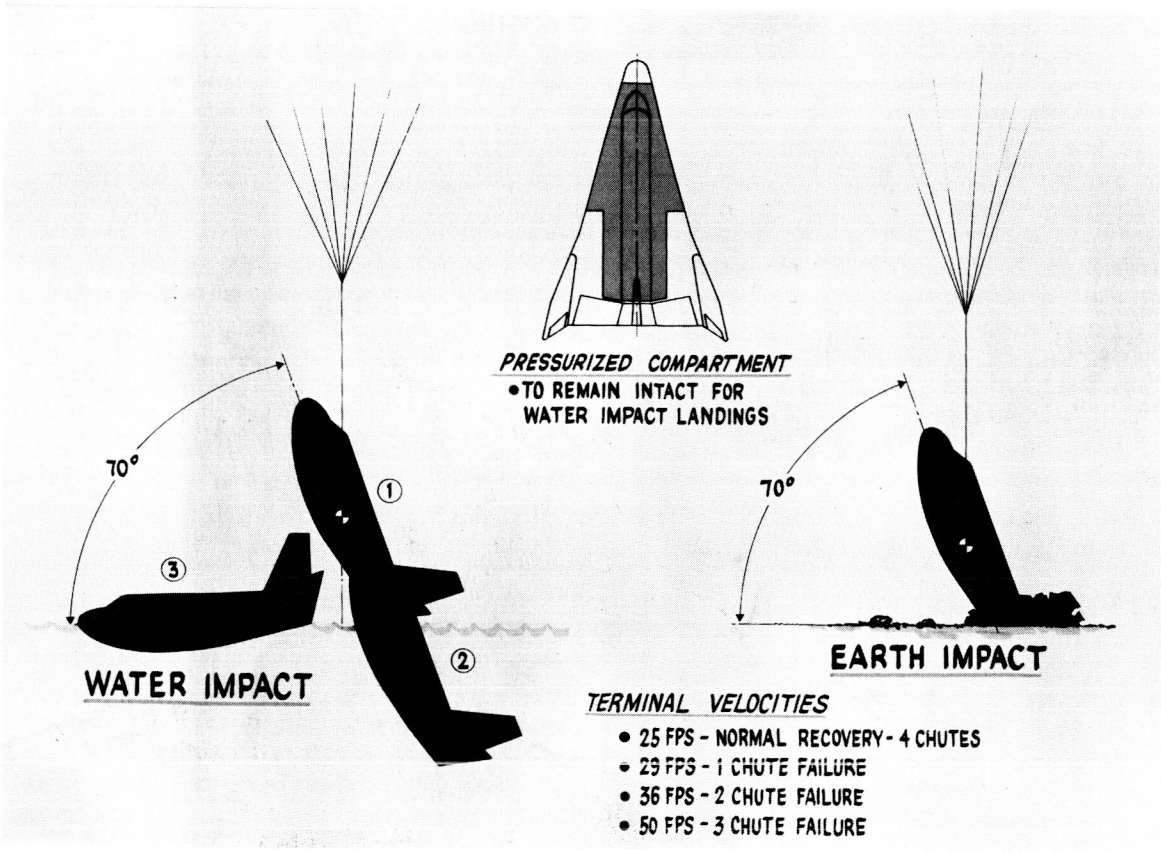

FIGURE 33. RECOVERY IMPACT

D. CREW STATION

This section describes the crew station studies conducted for the detail preliminary design of the D/3 vehicle. The primary effort centered around the fabrication and development of a spatial mockup of the D/3 crew station area. Three studies were conducted with the mockup: (1) pilot window visibility during landing, (2) instrument panel display area and arrangement, and (3) mobility including ingress and egress.

1. Visibility

An important early task in this study was to determine the need for a canopy on a research version of the HL-10. This study task, described in Part IV, compared a no-canopy design using various indirect viewing subsystems (e.g., television and periscopes) with a canopy design providing the pilot with direct vision through a transparent windshield. Relative visibility, structural weight, reliability and safety aspects were all considered. While there may be important reasons in a future mission application of the HL-10 for employing indirect visibility (such as greater freedom in internal crew arrangement and providing more than one crew member with approach and landing control capability), the decision was made to use a canopy and direct vision as the primary operational mode. Indirect vision subsystems will be a subject of the flight research program.

For a typical manned operational mission, the following visual contact with the outside is required or desirable:

(1) Orbital transfer and rendezvous: acquire rendezvous target for orbit transfer and control.

   (a) Acquisition phase: acquire rendezvous target and maintain visual contact up to physical contact.

   (b) Undocking: visually confirm separation.

(2) De-orbit: visually confirm separation from retro package.

(3) Entry: visually confirm entry altitude prior to atmospheric re-entry at 400 000 feet (121.9 km).

(4) Landing approach: at 50 000 feet (15.2 km) visually sight the landing area.

Of these requirements, the first four do not pose serious design or vehicle configuration problems and can be satisfied with small window ports or remote viewing devices.

The landing maneuver, however, is the critical condition. It demanded a more thorough investigation to determine if adequate visibility can be provided by the transparent area contained within the confines of the canopy aerodynamic shape specified for the study.

Landing visibility criteria. - Certain visibility requirements must be satisfied to enable the pilot to control the entry vehicle from his visual acquisition of the landing site to the final touchdown and slide out. The landing process can be divided into three phases: (1) search and acquisition, (2) approach, and (3) landing. The visibility requirements for these three phases change, and they are also dependent upon a control approach link that can be used to provide information to the pilot.

The visibility requirements for the search and acquisition phase are prohibitive for direct or indirect viewing systems unless ground or on-board radar is used to direct the pilot to properly orient the vehicle to see the landing site. A ground radar system is considered best for this program. It has been considered in establishing the visibility requirements.

Once visual acquisition has been achieved, the pilot selects a preflare aim point and starts the final approach maneuvers. During these maneuvers, he should have sufficient vision to track the aim point. If this approach is to consist of turns up to 360° (6.28 rad), as used on the X-15, some side vision is required to see the aim point during the turn.

During the final approach phase, when the flare is initiated, the pilot must have a clear unobstructed view of the runway. Through the flare to runway threshold, he should be able to see the horizon and at least the runway edges. Once over the runway, if he has adequate peripheral vision to make final adjustments to the sink rate and alignment, forward vision is not absolutely required, but it is still desired. Figure 34 summarizes the landing visibility requirements.

Landing visibility studies. -

(a) Landing profiles: The flight path angle and the attitude angle history are used in determining the field of view to the pilot. The landing profile is described here with the detailed landing profile and performance studies reported in Part III.

An altitude-range history representative of an HL-10 entering from orbit is presented in figure 35.

For a typical return from orbit, the HL-10 approaches the landing site at a range-to-touchdown of 80 nautical miles (148.2 km) with an altitude of 115 000 feet (35.1 km), and a speed of 3900 fps (1.2 km/sec). The time to touchdown is 6 minutes. The vehicle flies toward the runway to a high key position of 80 000 feet (24.4 km) altitude and 2200 fps (671 m/sec). At about 45 000 feet (13.7 km) altitude and 900 fps (275 m/sec), a mid-key position is reached about 15 nautical miles (27.8 km) uprange of the runway with about 3 minutes to touchdown (fig. 36). The HL-10 then banks to initiate a 180° (3.14 rad) turn with a load factor of 1.2 g which is maintained. The turn radius of about 5 nautical miles (9.3 km) is used to get aligned with the runway at the low-key point when the speed has decreased to 600 fps (354 knots) (183 m/sec). Depending on the orbit from which the HL-10 is returning, the turn may be less than 180° (3.14 rad).

Figure 37 shows a typical landing trajectory for a D/3 configuration with a canopy.

Typically, the landing trajectory can be divided into two phases: a flare phase, and a float phase. During the flare phase, angle of attack is continuously increased

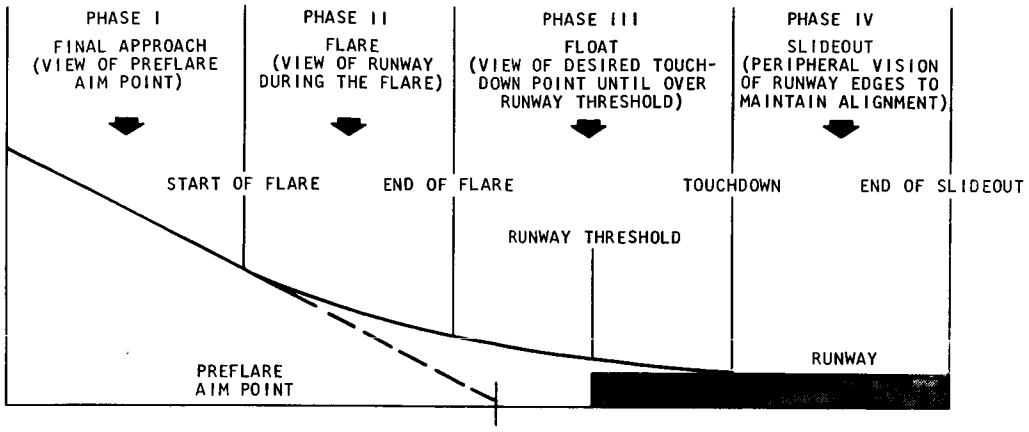

FIGURE 34. HORIZONTAL LANDING VISIBILITY CRITERION

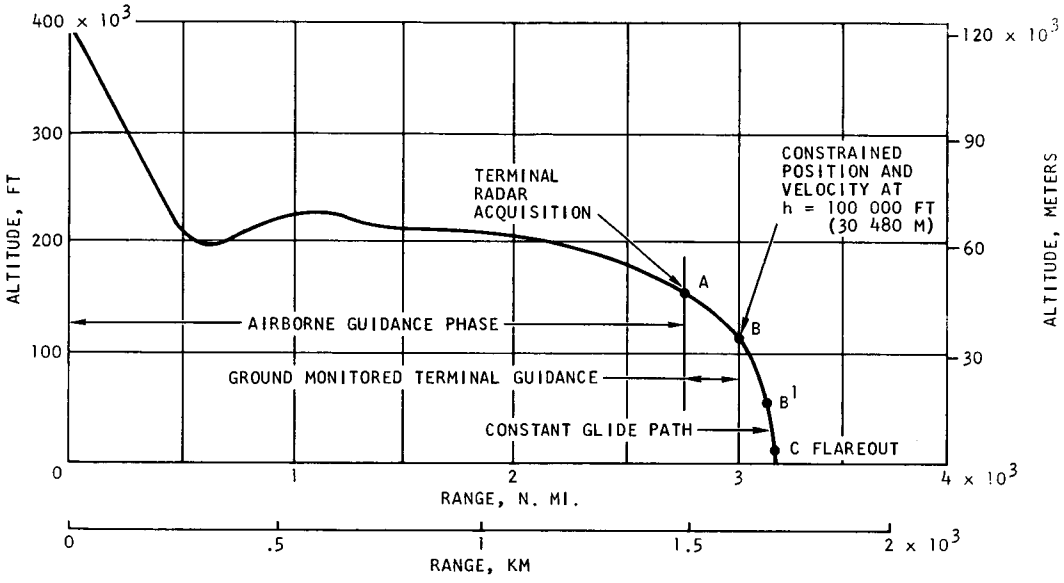

FIGURE 35. TYPICAL ALTITUDE--RANGE PROFILE

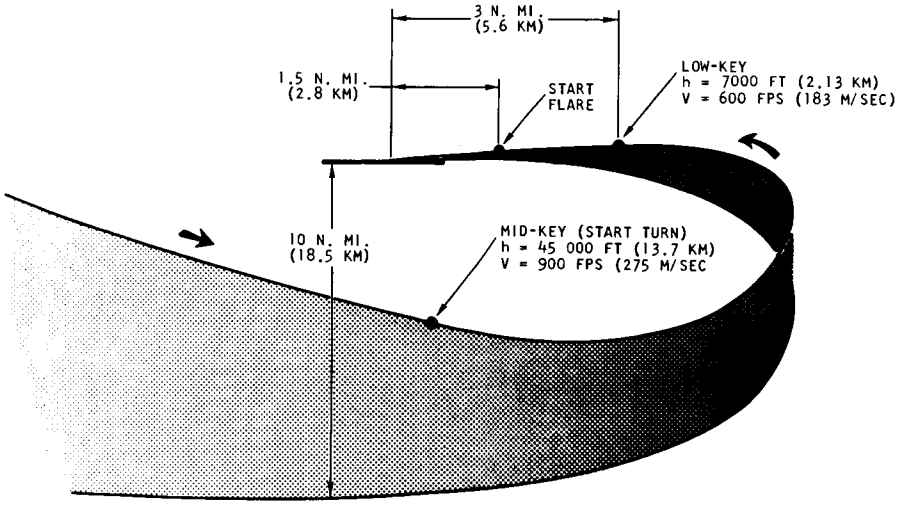

FIGURE 36. TYPICAL APPROACH PATTERN FROM ORBIT

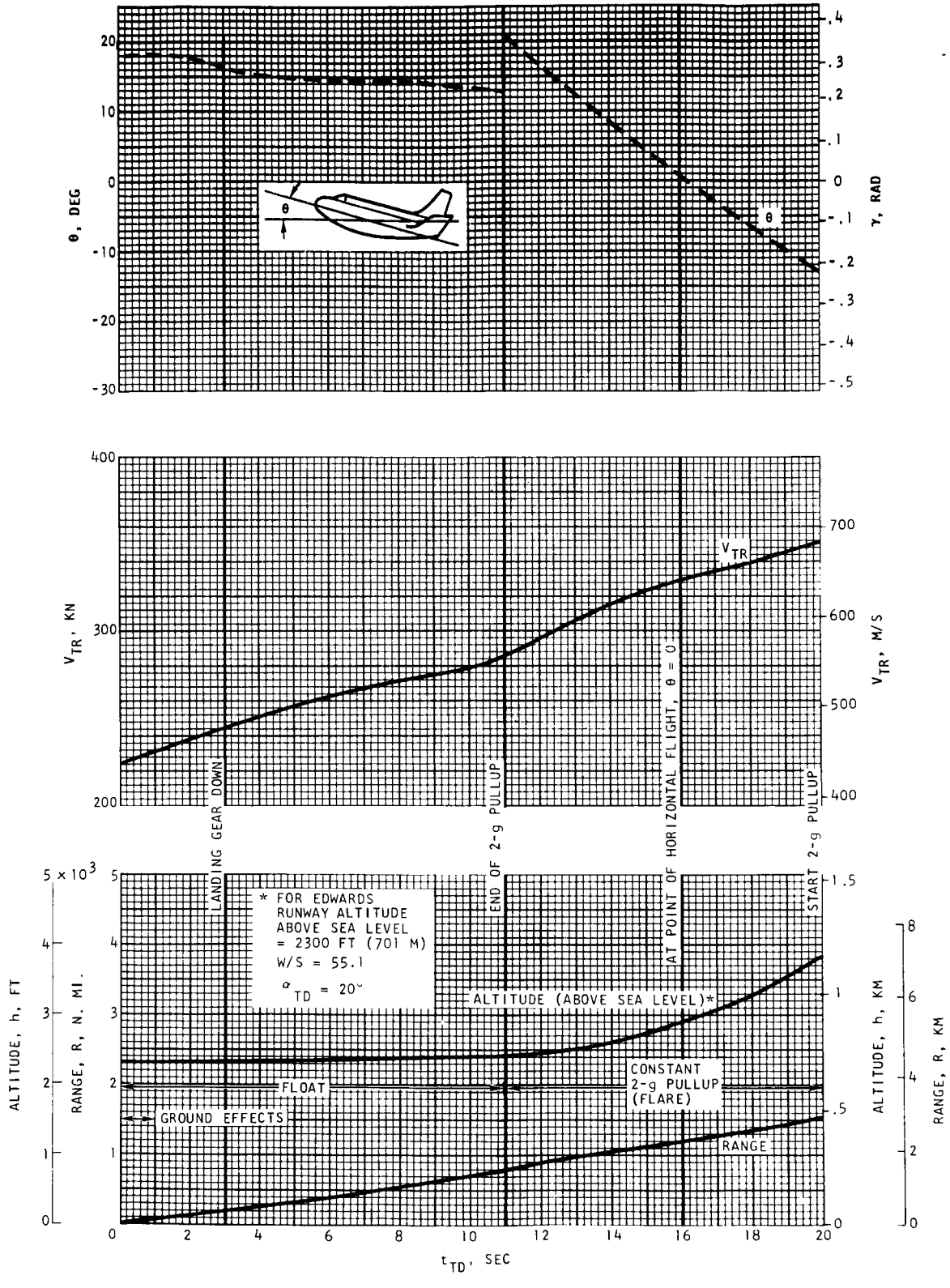

FIGURE 37. LANDING TRAJECTORY

to maintain a normal "pullup" load factor. This phase is required to reduce the normally high rate of sink to a value acceptable for touchdown (<13 fps) (4m/sec). Angle of attack is reduced sharply once the desired rate of sink is achieved and thereafter altered to maintain the desired rate of sink until touchdown.

The conditions at the time of flare initiation are usually established by pilot preference for high kinetic energy for added maneuverability. The flare begins at an altitude of about 1560 feet (475 m) above the runway and at a distance 1.56 nautical miles (2.9 km) uprange of the touchdown point. Pilot preference usually dictates a negative flight path angle of 30° (0.524 rad) and an indicated airspeed in excess of 300 knots (154 m/sec). In the case presented in figure 37, the indicated airspeed is 331 knots (170 m/sec), and the true airspeed is 351 knots (180 m/sec). The time is 20 seconds before touchdown. A 2-g pullup is maintained by increasing angle of attack as airspeed decreases. After 9 seconds, the rate of sink has been reduced to about 12 fps (3.7 m/sec), and the pullup maneuver is terminated and the period of float begins.

At float initiation, the vehicle is 151 feet (46 m) above the runway and 0.79 nautical miles (1.5 km) uprange from the touchdown point. The time to touchdown is 11 seconds. The landing gear are deployed 5 seconds before touchdown and are completely down and locked by 3 seconds before touchdown. At this time the vehicle is 38 feet (11.6 m) above the runway and 0.2 nautical miles (0.37 km) uprange from the touchdown point. In the last second before touchdown, there is a leveling off of the rate of change of angle of attack required to maintain the desired rate of sink. This effect is caused by the proximity of the ground.

Touchdown occurs at a velocity of 226 knots (116 m/sec) and an angle of attack of 20° (0.35 rad). Slide out is generally completed in 20 seconds after touchdown.

The trajectory used for the visibility study (fig. 37) was based on procedures recommended by NASA FRC personnel and represents conditions experienced during the HL-10 and M2-F2 air-launch programs. This trajectory produces smaller pitchup attitudes (θ) during the critical phase of the landing maneuver (from end of flare to touchdown) and consequently the best visibility. Trajectories producing higher values of θ would further degrade the already marginal field of view shown in this report.

(b) Description of canopy design: The basic external canopy follows the geometry, defined in the NASA reports (ref. 6) and referred to as canopy "D," is shown in figure 38. The conical windshield (fig. 39) falling within this shape was developed during this study.

Because the forward transparent areas cannot be exposed to the re-entry environment, a heat shield protective cover with an insulation layer must be provided, as shown in figure 40. At 75 000 feet (22.9 km) or below, this cover is jettisoned to disclose the wrap-around windshield that is free of post obstructions otherwise existing with a flat panel arrangement. The wrap-around design also presents a cleaner aerodynamic configuration because gaps are at a minimum and sharp corners or transitions are eliminated. The heat shield, however, will be set out from the outside mold line by 2-3/8 inches (0.12 m). Therefore, prior to jettisoning the shield, a modified canopy shape would exist.

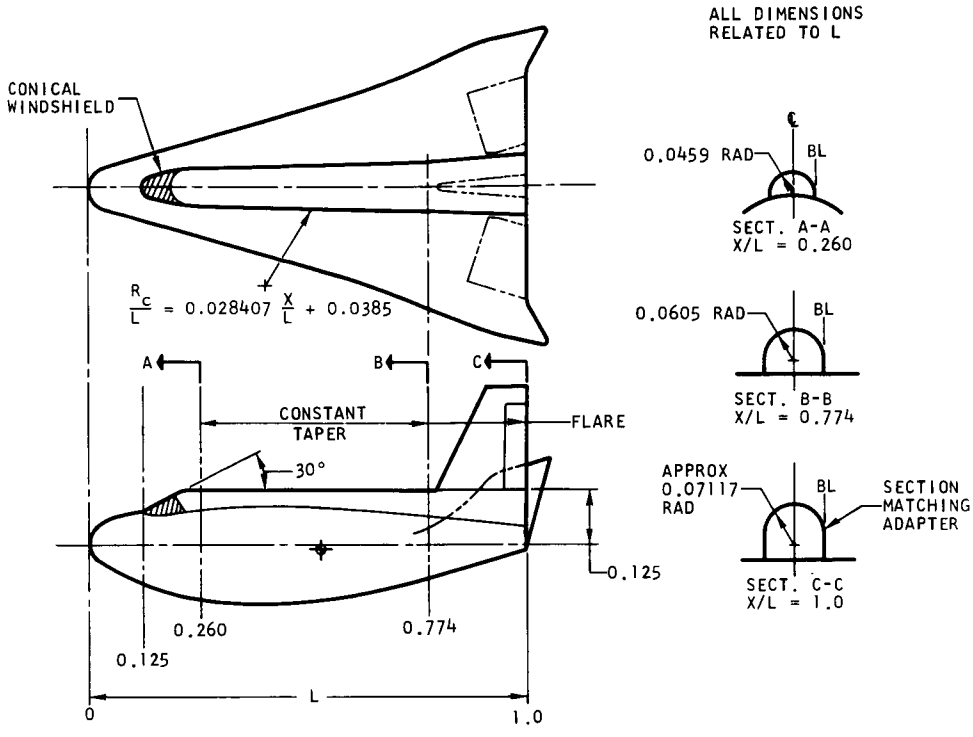

FIGURE 38. MODIFIED CANOPY CONFIGURATION DATA

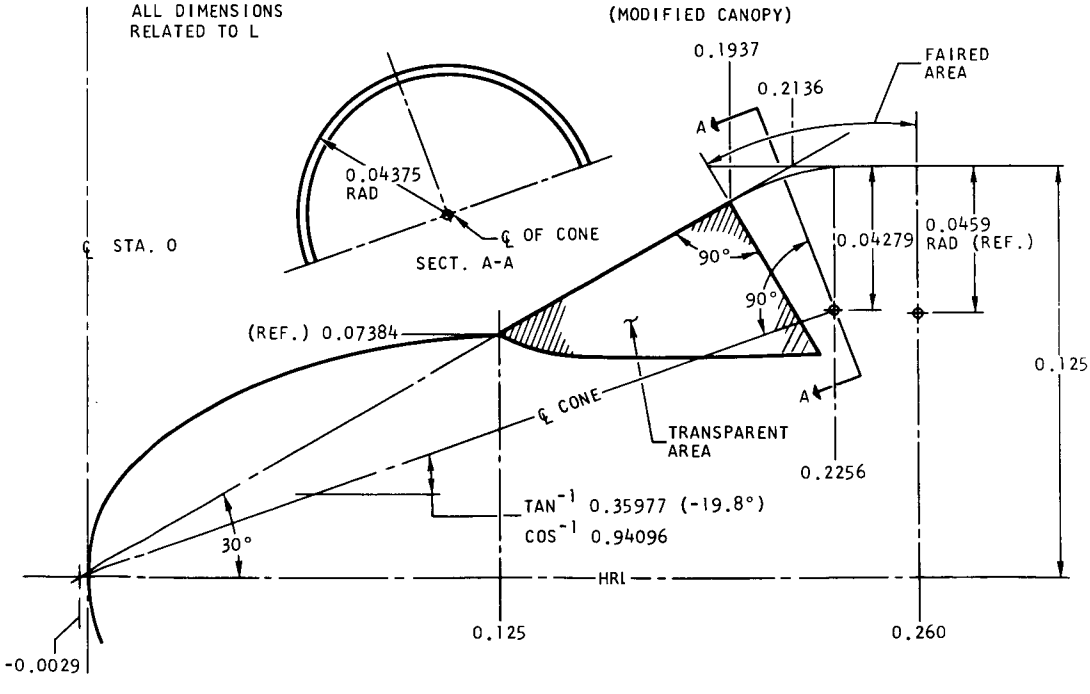

FIGURE 39. CANOPY GEOMETRY

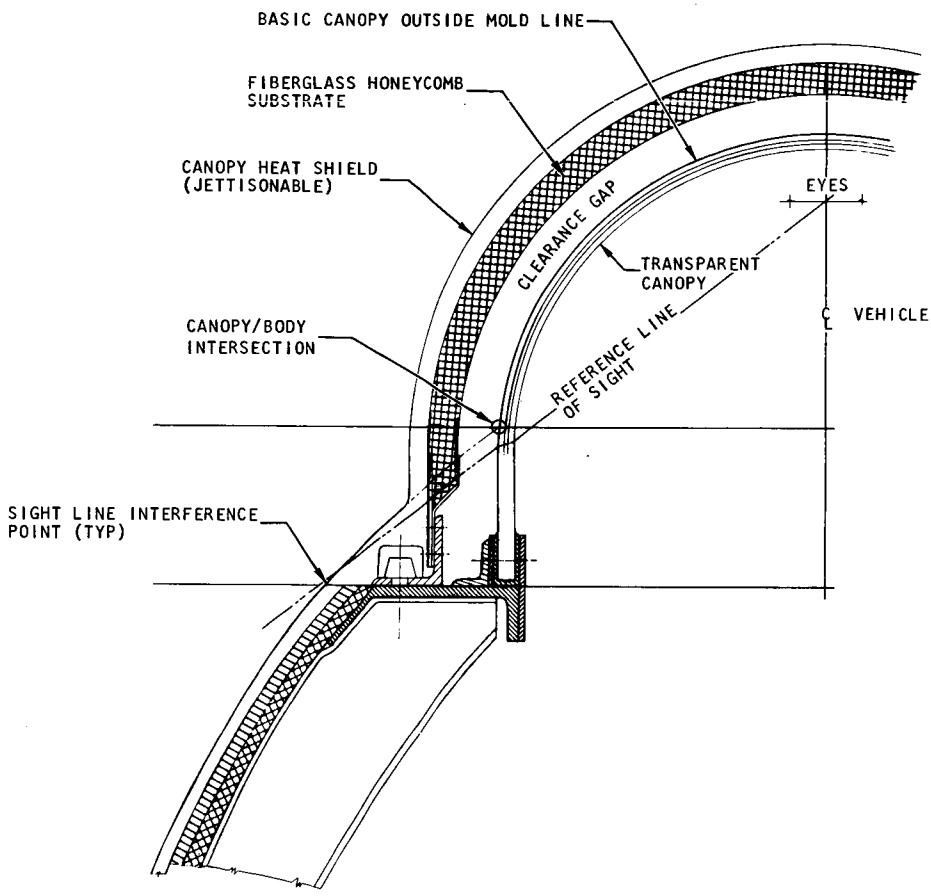

FIGURE 40. CANOPY/WINDSHIELD CROSS SECTION

No attempt has been made at this time to study fully the transparent installation and its host of problems, i.e., sealing, edge attachments, thermal breathing, etc. Past Martin Marietta studies in this area indicate that designs for an entry vehicle are well within the state-of-the-art; temperatures beneath the heat shield can be controlled to +200° F maximum, allowing the use of plastic or glass transparencies. If necessary, the conical shape windshield can be constructed from high-temperature glass to accommodate higher temperatures or space soak conditions that might be injurious to plastic materials. The principal area of concern for the study centered not on detail canopy hardware design but rather on the evaluation of visibility through the transparent area within the controlled geometry of the canopy.

For in-orbit requirements, direct visual contact with the outside is provided by an eight-inch diameter round port located on the left of the pilot's head. Through this window, the pilot can orient the vehicle with earth, confirm separation prior to entry, and confirm entry attitude. This window is exposed at all times. Temperatures in this area are not expected to exceed 1800° F, and a fused quartz multiple panel window can be installed with a metallic, hermetically tight seal.

For the main transparent area, studies indicate that the edge attachment can be contained below the canopy/body intersection line (figure 40). Therefore, maximum visibility is obtained. The clear area extends aft to a canted frame as shown in figure 39.

(c) Direct-vision sight-line interference envelop: A full-scale crew station mock-up of the D/3 vehicle (fig. 41) was used for determining the envelop of the pilot's sight-line interference with vehicle structure. Vision angles were plotted from the two eye positions shown in figure 42: the normal eye position at the vehicle centerline and a maximum head movement position determined by a subject wearing a high-altitude helmet (type A/P 225-2). For the latter, it was found the head could be moved comfortably to the side 6-1/2 inches where the helmet contacted the structure, and 3/4 inch forward considering the restraint harness and a comfortable body position to handle the flight controller. This head movement resulted in lowering the eye position 1-3/8 inches.

Vision angles were plotted from these positions using the wire method (fig. 43). Results are shown in figure 44.

(d) Pilot's field of view during the landing approach: Having studied the landing profile and vehicle attitude data and having designed a maximum of transparency into the forward canopy area, as shown in figures 39 and 40, it was possible to plot the visibility limits within this area (fig. 44). These data, together with the vehicle attitude data (fig. 37), permitted plots of the horizon and runway to be made, depicting the view that the pilot would obtain during critical phases of the landing maneuver. Figures 45 through 48 show these visual plots. For the study, a runway 300 feet (91.4 m) wide and 10 000 feet (3.1 km) long was used.

Forward vision of the runway is completely obscured from just prior to the end of flare to touchdown. However, the horizon can be seen during the entire landing operation. As shown in figure 49, at touchdown the runway edges are visible 321 feet (98 m) ahead, assuming the eyes are at the centerline of the vehicle, and 523 feet (159 m) if the head is moved to the second position just described.

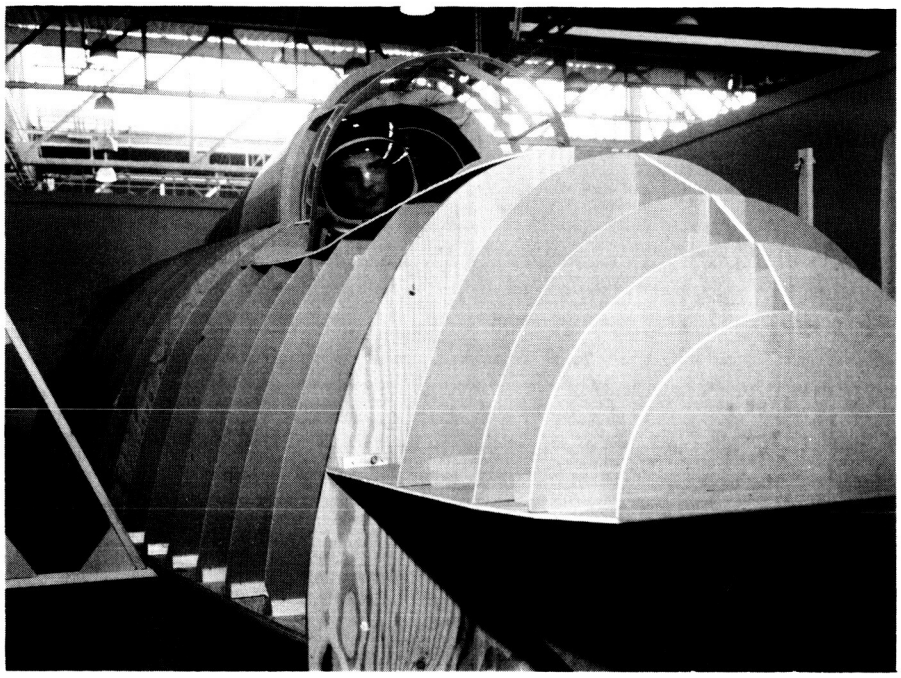

FIGURE 41. FULL-SCALE CREW STATION MOCKUP

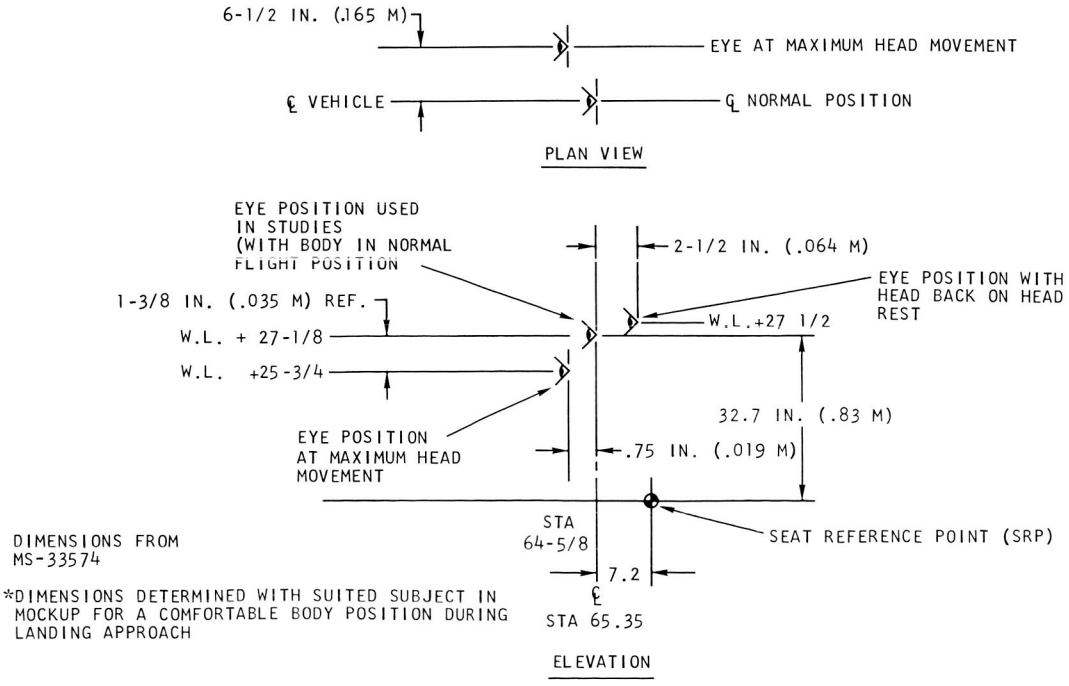

FIGURE 42. PILOT'S EYE LOCATION

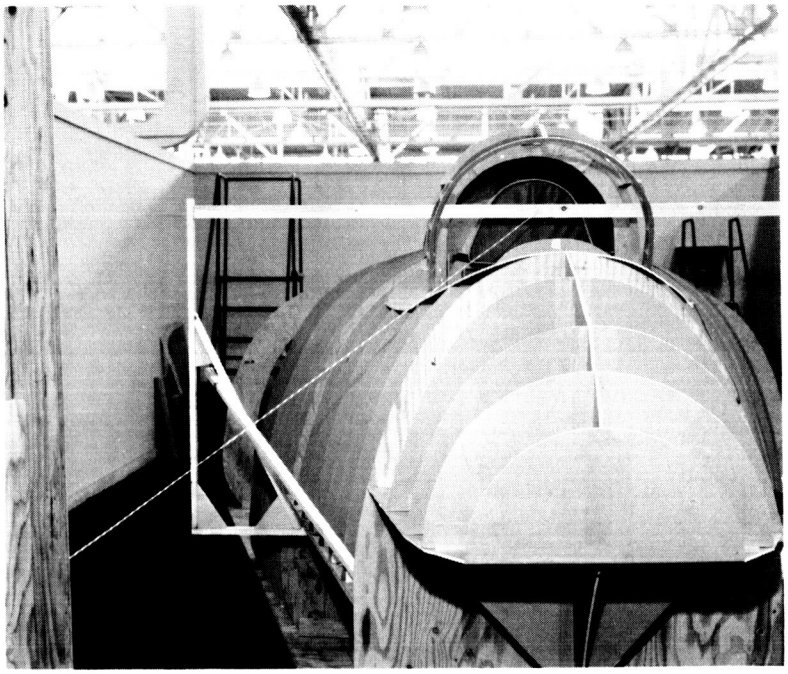

FIGURE 43. WIRE METHOD OF DETERMINING VISION ANGLES

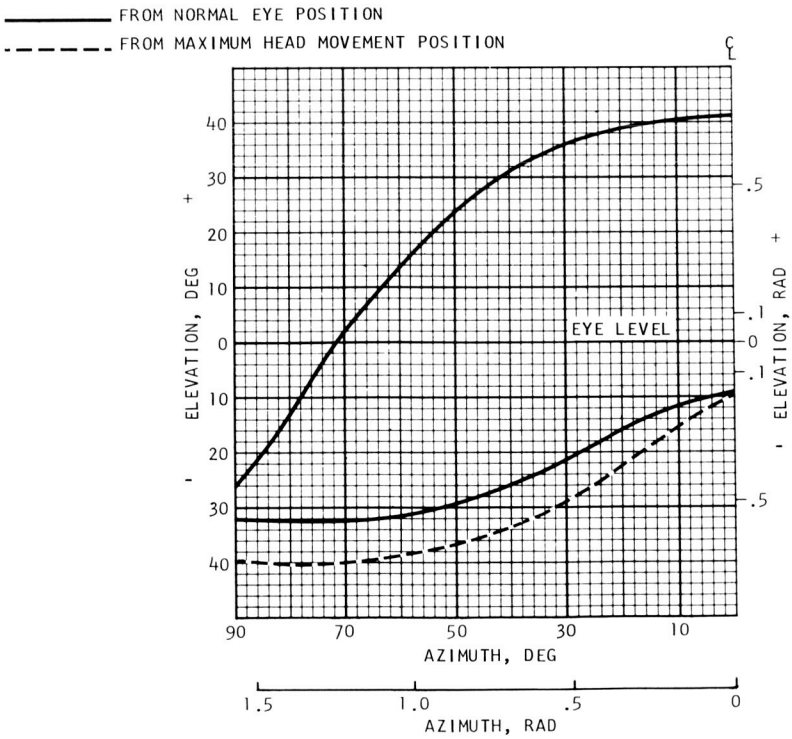

FIGURE 44. PILOT'S SIGHT LINE INTERFERENCE ENVELOPE

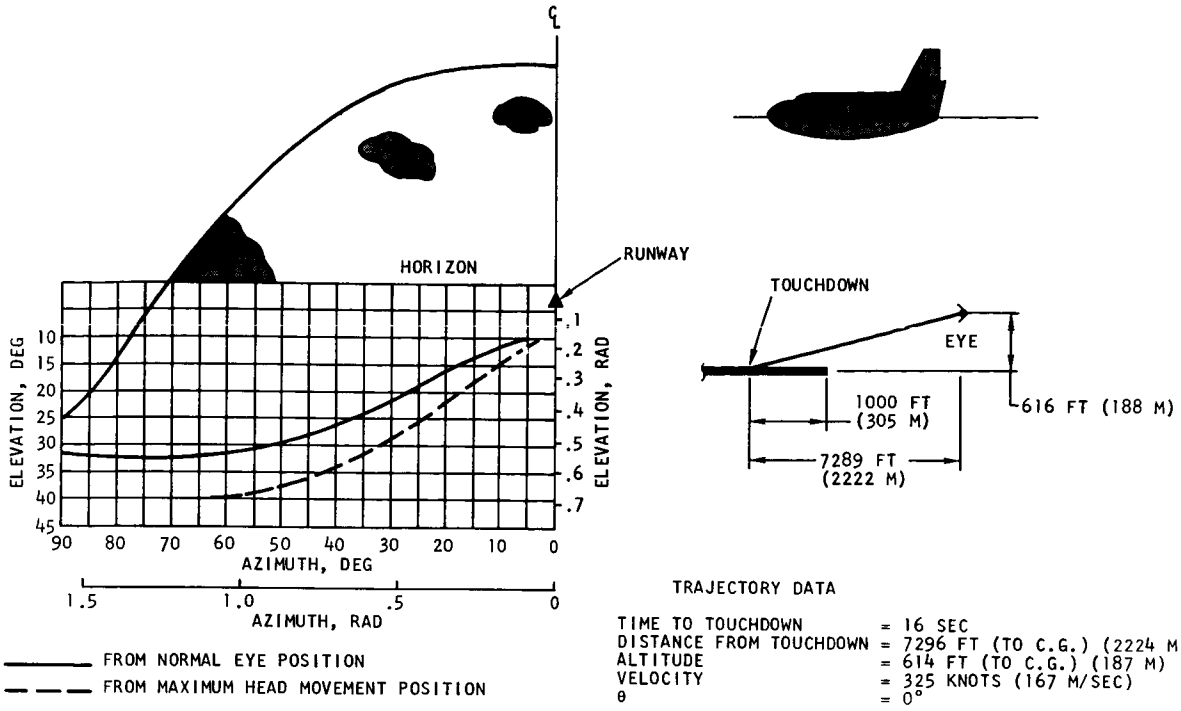

FIGURE 45. PILOT'S FIELD OF VIEW IN HORIZONTAL FLIGHT

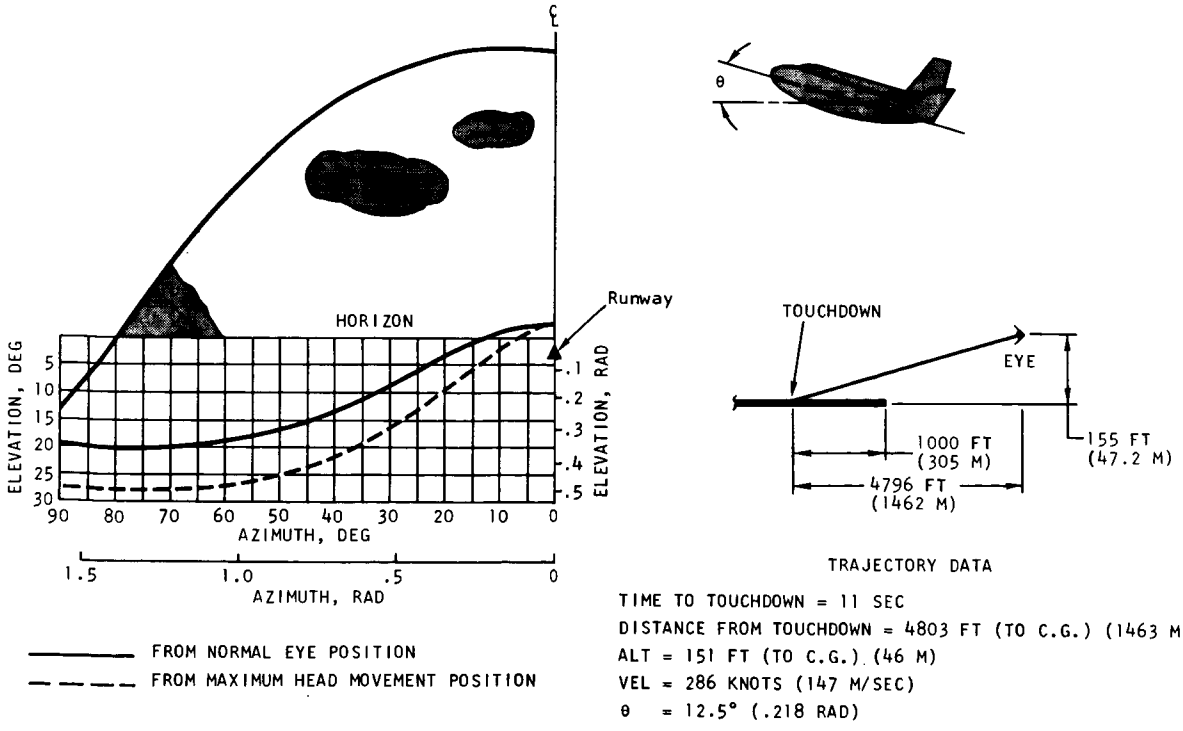

FIGURE 46. PILOT'S FIELD OF VIEW AT END OF FLARE

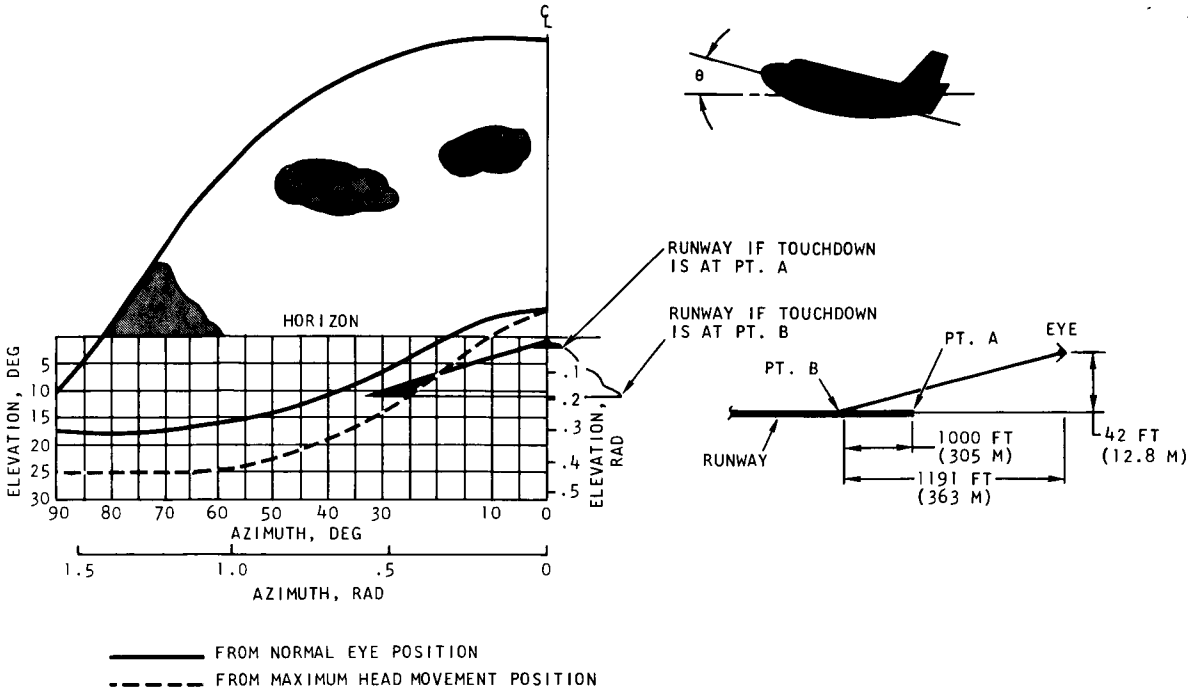

FIGURE 47. PILOT'S FIELD OF VIEW WITH GEAR DOWN

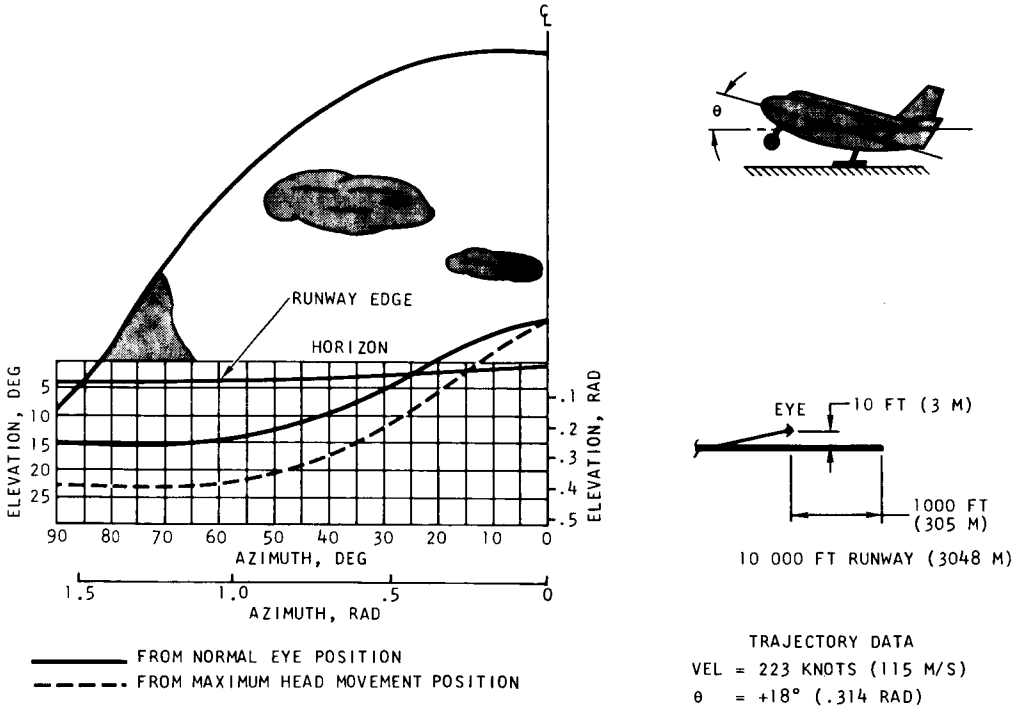

FIGURE 48. PILOT'S FIELD OF VIEW AT TOUCHDOWN

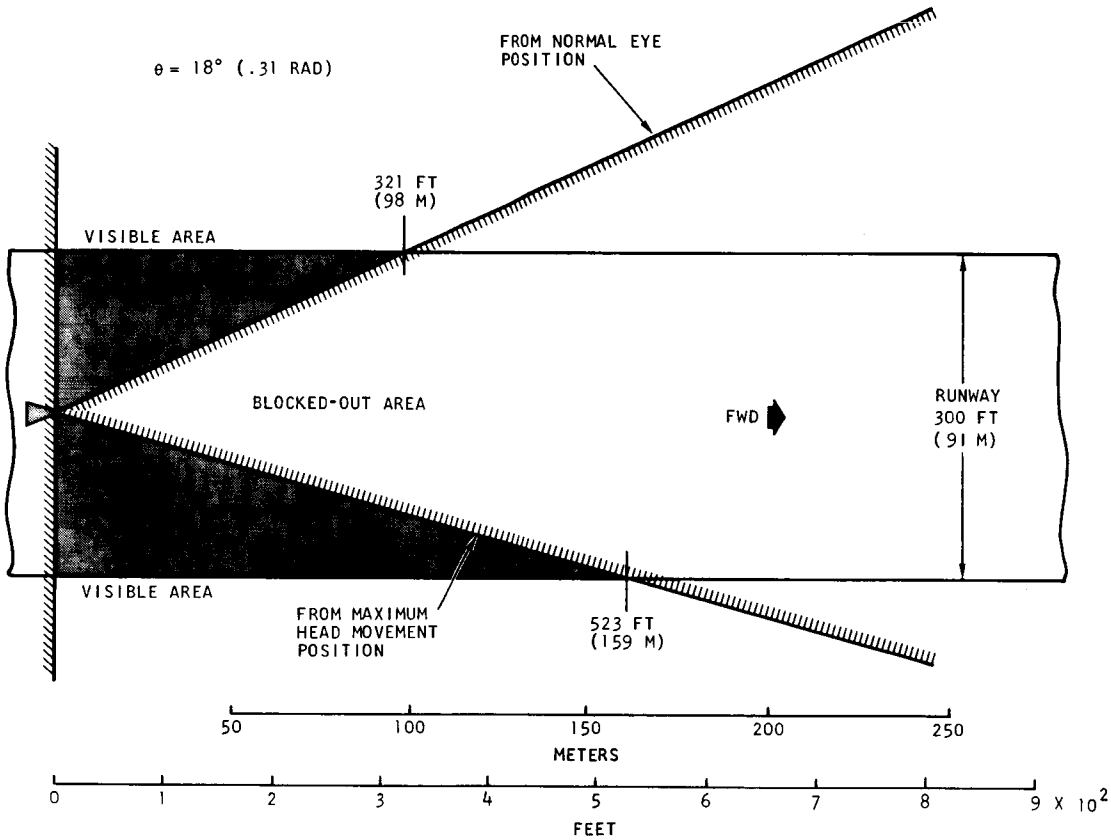

FIGURE 49. GROUND VISIBILITY PLAN VIEW AT TOUCHDOWN

In figure 47, with head movement, the runway edge comes into view if touchdown is 1000 feet (305 m) or more from the uprange end of the runway; otherwise, it is completely obscured. Periodic yawing of the vehicle 5° (0.087 rad) during the approach maneuver was considered to assist in runway alignment; however, the data presented in figures 46 and 47 , indicate a yaw angle greater than 10° (0.175 rad) would be required from end of flare to approximately runway threshold to obtain a view of the runway edge.

Four seconds after start of flare a horizontal vehicle attitude is achieved, and as shown in figure 45 ample up and down visibility is available. Uprange from this point, the pilot's field of view of the runway will improve since "nose down" attitudes prevail.

This analysis, although better substantiated than that conducted during the parametric phase of the study reported in Part IV, is still considered preliminary. Adequacy of the visibility provided by the D/3 should be further analyzed by dynamic ground simulation and will only be proven in the air launched flight test phase.

2. Control and Displays

The following controls and displays developed for the D/3 vehicle configuration are based on a three-man crew consisting of pilot, copilot/flight engineer and test experimenter.

Crew tasks. - On this basis, mission tasks were allocated as a function of crew member mission time/work load and available space for controls and displays. This philosophy provided the following task definition for each crew member.

The pilot's mission responsibilities are:

(1) Launch vehicle performance monitoring and launch abort backup to automatic abort system.

(2) Vehicle orbital attitude control

(3) Orbital maneuvering to station

(4) Propulsion management

  (a) Reaction control system

  (b) Abort and deorbit rocket system

  (c) Landing assist engine system

(5) Monitor and control hydraulic system

(6) Monitor malfunction warning system

(7) Backup autoflight control during entry

(8) Atmospheric flight control

(9) Visual acquisition of landing site

(10) Landing flight control

(11) Abort.

The copilot/flight engineer will be responsible for the following tasks:

(1) Monitor and control electrical system

(2) Monitor and control environmental system

(3) Control communication system

(4) Entry flight control training

(5) Rendezvous and docking control.

The primary tasks of the test/experimenter are delineated by those experiments to be conducted during a given flight. He will serve a secondary function as a backup for flight engineering tasks.

With these crew member tasks defined, it is now possible to assign those controls and displays necessary to perform the above tasks.

Control display arrangement. - Particular emphasis was given to the development of the flight control group. Soft mockups were utilized to develop crew station sizing, arrangement and vision. Special emphasis was directed within the cockpit area.

Vehicle size and shape in the cockpit area restricted the console space to 772 square inches within the pilot's useful vision and reach envelop. Additional space may be acquired by the use of foldout panels from within the inner skin structure. Systems that serve only during one unrepeated mission phase, such as the launch vehicle monitoring system, could be a plug-in unit that would be stowed after use.

Cockpit control panel areas were subdivided into visual and manual primary effectiveness zones, as defined in ASD-TR-61-91. They were utilized as the starting point for control/display area assignment (fig. 50).

The main display panel contains those instruments necessary for launch vehicle performance assessment, orbital and atmospheric flight control.

The right-hand console is devoted to the two-axis controller (rudder pedals are provided for yaw) malfunction warning system and suit environmental control system. Additional control panel space for orbit control can be obtained with a fold-out panel near the arm rest.

The left-hand console contains communication, lighting, abort-deorbit propulsion, abort system controls, hydraulics, reaction control and landing assist propulsion systems.

The central pedestal contains the energy management unit, landing engine emergency shutdown switch, landing gear and landing chute controls.

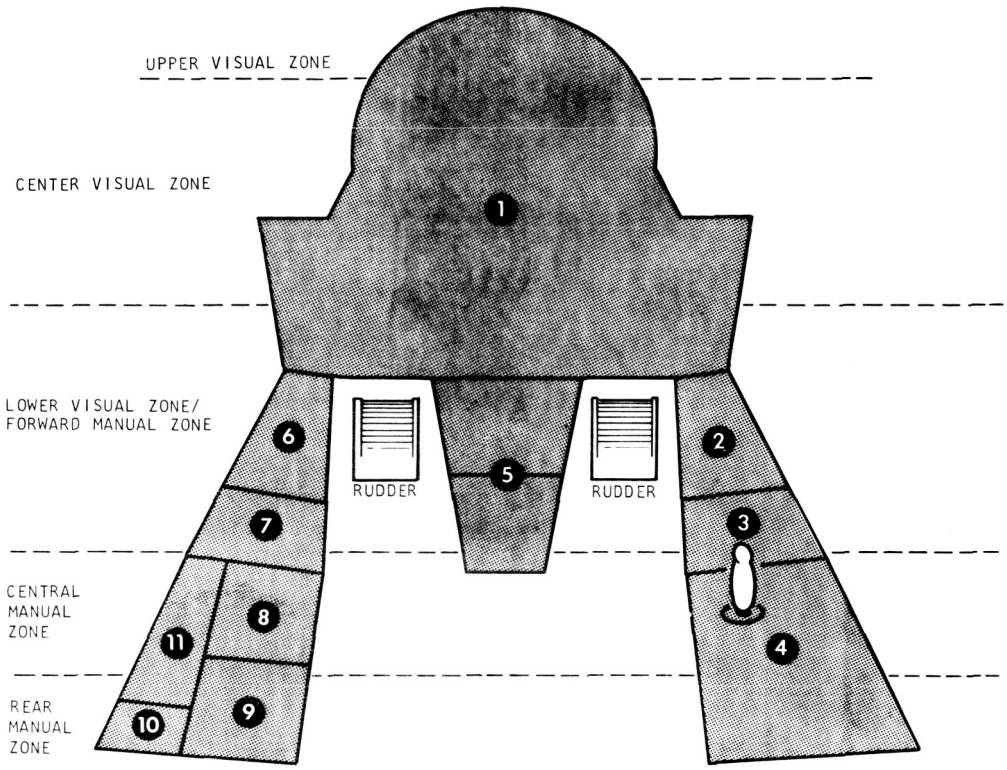

		AREA, SQ IN.
1	MAIN PANEL INSTRUMENTS	366
2	ECS CONTROL PANEL	173
3	MALFUNCTION WARNING	
4	CONTROLLER AND ARM REST	
5	LANDING SYSTEM AND COMPUTER	66
6	ABORT RECOVERY CONTROLS	173
7	HYDRAULIC CONTROLS	
8	RCS AND LANDING PROPULSION SYSTEM	
9	COMMUNICATIONS	
10	LIGHTING CONTROL	
11	ORBIT/DEORBIT PROPULSION CONTROL	

FIGURE 50. GENERAL LAYOUT AND VISUAL ZONES OF CONTROL PANEL

Figures 51 and 52 illustrate the physical control/display design and panel area arrangement within the cockpit area.

The two rear crew stations, copilot/flight engineer and test experimenter, are identical in size and arrangement. There are available 363 square inches of forward panel space. In addition, there are about 456 square inches of inner skin space available for additional use. This area would be limited to those nonessential instruments less than 4 to 8 inches in depth.

The copilot/flight engineer's training function will require that he have a duplicate set of orbital flight instruments and a three-axis controller. The flight instruments will be located on his lower forward panel. The three-axis controller is on his right-side console.

Primary electrical power and environmental control, displays and controls are located above the flight group. Secondary displays and controls plus communications are located on the side panels adjacent to the operator. Figures 53 and 54 illustrate the copilot's station.

The test experimenter's station, a mirror image of the copilot's station, will vary as a function of experimentation to be performed. His primary task is the control of experimentation. However, he will serve a secondary function of backup to flight engineering tasks. Figure 55 is typical for this station.

Component list. - A list of instruments, lights, and controls required at the crew stations is given in table 13.

Increased canopy volume at pilot's station. - Mockup studies of the pilot station demonstrated the critical nature of the space available for the pilot and his necessary functional equipment.

To obtain maximum forward downward visibility, it was necessary to locate the pilot at this most forward position. Although this forward position is minimum, and limited tests demonstrated it to be acceptable, a more detailed analysis of equipments and display would be required to assure complete adequacy of the display area. A more aft position of the pilot to gain volume for additional panel space can only be achieved at the expense of further degrading visibility.

The mockup studies also showed that an increase in shoulder room for a 95 percentile man would be desirable. To provide a total width increase at the shoulder level of 4 inches, it would be necessary to bulge the forebody and canopy. The geometry changes necessary to do this are shown in figure 56.

3. Ingress and Egress Provisions

A 24 by 34 inch hatch, located in the crown just aft of the pilot and midway between the aft crew members, provides access to both stations. This opening is sufficiently large to permit installation or removal of subsystem components.

If maintenance is required while in the launch position, ladders, platforms, etc., can be provided and installed inside the vehicle.

Crew loading of the aft station will be similar in procedure to that of Gemini. It should pose no difficulties and require a minimum of ground support equipment, as shown in figure 57. Since the canopy is fixed and the pilot's entrance is through the aft crown hatch, it will be necessary to move the pilot's seat aft to a position below the hatch. Then, with the aid of an assist device, the pilot would be inserted into the seat. The seat would then be rolled forward into the normal launch position. Figure 57 demonstrates this technique.

In the second method, the seat back rest is rotated aft. The pilot is inserted into the seat. The seat is then rotated into launch position. Figure 58 demonstrates this technique.

For normal egress while in the vertical position, the operation would be reversed. For normal egress after landing, the pilot would rotate his seat back and use the back rest as a step to climb over the coaming, as shown in the sequence pictures of figure 59. The aft crew could then use the pilot's seat as a step and proceed to evacuate in the same manner, or they could use the pilot's floor as a step, as shown in figure 60.

For emergency egress while in the vertical position, the pilot's canopy, consisting of a large wrap-around transparent windshield, could easily be sheared cleanly at the edge attachment with a shaped charge. The transparency could then be pushed out easily. The canopy cover required for entry heating protection would be first jettisoned in the normal manner. The aft crew would escape through the crown hatch after explosively shearing the hatch hold-down pins which would allow the hatch to fall clear of the vehicle.

For a crash landing, where crew activity is possible, the same procedure would be used. External hatch and canopy removal controls accessible to the ground crew would also be provided.

Perhaps the most hazardous escape situation would occur immediately following an emergency recovery over water where flooding occurs due to reptured structure. Providing the crew can perform evacuation duties, they would first remove the canopy and hatch, the aft crew would then jettison the survival kit which includes a three-man raft. Evacuation procedures developed for Gemini would then be followed by the suited astronauts.

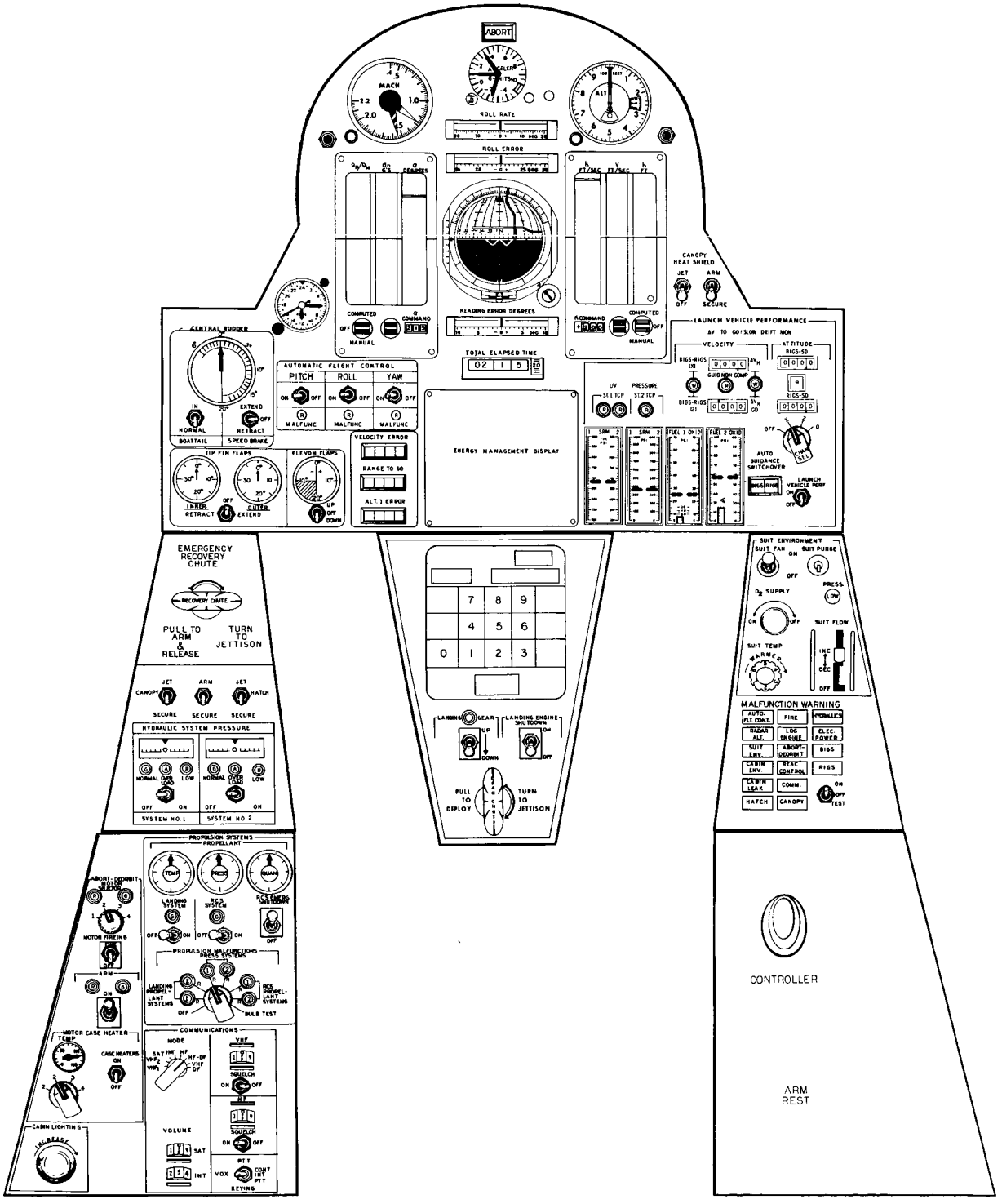

FIGURE 51. CONTROL PANEL INSTRUMENT LAYOUT

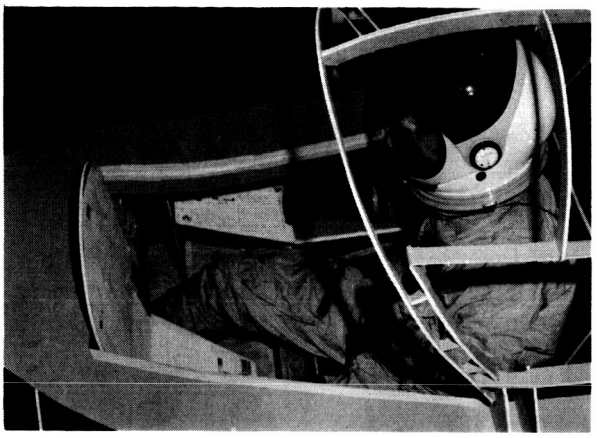

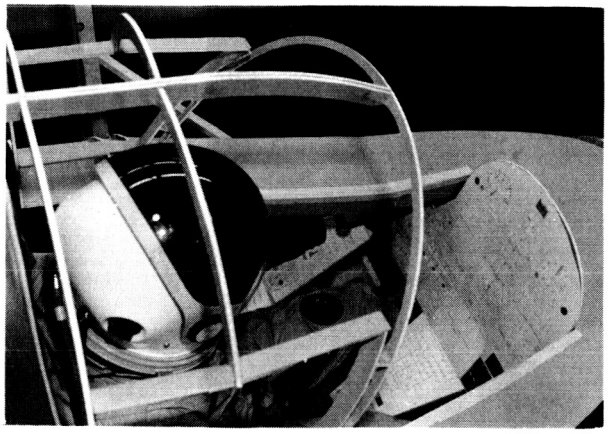

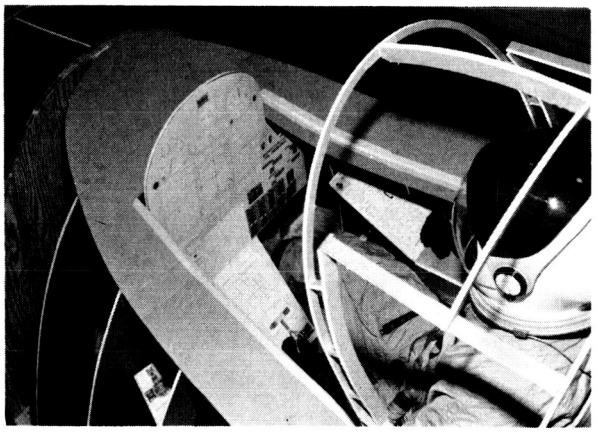

FIGURE 52. CONTROL/DISPLAY IN FULL-SCALE MOCKUP

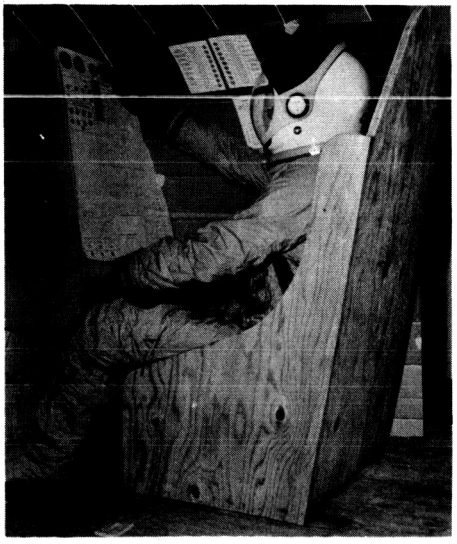

FIGURE 53. MOCKUP OF COPILOT'S STATION

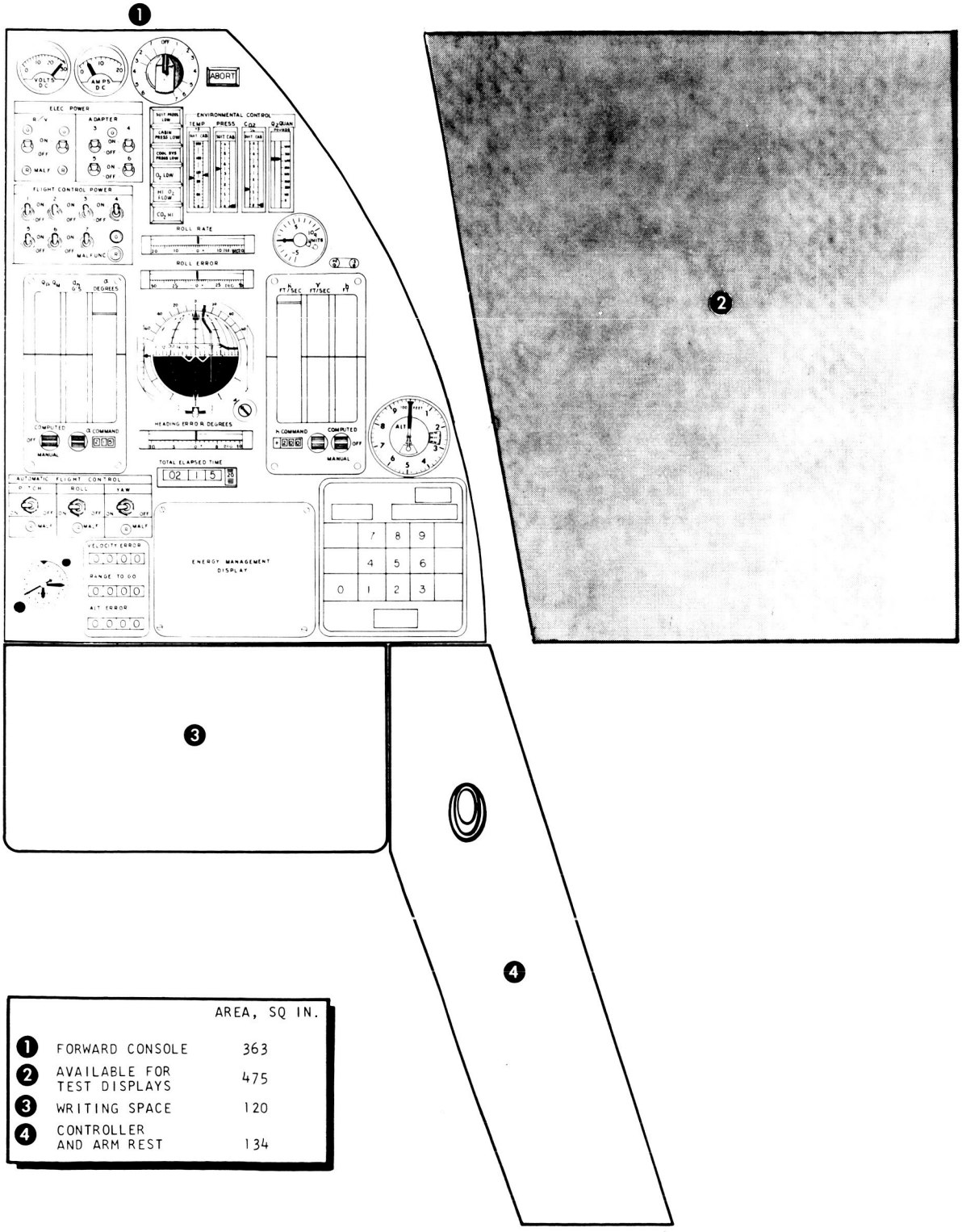

		AREA, SQ IN.
1	FORWARD CONSOLE	363
2	AVAILABLE FOR TEST DISPLAYS	475
3	WRITING SPACE	120
4	CONTROLLER AND ARM REST	134

FIGURE 54. COPILOT/FLIGHT ENGINEER'S STATION

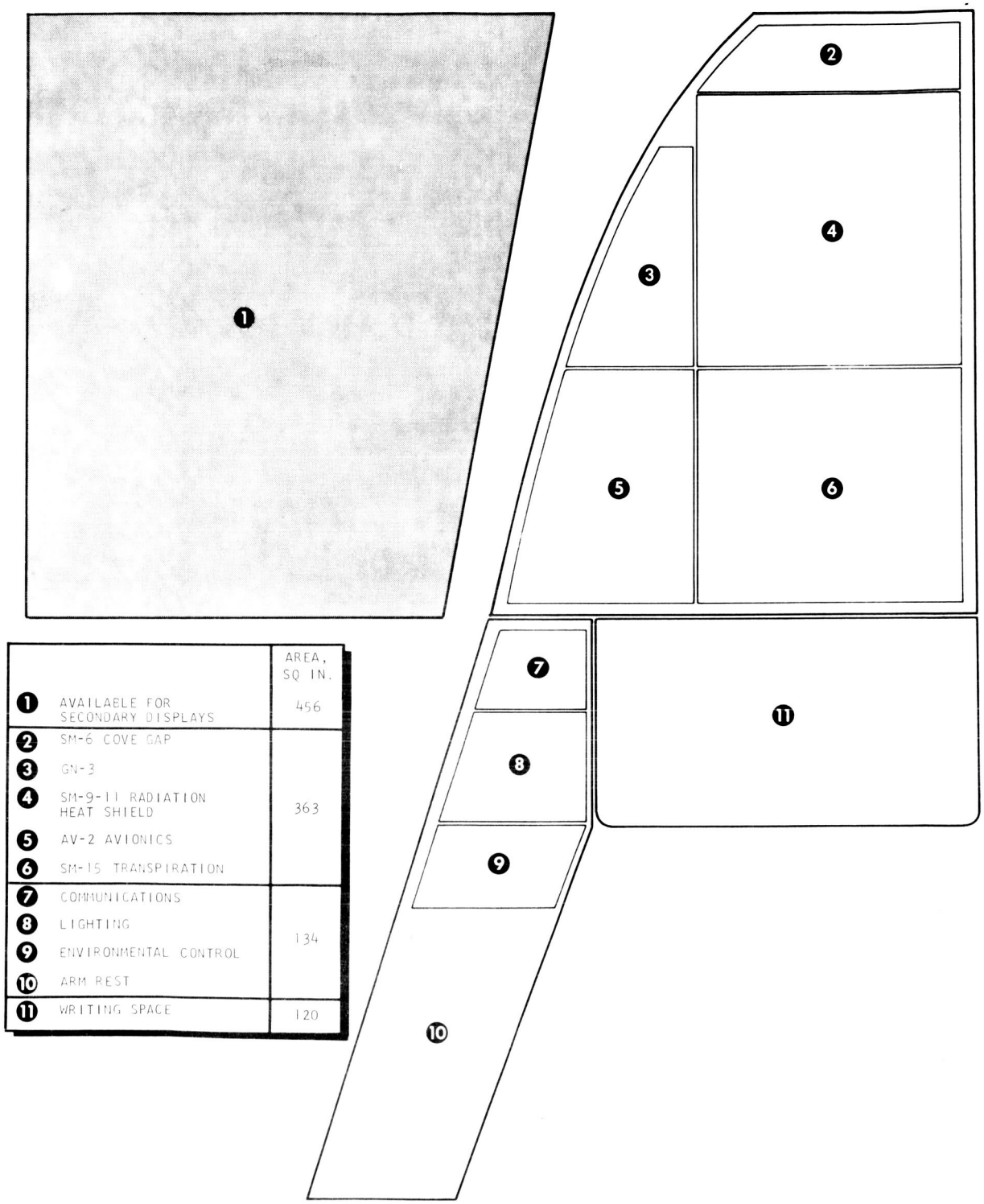

		AREA, SQ IN.
1	AVAILABLE FOR SECONDARY DISPLAYS	456
2	SM-6 COVE GAP	363
3	GN-3	
4	SM-9-11 RADIATION HEAT SHIELD	
5	AV-2 AVIONICS	
6	SM-15 TRANSPIRATION	
7	COMMUNICATIONS	134
8	LIGHTING	
9	ENVIRONMENTAL CONTROL	
10	ARM REST	
11	WRITING SPACE	120

FIGURE 55. TEST/EXPERIMENTER'S STATION, LEFT-HAND SIDE

TABLE 13

COMPONENT LIST

Instruments	Quantity	Location *	Lights	Quantity	Location *	Controls	Quantity	Location *
Environmental Control System								
Suit and cabin pressure	1	C	Low O_2	1	C	Suit Hi O_2 flow valve	1	C
Suit and cabin temperature	1	C	High CO_2	1	C	Water seal switch	1	C
Suit and cabin CO_2	1	C	Cabin pressure low	1	C	Cabin vent valve	1	C
O_2 quantity	1	C	Cooling system pressure low	1	C	Cabin recirculation	1	C
H_2O quantity	1	C	High O_2 flow	1	C	Suit flow valve	3	P, C, E
Glycol quantity	1	C	Suit pressure low	3	P, C, E	Suit temperature control	3	P, C, E
O_2 storage pressure	1	C				Suit fan switch	3	P, C, E
O_2 storage temperature	1	C				Suit demand regulator	3	P, C, E
Steam temperature	1	C				Suit purge valve	3	P, C, E
						Cabin temperature control	1	C
						Cooling pumps switch	2	C
						Cabin fan switch	1	C
						Suit inflow valve	1	C
						Suit bypass valve	1	C
						Cabin pressure regulator	1	C
						Cabin purge valve	1	C
						Cabin repressure valve	1	C
						Hi-flow atmosphere valve	1	C
						Atmosphere shutoff valve	1	C
						Crew emergency cooling valve	1	C
						H_2O flow override valve	1	C
						Accumulator valve	1	C
						Redundant cooling loop valve	1	C
Hydraulics System								
Pressure indicator system no. 1	1	P	System no. 1 normal	1	P	System no. 1 on/off	1	P
Pressure indicator system no. 2	1	P	System no. 2 normal	1	P	System no. 2 on/off	1	P
			System no. 1 overload	1	P			
			System no. 2 overload	1	P			
			System no. 1 low	1	P			
			System no. 2 low	1	P			
Communications System								
						Voice control center	3	P, C, E
						Each center contains:		
						Mode selector (7 position)	(1)	
						VHF on/off/vol	(1)	
						HF on/off/volume	(1)	
						VHF squelch on/off	(1)	
						HF squelch on/off	(1)	
						SAT on/off/volume	(1)	
						Internal on/off/vol	(1)	
						Voice transmittal selection and modulator switch PTT/VOX/ Keying/Cont Int PTT (4 position)	(1)	

TABLE 13.--Continued

COMPONENT LIST

Instruments	Quantity	Location *	Lights	Quantity	Location*	Controls	Quantity	Location *
Guidance and Control System								
Flight director	2	P, C	0.05 g	2	P, C	Side stick controller	2	P, C
8-day clock	3	P, C, E	0.02 g	2	P, C	AFC pitch on/off	2	P, C
Total elapsed time	3	P, C, E	Auto flight control malfunction indicator pitch	2	P, C	AFC roll on/off	2	P, C
Radar altimeter	1	P	AFC malfunction indicator roll	2	P, C	AFC yaw on/off	2	P, C
Mach meter	1	P	AFC malfunction indicator yaw	2	P, C	Boattail in/norm	1	P
Accelerometer	2	P, C				Speed brake ext/retract	1	P
Energy management display	2	P, C				Tip fin flaps inner/off/outer	1	P
Velocity error indicator	2	P, C				Elevon flaps down/off/up	1	P
Altitude indicator	2	P, C				Energy management computer entry unit	1	P
Range to go indicator	2	P, C						
Roll rate indicator	2	P, C						
Roll error indicator	2	P, C						
Heading error indicator	2	P, C						
Central rudder position indicator	1	P						
Tip fin flaps position indicator	1	P						
Elevon flaps position indicator	1	P						
$\dot{h}$ command ind								
$\dot{h}$ (ft/sec) tape	2 units	P, C						
V (ft/sec) tape								
h (ft) tape								
Q_p/Q_m tape								
α_n tape	2 units	P, C						
α_{deg} tape								
α command ind								
Landing Assist Engine System								
Fuel temperature	Common with RCS gages		Engine on	1	P	System on/off switch	1	P
Fuel pressure			Propellant system no. 1 malfunction	1	P	Emergency shutdown switch	1	P
Fuel quantity			Propellant system no. 2 malfunction	1	P	System test selector switch (8 position)	1	P
			Pressure systems 1 and 2 malfunction	2	P		Common with RCS control	
Malfunction Warning System								
			System warning	15	P	Master test switch	1	P
			Abort indicator	3	P, C, E			
			Summary malfunction indicator	2	P			
Landing System								
			Gear down indicator	1	P	Gear down switch	1	P
						Landing brake chute release and jettison handle	1	P
						Recovery chute release and jettison handle	1	P
Canopy and Hatch								
			Hatch latches open	1	C	Hatch jettison switch	1	C
						Canopy shield arm switch	1	P
						Canopy shield jettison switch	1	P

TABLE 13.--Concluded

COMPONENT LIST

Instruments	Quantity	Location *	Lights	Quantity	Location *	Controls	Quantity	Location *
Launch Vehicle Performance System								
SRM TVC pressure	1	P	Abort indicator	3	P, C, E	Slow drift selector switch	1	P
SRM thrust chamber pressure	1	P	Stage I thrust chamber pressure	2	P	System on/off switch	1	P
Stage I fuel and oxidizer tank pressure	1	P	Stage II thrust chamber pressure	1	P			
Stage II fuel and oxidizer tank pressure	1	P	Guid non compare	1	P			
BIGS-RIGS (X), V_H counter	1	P	BIGS-RIGS mode indicator	1	P			
BIGS-RIGS (Z), V_R counter	1	P	ΔV mode indicator	1	P			
BIGS-SD counter	1	P	Auto guid switch over	1	P			
RIGS-SD counter	1	P						
Attitude channel indicator	1	P						
Reaction Control System								
Fuel temperature	1	P	RCS on/off indicator	1	P	RCS on/off switch	1	P
Fuel pressure	1	P	Prop system no. 1 malfunction	1	P	RCS emerg shutdown switch	1	P
Fuel quantity	1	P	Prop system no. 2 malfunction	1	P	System test-selector (8 position)	1	P
			Press. system no. 1 malfunction	1	P			
			Press. system no. 2 malfunction	1	P			
Abort-Deorbit System								
Motor case temperature	1	P	Abort system go	1	P	Case heater on/off switch	1	P
			Abort system no/go	1	P	Motor temperature selector switch (4 position)	1	P
			Deorbit system go	1	P	Abort arm switch	1	P
			Deorbit system no/go	1	P	Abort pull handle	1	P
						Deorbit motor selector switch (4 position)	1	P
						Deorbit motor firing switch	1	P
Electrical Power System								
Voltage dc	1	C	Flight control power on	1	C	Flight control power on/off	1	C
Amperage dc	1	C	Flight control power malfunction	1	C	Adapter power on/off	1	C
			Adapter power on	1	C	R/V power system no. 1 on/off	1	C
			R/V power on system no. 1	1	C	R/V power system no. 2 on/off	1	C
			R/V power on system no. 2	1	C	Electric power test selector (14 position)	1	C
			R/V power system no. 1 malfunction	1	C	Circuit breaker switch	18	C
			R/V power system no. 2 malfunction	1	C			
			Circuit breaker open indicator	18	C			

* P--Pilot's station C--Copilot's station E--Experimenter's station

ER 14471-7

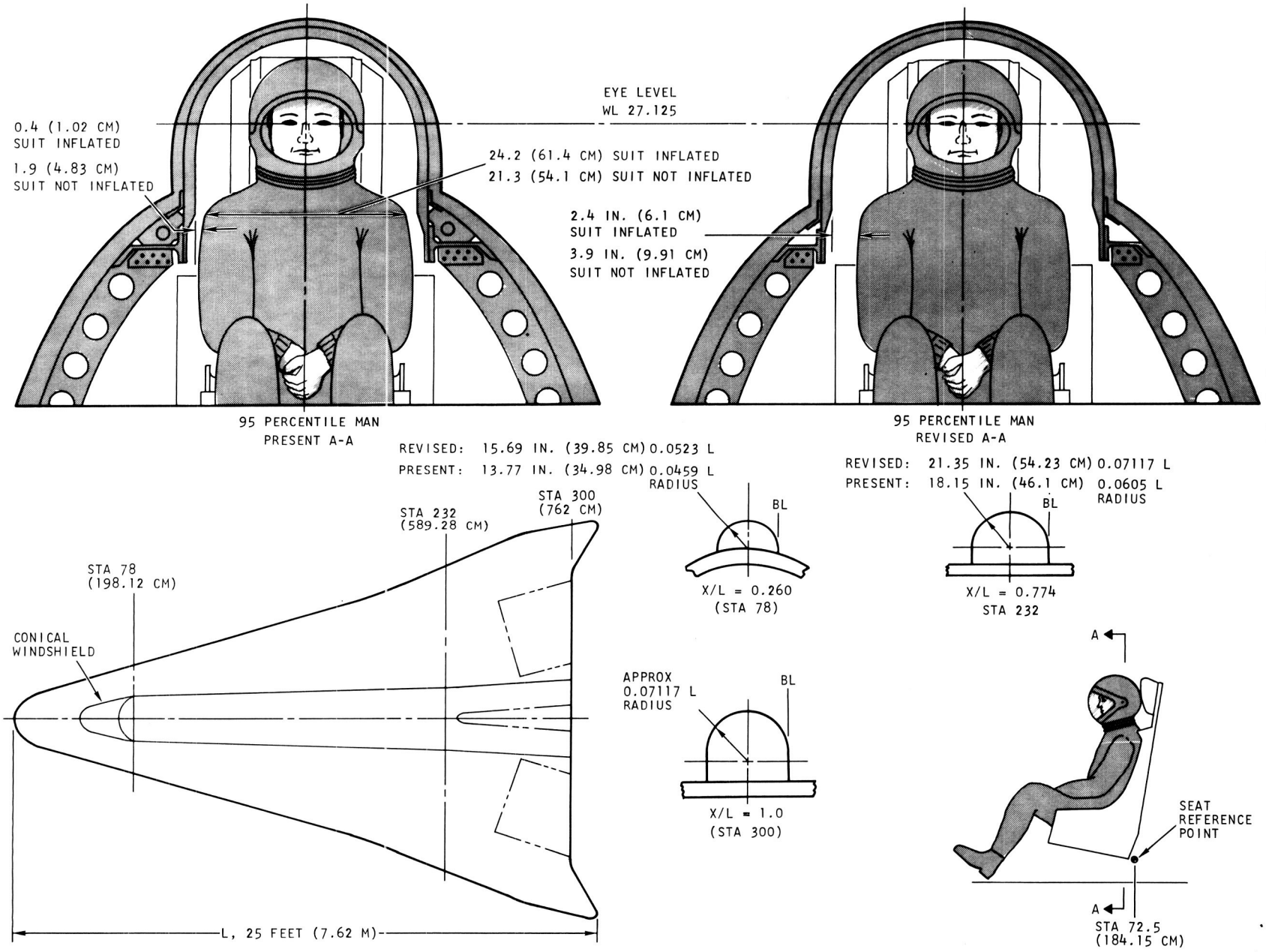

FIGURE 56. INCREASED CANOPY VOLUME AT PILOT'S STATION

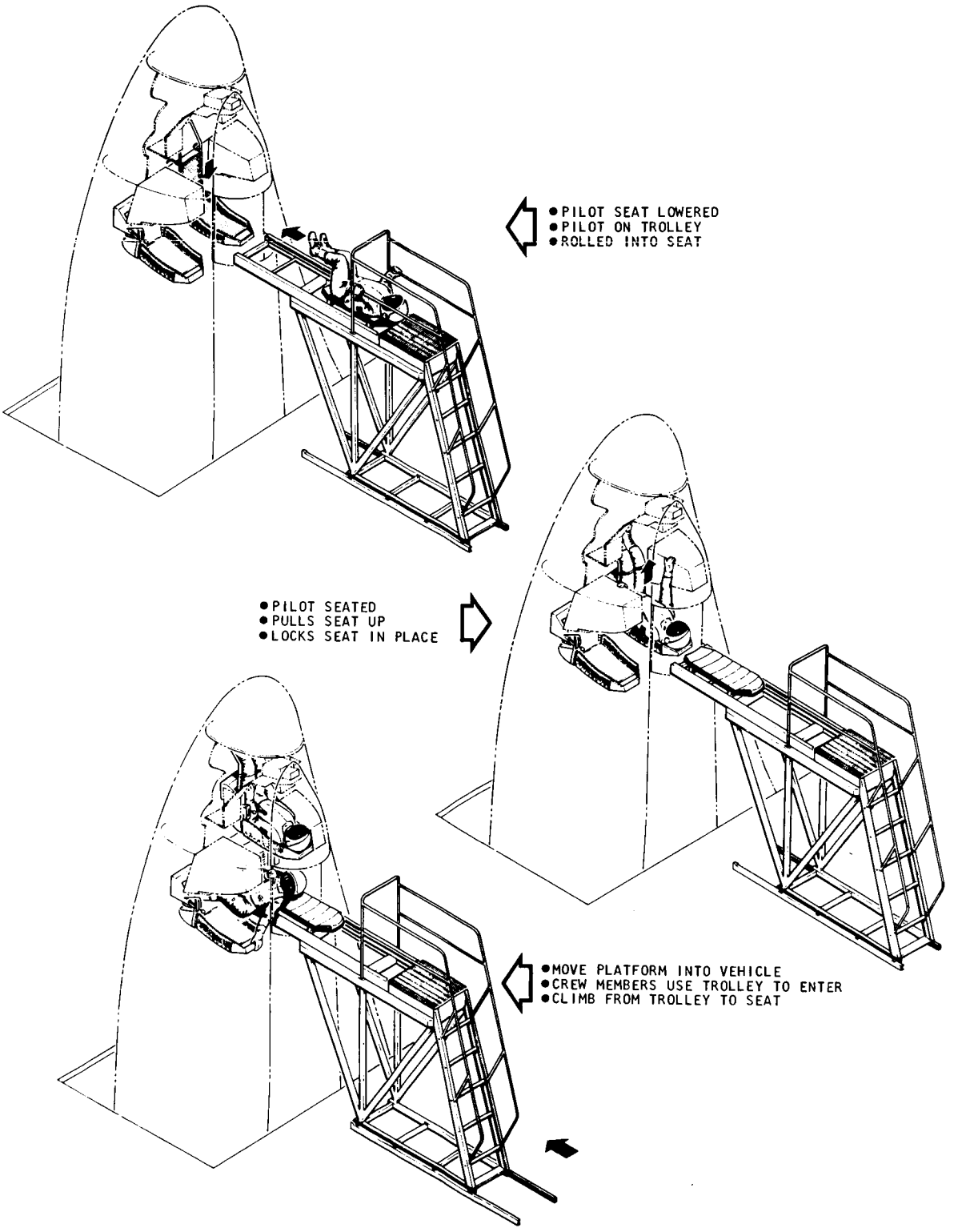

FIGURE 57. CREW INGRESS IN LAUNCH POSITION

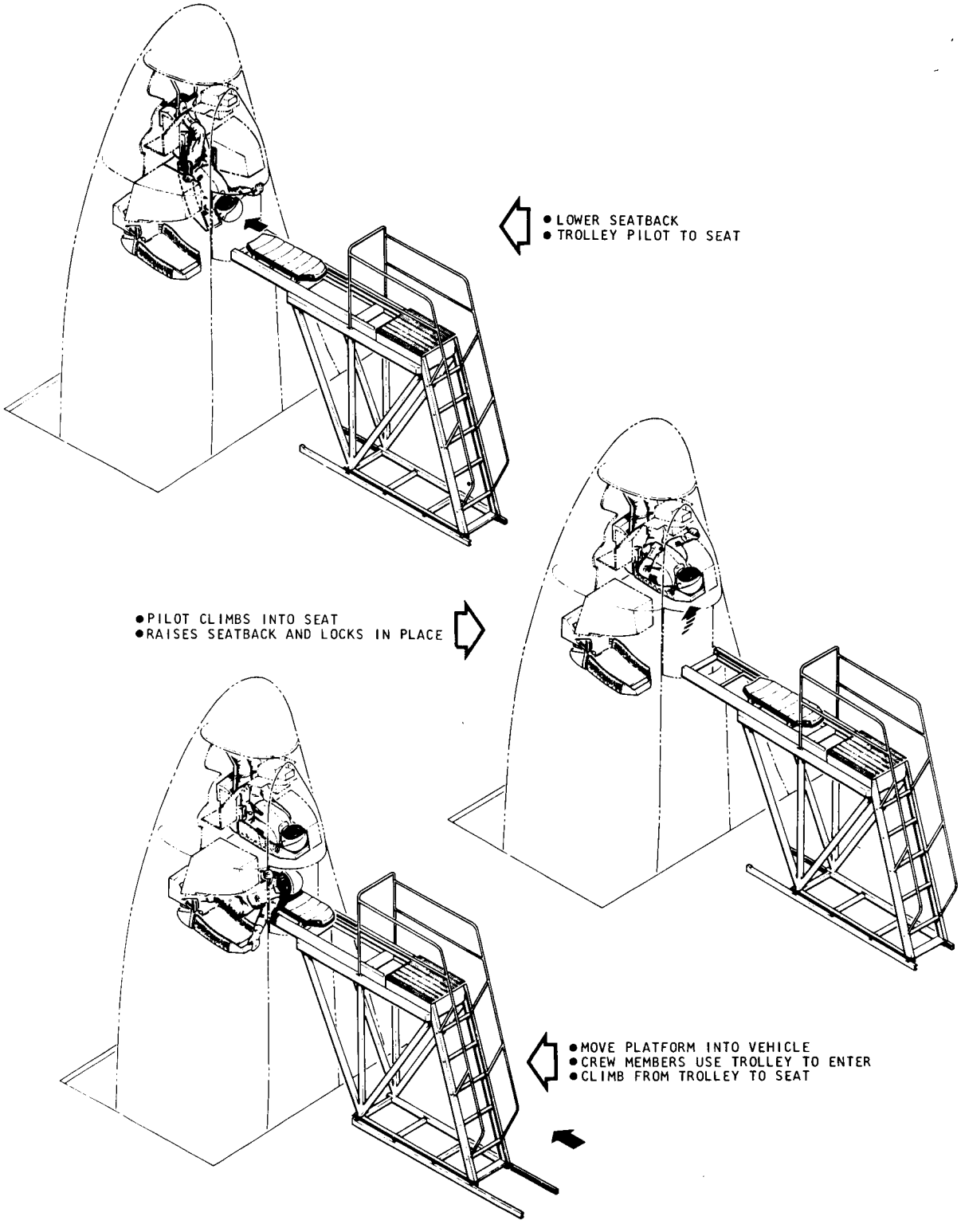

FIGURE 58. ALTERNATIVE METHOD OF CREW INGRESS

FIGURE 59. PILOT EGRESS AFTER LANDING

FIGURE 60. PILOT FLOOR AS STEP FOR AFT CREW EGRESS

E. NAVIGATION AND GUIDANCE SUBSYSTEM

Important subsystem design criteria include the maximum use of developed and flight-proven equipment compatible with the vehicle's research potential, plus the utilization of a simple logic for entry flight which considers the pilot as the primary controller.

The recommended approach, shown in figure 61, was evolved in accordance with these criteria and with the functional requirements throughout the mission. This evolution is presented in section VI-E of Part IV, along with pertinent functional descriptions, performance evaluations and a subsystem specification. These Part IV performance evaluations substantiated the adequacy of the recommended navigation and guidance approach through the couplete entry phase to the point of terminal flare initiation, despite simulated 3σ perturbations. As described in Part IV, the simple guidance logic makes use of preprogrammed reference curves for both the primary and backup modes. Navigation and guidance performance evaluations have been extended in this document to include results of simulated flights conducted specifically for the D/3 vehicle and the flight test trajectory entering from the recommended elliptic orbit. These performance results are summarized in the subsequent two sections, after which the recommended subsystem equipments are discussed.

1. Inertial Navigation Error Propagation

The proposed use of autonomous inertial navigation, from deorbit until acquisition by the landing area tracking radar, results in a vehicle position uncertainty that increases with time. This radial error buildup (in the horizontal plane) was determined for two HL-10 entry trajectories. Trajectories T_1 and T_2 (table 14) cover the flight duration from deorbit until Mach 5; T_1 corresponds to maximum L/D or flight time, and T_2 to the maximum practical crossrange case. The T_3 case assumes a ground transmitted navigation update just prior to atmospheric entry, otherwise it is the same as T_2. (The table 14 navigation errors are corrected by ground terminal guidance.)

Results show that initial conditions are the major sources of navigation error propagation and that the inertial sensor error contributions are relatively small. Also, an update at atmospheric entry does not reduce the error buildup due to initial misalignment, which is the major error source for trajectory T_2.

These navigation error results were obtained for the recommended primary navigation system from linear error equations, programmed by Autonetics on a 7094 computer. Similar results, provided by Minneapolis Honeywell, TRW and United Aircraft, substantiate that entry navigation error contributions due to 3σ inertial component errors will be minor compared to initial condition effects.

The primary navigation requirements, as defined in the subsystem specification in Part IV, include the ability to accurately navigate and guide throughout ascent--in event of a malfunction in the boost vehicle inertial guidance system. Its performance through boost and a three-quarter orbit coast was also evaluated, using digital computer simulation, by Autonetics and United Aircraft. Simulation results substantiate that the performance specifications in Part IV will be met.

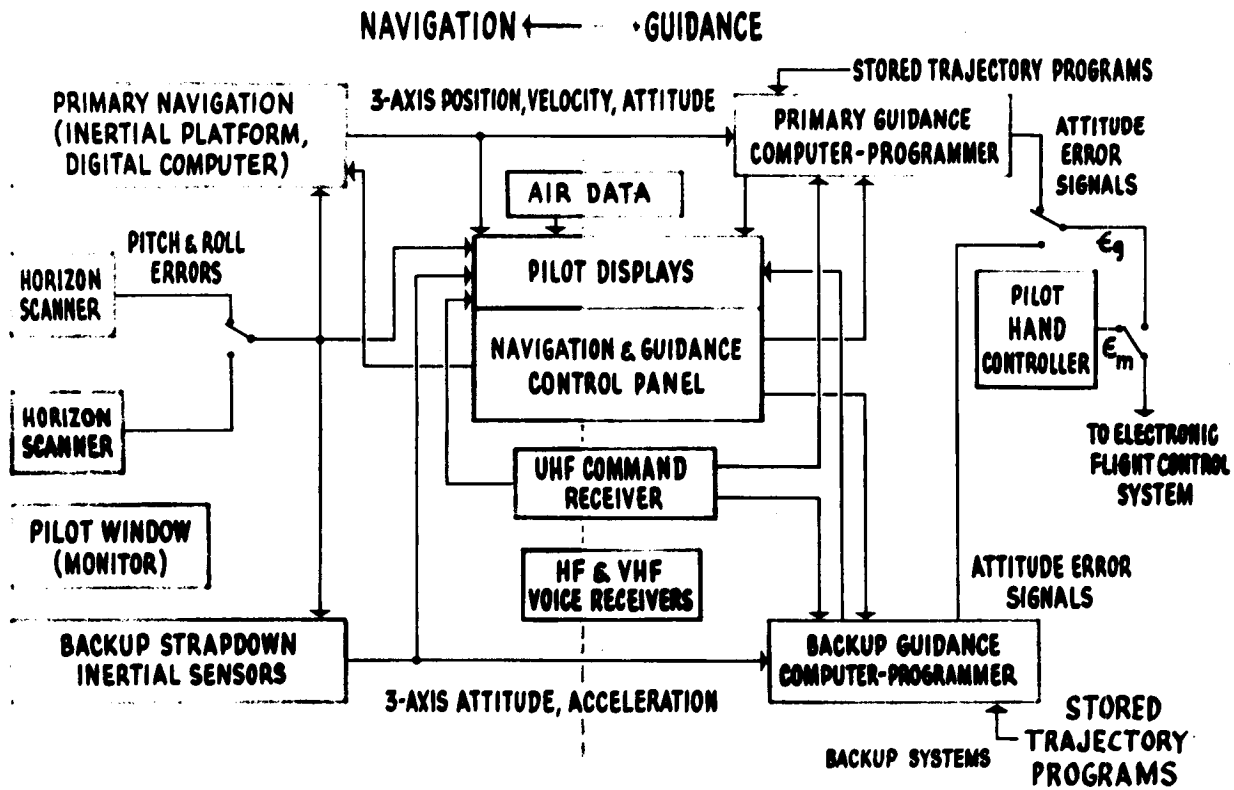

FIGURE 61. NAVIGATION AND GUIDANCE SUBSYSTEM

TABLE 14

NAVIGATION ERROR IN HORIZONTAL PLANE AT TERMINAL SITE RADAR ACQUISITION

Error source		Trajectory		
		T_1 (3630 sec)	T_2 (2592 sec)	T_3 (892 sec)
		Radial error, n. mi. (km)	Radial error, n. mi. (km)	Radial error, n. mi. (km)
Initial Alignment	$\Delta\phi_x$ = 18 min	5.0 (9.26)	6.3 (11.67)	6.3 (11.67)
	$\Delta\phi_y$ = 18 min	12.1 (22.41)	8.3 (15.32)	8.3 (15.37)
	$\Delta\phi_z$ = 18 min	4.0 (7.41)	3.2 (5.93)	3.2 (5.93)
Initial Velocity	$\dot{\Delta}x$ = 8 fps (2.44 m)	14.1 (26.1) *	5.1 (9.45) *	0.8 (1.48)*
	$\dot{\Delta}y$ = 8 fps (2.44 m)	12.0 (22.2) *	7.5 (13.89)*	0.8 (1.48)*
	$\dot{\Delta}z$ = 8 fps (2.44 m)	1.3 (2.41)	0 (0)	1.0 (1.85)
Initial Position	Δx = 0.5 n. mi. (0.926 km)	2.1 (3.89) *	0.5 (0.926) *	0.4 (0.741)*
	Δy = 0.5 n. mi. (0.926 km)	6.7 (12.41) *	3.8 (7.04) *	0.2 (0.37)*
	Δz = 0.5 n. mi. (0.926 km)	0.2 (0.37)	0.5 (0.926)	0.2 (0.37)
Accelerometers (3)		5.1 (9.45)	1.8 (3.33)	0.6 (1.11)
Gyros (3)		0.6 (1.11)	0.3 (0.56)	0.3 (0.56)
RSS total		24.6 (45.56)	14.8 (27.41)	11.0 (20.37)

* Without vertical channel stabilization

2. D/3 Entry Guidance Performance

The guidance performance evaluation presented in Part IV was conducted for an initial entry velocity of 25 320 fps (7740 m/sec), which results from applying a 520-fps (159 m/sec) velocity increment from a 100-nautical mile (185 km) circular orbit. These studies also utilized a C/2 vehicle. Several of these simulated guidance flights were repeated for the D/3 vehicle to evaluate sensitivity to vehicle size and to the higher initial entry velocity when deorbiting near apogee from the recommended baseline elliptic orbit.

Primary mode guidance evaluations again concentrated on the maximum practical crossrange case, using the Part IV guidance equations. The most critical 3σ error source again proved to be an L/D uncertainty of -7 percent. Resulting angle of attack, α, and bank angle, ϕ, response traces are presented in figure 62 for the nominal case and for simulated L/D perturbations of -7 percent and +14 percent. The relative L/D (or α) margins, during hypersonic flight, and the quantized α and ϕ command levels during the ground-based terminal guidance phase, can be observed. Specific results of these and other simulated flights are summarized in table 15.

Comparison of the table 15 nominal values with those in Part IV shows an 8 percent higher crossrange maneuverability due to the increased entry velocity, but also increased total heat. However, heating criteria and hypersonic L/D margin sensitivities to uncertainties and to error source perturbations show only minor differences. Performance is slightly improved for the D/3 vehicle trajectory with regard to negative L/D error tolerability. The lateral displacement errors at flare initiation altitude are significantly improved by simulating the ground radar location to be directly beneath the nominal flare initiation point, instead of at the runway as assumed for the Part IV simulations.

3. Recommended Equipment Summary

The equipments considered for the D/3 vehicle configuration were recommended by potential suppliers in response to a Martin Marietta request for information. This request was accompanied by the subsystem specification presented in Part IV.

Characteristics of the pertinent equipment recommended by various suppliers for the primary mode, backup mode, and experimental research task provisions are summarized in tables 16, 17 and 18. All are applicable to the specified requirements. Unless noted otherwise in the tables, the preliminary cost estimates include necessary design, development, test equipment, and seven flight units. Some of the alternative equipment summarized in table 18 may also prove applicable for the primary or backup modes, depending upon future development and tests.

The selected equipment for the D/3 vehicle is summarized in table 19. This equipment is described further in subsequent sections, which cover the specific units recommended by each contractor and include supporting data.

4. Autonetics Recommendations

Primary mode. - The HL-10 guidance and navigation system is a self-contained, automatic guidance and navigation system designed to function and control with the required accuracy through ascent, post-ascent abort, in-orbit, deorbit and entry. As summarized in table 19, the system is composed of an N16 Inertial Reference Set (IRS), two horizon scanners, and a D-103H general-purpose computer.

The N16 IRS, when integrated with the D-103H digital computer, functions both as a sensor of inertial acceleration components along a set of space-stabilized orthogonal axes, and as an attitude reference. The system block diagram is shown in figure 63. The IRS is designed to accept external mode commands and gyro torquing signals for operation in an align/navigate mode.

Inertial reference set: The IRS consists of a stable platform assembly and its associated control electronics and power supplies. The platform is an all-attitude device on which are mounted three VM8S velocity meters (integrating accelerometers). The VM8S output is in the form of two square-wave resolver signals, 90° out of phase. The platform is stabilized by two 2-axis G9 gyros.

The gyro operates in a pulse-torquing mode. The torquing signals provided by the external computer are converted in the IRS to binary pulse form. The pulses are of constant amplitude and width increments; they change in sign under digital computer control to produce the desired torquing rate. Zero torquing rate is generated by alternate plus and minus pulses. Maximum torquing rate of 50° per hour occurs when the binary signal remains in the plus or the minus state.

The platform uses a one- and eight-speed resolver assembly on each of the roll, pitch; and azimuth axes. The outputs are transformed to synchro form in the driving amplifiers, and also electronically encoded to whole-word digital form. Sine and cosine of the roll angle are also encoded.

IRS precision parameters, such as gyro and velocity meter biases, scale factors, and axis alignments, are stored in a small memory module located in the IRS. Most of these parameters are determined and stored during a system-level automatic calibration run; others are manually entered at the time of inertial instrument change and prior to system calibration. When the IRS is mated with the external D-103H computer, the precision parameters are read out to the memory of the external computer for use in the navigation mechanization.

Conversion and tie-in equipment: Conversion electronics are required for compatible interface between the IRS velocity meters and gyros and the external D-103H computer for: (1) converting the IRS platform gimbal angle resolvers to the desired analog and digital forms, (2) validity and parity checks, and (3) digital communication between the memory of the IRS and the external computer.

D-103H computer: The computer proposed for use in the HL-10 baseline guidance and navigation system is a microminiaturized general-purpose computer.

The D-103H computer consists of an arithmetic and control unit, coincident-current core memory, input-output, and the power supply--all combined into a single chassis.

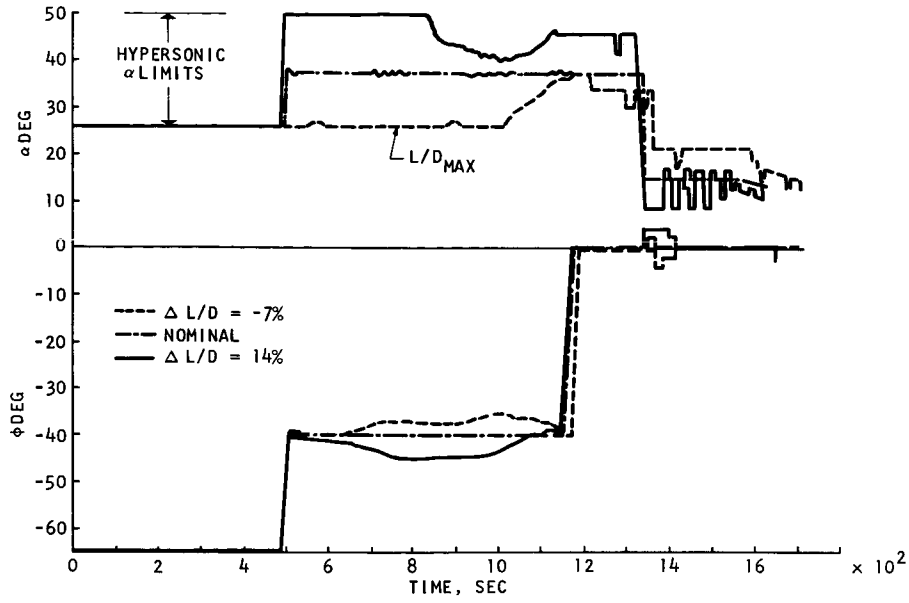

FIGURE 62. D/3 GUIDANCE SIMULATION WITH L/D PERTURBATIONS, MAXIMUM PRACTICAL CROSSRANGE

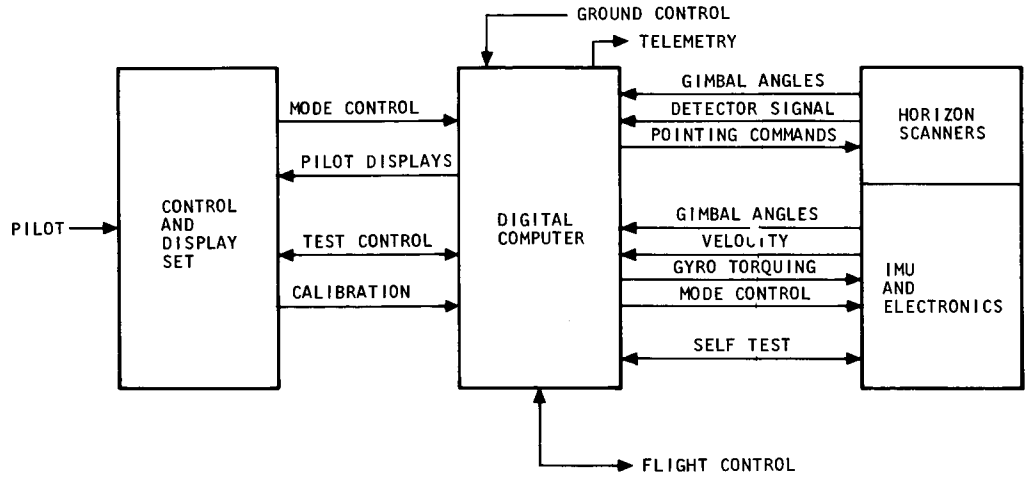

FIGURE 63. PRIMARY SYSTEM SCHEMATIC

ER 14471-7

TABLE 15

ENTRY GUIDANCE SIMULATION RESULTS, MAXIMUM PRACTICAL CROSSRANGE TRAJECTORY FOR D/3 VEHICLE

Condition	Deviation from nominal, Max. heat rate		Deviation from Nominal at Altitude of 670 feet (204.2 m)									Approximate hypersonic L/D margin, % (relative)
			Total heat		Time, sec	Lateral Displacement		Downrange		Velocity (R)		
	Btu/ft^2 sec	MN/m^2	Btu/ft^2	MJ/m^2		ft	m	ft	m	f/s	m/s	
Nominal	(178)	(2.02)	(89.6 x 10^3)	(1.02)	(1656)	(0)	(0)	(0)	(0)	(506)	(152)	100
$\Delta L/D = -7\%$	+4	+0.05	+12.7	+0.14	+57	0	0	-97	29.6	-15	-4.5	26
$\Delta L/D = -8\%$	+5	+0.06	+13.6	+0.15	+79	-1	-0.3	-110	-33.4	-19	-5.8	5
$\Delta L/D = +14\%$	-9	-0.10	-9.3	-0.11	-31	-2	-0.6	+134	+40.7	+15	+4.5	34
Atmospheric density change of +60%	+7	+0.08	+6.1	+0.07	+41	-3	-0.9	+182	+55.6	-58	-17.4	51
Atmospheric density change of -30%	-6	-0.07	-0.6	-0.01	-8	0	0	-176	-53.7	+34	+10.2	65
$\Delta V_i = -100$ fps (30.48 m/s)	+13	+0.15	+8.6	+0.09	+18	+2	+0.6	+103	+31.5	-5	-1.5	34
Initial flight path angle deviation of -0.12°	+13	+0.15	+8.5	+0.09	+11	+2	+0.6	+24	+7.4	0	0	42
$\Delta h_i = 14\,100$ ft (4297.7 m)	+4	+0.05	+8.1	+0.09	+5	-	0	-18	-5.6	+1	+0.3	51
Constant north wind of 100 fps (30.48 m/sec)	+1	+0.01	+1.2	+0.01	+72	-2	-0.6	-304	-92.6	-179	-54.6	96
Angle of attack reference error of +2.0°	-7	-0.08	-0.8	+0.01	+5	-4	-1.2	+261	+79.6	-6	-1.8	87
Bank angle reference error of +2.0°	-4	-0.05	-0.3	-0.01	+3	+1	+0.3	0	0	-1	-0.3	79
$\Delta X_R = 74$ n.mi. (137 km) $\Delta R = 67$ n.mi. (124 km)	+1	+0.01	+13.6	+0.15	+48	-1	-0.3	+30.4	+9.3	0	0	32

Initial position deviations:

Crossrange = 74 n.mi. (137 km)

Downrange = 67 n.mi. (124 km)

Nominal initial conditions: h = 400 000 ft (121.92 km), γ(I) = 1.50°, velocity, (I) = 25 860 ft/sec (7882 m/sec)

Nominal end conditions: γ(R) = -17.6°, velocity (R) = 506 ft/sec (154 m/sec), downrange = 3749 n. mi. (6943 km), crossrange = $\pm$676.5 n. mi. (1253 km)

TABLE 16

CANDIDATE NAVIGATION AND GUIDANCE EQUIPMENT FOR BASELINE PRIMARY MODE

Contractor	Equipment	Weight, lb (kg)	Volume, ft^3 (m^3)	Power watts	MTBF, hr	Cost, $	Development Status
Autonetics	N-16 IMU, D103-H computer, Dual horizon scanners	149.4 (22.4)	3.62 (0.103)	522	2620	7.7×10^6	Components being developed for F-111 , SRAM and OGO
Honeywell	IMU platform, SIGN III computer	70 (31.8)	1. (0.028)	280	800	6.	Gemini platform, developmental computer
A.C. Electronics	IMU, computer, display and keyboard, wiring harness	225 (102.1)	--	400	--	7.6*	Apollo Lunar Module system
Raytheon	Computer (only)	52 (23.6)	0.8 (0.023)	110	2850	3.5*	Apollo, modified Block II

*Cost estimate based on seven unmodified units only.

TABLE 17

CANDIDATE NAVIGATION AND GUIDANCE EQUIPMENT FOR BASELINE BACKUP MODE

Contractor	Equipment	Weight, lb (kg)	Volume, ft^3 (m^3)	Power watts	MTBF, hr	Cost, $	Development Status
Honeywell	Strapdown IMU, computer-programmer, power supply	38.5 (17.5)	0.55 (0.016)	200	2200	3.0×10^6	Being used in PRIME flight test program
United Aircraft	Strapdown IMU, digital processor	31. (14.1)	0.5 (0.014)	100	2000	2.6	IMU developed for Apollo Lunar Module, developmental computer
Autonetics	Strapdown IMU, DDA computer	28. (12.7)	0.77 (0.022)	52	--	1.3	Being developed under company funds

ER 14471-7

TABLE 18

CANDIDATE EXPERIMENTAL NAVIGATION AND GUIDANCE EQUIPMENT

Contractor	Equipment	Weight, lb (kg)	Volume, ft^3 (m^3)	Power watts	MTBF, hr	Cost, $	Development Status
TRW	Strapdown IMU, computer, and DEDA	60.7 (27.5)	1.6 (0.045)	175	1530	6.5×10^6	Developed for Apollo Lunar Module
Honeywell	SIGN III (strapdown IMU and computer)	42. (19.1)	0.6 (0.017)	176	2135	3.0	Computer has been packaged and tested. IMU will be tested this year.
Autonetics	N-35S IMU, computer, star tracker and earth landmark tracker	123 (55.8)	3.1 (0.088)	432	7500	13.9	Being developed. Except for landmark tracker, functionally equivalent components have been flown.

TABLE 19

SELECTED D/3 NAVIGATION AND GUIDANCE EQUIPMENT

Contractor and Function	Equipment	Weight, lb (kg)	Volume, ft^3 (m^3)	Power, watts	MTBF, hr	Development Status
Autonetics	IN-16 IMU	67 (30.4)	2.3 (0.065)	250	3 250	Sled and flight tested; being developed for F-111
Baseline Primary mode	D-103H digital computer	56 (25.4)	1.17 (0.033)	250	13 600	Being developed under Air Force contract
	Dual horizon scanners	26.4 (12.0)	0.30 (0.008)	22	71 230	Developed by ATL for OGO
Honeywell	Strapdown IMU	21.5 (9.8)	0.28 (0.008)			Successfully completed initial PRIME flight tests
Baseline backup mode	Computer programmer	8 (3.6	0.16 (0.005)	200	2 200	
	Power supply	9 (4.1)	0.11 (0.003)			
TRW Systems	IMU	19.8 (9.0)	0.3 (0.008)	74	3 200	Apollo Lunar Module abort guidance system
Experimental research tasks	Digital computer	32.5 (14.7)	1.14 (0.032)	90	4 000	
	Data entry and display assembly	8.4 (3.8)	0.15 (0.004)	11	11 000	

Integrated circuits are mounted on 5 by 7-5/8 inch circuit boards. Interconnections for these boards are provided by a multilayer interconnection board to simplify wiring. Forced air and conduction cooling are used to maintain the components within specified temperature limits and to provide environmental protection with a sealed chassis.

Functionally, the D-103H is a binary, parallel, single-address computer capable of performing logic and arithmetic operations for the HL-10 baseline primary N and G system.

The characteristics of the D-103H computer are summarized in table 20.

Horizon scanners: The selected horizon sensors unit features four tracking heads spaced 90° in azimuth around the yaw axis of the vehicle. Two tracker heads are mounted on a single casting, so that only two castings are mounted on the vehicle. In operation, the trackers supply measurements of the horizon angle at four different azimuth positions. Pitch and roll can both be computed from any three out of the four measurements by performing analog computations of the typical forms:

$$\text{Pitch (or roll)} = \frac{\theta_A + \theta_B}{2} - \theta_C$$

or

$$\text{Pitch (or roll)} = \theta_C - \theta_A$$

where θ_A, θ_B, and θ_C are three properly chosen horizon-angle measurements.

Any one of the four trackers can fail, therefore, and undegraded performance can still be achieved by properly switching the inputs to the pitch and roll computing circuitry. Similarly, if the sun appears in the field-of-view of any of the four trackers, that tracker will be removed from the computation and full performance can still be realized.

Self-contained performance monitoring: During system operation, critical points can be continually monitored by the digital computer through a logic network to provide a discrete indication of a failure in any of the system functional areas. This information will then be available for prelaunch readout or for telemetering to a ground station during test flights.

The functional areas, monitored during automatic checkout as well, are the following: power supplies, platform control loops, gyro torquing loops, velocity meter control loops, optical tracker loops, the digital computer, and auxiliary equipment outputs.

Automatic checkout: A thorough and accurate assessment of the functional integrity of the system can be obtained from a computer-controlled system checkout. Automatic checkout provides a rapid, uniform procedure, free from human fallibility and the requirement for operator skill in application and interpretation.

During prelaunch checkout, a thorough test must be administered by the computer which will quickly verify system functional integrity or isolate a malfunction to a readily replaceable major assembly such as the IRS, the optical trackers, the horizon scanner,

TABLE 20

D-103H COMPUTER CHARACTERISTICS

Functional	
Type	Parallel processor--internally stored program--tape filled
Synchronous clock rate	1.11 Mc (0.9 μsec per bit time)
Data word length	24 bits including sign
Number system	Binary 2's complement
Instruction format	Single address--32 basic instructions--plus input-output and modified instructions--24-bit instruction length
Memory capacity	16 384 24-bit words
Memory type	DRO core
Special features	34 interrupts--internal and external with wired priority
	Built in program interrupt protection
	Built-in 50-millisecond real-time interrupt
	Built-in double precision add, subtract, clear, and add and store instructions
	Bootstrap fill capability
	Special instructions
	Power transient or failure memory protection
Performance Data	
Memory cycle time	3.6 μsec
Arithmetic instruction times	Add/subtract, single precision . . 7.2 μsec
	Add/subtract, double precision (built-in) . . . . . 10.8 μsec
	Multiply--single precision . . . . 18 μsec
	Multiply--double precision (programmed) . . . . . 152 μsec
	Divide--single precision . . . . . 29.7 μsec
Addressing modes	Direct addressing for up to 32 768 words
	Indexed addressing--7 index registers stored in memory, unlimited levels of indexing.
	Indirect addressing--unlimited levels of indirect addressing and indexed indirect addressing

Memory expansion: up to 16 000 words internally, plus another 16 000 words in external package (located up to 30 feet from basic computer) without modifications to basic computer.

the IRS electronics, the computer, the experimental system sensor equipment, or the backup strapdown system.

Development status: The N16 IRS navigation system has successfully completed flight testing at Holloman Air Force Base. An advanced version of the N16 system is presently under development for the Mark II avionics system for the F111 aircraft.

The D-103H computer is currently under development by Autonetics' Data Systems Division for use in an Air Force military application. Development and delivery schedules lead the HL-10 program sufficiently to provide a well-developed and flight-tested computer for the HL-10 flight program.

Development of the horizon sensor package was completed for the Orbiting Geophysical Observatory.

Backup mode.- The backup strapdown navigation and guidance system consists of a modularized inertial sensor package and a special-purpose DDA computer. The inertial sensor package consists of two Autonetics G10B gyros, three Autonetics A40 electromagnetic accelerometers, gyro electronics, a clock (to be used also by the DDA's), and a power supply. Its characteristics are summarized in table 17.

G10B gyro: The Autonetics G10B free-rotor gyro is a two-axis displacement gyro capable of torquing rates of up to 20° per second. Except for the increased torquing capability, it is identical to the G10A gyro used in the N35S Inertial Measuring Unit (IMU) experimental system.

A40 electromagnetic accelerometer: The electromagnetic accelerometer is a single-axis, closed-loop, force servo type. Although it is inherently an analog accelerometer, a digital velocity output is obtained when it is combined with current-digitizing components in the force-servo loop. The acceleration sensing member is a fused-silica proof mass which is attached to the accelerometer stator members by means of an integral flexure section. The proof mass and the flexure section are made of a single, precisely lapped and etched disk of fused silica to attain dimensional stability with respect to temperature, time, and acceleration environment.

DDA special-purpose computer: The computer requirements for the baseline backup navigation and guidance system will be met by a small special-purpose DDA computer, incorporating components and techniques within the limits of existing technology. The computer will consist of 60 to 100 metal-oxide-semiconductor integrators, one bit counter, one 30-bit shift register, a small serial storage device, and some initialization and input/output selection logic. The serial storage device will be used for storage of platform parameters and preprogrammed trajectory data.

The MOS integrators and associated logic will be contained on two 5 by 8 inch or smaller cards. The volume of the logic package will not exceed 0.1 cubic feet. The total weight of the computer will not exceed 2 pounds and will not require more than 5 watts of power.

Experimental research equipment.- In its basic form, the system is composed of an Inertial Measuring Unit (IMU), an optical tracker, and a digital computer. An additional known-landmark tracker to perform Task GN-3 is added to the basic system without the need for very precise mechanical tie-in with the IMU. The N35S IMU is an

adaption of the N16 IRS proposed for the baseline system. The basic difference between the N16 and the N35S is that the use of the star tracker in the N35S system requires the N35S to use precision optical gimbal angle readouts, but allows the IMU to use non-case-rotated gyros. Otherwise, the N35S is identical to the N16 proposed for the baseline system. The N35S IMU platform is stabilized by two G10A gyros, miniaturized versions of the two-axis, free-rotor, gas spin bearing gyro (G6B4). Precision optical angle readouts are used for gimbal angle resolvers.

The computer proposed for use in HL-10 experimental systems is the D-103J, a smaller version of the D-103H proposed for the baseline primary navigation and guidance system. This computer possesses features making it capable of satisfying the stringent requirements of the experiments to be performed. The D-103J memory can be expanded to 16 384 words (the D-103H), and thence to 32 768 words to meet increases in system requirements. This is accomplished by the addition of a 16 384-word memory module which can be located remotely from the computer.

The N35S optical star tracker consists of a telescope, mounted in a two-degree-of-freedom gimbal system with a torquer and optical angle readout on each of the two axes. A solid-state photodetector is mounted in the focal plane of the telescope. To ensure a large viewing solid angle at all times, the tracker will be mounted separately from, but on the same base with, the IMU.

The known-landmark tracker is identical to the star tracker with the exception of the focal-plane detector. The landmark tracker has star detector as well as a landmark detector capability to permit inflight calibration.

Because the N35S is identical to the N16, with the exception of the gyros and gimbal angle readouts, a high degree of confidence can be placed in the quoted physical characteristics of the N35S. The gyros used are the developed G10A gyros which are presently used on the Elliott Brothers' E5 autonavigator. The gimbal readouts are the optical angle readouts which were developed for the N16S autonavigator.

Development status: Daylight star acquisition and tracking were successfully demonstrated in 1952 by the Autonetics XN-2 inertial navigator. Since 1955, successors to this first stellar-inertial navigator have included N2C, N2J, N3A, N3B, and N7D. These systems have undergone thousands of hours of test and actual use in such vehicles as T-29, B-58 and C-121 aircraft, and marine surface craft. Current development programs include a company-funded N16S tracker subsystem and the Air Force-funded Unknown Landmark Tracking (ULTRA) Feasibility Study.

5. Honeywell Recommendations

Primary mode. - The system consists of a stable platform IMU and a SIGN-III computer. Its characteristics are summarized in table 16. The IMU is an all-attitude, four-gimbal type derived from various programs, including Gemini. It utilizes three GG177 flexure pivot accelerometers and three GG8001 miniature integrating gyros. The computer utilizes a random-access, coincident-current magnetic core memory with a storage capacity of 4096 20-bit words. Typical computation times are: add (4 μsec), multiply (24 μsec), and divide (24 μsec).

Backup mode. - The navigation and guidance backup system characteristics are summarized in table 19. It provides information to the pilot and/or vehicle flight critical electronics which allow the vehicle to be guided to a predetermined area for terminal radar acquisition. The system also provides instrumentation for postflight data analysis.

The system consists of a strapdown inertial measurement unit, a computer/programmer, and a power supply.

IMU: The IMU contains three type GG87-B16, miniature, floated, single-degree-of-freedom, rate integrating gyros and three type GG177-B17, fluid-filled, hinged-pendulum, linear accelerometers. Both the gyros and accelerometers are operated in a pulse-rebalance mode.

Computer/programmer: The programmer section provides the computer section with stored functions: acceleration, alpha limits, roll angle, etc. It can operate in a continuous or standby mode. The latter facilitates long flight periods that require no input.

The computer section performs all computations required to implement the entry guidance law.

Development status: The backup system is being flight verified on the PRIME program as the navigation and guidance system. Minor modifications are envisioned, primarily to the computer/programmer, to facilitate the longer, multiorbital HL-10 mission. This should not, however, invalidate PRIME flight testing that will have been achieved.

Experimental research equipment. - The SIGN III inertial guidance system is contained within one package which includes the strapdown inertial sensor, computer, and associated electronics. Its characteristics are summarized in table 18.

The inertial sensor assembly contains three pulse-rebalanced gyros for measuring incremental angular rotations at body rates up to 200° per second, and three pulse-rebalanced accelerometers for measuring incremental velocities during linear acceleration up to 20 g.

The SIGN III computer is a fast, general purpose computer with special hardware to facilitate high-speed incremental arithmetic. Its important features include:

Memory size	4096 words, standard
Expendable	Yes
Data word length	20 bits
Instruction word length	20 bits
Add time	4 μsec
Multiple time	24 μsec
Divide time	24 μsec
Index registers	3 in memory
Number of instructions	56

The processor uses two-complement, fixed-point, fractional arithmetic. While the 20-bit data word is adequate for the majority of the calculations, several instructions have been provided for double-precision arithmetic. For example, the double-precision add instruction can add two 40-bit words in 6 microseconds. Memory sizes up to 4096 words can be accommodated directly. Larger sizes may be handled conveniently by using an output discrete as a bank change command. The special-purpose, wired-program sequencer processes the incremental inputs (velocity and attitude pulses) at a rate of 3200 iterations per second.

A functional block diagram of the SIGN III is shown in figure 64.

6. TRW Systems Recommendations

The lunar module abort guidance section is a strapdown, all-attitude, inertial guidance subsystem being developed and produced by TRW systems for NASA's Manned Spacecraft Center under subcontract to Grumman Aircraft and Engineering Corporation. The AGS is a light-weight, low-powered guidance subsystem which offers sufficient flexibility for application to a wide variety of manned and unmanned missions. Its characteristics are summarized in table 19. With minor modifications, it can be employed for the experimental research tasks and also for the primary or backup modes.

The abort guidance system consists of three subassemblies: the abort electronics assembly, the abort sensor assembly, and the data entry and display assembly. A brief description of each of these major subassemblies is contained in the following paragraphs.

Abort electronics assembly (AEA). - The AEA is a general-purpose digital computer designed by TRW for use with strapped-down gyros and accelerometers. This general purpose computer incorporates a core memory with a 5-microsecond access time and has a word length of 17 bits plus sign. All circuits have been designed using "worst-case" techniques in order to meet the stringent reliability requirements of the lunar module program.

The general characteristics of the lunar module AEA are:

Memory capacity	4096 words
Clock frequency	1.024 Mc
Word length	18 bits
Repertoire	27 instructions
Computation time	
Add	10 μsec
Multiply	70 μsec

The memory system is a partially hard-wired, partially scratchpad, 18-bit, 4-millisecond cycle time, ferrite core type. The memory is currently half hard-wired and half soft-wired, with 512 words of the soft-wired portion being scratchpad. The logic design

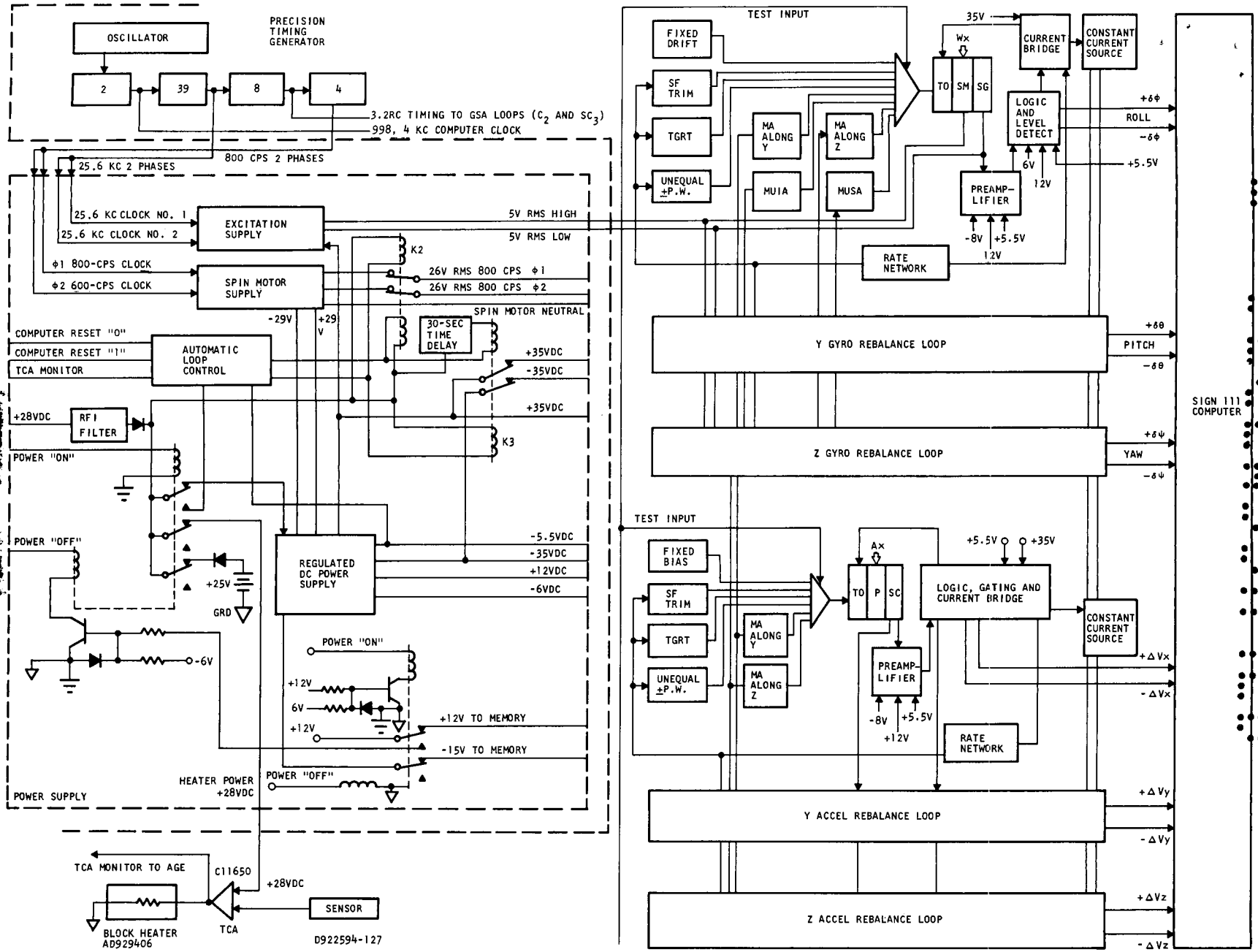

FIGURE 64. SIGN III BLOCK DIAGRAM

CONFIDENTIAL
ER 14472-7

is such that allowance for expansion has already been designed for extension from 4096 words of memory to 8192. The scratchpad memory is electrically alterable through established loading equipment.

Abort sensor assembly (ASA). - The inertial reference unit for the abort guidance section, the ASA, is being developed and produced by United Aircraft Corporation Systems Center under subcontract to TRW. This inertial sensor assembly utilizes three Norden RI-1139B single-degree-of-freedom, floated, rate integrating gyros, and three Bell VII pendulous accelerometers as inertial instruments. The ASA is essentially a self-contained subassembly in that it includes, in addition to the inertial sensors, an integral power supply, inertial sensor pulse rebalance electronics or pulse torque servo amplifiers, thermal control electronics, and a frequency synchronizer or control subassembly.

The gyros and accelerometers are both operated in a torque-rebalance or forced-limit cycle mode. The gyros sense angular rotation about each of the vehicle axes and are pulse-torqued to remain at null. The pulses represent incremental body rotations, $\Delta\theta$, which are processed by the AEA. Similarly, the pulse-rebalanced accelerometers measure incremental velocity changes, and the pulses are proportional to incremental vehicle velocity components along the respective accelerometer input axes.

General characteristics of the ASA are:

Maximum design turning rate	±25 deg/sec
Maximum design acceleration	+100 ft/sec^2
Sensor scale factor (approximate)	
Angular	3 arc sec/pulse
Translational	0.003 ft/sec/pulse

The current ASA design (see functional block diagram in figure 65) takes advantage of the AEA's capability to provide compensation of certain error sources and of the capability of the lunar module primary guidance subsystem for providing initial alignment under some operating modes. Other mission applications for which the abort guidance system might be considered would require certain ASA modifications, such as the addition of a porro prism for optical azimuth determination and a change of the accelerometer scale factor. This later change can be accomplished within the accelerometer pulse torquer servo amplifier because the instrument itself is capable of measuring in excess of 20 g.

Data entry and display assembly (DEDA). - The DEDA enables the astronaut to manually enter data into the computer and to readout data stored within the computer. The entry or readout of data is accomplished via a keyboard. As data are assembled, they are displayed on an electroluminescent panel for verification by the operator prior to initiation of either an entry or readout command. In the event data are incorrectly entered or an incorrect mode commanded, an operator error lamp is lighted, indicating to the astronaut that an error was committed. The address of the memory location where data are to be entered or read out consists of three octal digits.

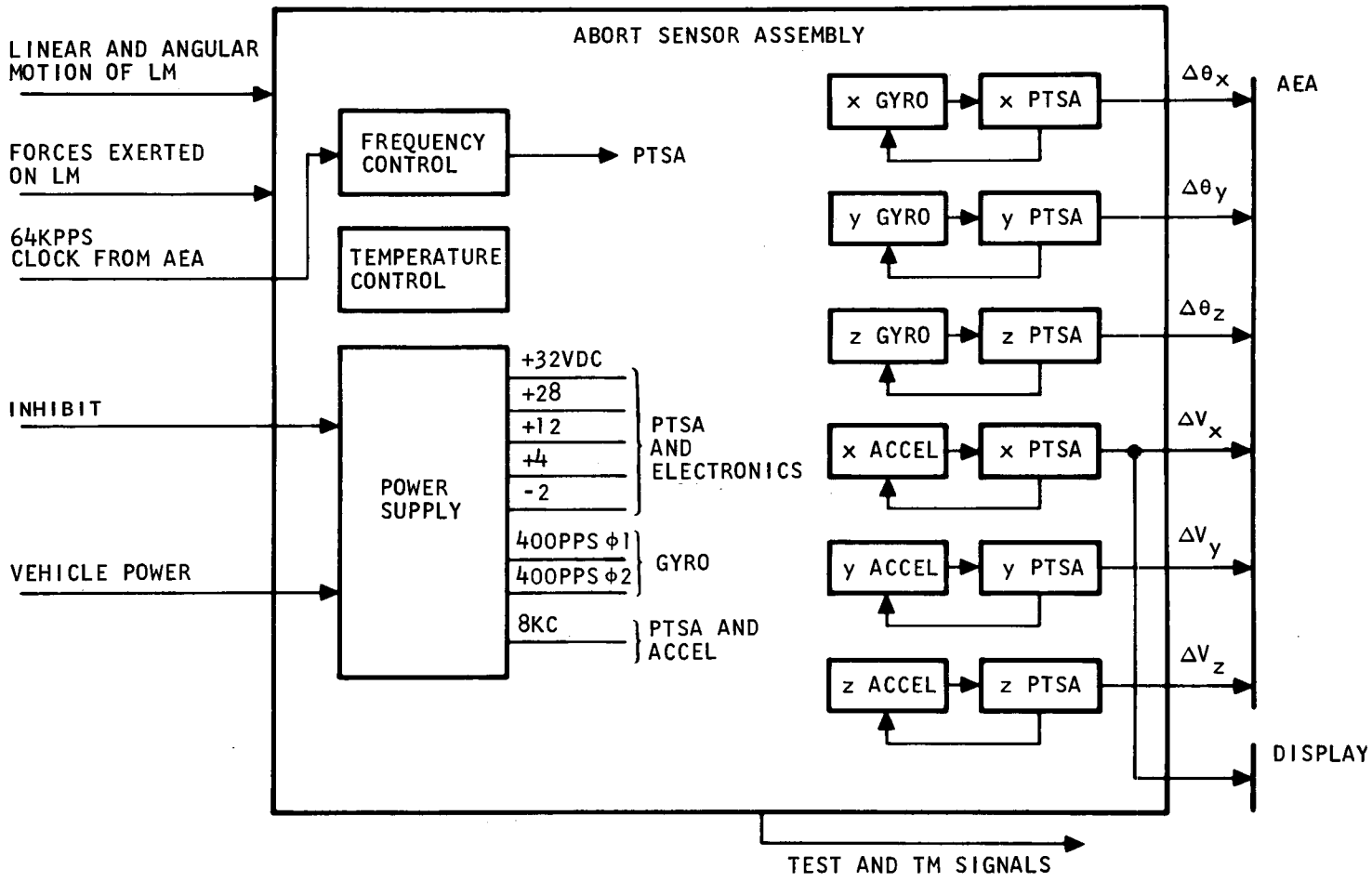

FIGURE 65. ASA FUNCTIONAL BLOCK DIAGRAM

Data are composed of five decimal digits and a plus or minus sign. Additional controls consist of a "clear" button for clearing data incorrectly entered or for terminating a readout mode and a "hold" button for terminating the update of data being read out of the computer.

7. United Aircraft Recommendations

The proposed backup mode equipment consist of a three-axis strapdown inertial measurement unit (SDIMU) and a special purpose digital data processor. The SDIMU contains three Norden RI-1139 gyros, three Bell VII accelerometers, pulse torquing servo amplifiers, and other associated electronics. The data processor converts the sensor body attitude reference to an equivalent inertial reference. Equipment characteristics are summarized in table 17.

Strapdown inertial measurement unit. - The strapdown inertial package is that developed for the Centaur Phase II program. It is essentially the lunar module/abort sensor assembly redesigned to accommodate the boost environment of the Centaur. It is expected that modifications, if any, would be minor to satisfy HL-10 requirements.

Digital data processor. - The platform equivalent electronics package is a special purpose digital data processor designed by United Aircraft for use with the strapdown inertial sensor package. The pulse outputs of the sensors are used to calculate sensor attitude in inertial coordinates.

The computer memory system contains a 512-word linear core rope for the program memory, plus a 256-word by 24-bit coincident current toroidal core matrix for data memory. The core rope memory is used for the portion of the program which remains constant regardless of the mission. The scratch-pad" memory is utilized for those sections of the program and data which are mission- and time-dependent. Thus, targeting flexibility and reaction time are preserved with a savings in weight and cost.

The core rope memory utilizes toroidal cores which have a linear B-H curve. These cores permit low power operation because the cores are not switched and do not have to be primed. The entire memory system logic circuitry consists of integrated circuits, including core rope drivers and sensing circuits. The coincident current memory utilizes integrated circuits for matrixing and sensing and discrete components for the core drivers.

8. A.C. Electronics Recommendations

The Apollo navigation and guidance configuration which would come closest to satisfying the specified HL-10 requirements is a Lunar Excursion Module (LEM) system which consists of two wiring harnesses, inertial measurement unit, pulse torque assembly, power servo assembly, electronic component data unit, LEM guidance computer, and display and keyboard. The display and keyboard does contain certain pilot displays, and the computer can be programmed to display any of its information.

As summarized in table 16, the LEM system weighs approximately 225 pounds and requires 400 watts of 28 volts dc power. At the present time the ninth LEM system is in

final checkout and is fully qualified for the Apollo program. The differences in environmental requirements are estimated to have no impact on the design. By the date of the HL-10 need, the system will have been fully flight tested.

9. Raytheon Recommendations

The Apollo guidance computer is a parallel, single-address stored program, general purpose computer, characterized by core rope modules containing 6144 words. The core rope modules are designed to be inserted into the computer in pairs, so the guidance computer could operate with 12 288 words to 36 864 words of fixed memory. The HL-10 application can be met with one pair of core rope modules supplying a capacity of 12 288 words of fixed memory and 2048 words of erasable memory. Computer physical characteristics are summarized in table 16. The computer capacity is more than adequate for the baseline primary mode requirements, and also appears to be well suited for accomplishing research tasks GN-3 through GN-6 in Part II.

Salient features of the Apollo guidance computer are listed below:

Organization	Parallel
Number system	1's complement
Power (operating)	100 watts
Power (standby)	10 watts
Clock frequency	2 Mc
Memory (fixed)	36 864 words
Memory (erasable)	2048 words
Word length	15 bits plus parity
Volume	Approximately 1 ft^3
Weight	Approximately 70 lb
Add time	24 μsec
Double precision add	36 μsec
Multiply time	48 μsec
Double precision multiply	480 μsec
Divide time	84 μsec
Memory density (NDRO)	3000 bits per cubic inch
Memory density (DRO)	1000 bits per cubic inch

F. ELECTRONIC FLIGHT CONTROL SUBSYSTEM

The electronic flight control subsystem generates output signals to the reaction jets and to the surface control actuators in accordance with input commands from the pilot's hand controller or the guidance computer (primary or backup, as indicated in fig. 61).

The tradeoff studies have emphasized maximum utilization of proven techniques and equipments compatible with vehicle research potential. Initial tradeoffs of current subsystem technology and research needs were conducted. These tradeoffs involved: (1) complete dependence on pilot fly-by-wire inputs to the surface control actuators versus a mechanical link (for backup, at least), (2) the use of conventional versus adaptive or supervisory loop techniques for varying the autopilot gains and surface trim settings, and (3) analog versus digital mechanizations. These tradeoffs--along with a description of the recommended approach, a preliminary performance evaluation, and a subsystem specification--are presented in section VI-F of Part IV.

The baseline functional block diagram (fig. 66) uses conventional gain programming for stability augmentation and fly-by-wire pilot input commands. It makes use of three parallel channels per axis for reliability enhancement, with automatic switching via comparator circuits.

1. Recommended Equipment Summary

The equipments considered for the D/3 vehicle configuration and described in some detail in this section were recommended by potential contractors in response to Martin Marietta's request for information. This request was accompanied by the subsystem specification in Part IV.

Table 21 summarizes pertinent equipment characteristics, as recommended by various potential suppliers. The preliminary cost estimates include necessary design, development, test equipment, and seven flight units. Physical descriptions of the equipments selected for use in the detailed configuration design of the D/3 vehicle are summarized in table 22. They are further described in subsequent sections, which cover the specific equipments recommended by each contractor and provide supporting data.

2. Sperry-Phoenix Recommendations

In accordance with the subsystem specification, the proposed baseline equipment incorporates pilot fly-by-wire inputs and conventional gain programming.

System operation. - To provide full authority over the entire trajectory, inner loop and outer loop gain variations are implemented. The gain variation is mechanized for complete versatility in that it can be addressed from a multiplicity of sources using a d-c voltage for control. The control voltages can be either continuously varying or discrete. Hypersonically, the gains are varied by inertial components sensing body axis accelerations. As the vehicle veolocity becomes less than hypersonic, the gains are controlled from air data inputs or ground-updated inertial navigation velocity from

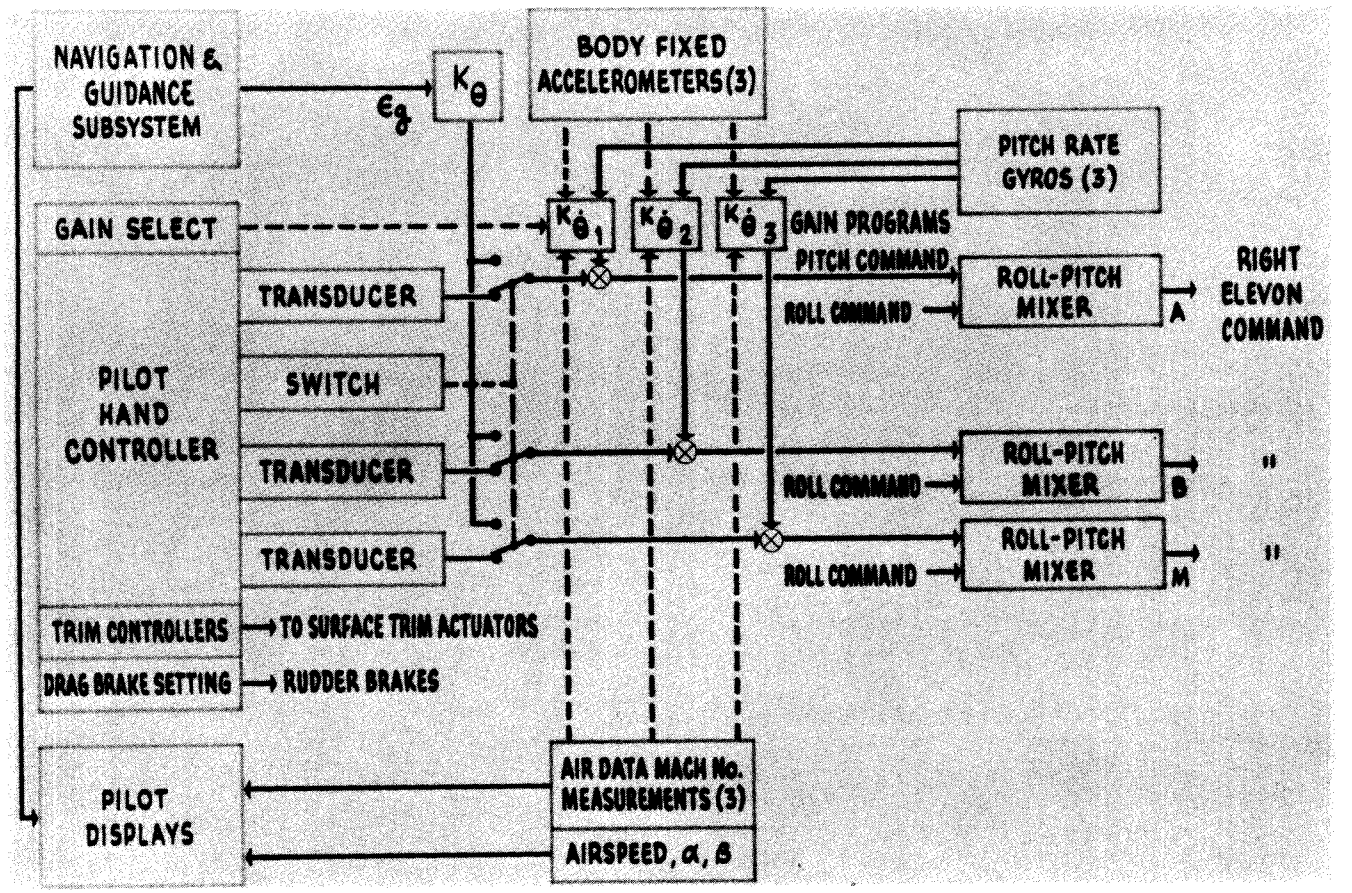

FIGURE 66. ELECTRONIC FLIGHT CONTROL SUBSYSTEM--PITCH CONTROL

TABLE 21. CANDIDATE ELECTRONIC FLIGHT CONTROL EQUIPMENT

Contractor	Equipment	Weight, lb (kg)	Volume, ft^3 (m^3)	Power, watts	MTBF, hours	Cost, $	Development status
Baseline System:							
Sperry-Phoenix	Triplex Autopilot	25 (11.3)	0.38 (0.011)	97	50 000	1.2×10^6	Rate sensors and electronic modules developed for PILOT (SV-5) drop test program.
Autonetics	TRISAFE Autopilot	35 (15.9)	0.54 (0.015)	85	1 000 000	0.6	Pitch channel tested. Funded contract to install P&Y system on F-101B.
Honeywell	Modified MH 132 Autopilot	85 (38.6)	1.91 (0.054)	165	50 000	3.275	Circuits being developed for the C5A program.
Experimental System:							
Autonetics	Adaptive Autopilot (SIDAC)	42 (19.1)	0.71 (0.020)	85	3 000 000	1.8 for 3 SIDAC and 3 digital	Being mechanized for 1967 flight tests.
Autonetics	Digital Autopilot (2 computers)	26 (11.8)	0.4 (0.011)	90	1 200 000		Developmental computer.

TABLE 22. SELECTED D/3 ELECTRONIC FLIGHT CONTROL EQUIPMENT

Contractor	Equipment	Weight, lb (kg)	Volume, ft^3 (m^3)	Power, watts
Sperry-Phoenix	Pitch Autopilot Assembly	7 (3.2)	0.11 (.003)	26
	Lateral Autopilot Assembly	10 (4.5)	0.12 (.003)	51
	Command Coupler Assembly	8 (3.6)	0.15 (.004)	20

the navigation subsystem digital computer. Flight control system (FCS) gains can also be changed in a discrete manner, based on FCS mode or pilot input for the manned mission. For the adaptive FCS research task, the baseline FCS can accept gain control inputs based on a d-c signal generated by an "adaptive computer" gain control. As a result, the "adaptive computation" will not jeopardize the baseline FCS reliability; any of the gain variation d-c control voltage inputs can be overridden either automatically or manually by the pilot.

The inner loop control provides for rapid attitude rate responses to various commands, including pilot manual inputs. The control law includes integral and displacement computations as well as high frequency compensations. The outputs are surface-actuator position command signals. Since outer-loop yaw commands are not required, yaw control is primarily for vehicle yaw damping. Inertial sensors for inner-loop control are floated, self-test rate gyros.

For exoatmospheric control, the inner-loop error signal, after appropriate shaping, is processed through a threshold detector with pseudo rate feedback. Jet select logic routes the on-off control signal to the proper jet thrustor to achieve the desired motion.

The inner-loop atmospheric FCS is triplex for fail-operational performance in all three axes. The front-end "fault isolation and monitoring" function senses and isolates faults occurring during flight for rate sensors and front-end electronics. All three command signals in each axis are processed through a mid-value logic signal selector (MVL). As a result, all three elevon pitch-roll mixing amplifiers see the same consistent axis command signal, even in the presence of a front-end failure.

Unit descriptions.- The electronic FCS for atmospheric and exoatmospheric control is made up of three units: the Pitch Autopilot, Lateral Autopilot, and Command Coupler. Functional high-density, but readily maintainable, packaging is used. The electronics consist of hybrid microcircuit discrete-embedded modules, mounted on removable card assemblies.

Pitch autopilot assembly: This fail-operational unit contains:

(1) Three miniature, precision pitch rate gyros. The gyros include spin motor detection signals and self-test torquers.

(2) Signal demodulation and adjustable inner-loop control laws with control stick inputs.

(3) Precision gain multipliers for inner-loop gain variation. They are addressable by external as well as internally generated gain changing commands.

(4) A low impedance interface with the atmospheric actuator assembly.

(5) On-off command signals for exoatmospheric jet reaction rocket control.

(6) Telemetry signals.

(7) Failure status reporting.

(8) Roll-pitch elevon command mixing.

Lateral autopilot assembly: This fail-operational assembly consists of:

(1) Six miniature precision rate gyros, three for roll rate and three for yaw rate. The gyro orientations are adjustable to provide any degree of yaw-roll coupling desired. The gyros include spin motor rotation detection signals and self-test torquers.

(2) Signal demodulation and adjustable inner-loop control laws with roll and yaw control stick inputs.

(3) Precision gain multipliers for inner-loop gain variation. They are addressable by external as well as internally generated gain changing commands.

(4) A low impedance interface with the atmospheric actuator assembly.

(5) On-off command signals for exoatmospheric reaction rocket control.

(6) Telemetry signals.

(7) Failure status reporting.

(8) Roll-pitch elevon command mixing.

Command coupler assembly: This unit contains:

(1) Adjustable outer-loop control laws.

(2) Precision gain multipliers for outer-loop gain variation. These are addressable by external as well as internally generated gain changing commands.

(3) Guidance error processing.

(4) Three accelerometers for inner-loop gain variations.

3. Honeywell Recommendations

Three possible approaches which meet or will meet the HL-10 requirements with minimal modification are: (1) the MH-96 adaptive flight control system which has been flight-proven and is still operational in the X-15, number 3, (2) the MH-132 which was developed, fabricated, and environmentally tested for the X-20, and (3) a microelectronic version of the MH-132, the circuits of which have been mechanized and tested.

MH-96 (X-15). - The MH-96 adaptive flight control system provides for both aerodynamic and reaction control with automatic blending to minimize onboard fuel consumption. The system is dual-redundant with fixed gain backup which, along with the adaptive gain changer, meets the fail operational requirement. Redundant adaptive gain changers, which are mechanized in all three axes (roll, pitch, and yaw), adjust for control surface effectiveness changes regardless of the reason for the change. The main components of the MH-96 system are:

DGG124B1	function selector (primarily stability augmentation)
DGG127A1	function selector (primarily outer loop modes)
DBG183A1	adaptive controller
DLG56B1, DLG59A1, DLG60A1	dual-redundant stick and rudder pedal displacement pickoff assemblies
DVG26A1	(two per system) DVG27A1 solenoid valve assemblies (for hydrogen peroxide reaction system)
DGG182A1	dual normal accelerometers
DGG183A1	dual lateral accelerometers
603R071G02	three-axis rate gyro assembly (two per system)
DSG29A1	solenoid held engage switch
DSG27A1	control stick steering button

Also, two automatic airborne checkout equipment (DUG1331A1) and one ground test unit (DUG1120A1) were provided for the X-15 flight program.

MH-132 (X-20 Dyna-Soar). - The MH-132 self-adaptive flight control system provides a combination of aerodynamic surface control, reaction control, and thrust vector control to augment both dynamic and static stability in addition to providing a damping function. The system has four basic control modes:

(1) Manual direct (fly-by-wire)

(2) Manual-augmented (self-adaptive)

(3) Pilot-selectable (fixed gain augmented)

(4) Automatic (tie-in to guidance system).

A hybrid dual-triple redundant mechanization, in which the electronics are triplicate while the sensors and actuators are duplicate, provides a high mission reliability and fail-safety in the event of any single failure. The self-adaptive circuitry in each of the three control axes is similar to that of the MH-96 (X-15) system, with certain

improvements and refinements incorporated. The MH-132 consists of the following components:

BG197A1A	electronic computer	
CG138A1A	control mode selector	
CG139A1A	control trim selector	
GG208A1	accelerometer unit (normal and lateral axis)	
GG209A1A	pitch	rate gyro groups
GG210A1A	roll	rate gyro groups
GG211A1A	yaw	rate gyro groups

In addition, a DUG1414B-1 bench level analyzer is used to check out the MH-132 flight control system equipment.

MH-132 (Microelectronic Version). - The microelectronic version of the MH-132 is functionally identical to the MH-132. The difference between the two systems involves only the electronic computer mechanization.

In the past two years, studies have been made in simplifying and improving the reliability of electronic circuits through the use of integrated circuits. Circuits similar to those of the MH-132 have been under evaluation for more than a year and now represent state-of-the-art mechanization. In the microelectronic version of the MH-132, use of integrated circuits is proposed only in those cases of proven capability. A completely microelectronic computer mechanization would be smaller and lighter, but it would also require more development effort and a higher risk element. It is anticipated that HL-10 microelectronic equipment and requirements will be verified through hardware contract work being performed on the C5A.

An automatic flight control system consisting of a stability augmentation system and autopilot with three channels in each of three axes will be built in 1967 and tested in 1968. The estimated system characteristics are summarized in table 21.

4. Autonetics Recommendations

The functional interface of the FCS is shown in figure 67 with the electronic FCS indicated within the dashed-line enclosure. The proposed FCS is comprised of three major elements: sensor package, pilot controller transducers, and a control computer. The sensor package, pilot controller transducers, and the exoatmospheric control portion of the control computer are assumed as common to all systems whether baseline, alternate, or experimental.

The remainder of the FCS, the control computer during atmospheric portions of flight, has four considerations. First is a baseline system having three independent, parallel channels for each axis with voting in the servo valve portion of the hydraulic actuators. Second is an alternate system designated Tripple Redundancy Incorporating

Self-Adaptive Failure Exclusion (TRISAFE), having three channels per axis with numerous common tie points throughout the electronics. Third is an adaptive SIDAC system which identifies parameters for adaptive control experimentation. Fourth is a digital system for experimentation. Their characteristics are summarized in table 23.

Baseline system and common components. -

Exoatmospheric control: Attitude control during the exoatmospheric portion of the mission may be achieved by several different combinations of subsystems. Since the use of a rate gyro is indicated for atmospheric entry, it will be retained for attitude control. However, the use of derived rate, analog or digital, would normally be adequate for attitude control.

The performance to be expected from the attitude control system is a function of sensor accuracy, system electronic gains, dead-zone setting, vehicle inertial properties, and jet thrustor sizing. No problems are foreseen in meeting the specified performance requirements (Part IV).

Baseline components: The electronic components, the functional electronic cards, sensors and the packaging are similar to those subsequently described for the TRISAFE control computer, with the exception that each redundant channel for the baseline system will be mechanically isolated and electrically isolated with separate power supplies.

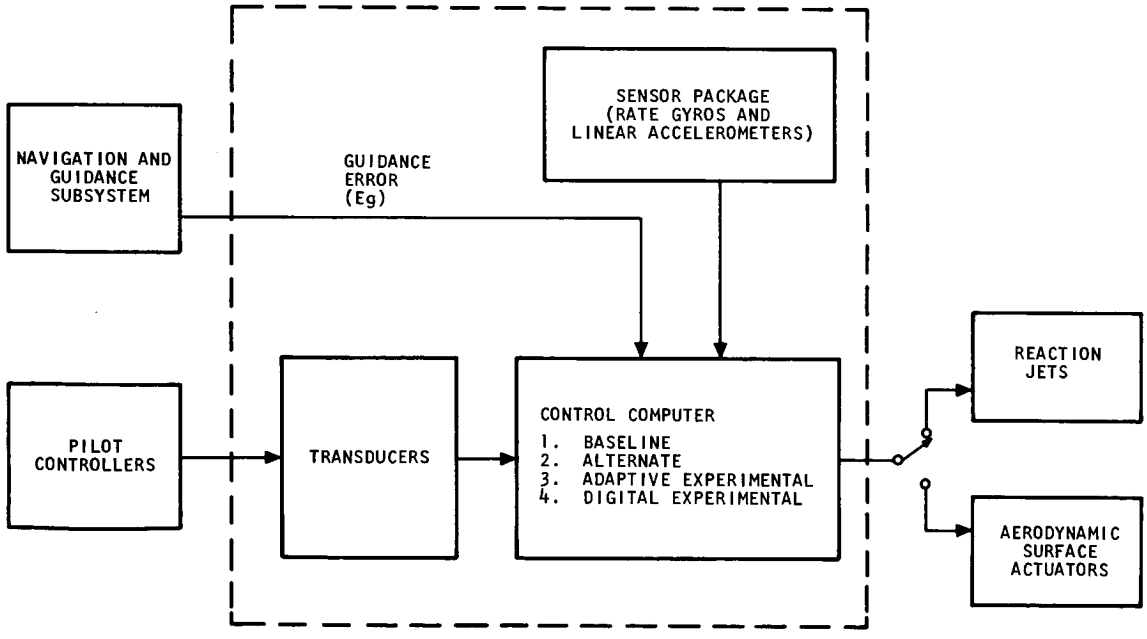

FIGURE 67. FLIGHT CONTROL SYSTEM FUNCTIONAL INTERFACE

Sensor packages: The sensor package is regarded as the same for all considerations: baseline, alternate, adaptive, and digital.

Rate gyro package: The TRISAFE rate gyro package size is 5-1/2 by 6 by 2-3/8 inches, and its weight is 4-1/2 pounds maximum. It contains three rate gyros with the same alignment, and identical units are used for pitch, yaw, and roll rate sensing by varying the mounting alignment in the aircraft. Within the unit, a base plate is employed for mounting the following components: three rate gyro modules; three chokes for pickoff phasing; three spin-motor phasing capacitors; three power transformers (115 to 26 V) for spin motors and pickoffs; and three trimming networks. The rate gyro modules are rugged subminiature, fluid-damped units with temperature-compensated damping and self-test features which include a spin-motor rate detector and a d-c gimbal torquer. The gyros exhibit adequate characteristics to fulfill mission requirements.

Linear accelerometer package: The linear accelerometer will be used in the TRISAFE configuration to measure accelerations. The accelerometers are a subminiature, solid-state design. This solid-state design consists of a flexible silicon beam attached to the frame, with a seismic mass attached to the free end. Piezoresistive strain elements, diffused in each side of the beam, provide an electrical output proportional to acceleration. This simple construction, without moving mechanical parts, is conducive to high inherent reliability.

Each unit contains a forcing coil for self-test purposes. The triple accelerometers for a given axis are contained in a single package. Each package weighs approximately 2.0 pounds and is 3-1/2 by 2 by 1-1/2 inches in size. A separate 115/26-volt, 400-cps power transformer is associated with each accelerometer.

TABLE 23. SUMMARY OF FCS PHYSICAL CHARACTERISTICS

Control system component	Size, inches	Weight, pounds	Power	MTBF, hours
Common Components				
Rate gyro packages (3)	5-1/2 by 6 by 2-3/8 x (3)	13-1/2	115 V, 400-cps, 60 W	Included in Computer MTBF
Accelerometer package	3-1/2 by 2 by 1-1/2	2	30 V ac or dc, 0.9 W	Included in Computer MTBF
Pilot controller transducers	--	1-1/2	--	Included in Computer MTBF
Control Computers				
Baseline Control Computer	8 by 5-1/2 by 13	16	115 V, 400-cps, 16 W 28 V dc 5 W	710 (each channel of each axis)
Alternate-TRISAFE Control Computer	8 by 5-1/2 by 15-1/2	18	115 V, 400-cps, 18 W 28 V dc, 5 W	0.9×10^7 (1-hr mission) 0.9×10^6 (10-hr mission)
SIDAC Adaptive Computer	12 by 5-1/2 by 15-1/2	25	115 V, 400-cps, 25 W	3×10^7 (1-hr mission) 3×10^6 (10-hr mission)
Digital flight control system (2)	(0.2 cu ft) x (2)	26	90 W	1.2×10^7 (1-hr mission) 1.2×10^6 (10-hr mission)

Approximately 200 units have been produced over the last two years. It has been used on several military programs and flight tested in the Raytheon Hawk missile.

Force and position transducer: The existing pitch force transducer has an adjustable deadband feature that allows the deadband to be adjusted to zero. The electrical output is a potentiometer excited by a d-c voltage.

The linear position transducers are mounted across the rudder bungee spring and provide a triple redundant electrical output proportional to control position or spring pressure. This unit is provided with three independent position transducers in each package. Center tap on the secondaries provide self-test capability.

TRISAFE computer. - The alternate TRISAFE gain scheduling system for atmospheric control employs body-referenced acceleration-derived gain adjustment for hypersonic flight and dynamic pressure-derived gain adjustment for speeds below hypersonic. Some of the features of this system and, finally, its developmental status are described below:

TRISAFE redundancy: This method of achieving redundancy will provide a higher MTBF than the single end point comparison method; it is achieved as a result of the high redundancy efficiency. TRISAFE has been so named because failure correction takes place without any predetermined decision process.

Switch fading: During the transition between manual and automatic control or during the transition from acceleration to air data gain scheduling, error signals may be present which can cause significant switching transients. They are confusing to the pilot and may be interpreted as a failure by him. By providing a controlled transition from one mode to another, the transient is minimized.

High bandwidth stability augmentation: The purpose of high bandwidth is to minimize the effect of aircraft parameter variations on control system performance for a given value of the scheduled gain. To achieve this, it is necessary to feed back all the vehicle states, either directly or as derived from a sensor output. The degree of success in fully achieving this goal is usually dependent upon the vehicle aeroelastic characteristics and the control movement device response characteristics.

Input signal processing: For a manned vehicle which operates in exoatmosphere conditions, in the atmosphere with high dynamic pressure associated with abort conditions, and at low dynamic pressure associated with the critical landing task, it is important that the pilot have direct control over that variable which is important during the various flight conditions. Pilot input signal shaping is an aid in achieving this and in achieving minimal variation in response of the desired output variable to his input. In the automatic mode, input signal shaping will minimize steady-state errors without significantly influencing the basic stability augmentation system bandwidth.

Dynamic pressure gain scheduling: Below hypersonic speeds, dynamic pressure is estimated to vary over a wider range than the variations in control surface movement effectiveness due to Mach number. Considering the usable range of lift coefficient, bank angle range required for maneuvering, landing speed, off-nominal conditions,

and trajectory overshoot, a 6-to-1 range in dynamic pressure is possible. The estimated aerodynamic data indicate a 3-to-1 variation in pitch control surface moment derivative due to Mach number. Therefore, it is recommended that dynamic pressure gain scheduling should be used below hypersonic speeds and that the high bandwidth characteristics should be used to minimize the Mach number effects.

Development status: The ability of the TRISAFE mechanization concept to compensate for failures has been demonstrated by all units used in a flight control system. Examples are sensors, signal shaping networks, gain scheduling, and hydraulic actuation. The output of these units and the complete autopilot exhibits negligible change in response due to many types of multiple failures within the unit.

The TRISAFE mechanization concept has been under development at Autonetics for several years. A pitch channel system has been successfully tested and evaluated by the Air Force. This, in turn, has led to the current Air Force-funded contract to design, develop, and flight test a demonstration model in the F-101B aircraft. This system, which will control the pitch and yaw axis, will have provision to simulate many failures while in flight to demonstrate the fail-operational capability.

SIDAC adaptive computer. - Operational requirements of entry lifting bodies may require an adaptive control system to adjust for wide variations in environmental conditions. Among many types of adaptive control, the concept of parameter identification called SIDAC appears promising. In this concept, the outputs from a relatively simple parameter tracking computer are used to adjust parameters in a flight control system, thereby compensating for variations in airframe dynamics. The system not only works in the presence of load disturbance noise, but utilizes it as well as control commands in the identification process. This is made possible by the inclusion of disturbances or wind gust terms in the identification model. Figure 68 shows the block diagram of a pitch-axis SIDAC system.

The system's ability to function with almost any type of disturbance is a direct consequence of the airframe being represented in its true form as a multivariable system, thereby accounting for all inputs and outputs. Implementation of the multivariable approach proceeds as follows:

(1) The differential equations describing the airframe motion are written in conventional form.

(2) All inputs and outputs which are not easily measured are eliminated algebraically.

(3) An error expression is formulated for the aircraft model. If the unknown coefficients of the error expression are adjusted to their true values, the error becomes zero.

(4) The coefficient of each of the measured variables is adjusted automatically by a standard gradient approach to drive the error toward zero. As the error approaches zero, the parameters approach the correct values.

(5) The parameter values are then used to adjust the gain and compensation of the control loop.

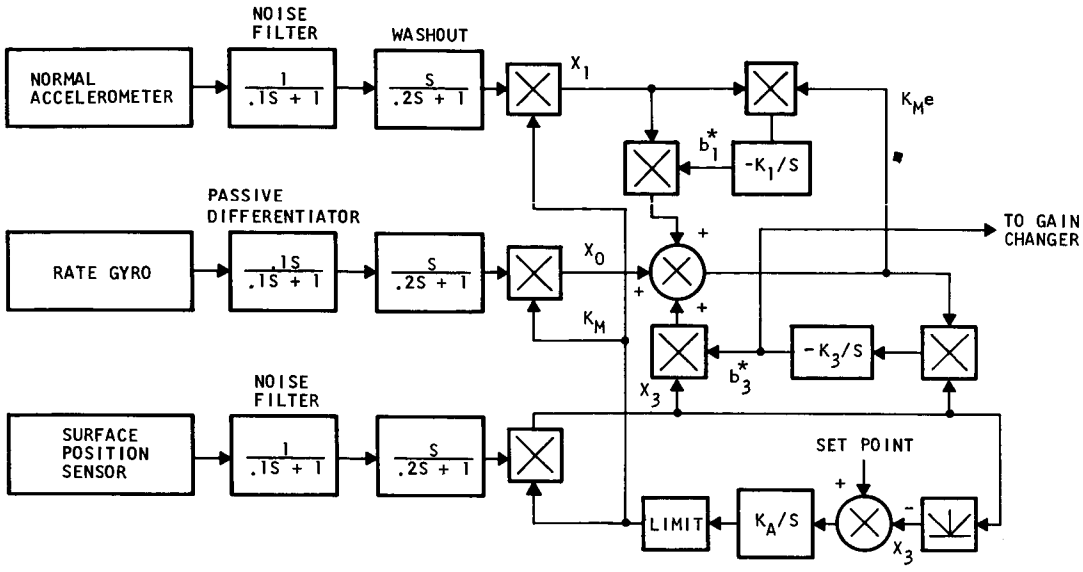

FIGURE 68. PITCH SIDAC IDENTIFICATION SYSTEM

The aircraft model equation can be represented by:

$$\ddot{\theta} = b_1 N_z + b_2 \dot{\theta} + b_3 \delta$$

If the b's are correct, the equation becomes:

$$\theta = X_0 + \sum_{i=1}^{3} b_i^* X_i$$

If the b's are incorrect, an error equation is formed by:

$$e = \sum_{i=1}^{3} b_i^1 X_i$$

where

$b_i^1 = b_i - b_i^*$

b_i^* = estimated value

b_i = exact value

The adjustment of the desired b_i coefficient is accomplished by:

$$\dot{b}_i = -2Ke\,\overline{X_i}$$

The coefficient b_3 approximates the elevator effectiveness. It is approximately proportional to dynamic pressure divided by moment of inertia. Hence, the gain in the stability augmentation loop is adjusted as a function of $1/b_3$.

The washouts on the instrument outputs are employed to eliminate trim and bias information. The noise filters are used to reduce the effects of sensor noise and dynamic cross-coupling effects from other axes.

The proposed SIDAC computer is used as an adjunct to the alternate control system. It is used in place of the body-fixed accelerometer or air data information to provide control loop gain adjustment.

Development status: The SIDAC concept has been developed under contract to the Air Force. Many simulation studies of the system have been conducted both by the Air Force at Wright-Patterson Air Force Base and by Autonetics, using X-15 and X-20 vehicle dynamics. Presently, the system is being mechanized in the TRISAFE format for flight testing in early 1967 on an F-101 aircraft under the sponsorship of the Air Force.

Digital control computer. - Digital computers have long been used in airborne vehicles to perform complex guidance calculations. However, not until the late 1950's was the idea conceived for forming flight control calculations in conjunction with guidance calculations. The concept was successfully implemented by Autonetics in the design of the digital computer for the Minuteman ICBM. The soundness of this approach to flight control was demonstrated by the success of the first Minuteman flight test missile in 1961 and the subsequent large number of successful flights. Presently, it is the only operational vehicle in the USA employing a digital flight control system.

Despite these successes, however, digital control systems have not been used on manned aircraft. Primarily, this has been due to the high costs of digital systems, especially when the requirements of fail safety/fail operability were imposed. However, because of recent technological advances in microelectronics, this is no longer a valid reason. Not only are significant reductions in costs occurring, but also reductions in power and size--all of which will make near-term digital flight control for manned aircraft a reality.

The key to an operational manned digital flight control system is its fail safe/fail operational characteristics. It is proposed, therefore, to evaluate such a mechanization experimentally. To provide a realistic simulation of an operational flight control system, separate digital flight control computations should be performed by the experimental system rather than by a central computer. In other words, the guidance and control calculations should be separated because of the different requirements imposed on the flight control system for manned applications. Moreover, the separation of the flight control and guidance computations is expected to be the more cost-effective mechanization approach for operational systems.

For digital control systems, fail safe and/or fail operational operation can be achieved by utilizing either one, two, or three computers in conjunction with the inherent self-test capability of a digital computer. Several approaches are possible. For fail safe digital mechanizations, the candidates are: (1) a single computer with self-test capability and (2) dual computers with monitor.

For fail safe/fail operational digital mechanizations the candidates are: (1) dual computers with self-test capability and (2) triple computers with monitor.

The preferred approach for the experimental system is dual computers with self-test capability. In this approach, one computer is primary and the other is secondary. The primary computer supplies the command signal to the actuation system, while the secondary computer provides an output signal for comparison with the output of the primary computer. If a discrepancy exists, the secondary computer, which is continuously under self-test, determines whether its output is valid or not. If valid, it removes the primary computer and inserts itself into the role of providing the system command signal. For the case of an invalid check, the primary computer continues to supply the command signal.

In summary, the purpose of the experiment would be twofold: (1) to evaluate the ability of a digital system to provide fail safe/fail operational characteristics similar to an analog system (e.g., TRISAFE) and (2) to evaluate the stability and dynamic performance of the system.

Development status: The computer previously described has been developed and flight tested. Although it was not specifically designed to perform flight control computations, it has sufficient capability to do so. It is therefore suited for use in an experimental type flight control system. For operational systems, Autonetics will have under development in early 1967 a digital computer designed specifically to the flight control requirements of manned aircraft. The development of such a computer will make economic use of digital control possible for future operational vehicles.

G. FLIGHT CONTROL ACTUATION SYSTEM

The primary flight control surfaces, elevons, and rudders are actuated by a dual hydraulic system, consisting of two independent hydraulic subsystems which provide the required redundancy. Each individual subsystem is designed for the loads associated with normal entry and landing, and both subsystems together are designed for the loads associated with ascent abort. In normal operation, both subsystems are active and share the load at the actuator.

1. Hydraulic System

Each hydraulic subsystem consists of an electric motor-driven hydraulic pump, a reservoir, an accumulator, filters, miscellaneous valves and instruments, and one-half of a dual tandem servoactuator for each elevon and rudder surface (fig. 69). The motor pump and reservoir are packaged as a unit to facilitate heat transfer and to reduce the number of external connections and external seals. This unit also includes provisions for evaporative cooling of the motor, pump, and fluid. The return line filter, the relief valve, the fill ports, instrumentation, and miscellaneous components are packaged as a unit to minimize the number of external seals and connections. Each servoactuator unit consists of pressure line filters, electrohydraulic servo valves, transfer valves, and switching logic. The piston-type accumulators connect to the filter unit but are mounted separately.

The ten major components of the system are interconnected with stainless steel tubing. Fittings and connections are permanently brazed to reduce weight and reduce the possibility of external leakage (Aeroquip Space-Craft fittings or equivalent). Flexibility at actuator connections is provided by coiled tubes or swivel joints.

The system weights are as shown in table 24. The motor pump unit weight and the servoactuator weights are based on vendor proposals. Other weights are based on similarity to standard components.

TABLE 24

FLIGHT CONTROL ACTUATION SYSTEM WEIGHTS

Item	Name and description	Weight lbM	Weight kg
1	Motor pump units including reservoir (2)	92	41.8
2	Accumulators, piston type (2)	14	6.4
3	Filter units including miscellaneous components (2)	20	9.1
4	Servoactuators, elevon (2)	90	40.9
5	Servoactuators, rudder (2)	50	22.7
6	Plumbing, lines and fittings	30	13.6
7	Hydraulic fluid	22	10.0
8	Actuators, mechanical and elevon flap (2)	34	15.4
9	Actuators, mechanical and tip fin flap (4)	36	16.7
10	Supports and miscellaneous	32	14.6
	Total system	420	191.2

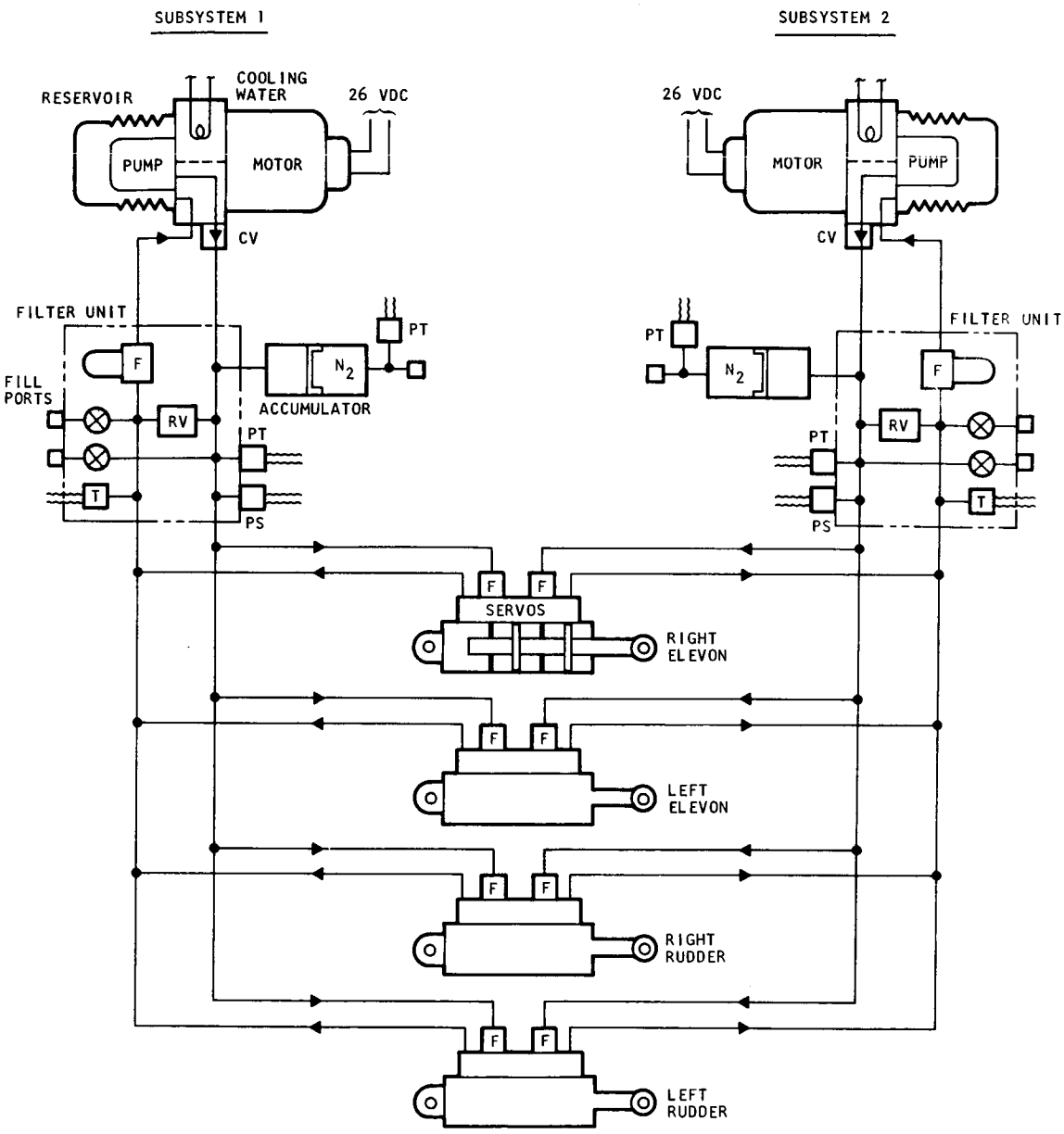

FIGURE 69. HYDRAULIC SYSTEM

The hydraulic system is a 3000 psi (20.68 MN/m^2), high temperature, aircraft hydraulic system in general accordance with specification MIL-H-8891. The hydraulic fluid is a deep dewaxed, superrefined mineral oil, in accordance with specification MIL-H-27601A, which is being used successfully in the PRIME vehicle.

The pump flow rates and the motor input current and power for the various phases of flight are shown in table 25. Motor input power is at a nominal 26 volts dc.

TABLE 25

HYDRAULIC FLOW AND POWER INPUT (PER SUBSYSTEM)

Operating phase	Pump flow gpm	Pump flow m^3/sec	Current, amperes	Power, kw
Peak (rated)	5.80	366×10^{-6}	473	12.30
Standby	1.08	68	182	4.73
Entry	1.62	102	216	5.60
Landing	2.85	180	290	7.55

Other hydraulic system inputs are electrical control signals to the electro-hydraulic servo valves in each servoactuator, and cooling water to each motor pump unit.

2. Motor Pump Unit

The motor pump unit consists of a pressure compensated hydraulic pump, a self-pressurizing reservoir, and a direct current electric drive motor. These items will be packaged as an integrated unit which includes provisions for cooling of the motor and the hydraulic fluid.

The pump supplies flow rates of up to 5.8 gpm (0.000366 m^3/sec) at a pressure of 3000 psi (20.68 MN/m^2). The pump operates with fluid temperatures of -20° to +450° F. The design duty cycle consists of nominal operation at 45 percent of rated flow, with peaks to 100 percent of rated flow for one second in every 30 seconds. The design operating time per flight will be 60 minutes (3600 sec).

The motor operates on an electrical input of 26 volts dc, and includes a radio noise filter. The unit will be functional during and after exposure to a sheltered space vacuum environment for periods of up to 8 hours.

The self-pressurizing reservoir has an active volume of 240 cubic inches (0.00393 m^3) to allow for fluid expansion and accumulator action.

Configuration. - The motor pump unit selected for the D/3 vehicle is a Pesco Model No. 115096-100. This unit was proposed by Pesco Products Division of Borg-Warner Corporation to meet the specified HL-10 requirements (ref. 7).

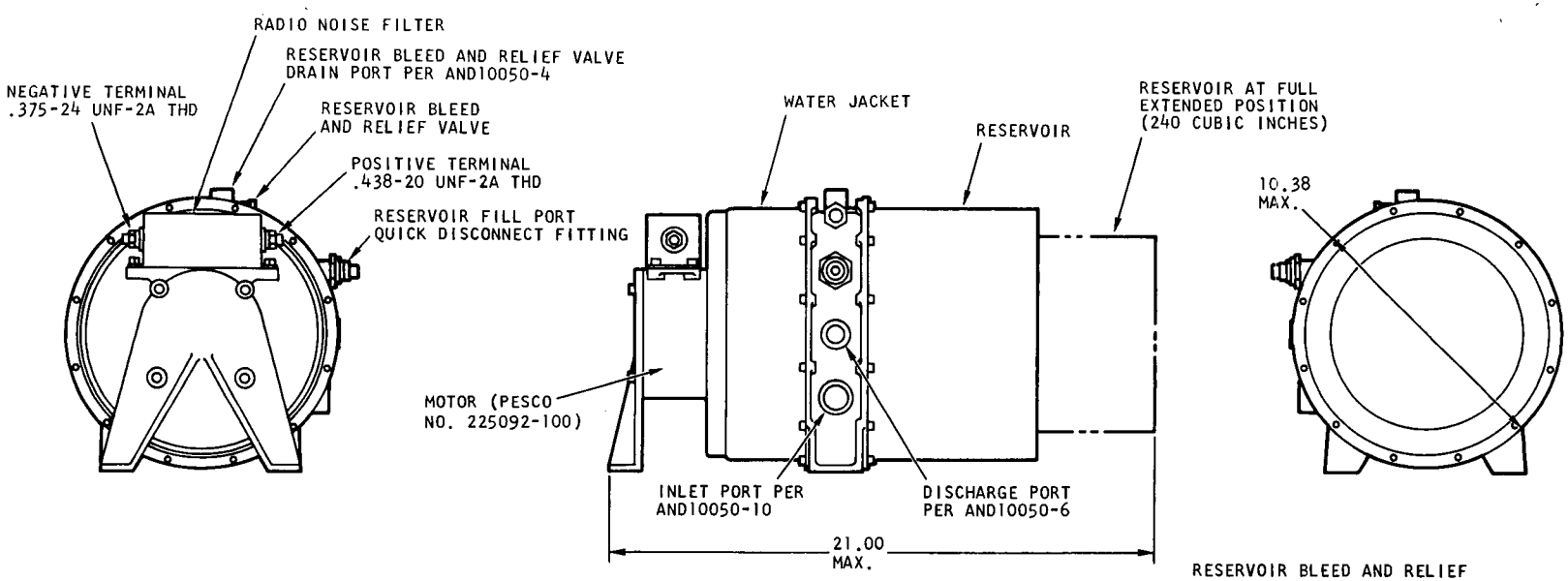

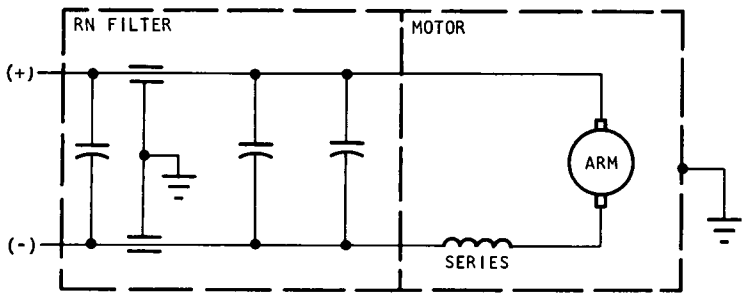

SCHEMATIC WIRING DIAGRAM

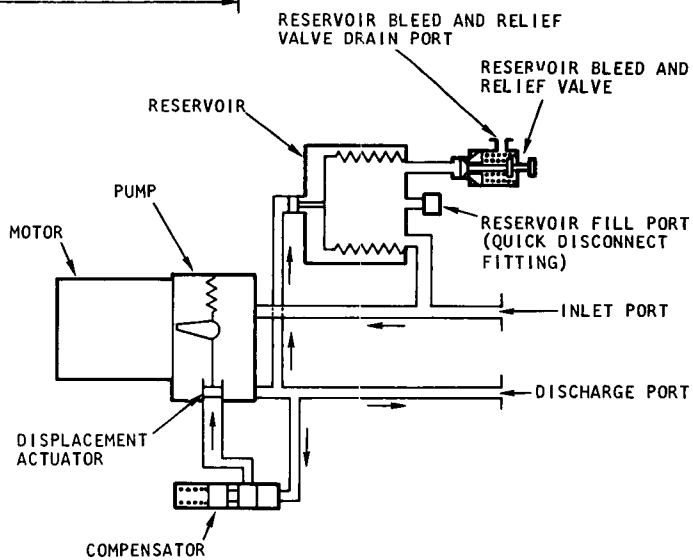

SCHEMATIC FLOW DIAGRAM

1. WEIGHT: 45.6 LB DRY (ESTIMATED)
   TOTAL WGT. INCLUDING HYD. FLUID AND WATER = 60.3 LB (ESTIMATED)
2. PERFORMANCE: 5.8 GPM AT 3000 PSI and 26 VDC PUMPING
   HYD. FLUID CONFORMING TO MIL-H-8446 OR EQUIVALENT
3. FLUID TEMPERATURE: -20° F TO 450° F
4. DUTY CYCLE: 5.8 GPM FOR 1 SEC OF EVERY 30 SEC;
   2.6 GPM for 29 SEC OF EVERY 30 SEC
   TOTAL CONTINUOUS OPERATING TIME PER CYCLE = 30 TO 60 MINUTES
5. WATER JACKET FILL AND BLEED PORT LOCATIONS TO BE DETERMINED BY FLIGHT ATTITUDE OF VEHICLE

FIGURE 70. MOTOR PUMP UNIT

The external configuration of the unit is as shown in figure 70. The weight of the unit is 45.6 pounds (20.7 kg) dry.

The manifold casting, located in the center of the unit, contains the mounting face, the pump rotating parts, the fill and bleed ports, and the pump inlet and discharge ports. The electric motor and hydraulic reservoir are also mounted to the central casting. The pump is of pivoted barrel design and operates totally submerged in the reservoir. The electric motor drives the pump through a splined coupling. The pump and motor are integrated in such a way that one of the motor bearings also serves as a pump bearing. The radio noise filter is attached to the electric motor. The electric power terminations are pigtail leads attached to the radio noise filter.

The motor pump unit is self-contained and requires no additional external components. The unit provides its own hydraulic pressurization system at startup and is immediately responsive to all flow demands up to rated flow when supplied with electric power at 26 volts dc. During periods of storage, the reservoir maintains an internal hydraulic pressure of 5 psig (34.47 kN/m^2) at normal fill levels.

Hydraulic fluid is sealed at the drive shaft interface by a spring-loaded and pressure-balance seal disc rotating against a stationary carbon seal face. There are only two external high pressure static seals, one at the high pressure service port and one at the pump displacement control valve. There are three pressure seals, one at the low pressure service port, one at the system return port and one at the hydraulic reservoir flange.

The variable displacement hydraulic pump is infinitely variable between the rated flow and zero flow. The displacement is controlled by a pressure-responsive compensator which operates on a differential of less than 100 psi (0.69 MN/m^2) above the rated pressure. The pump contains five pistons within a rotating barrel which is inclined at an angle with respect to the pump drive shaft. This angle establishes the pump displacement. The lightweight pistons are of a unique spherical design incorporating line-contact piston rings to reduce piston contact with the cylinder wall and provide zero piston-bore clearance. Pistons of this design are insensitive to contamination. This pump is similar to the pump used on the first stage of the Minuteman missile.

The proposed motor is designed and fabricated by Pesco. It is a direct current, ungrounded, series-wound explosion-proof machine incorporating design features and processes developed and proven in missile and aircraft applications. The motor will utilize Pesco's "E" frame (4.75-inch diameter, 0.121 m) laminations, comutator and other miscellaneous hardware from production tooled designs. The stator housing and bells, water jacket, and radio noise filter will be detailed as necessary to meet the application. The motor will be sealed to retain an internal atmosphere when subjected to an external vacuum.

The reservoir is a bellows type, operating on the "bootstrap" principle. The swept volume of the reservoir is 240 cubic inches (0.00393 m^3). The bellows assembly is fabricated of stainless steel completely welded into a single unit. The flexible bellows

act as a spring to maintain a constant pressure on the fluid in this system while inoperative. The reservoir completely encompasses the pump, submerging it in hydraulic fluid. There is one external hydraulic static seal at the joint between the reservoir and the unit manifold housing. A seal wiper ring is incorporated to eliminate the possibility of airborne contamination entering the area between the inner shell and the bellows. Graduations on the side of the inner shell provide a visual gage of reservoir fill level.

A dual-channel radio interference filter will be provided on the motor to suppress generated noise to within the limits of MIL-I-26600. The filter will utilize circuit techniques and components developed on similar applications to provide maximum attenuation with minimum size and weight. The components will have demonstrated capabilities at the anticipated operating temperatures expected in this application.

Performance.- The rated delivery and pressure of the motor pump unit is 5.8 gpm (0.000336 m^3/sec) at 3000 psi (20.68 MN/m^2). The rated inlet pressure to the pump is 55 psi (0.38 MN/m^2), which is supplied by the self-pressurizing reservoir. A minimum system flow of 0.5 gpm (0.00003 m^3/sec) is necessary to provide pump cooling. The anticipated unit performance characteristics are shown in figure 71. The power loss and the overall "wire to oil" efficiency are shown as a function of output flow. The power losses for this unit are approximately 5 percent higher than the losses assumed by the pump model curves used in the tradeoff studies. The motor is designed to deliver 12 horsepower at 7500 rpm, and 7.5 horsepower at 8500 rpm with an input of 26 volts dc.

The operating life of the unit will be 36 hours at the specified operating duty cycle. This is a conservative estimate based upon the 50-hour operating life achieved by a similar unit. The estimated mean-time-between-failure (MTBF) for the unit is 200 hours, based upon actual reliability performance demonstrated by a similar unit.

Development status.- The proposed motor pump unit is a new package design based on the component designs used by Pesco in the Minuteman and Polaris missile hydraulic power units. Actual data from the Stage I Minuteman units were used as a basis for establishing anticipated performance, life, and MTBF values for the proposed unit.

Alternate sources.- The motor pump unit could be developed by other contractors in addition to Pesco whose proposed unit has been described. Vickers Incorporated, Division of Sperry Rand Corporation, is in the process of developing and qualifying a pump model PV3-022 which may be suitable for this application. At the time of this study, however, Vickers was unable to supply size, weight or performance data for the complete motor pump unit.

3. Hydraulic Servoactuators

The hydraulic servoactuator (the unit) is a dual tandem actuator which receives hydraulic power from two independent hydraulic subsystems and receives electrical command signals from a fly-by-wire flight control system. The unit contains the servo valves, transfer valves and switching logic necessary to continue safe operation in the

event of any single failure. Both of the redundant hydraulic subsystems are active simultaneously and share the load at the actuator. A failure in either subsystem will cause that subsystem to be switched out.

The unit operates with hydraulic input pressures of 3000 psi (20.68 MN/m^2) and hydraulic fluid temperatures of -20° to +450° F. The unit has rate and response characteristics consistent with use on a high performance flight vehicle. Total operating time per flight will be 60 minutes (3600 sec). The unit will be functional during and after exposure to a sheltered space vacuum environment for periods of up to 8 hours.

The actuator uses equal-area pistons and four-way servo valves. The elevon actuator has an area of 6.67 square inches (0.0043 m^2) per subsystem, a stroke of 8 inches (0.203 m) and a no-load rate of 3.14 inches per second (0.080 m/sec). The rudder actuator has an area of 3.14 square inches (0.002m^2) per subsystem, a stroke of 4 inches (0.102m), and a no-load rate of 2.1 inches per second (0.051 m/sec).

Configuration. - The servoactuators selected for the D/3 vehicle are Hydraulic Research and Manufacturing Company part numbers 30001250 and 30001260 for the elevons and rudders, respectively. These actuators were proposed by this company to meet the specified HL-10 requirements.

The outline dimensions and weights of the actuators are shown in figure 72. Each actuator consists of a dual-tandem power cylinder, three electrohydraulic servo valves, two engage valves, and logic circuitry.

Functional operation. - The servoactuators incorporate a hydraulic logic system which operates to disconnect either of the redundant hydraulic subsystems in the event of a failure in that subsystem. The logic mechanization is based on measurement and comparison of servo valve power spool positions. The actuator functional diagram is shown in figure 73.

The actuator has two active command channels and one monitor channel. Each active channel consists of a conventional two-stage servo valve which connects, through an engage valve, to one-half of the tandem cylinder. The monitor channel consists of an identical servo valve which provides the third position reference. Each servo valve has a monitor which is used to measure spool position and transmit a pressure signal, proportional to the power spool stroke, to the comparators. Each comparator receives signals from a pair of monitors and detects any phase or amplitude difference between them. A disagreement of phase and/or amplitude will cause the comparator output to change. This output change is used to drive the engage valves which operate to disconnect control pressure of the failed channel from one-half of the tandem cylinder and to bypass that half of the cylinder to return.

A failure in channel 1 appears as a disagreement in both comparators 1 and 2, and causes the engage valve 1 to close. A failure in channel 2 appears as a disagreement only in comparator 2 and causes engage valve 2 to close. A failure in the monitor channel appears as a disagreement only in comparator 1 and causes neither engage valve to close. Electrical switches in the actuator will provide an indication when a failure is detected.

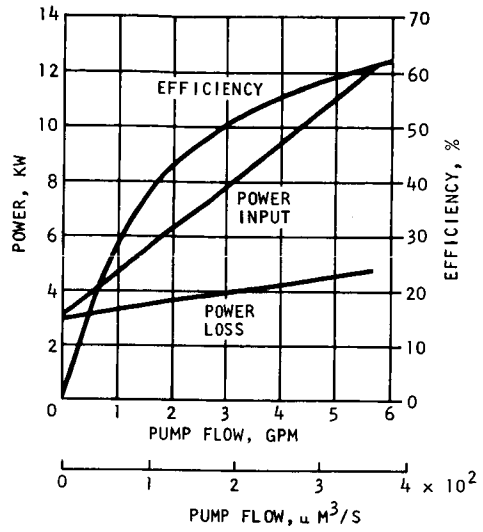

FIGURE 71. MOTOR PUMP UNIT POWER INPUT VERSUS FLOW

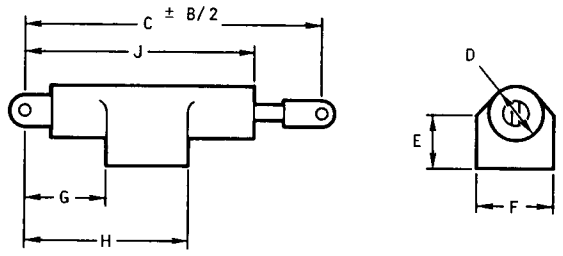

SYM.	ENVELOPE DIMENSION	UNITS	ITEM 1 (ELEVON)	ITEM 2 (RUDDER)
	AREA PER SUBSYSTEM	SQ. IN.	6.67	3.14
B	STROKE, TOTAL	IN.	8.0	4.0
C	LENGTH, NOMINAL	IN.	40.0	24.0
D	OUTSIDE DIAMETER, MAX.	IN.	5.0	3.5
E	MAX.	IN.	5.0	4.0
F	MAX.	IN.	5.0	4.0
G	MIN.	IN.	10.0	6.0
H	MAX.	IN.	20.0	14.0
J	MAX.	IN.	34.0	20.0
	WEIGHT	LBM	45.0	25.0

FIGURE 72. HYDRAULIC SERVOACTUATOR

No separate tandem power spool is used. Both active channel servo valves control the actuator directly. In such arrangements, a force flight always exists between the channels when both servosystems are not in exact agreement (null shifts, etc.). These problems are overcome in this system by:

(1) Reducing the servo valve pressure gains to those of a normal power spool.

(2) Significantly reducing random null shifts by improved design techniques and much tighter internal feedbacks.

(3) Using an upstream electrical voter to pass only one signal to all channels (also improving the failure-mode analysis for the total system).

(4) Designing the system so that when one channel drifts outside of an acceptable tolerance the hydraulic logic automatically rejects that channel and the remaining channel continues in control.

Alternate source. - The servoactuators could be developed by other contractors in addition to Hydraulic Research whose proposed units have been described. Moog Incorporated also submitted recommendations for servoactuators for the HL-10 application (ref. 8).

Moog recommended a three-channel, majority voting, dual system, single-piston design. This basic design has been developed at Moog, and hardware has been built and evaluated for NASA-Huntsville under contract NAS 8-11998 (ref. 9).

This basic actuator design is also being developed for use on three stages of the Manned Orbital Laboratory (MOL) booster. The three-channel majority-voting type actuator was selected for the MOL after a study compared various redundancy approaches (ref. 10).

The actuator for the MOL program includes provision for operation on either of two supply pressures, with automatic supply pressure switchover (or switch back) incorporated within the servoactuator package. This actuator differs slightly from the HL-10 requirement in that a tandem, load sharing, cylinder-piston is not used.

This single-piston actuator design would require that the actuator, and each of the hydraulic subsystems, be sized to meet the full abort hinge moments, rather than one-half of the abort moments required when a tandem-piston actuator design is used. This would result in a greatly increased power requirement.

As an alternate design, Moog suggests that a three-channel, majority voting, tandem-piston design could be developed. This design would be essentially identical to the MOL design except that a tandem second stage spool would be used to power a tandem piston, and hydraulic source pressure logic would be applied to the first stage only (i.e., the three-channel, majority voting first stage would be driven by either of the dual sources, with preference determined by a transfer valve). This concept would fulfill the HL-10 requirements.

4. Filter Package

The filter package contains the return line filter, the system relief valve, fill ports with shut-off valves, and pressure and temperature transducers. These components are assembled into a common manifold to eliminate interconnecting tubing and reduce the number of external seals. The relief valve and shut-off valves are of the cartridge type.

The filters will provide filtration of 10 microns nominal and 25 microns absolute. The filters have a pressure drop indicator button to indicate when the pressure drop, due to contaminants, reaches a predetermined value.

A temperature sensor with a range of 0 to 450° F is provided to monitor the fluid temperature in the return line. A pressure transducer with a range of 0 to 4000 psi (27.58 MN/m^2) is provided to monitor subsystem pressure. A pressure switch gives a warning to the pilot when subsystem pressure drops below a predetermined value.

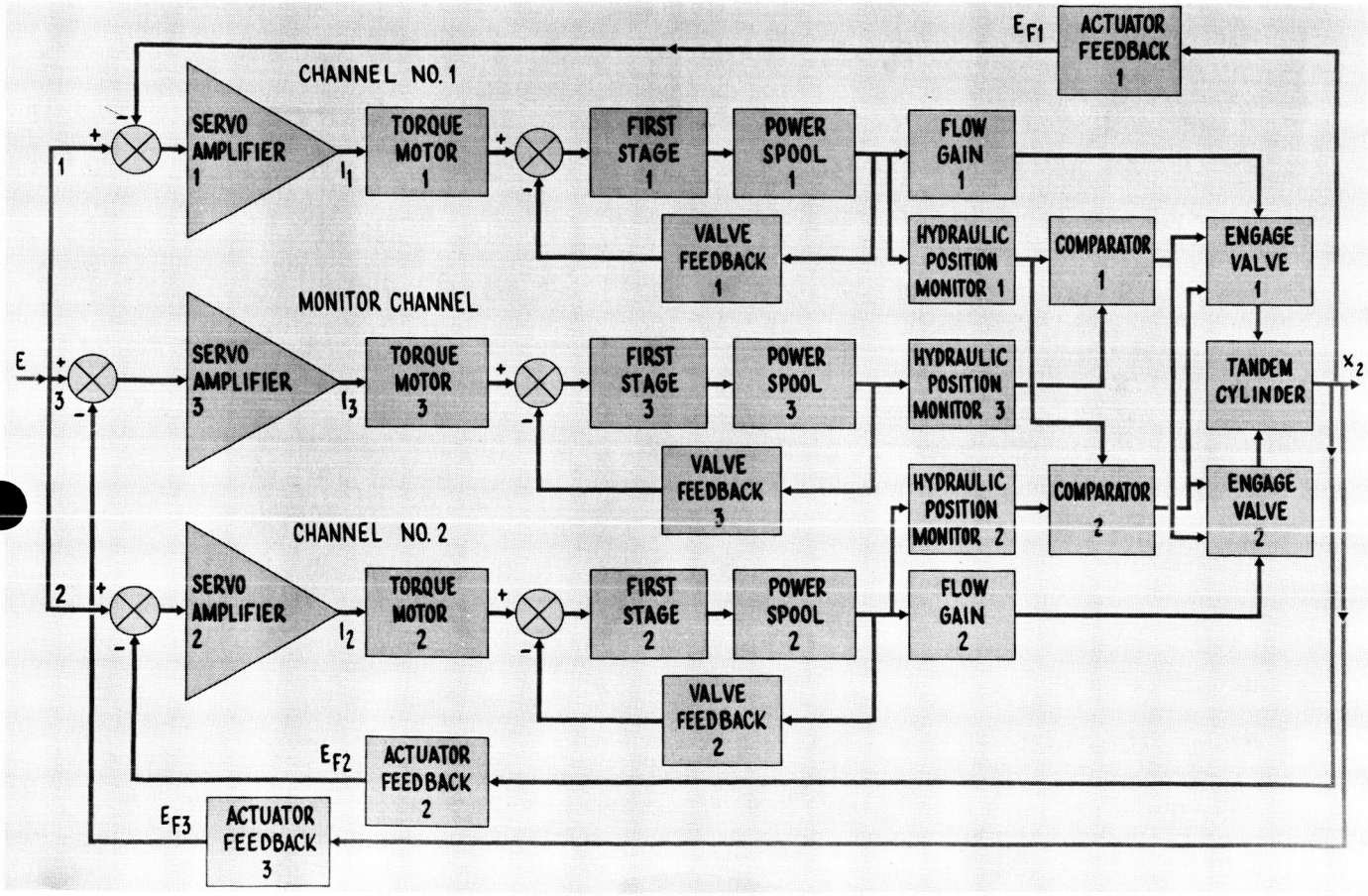

FIGURE 73. SERVOACTUATOR FUNCTIONAL DIAGRAM

H. PROPULSION AND ORDNANCE

The propulsion subsystems for the D/3 vehicle are: (1) the integral abort/deorbit and (2) the integrated reaction control system and landing assist system (RCS/LAS) subsystems. Design and performance criteria for these subsystems, as well as the general analytical approach used in determining such criteria, are contained in Part IV, section VI-H. The 25-foot D/3 entry vehicle was used as the example to illustrate the techniques employed in Part IV to develop the propulsion subsystem parametric data. In consideration of this, the calculations for determining propellant quantities, thrust levels, burning times, and similar parameters will be omitted from this present section of the report. However, pertinent data are extracted for tabulations and discussions in the following paragraphs.

The ordnance subsystem for the D/3 vehicle provides many of the same functions for which pyrotechnics were used on the Gemini spacecraft. The design described in subsection 3 overlaps a number of other D/3 subsystem descriptions and, therefore, the discussion of ordnance is limited to a functional description.

1. Abort/Deorbit Propulsion

The abort/deorbit propulsion subystem for the D/3 entry vehicle consists of two pairs of spherical solid propellant rocket motors. These motors are located in a short section of the adapter for the entry and launch vehicles (fig. 19).

Each motor in one pair, designated 1 and 2, is sized to produce the required impulsive velocity of 130 $\pm$ 1.3 fps (39.6 m/sec) to the orbiting vehicle for the deorbit function. In addition, these same motors will have a combined thrust level and burning time sufficient to perform the pad abort function associated with entry vehicle shock overpressure limitation of 7 psig (48.263 kN/m^2). The other pair of motors, designated 3 and 4, is sized to augment motors 1 and 2 to result in an impulsive velocity equivalent of at least 520 fps (158.5 m/sec), based on sea level rocket motor performance for all four motors, to provide for vehicle recovery by parachute from a pad abort. In addition, the thrust level and burning time of all four motors will be at least sufficient to perform a successful abort at maximum "q" flight conditions for the entry vehicle shock overpressure limit, when fired simultaneously.

All four motors are required to provide a total impulsive velocity of at least 570 fps (173.7 m/sec) to the orbiting vehicle (at vacuum conditions) to preclude an African landing in the event of a booster shutdown at a velocity of about 23 000 fps (7010.4 m/sec) (see Part III). This particular functional operation requires all four motors to be carried to orbit velocity, thereby precluding a normal boost phase abort motor jettisoning requirement.

The physical and performance characteristics of the spherical solid propellant rocket motors selected for application in the D/3 vehicle integral abort/deorbit propulsion subsystem are presented in table 26. This table shows that the physical characteristics of the selected motors are compatible with vehicle physical limitations. Table 27 presents a comparison of the required and available performance characteristics of the selected subsystem. It should be noted that the integral system arrangement meets the deorbit impulsive velocity requirement and, in general, exceeds all others by a small margin. All thrust level requirements, as well as the respective burning times, are met.

TABLE 26

D/3 ENTRY VEHICLE ABORT/DEORBIT MOTOR CHARACTERISTICS

	Motor 1 or 2	Motor 3 or 4
Chamber pressure	1000 psi (6.9 MN/m^2)	1000 psi (6.9 MN/m^2)
Thrust, sea level	16 285 lbF (72.436 kN)	18 330 lbF (81.532 kN)
Maximum "q"	17 272 lbF (76.826 kN)	19 388 lbF (86.238 kN)
Vacuum	17 836 lbF (79.335 kN)	20 090 lbF (89.360 kN)
I_{SP}, sea level	250 sec	250 sec
Maximum "q"	265 sec	265 sec
Vacuum	274 sec	274 sec
Total impulse, sea level	51 786 lbF-sec (0.23 MN-sec)	64 888 lbF-sec (0.289 MN-sec)
Maximum	54 925 lbF-sec (0.24 MN-sec)	68 634 lbF-sec (0.306 MN-sec)
Vacuum	56 718 lbF-sec (0.25 MN-sec)	71 118 lbF-sec (0.316 MN-sec)
Burning time	3.18 sec	3.54 sec
Propellant weight (useful)	207.3 lbM (94.1 kg)	259.4 lbM (117.8 kg)
Nozzle area ratio	10	10
Mass fraction	0.90	0.90
Overall length (max.)[a]	36 in. (0.914 m)	36 in. (0.914 m)
Overall diameter (max.)[a]	22 in. (0.559 m)	22 in. (0.559 m)
Overall length	27.3 in. (0.693 m)	29.8 in. (0.757 m)
Overall diameter	19.6 in. (0.498 m)	21.0 in. (0.533 m)

General (each motor)

Ignition delay (max.)--0.05 sec

Reliability (min.)--0.994

Thrust misalignment (max.)--0.1 degree

Operational voltage range--24 to 30 Vdc

Man rated

Total impulse must be within ±1% of that specified

(a) Limited by EV adapter geometry

TABLE 27

ABORT/DEORBIT PROPULSION SUBSYSTEM CAPABILITIES

Event	Required				Available				Motors Used
	F/W_{EV^*}	W_P/W_{EV^*}	t_b sec	ΔV	F/W_{EV^*}	W_P/W_{EV^*}	t_b sec	ΔV	
Pad abort a) Shock over-pressure = 7 psig	2.31	0.0189	2.04		2.31	0.0294	3.18		1 and 2
b) 15 000-ft altitude		0.0627		520 fps (158.5 m/sec)	2.31 2.61	0.0294 0.0367	3.18 3.54	542 fps (165.2 m/sec)	1 and 2, then 3 and 4
Maximum "Q" abort	5.20	0.0490	2.494		5.20	0.0661	3.18 3.54		All
Africa avoidance		0.0628		570 fps (173.7 m/sec)				585 fps (178.3 m/sec)	Selected sequence
Deorbit		0.0147		130 ± 1% fps 39.6 ± 1% m/sec	1.265	0.0147	3.18	130 ± 1% fps 39.6 ± 1% m/sec	1 or 2

The selected motors have the capability to meet all the functional, performance and dimensional requirements specified for these propulsion subsystems on the D/3 vehicle.

In the course of the parametric studies phase, the abort/deorbit motors characteristics for a C/4 size vehicle were submitted to Aerojet-General Corporation, Sacramento and Thiokol Chemical Corporation, Elkton Division, in the form of a preliminary subsystem specification. Each corporation responded with recommended motor designs and pertinent discussion relative to utilizing their previous experience and manufacturing techniques (existing state-of-the-art) to permit delivery of hardware on time and at lowest development cost. Both manufacturers indicated that the two different motor requirements could be accomplished within a single development program. Because of the man-rating, installation envelope, and total impulse control ($\pm 1\%$) requirements, off-the-shelf hardware was not directly applicable.

It was concluded from the data received that the motors would be approximately 5 percent heavier than expected. This increase is primarily associated with a lower specific-impulse capability (approximately 5%) than that assumed in the parametric phase of the present study.

Automatic motor firing sequences for abort conditions are selected by the onboard programming equipment. Actual firing of the selected motors is accomplished by the pilot pulling the abort control handle. For the deorbit function, the pilot can select the motor to be used; he is also able to fire the selected motor. Each motor is temperature controlled to assure that the delivered thrust and burning time meet the abort and deorbit performance requirements.

Crew controls and instrumentation consist of a four-way selector switch, temperature gage, arming switch, firing switch (deorbit function), heater switch, and go-no-go indicator light. At launch countdown the heater switch and arming switch must be turned on. Data relative to the abort/deorbit system condition and flight programmer motor firing sequence storage are sent to the malfunction detection system, where a go or no-go condition is determined. A no-go condition will cause the go-no-go indicator red light to turn on. The other controls and indicators are used to monitor the condition of each motor and circuit and to permit the crew to select and fire the deorbit motor.

2. Integrated RCS/LAS Propulsion Subsystem

The reaction control system (RCS) provides the means to orient and control the attitude of the entry vehicle during phases of the mission when aerodynamic control is not practicable. The landing assist system (LAS) provides a thrust equal to 0.1333 times the D/3 entry vehicle landing weight, for a period of 10 seconds (maximum), to extend the landing touchdown distance.

An integrated RCS/LAS design approach was selected, as shown schematically in figure 74. This arrangement is a desirable compromise between the various performance, weight, installation, reliability, and hardware availability arguments associated with a multimission, reusable subsystem. Specifically, the selected arrangement incorporates the least number of thrustor assemblies possible as well as a common propellant and pressurization system.

[redacted]

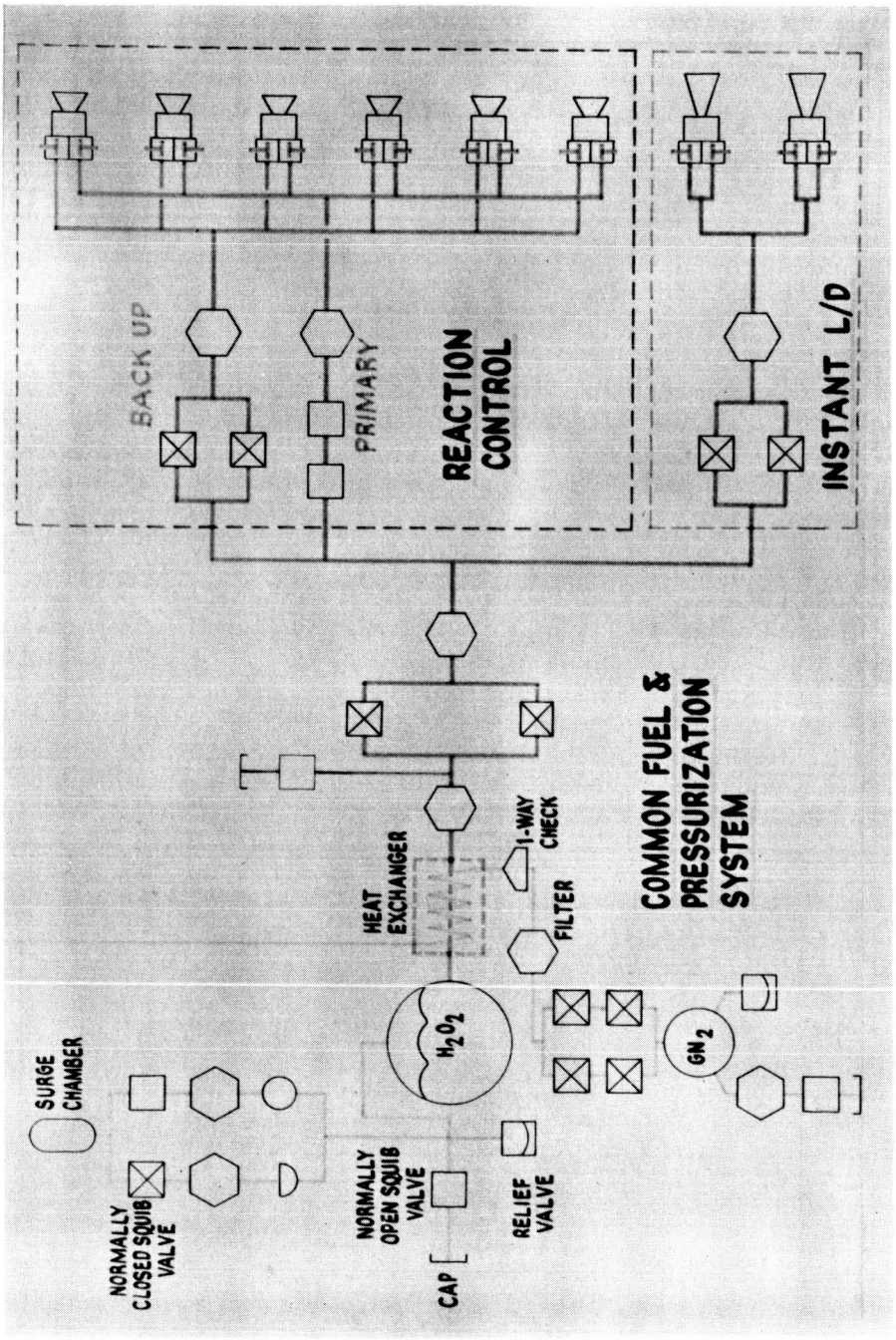

FIGURE 74. INTEGRATED RCS/LAS SCHEMATIC

[redacted]

A preliminary reliability analysis was conducted to determine the effect of nonredundant thrustor assembly utilization on subsystem mission reliability. Available data indicated a thrustor assembly failure rate was several orders of magnitude less than that for a propellant valve. Considering this rate comparison, it was concluded the nonredundant thrustor assembly subsystem design selected would have a mission reliability practically the same as that for the fully redundant design. The selected subsystem design meets the reliability apportionment assigned to the subsystem (see Part IV).

The RCS/LAS system will be packaged in modular assemblies to minimize installation weight (brackets, etc.) and to enhance checkout and refurbishing tasks. Squib valves and filters are incorporated in a block assembly to minimize the number of fluid couplings. This arrangement will significantly decrease leakage sources and enhance refurbishing and checkout operations. A simple heat exchanger has been incorporated in the propellant tank discharge header to provide a constant temperature pressurization gas supply to the pressure regulation subsystem. Incorporation of the heat exchanger is recommended to preclude regulator failure during the final LAS operating period. Analyses of various test data indicated that pressure regulator failure may be affected by the marked decrease in pressurizing gas temperature normally encountered in the final operating period of an extended, continuous, final thrusting phase. For this type of operation, the pressurizing gas supply does not have sufficient time to pick up heat from its surroundings to compensate for the work function temperature effect. Application of the simple heat exchanger will provide a final gas temperature within a few degrees of the initial storage temperature.

The various functional operations and associated RCS/LAS propulsion subsystem requirements are listed in table 28. Performance requirements for these functional operations are summarized in table 29. Calculation procedure for the performance data is presented in Part IV where the D/3 entry vehicle was used as the example to demonstrate the application of the analytical techniques in developing the RCS/LAS propulsion subsystem parametric data. Installation of the integrated RCS/LAS propulsion subsystem in the D/3 entry vehicle is shown in figure 75.

A preliminary subsystem specification was also prepared for the integrated RCS/LAS propulsion subystem. This specification was sent to Kidde Aerospace and Bell Aerosystems. Each company responded with recommended equipment applications and minor subsystem design changes, based on their individual hardware application or techniques.

In the case of the D/3 vehicle, all RCS, pressurization, and propellant subsystem components are considered to be available. Some development will be required for the LAS thrustor-catalyst bed assembly due to the higher thrust required for the larger vehicle. Typical thrustor assemblies for the RCS application could be:

Pitch/roll--Kidde P/N 874093

Pitch/roll--Bell Model 8233

Yaw--Bell Model 8093

[redacted]

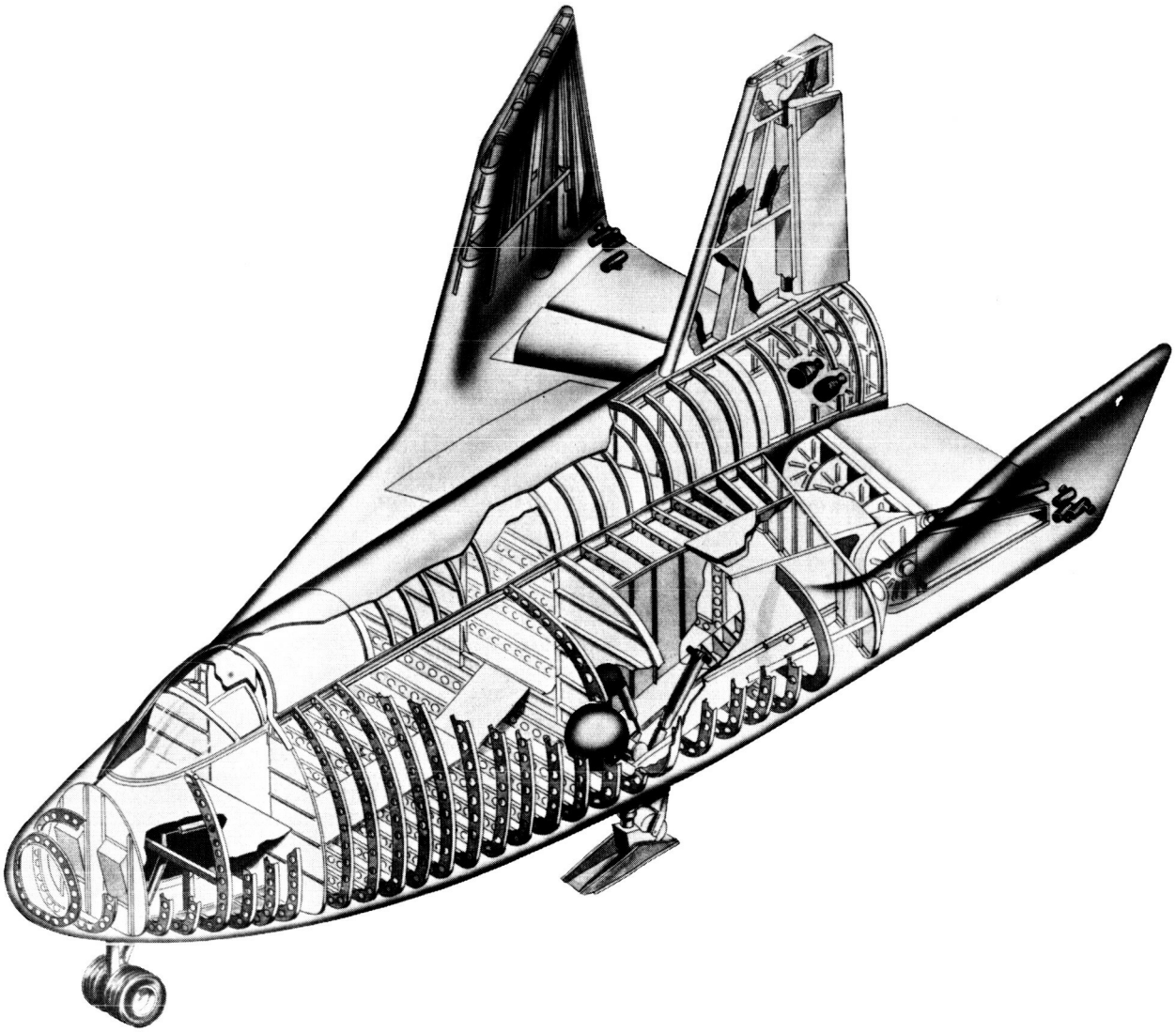

FIGURE 75. RCS/LAS INSTALLATION

[redacted]

TABLE 28

INTEGRATED RCS/LAS PROPULSION SUBSYSTEMS FUNCTIONAL REQUIREMENTS

Reaction Control System

Orbit Phase

1. Stabilization after booster separation (take out 2°/sec angular velocity)
2. Limit cycle operation (±5° dead band, 8-hour duration)

Retro/Pre-entry Phase

1. Maneuver for retro (180° pitch, 90° yaw, 90° roll; up to 6 minutes to accomplish)
2. Alignment for retro (±1° dead band, 2-minute duration)
3. Transient arrest during retro (3.5 second duration)
4. Maneuver for entry (180° pitch, 90° yaw, 90° rollup to 5 minutes to accomplish)
5. Stabilization after abort/deorbit package separation (null out 10°/sec angular velocity)
6. Limit cycle to pre-entry (±5° dead band, 20-minute duration)
7. Alignment prior to atmospheric entry (±1° dead band, 5-minute duration)

Entry

1. Stabilization to aerodynamic takeover (±2° dead band, 5-minute duration)

Landing Assist System

Landing Phase

1. Modification of L/D characteristics during final landing phase (F/W_{EV} = 0.1333 for 10 sec)

Selection of 90 percent hydrogen peroxide (H_2O_2) as the propellant was primarily associated with the minimum refurbishment requirement for at least five mission reuses. Extensive data exist to indicate that available H_2O_2 system hardware will be able to satisfy the reuse requirement. The maximum gas temperature of approximately 135° F for H_2O_2 decomposition products will not impose thermal insulation problems on the vehicle. Incorporation of a thermal block between the thrustor assemblies and propellant valves will permit the propulsion subsystem to tolerate the normal entry trajectory environment conditions without difficulty. Such thermal blocks are incorporated in present H_2O_2 systems to prevent thermal feedback associated with normal engine operation for designs where the propellant valves are close-coupled to the decomposition chamber.

TABLE 29

RCS/LAS PROPULSION SUBSYSTEM PERFORMANCE REQUIREMENTS

Reaction Control System

Pitch/roll motors (4 vertically oriented motors, 2 up and 2 down, used in pairs of same orientation for pitch and opposite orientation for roll control)

F_{VAC} = 29 lbF each (129 N)

Minimum pulse width = 0.06 sec

N_P = 240 pulses/mission (max.) in pitch

N_R = 420 pulses/mission (min.) in roll

N_{max} for a thrustor = 660 pulses/mission

$t_{b(max)}$ for a thrustor = 134 sec/mission

P_c = 250 psi (1.724 MN/m^2)

Yaw motors (2 side-oriented motors)

F_{VAC} = 58 lbF each (258 N)

Minimum pulse width = 0.06 sec

N_Y = 200 pulses/mission (max.) in yaw

$t_{b(max)}$ for a thrustor = 134 sec/mission

Landing Assist System

Two aft firing thrust chambers

F_{SL} = 825 lbF (3.67 kN)

$t_{b(max)}$ = 10 sec/mission

Propellant (common, for both RCS and LAS usage)

Pressurized, positive expulsion system

W_P (useful) = 170 lb; 35 for RCS and 135 LAS (77.1 kg)

I_{SP} = 122 sec

Type 90% H_2O_2

TABLE 29.--Concluded

RCS/LAS PROPULSION SUBSYSTEM PERFORMANCE REQUIREMENTS

Operating pressure = 412 psia (2.841 MN/m^2)

Volume = 3800 cu. in. (0.111 432 m^3)

Temperature = 60° F to 80° F (289 to 300° K)

Pressurant

Weight stored 5.92 lbM (2.685 kg)

Type N_2 gas

Initial storage pressure = 3000 psia (20.684 MN/m^2)

Final storage pressure = 600 psia (4.137 MN/m^2)

Storage tank volume = 710 cu. in. (0.011634 m^3)

The RCS subsystem is provided essentially with a backup by virtue of the incorporation of redundant pressurization and propellant distributions circuits. Primary pressurization system control is accomplished by a pressure regulator valve, operating between 400 and 420 psia (2.758 to 2.896 MN/m^2. Should the regulated tank pressure go beyond these limits, the appropriate squib valves are actuated to lock out the pressure regulator valve circuit and to open the backup, bang-bang type pressure control circuit. Similarly, a lack of response from a thrustor causes squib valves to close the propellant circuit in use at the time of malfunction, and to open the backup propellant circuit. This action simultaneously transfers the RCS firing control signals to the appropriate propellant valves incorporated in the backup propellant circuit.

The pilot has control of arming the RCS and LAS subsystems. Automatic pressurization control switchover is accomplished if the propellant tank pressure exceeds a safe limit. Manual pressurization circuit and propellant circuit selection is provided by the pilot for other cases. Warning lights inform the pilot of the status of the subsystem. The RCS thrustor control is tied to the guidance and control system and the LAS thrustor is pilot-controlled (off or on only).

Other monopropellant systems are presently being developed. However, they are considered to have insufficient application background and a lack of available hardware for use in the HL-10 subsystems.

Earth-storable bipropellant systems hardware development and applications are well-funded. The Apollo and Gemini systems utilize such hardware. Reuse of such hardware for several missions, however, is open to question at this time. The propellant performance is 250 percent of that for 90 percent H_2O_2 and will certainly require consideration for missions of extended operational time. The HL-10 mission

requires a maximum of 8.5 hours operation. Consequently, it has such a low RCS propellant weight requirement that the advantages associated with use of the bi-propellant system are considered to be overcome by those for the H_2O_2 system hardware status and reuse potential.

3. Ordnance Subsystem

Ordnance devices are used extensively throughout the entry vehicle and the adapter for a wide variety of functions. These devices provide for characteristically fast and positive action and offer inherently high reliability with low weight penalties for redundancy. The devices take the form of squibs for valve and piston actuation and solid rocket motor ignition; explosive nuts, bolts and latches for severing structural connections; and shaped charges or primacord for metal cutting. The specific functions to be performed by the ordnance devices are described in table 30. The location of certain of these devices is depicted in figure 76.

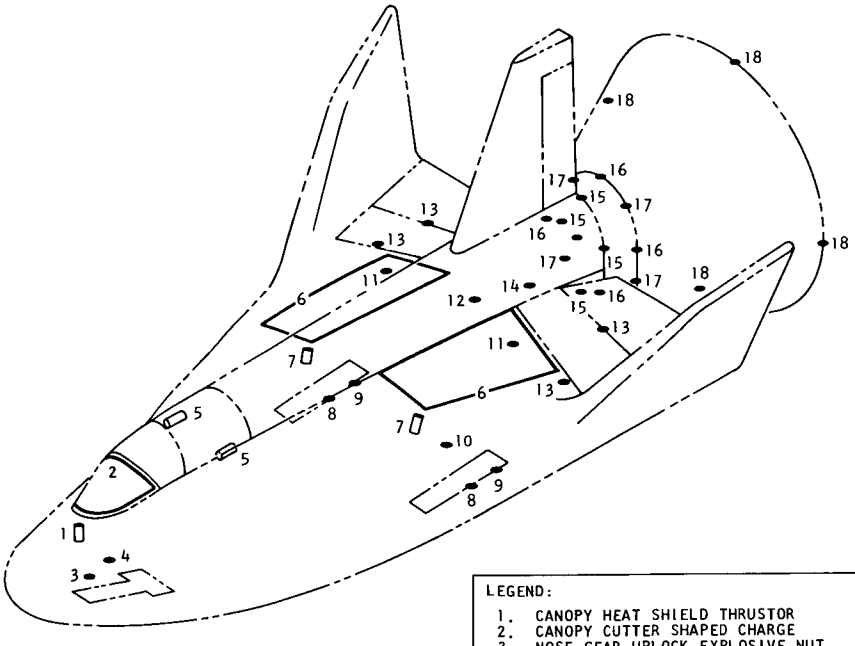

LEGEND:

1. CANOPY HEAT SHIELD THRUSTOR
2. CANOPY CUTTER SHAPED CHARGE
3. NOSE GEAR UPLOCK EXPLOSIVE NUT
4. NOSE GEAR GAS ACTUATOR
5. HATCH PIN EXTRACTORS
6. SHAPED CHARGE RECOVERY CHUTE WELLS
7. CHUTE CONTAINER POSITIONING ACTUATORS
8. MAIN GEAR GAS ACTUATORS
9. MAIN GEAR UPLOCK EXPLOSIVE NUTS
10. 17 SQUIBS RCS/LAS PRESSURIZATION AND PROPELLANT FLOW CONTROL
11. PILOT CHUTE EJECT MORTARS
12. EXPLOSIVE NUT, RECOVERY CHUTE BRIDLE REPOSITIONING
13. UPPER AND LOWER FLAP RIGID LINK RELEASE
14. BRAKE CHUTE EJECT MORTAR
15. ADAPTER ATTACHMENT TO ENTRY VEHICLE EXPLOSIVE NUTS
16. EXPLOSIVE BOLTS ORBIT PROPULSION MODULE TO AFT ADAPTER SECTION
17. ABORT AND DEORBIT MOTOR IGNITERS (4) AND INITIATORS (16)
18. EXPLOSIVE BOLTS ADAPTER TIE TO LAUNCH VEHICLE

FIGURE 76. ORDNANCE SUBSYSTEM

TABLE 30

ORDNANCE SUBSYSTEM COMPONENTS, LOCATION AND FUNCTION

Igniters:	To provide for ignition of the abort rockets, the deorbit rockets, and the adapter separation rockets. These devices are composed of squib initiators which ignite a pyrotechnic which, in turn, ignites the solid rocket propellant grain. Dual igniters will be employed for each motor with dual initiators for each igniter to provide the desired redundancy. In all, 8 igniters and 16 initiators will be employed in the 4 solid rocket motors.
Explosive nuts:	Explosive nuts are used to provide release of structural fasteners for adapter tie to launch vehicle; "on-orbit" propulsion module tie to after portion of adapter; propulsion module tie to entry vehicle; and forward firing of adapter to entry vehicle. Explosive nuts are used in conjunction with standard bolts to physically fasten the gear to the vehicle structure in the stowed position. An explosive nut installation is also used to hold the vehicle recovery bridle to the after end of the vehicle for the period during chute opening and vehicle deceleration. At terminal velocity of vehicle, the chutes are dereefed and bridle attachment point is shifted from the after end of the body to the forward end of the body to position the vehicle for land or water impact. Explosive nuts are used to break the rigid links of the upper and lower flaps.
Shaped charge:	Shaped charges are used to cut the skin panels immediately above the recovery chute containers, located one each in the left and right hand main landing gear wells. Since the recovery system is an emergency system, throughskin structure was used in lieu of compartment doors. A shaped charge is used to cut the windshield transparent area for emergency egress prior to launch or after recovery.
Mortars:	Mortars are used in three phases in the recovery system, one to eject the decelerating brake chute used during vehicle slide out. The recovery chute package and mortar are located in the most aft section of the body. The other two applications are for ejecting the pilot chutes which, in turn, extract the main chute packages. The pilot chute mortars are located in the after end of the recovery chute containers located in each main gear well.
Gas actuators/ thrustors:	Pyrotechnic gas generators are used to provide individually pneumatic energy required for the three landing gear extension actuators and the two positioning actuators containers for chute extraction. In each application, the gas-generating cartridge is mounted in the head end of the actuating cylinders. An explosively charged thrustor is used for removal of the canopy heat shield cover.
Pin extractors:	Explosively fired latch pin extractors are used to free the hatch from the vehicle during emergency egress during the prelaunch activities or after recovery.
Squibs:	Seventeen squibs located in a centralized area are used in the pressurization and propellant flow control systems for the reaction control system (RCS) and the landing assist engine (LAS).

I. COMMUNICATION SUBSYSTEM

In accordance with the design criteria and tradeoffs presented in Part IV, the approach to communication subsystem design involves: (1) maximum use of the existing ground network, (2) antenna coverage for the spacecraft with a minimum of antenna switching, and (3) consideration of the communication, tracking and telemetry ground equipment costs at the selected landing area (Edwards Flight Research Center). The ground network that best satisfies these design criteria is a nonunified S-band system which consists of equipment that has been previously qualified on existing programs. The ground network is discussed in Part V.

The airborne equipments selected to implement the nonunified S-band system are described in this section. The first subsection contains a description of the selected electronic equipments along with a link analysis showing performance margins. The following two subsections contain a description of the antennas and the radiation coverage that can be expected for selected locations on the spacecraft.

1. Equipment Description and Performance

The equipments selected for the communications system are shown in table 31, based on performance characteristics and circuit techniques that have been qualified for space use. Figure 77 is a block diagram of the communication system.

UHF digital command receiver. - The digital command receiver system consists of two antennas coupled by a hybrid which, in turn, couples and divides the received power between two receivers. The command system is designed to receive digital information to perform three functions: (1) To enter words into the guidance computer, (2) to update the central timing equipment, and (3) to receive real-time commands to turn equipment on and off by ground control.

The receiving system consists of two receivers, a sub-bit detector and a decoder. The sub-bit detector recovers the timing information from a composite audio signal by means of a narrow-band phase-locked loop and detects digital information by means of an optimum filter design. The decoder detects the vehicle address and system address, stores and checks data, and processes the data to the appropriate spacecraft system.

Data are transmitted by a phase shift keying (PSK) tone. A second tone is linearly added to the phase-shifted tone to provide bit synchronization. This composite signal is then used to frequency modulate (fm) an ultra high frequency (uhf) carrier (400 to 450 Mh(z) for transmission to the spacecraft.

A word length is composed of 64 bits which contains three bits each for vehicle address and system address to provide choice of different vehicles and systems. The remaining bits comprise a real-time command, a computer word, central timing, and update or a test message.

After command receiving, detecting, and decoding, the command (upon complete validation) is transferred to the respective spacecraft system. After proper transfer of the command, a verification signal is transmitted via pulse code modulation (PCM) telemetry to the command station (ref. 11).

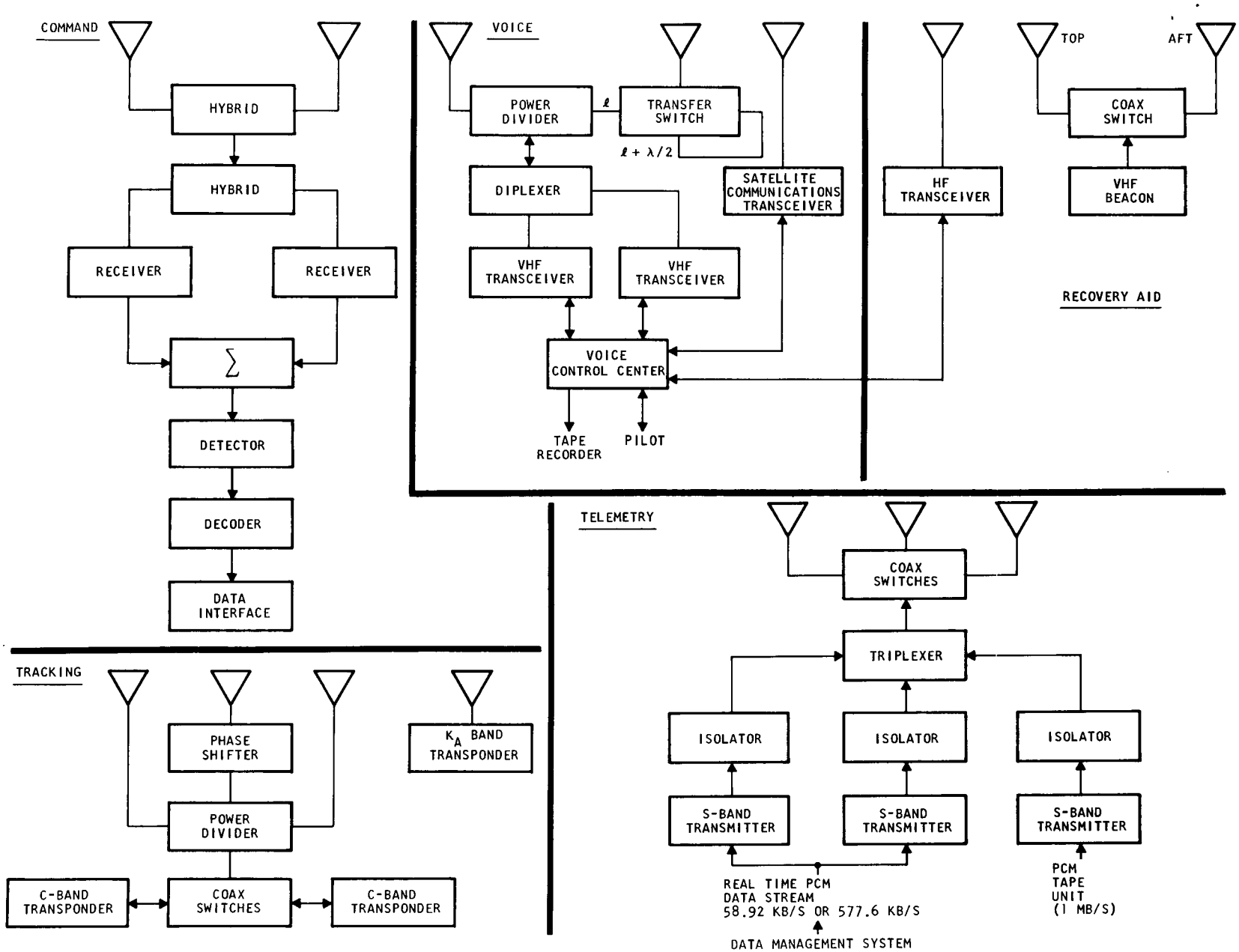

FIGURE 77. AIRBORNE COMMUNICATIONS SYSTEM

Performance margins of the command system are shown in table 32.

VHF/AM voice communications. - The very high frequency/amplitude modulation (VHF/AM) voice communications system consists of two slot radiators connected to a diplexer through a power divider to two receiver-transmitters.

Each of the receiver-transmitter combinations is operated at a separate frequency so that two conversations with the ground stations can be conducted simultaneously. Voice power is enhanced by speech clipping which produces a square wave radio frequency (rf) envelope. Noise is reduced during speech lulls by a suppression oscillator.

The two transmitters and receivers are assembled within a single enclosure. Modulation employed is low-level clipped speech, where the waveform is reduced to a square wave envelope. This speech processing provides nearly maximum voice power and retains high intelligibility and natural voice sound.

The operational modes are selectable. The modes of operation are: (1) two simplex, (2) two duplex, and (3) two receive-only combinations. Simplex operation occurs when the transmitter and receiver are on the same frequency. Duplex operation occurs when one transmitter is used with the other receiver. Performance margins of the voice communication system are shown in table 33.

S-band telemetry. - The S-band telemetry system consists of three transmitters, operated simultaneously on separate frequencies and connected to an antenna system through a triplexer. The antenna system consists of three selectable antennas to prevent interference nulls during transmission. Antenna selection is nominally pilot-controlled, with additional control through commands and attitude control.

Two transmitters transmit redundant data on separate frequencies during the entire mission. The telemetry baseband data format from the data management system is 58.9 kilobits during launch and orbit. At entry, the rate is increased to 577.6 kilobits to accommodate the increased data generated by the experiments. The 577.6-kilobit data rate is continued through landing.

The third transmitter operates on a third frequency at a one-megabit rate; it is activated after the effects of plasma attenuation have subsided to read out a tape recorder. The tape recorder contains data stored during the entry portion when communications blackout exists. A high data rate is required to read out all entry data before landing is initiated.

The S-band telemetry multiple frequencies are compatible with the receiving stations of the unified S-band system. Performance of the telemetry system for the various mission modes is shown in table 34.

C-band tracking. - The C-band tracking system consists of two transponders, one operating and one on standby, connected through a power divider to the antenna system. The antenna system consists of three antennas, with a phase shifter connected to one antenna to reduce the effect of interference nulls.

The C-band transponder receives and decodes pulses and replies with a transmitted pulse. The transponder performs primary tracking during all phases of the mission. It is compatible with all AN/FPS-16 and AN/FPQ-6 type radars.

TABLE 31

COMMUNICATIONS EQUIPMENT

Tracking							
Transponder	Scope	5.25 x 4.25 x 3.8 (13.4 x 10.8 x 9.3)	4.3 (1.96)	500	32	2	2
Coax switch			2.0 (0.91)	--	--	1	1
Power divider			1.5 (0.68)	--	--	1	1
Phase shifter			1.5 (0.68)	--	3	1	1
C-band antenna			0.5 (0.23)	--	--	3	3
Window			0.7 (0.32)	--	--	3	3
Voice							
vhf transceiver package	Collins	12 x 6 x 14.7 (30.5 x 15.2 x 37.4)	13.5 (6.15)	5	33		1
vhf antenna			6.1 (2.78)	--	--		2
Window			2.0 (0.91)	--	--		2
vhf power divider			1.0 (0.46)	--	--		1
Coax transfer switch			2.0 (0.91)	--	--		1
vhf diplexer			2.5 (1.13)	--	--		1
hf transceiver	Collins	8.5 x 4.0 x 6.0 (21.6 x 10.2 x 15.3)	6.3 (2.87)	5	20		1
hf antenna			6.7 (3.05)				1
Voice control center	Collins	8.65 x 4.66 x 4.7 (22 x 11.8 x 12)	7.9 (3.6)		20		1
Satellite comm transceiver	Bendix		20 (9.1)	500	1250*		1
vhf antenna			15 (6.8)	--	--		1
Window			4.0 (1.82)				1
Recovery aid							
vhf beacon	Collins	6.75 x 4 x 4 (17.2 x 10.2 x 10.2)	2.5 (1.81)	4	7.5	1	1
vhf antenna			1.5 (0.68)			2	2
Coax switch			2.0 (0.98)			1	1
K_a-band beacon	Bell	5.25 x 3.8 x 4.5 (13.4 x 9.3 x 11.4)	4.5 (2.05)	500	40	1	1
K_a-band antenna			0.25 (0.14)	--	--	1	1
Window			0.40 (0.18)	--	--	1	1

*Limited duty transmission.

TABLE 31--Concluded

COMMUNICATIONS EQUIPMENT

System Component	Source	Dimensions in. (cm)	Weight (each), lb (kg)	Power output (each), watts	Power (each), watts	Number required	
						Unmanned	Manned
Command							
Receiver package	Motorola	7 x 8-1/4 x 11 (17.6 x 20.6 x 28)	20 (9.1)	--	11	1	1
uhf antenna			3.2 (1.45	--	--	2	2
Window			1.4 (0.64)	--	--	2	2
Hybrid			0.7 (0.32)	--	--	2	2
Telemetry							
Transmitter	Collins	6.8 x 2.3 x 2.2 (17.3 x 5.8 x 5.6)	1.6 (0.73)	3	23	3	3
Triplexer			3.0 (1.36)	--	--	1	1
rf isolator			0.75 (0.34)	--	--	3	3
Coax switch			2.0 (0.91)	--	--	1	1
Window			1.0 (0.46)	--	--	3	3
S-band antenna			0.7 (0.32)	--	--	3	3
Autopilot adapter			15 (6.8)	--	--	1	

TABLE 32

LINK DETERMINATIONS--COMMAND

Frequency: 453 MHz, modulation: FM

	Data update at 1000 n. mi. (1850 km), dbm	Entry command at 200 n. mi. (370 km), dbm
Transmitter power (600 watts)	57.8	57.8
Ground rf losses	-1.2	-1.2
Ground antenna gain	18	18
Free space loss	-150.6	-136.6
Spacecraft antenna gain	0	0
Polarization loss	-3	-3
Char loss		-2
Spacecraft rf losses	-5	-5
Received carrier power	-84	-72
Required receiver carrier power	-99	-99
Margin, nominal	15	27
Margin, adverse tolerances	12	24

dbm = db below 1 milliwatt

TABLE 33

LINK DETERMINATIONS--VOICE

Frequency: vhf, modulation: am

	300 MHz				125 MHz	
	Spacecraft to ground at 1000 n. mi. (1850 km), dbm	Ground to spacecraft at 1000 n. mi. (1850 km), dbm	Spacecraft to aircraft at 1000 n. mi. (1850 km), dbm	Aircraft to spacecraft at 1000 n. mi. (1850 km), dbm	Spacecraft to satellite at 22,300 n. mi. (41,500 km), dbm	Satellite to spacecraft at 22,300 n. mi. (41,500 km) dbm
Transmitter power	37	50	37	50	57	55 (radiated)
Transmitter rf losses	-2	-0.5	-2	-6.9	-1	
Transmitter antenna gain	0	-18	0	-12	4	
Free space loss	-147.5	-147.5	-147.5	-147.5	-166	-166
Polarization loss	-3	-3	-3	-3		
Receiver antenna gain	18	0	12	0	0	4
Receiver rf losses	-0.5	-2	-3	-2	-1	-1
Received carrier power	-98	-85	-106.5	-97.4	-107	-108
Required receiver carrier power	-118	-110.0	-118	-110.0	-118	-115
Margin, nominal	20	25	11.5	12.6	11	7
Margin less adverse tolerances	18.5	23	9.5	10.6	9	5

TABLE 34

LINK DETERMINATIONS--TELEMETRY

Frequency: 2200 to 2300 MHz (S-band), modulation: PCM-PM

	Orbit to ground at 1000 n. mi. (1850 m) and 60 kilobits/sec, dbm	Orbit to aircraft at 1000 n. mi. (1850 m) and 60 kilobits/sec, dbm	Deorbit to ground at 300 n. mi. (360 km) and 600 kilobits/sec, dbm	Entry to ground at 200 n. mi. (370 km) and 1 megabit/sec, dbm	Entry to aircraft at 200 n. mi. (300 km) and 1 megabit/sec, dbm
Transmitter power (3 watts)	34.7	34.7	34.7	34.7	34.7
Spacecraft rf losses	-2	-2	-2	-2	-2
Window loss	-1	-1	-1	-1	-1
Char loss				-2	-2
Spacecraft antenna gain	3	3	3	3	3
Free space loss	-165	-165	-154.5	-151	-151
Receiver antenna gain	43.5	29.5	43.5	43.5	29.5
Received carrier power	-86.8	-100.8	-76.3	-74.8	-88.8
Equivalent receiver noise density (incl rf loss)	-173.1	-169.7	-173.1	-173.1	-169.7
Receiver noise bandwidth	48.8	48.8	58.8	61.2	61.2
Desired signal/noise ratio	10	10	10	10	10
Desired carrier power	-114.3	-110.9	-104.3	-101.9	-98.5
Margin, nominal	27.5	10.1	28	27.1	9.7
Margin, adverse tolerances	24.0	6.6	24.5	23.6	6.2

The performance of the tracking system is shown in table 35.

VHF satellite voice communications. - The vhf satellite voice communications system consists of a vhf/am (120 MHz) transmitter and receiver connected directly to an antenna. The satellite voice communications system provides the capability of continuous voice coverage throughout the mission, including periods when the spacecraft is out of view of ground stations.

Currently, experimental tests are being conducted by NASA with the Applied Technology Satellite (ATS) to determine optimum system characteristics.

Modulation employing low-level clipped speech, using a square wave envelope, will provide nearly maximum voice power and still retain high intelligibility and natural voice sound.

Simplex operation is planned. The performance of the system is shown in table 33.

VHF landing and recovery beacon. - The vhf (243 MHz) landing and recovery system consists of two selectable antennas connected through a switch to a transmitter. One antenna is located aft on the spacecraft and is extended after entry. After landing, the aft antenna is switched out and the top antenna is employed.

The vhf beacon is a tone-modulated am transmitter that provides a signal for line-of-sight radio direction finding. The beacon operates automatically with a transmission interruption cycle of two seconds on and three seconds off. During the two-second transmit interval, the transmitter output is 30 percent modulated by a one-kilocycle square wave.

HF transceiver. - The high frequency (hf) transceiver is directly connected to an extendable antenna. The transceiver primarily provides a signal for direction finding and voice communications beyond the line-of-sight after emergency landing. Transmission from orbit is unreliable and intermittent.

The operating modes are single side band (SSB), compatible am, or continuous wave (cw) with preassigned carrier frequency (8 to 15 MHz). The power output is 20 watts peak envelope power (PEP) in SSB, and 5 watts carrier in am and cw.

K_a-band tracking. - The K_a-band 35.0 GHz) tracking system consists of a transponder connected to an antenna. The transponder is used during the landing phase, when it extends the tracking range of the radar associated with the automatic landing system. High frequency is utilized on the radar so that a narrow tracking beam can be generated to avoid ground interference and accurately track at low elevation angles.

The automatic landing system is based on the AN/SPN-42 being developed for carrier landing by the Navy. When unmanned spacecraft are being landed, an autopilot adapter is planned in place of the pilot.

Audio center. - The audio center is an audio amplification and control unit that provides a complete and independently operated audio station for each crew station in the spacecraft. The unit provides each crewman with microphone and earphone amplifiers, switching circuits that control audio signals to and from operating rf equipment or an

intercommunication system common to other crewmen, and voice operated transmission (VOX) circuitry to permit voice keying of transmitters. Control panels associated with the crew positions are:

(1) Selection of input to the earphones

(2) Selection of audio outputs for the microphones

(3) Adjustment of the level of each receiver or intercom signal and overall level of the earphones

(4) Selection of either push-to-talk (PTT) or VOX operation

(5) Control of VOX sensitivity.

2. Antenna System

The antenna subsystem portion of this study consisted of specifying generic types for use with the various communication systems on the HL-10 and their location on the vehicle structure This subsection describes each antenna system and recommended locations. The following subsection will contain selected principal plane radiation patterns and contour maps.

The primary requirement governing the choice of antenna location is the extent of spherical radiation coverage provided. Most of the locations recommended for the final configuration of HL-10 vehicle were based on the study of radiation patterns taken on simulated 1/24- and 1/4-scale model vehicles. Test equipment limitations precluded obtaining patterns for the S-, C- and K_a-band systems. However, the successful performance of the antennas in the recommended locations for these systems can be reasonably well predicted.

HL-10 antenna installation. - The previously recommended HL-10 antenna system configuration (ref. 12) called for several installations in the center fin. Radiation patterns of these antennas were examined, and coverage was found to be marginal. With the exception of uhf command, the antennas were relocated to the vehicle body. The type of antenna for uhf use was changed and its present center fin location retained. While it is probable that a vhf antenna could have been designed to give satisfactory coverage from the fin, the number of antennas in this part of the structure should be kept to a minimum for mechanical, maintenance, and refurbishment reasons. Electrical disadvantages of fin installations, especially at the higher frequencies, include excessive line loss.

The revised HL-10 antenna system is shown in figure 78. The center fin is utilized for the command system only. The DeHavilland boom used for hf communication is retained at the base of the center fin as before. A new vhf voice communication antenna utilizes two "pancake" cavity-backed slot antennas, one on each side near the front of the vehicle. The slots can be fed either "in-phase" or "out-of-phase" at the discretion of the crew. The out-of-phase hookup provides broad coverage in the roll plane and should be more useful while in orbit. After entry and during landing, the in-phase configuration should provide the better coverage, i.e., toward the front and sides of the vehicle.

TABLE 35

LINK DETERMINATIONS--TRACKING

Frequency: 5765 MHz, modulation: Pulse radar

	Up at 1000 n. mi. (1850 km) dbm	Down at 1000 n. mi. (1850 km) dbm
Transmitter power	90	57
Transmitter rf losses	-1	-6
Transmitter antenna gain	44	0
Free space loss	-173	-173
Spacecraft window loss	-1	-1
Receiver antenna gain	0	44
Receiver rf losses	-6	-1
Received carrier power	-47	-80
Required receiver carrier power	-70	-100.5
Margin, nominal	23	20.5
Margin, adverse tolerances	19.5	17.5

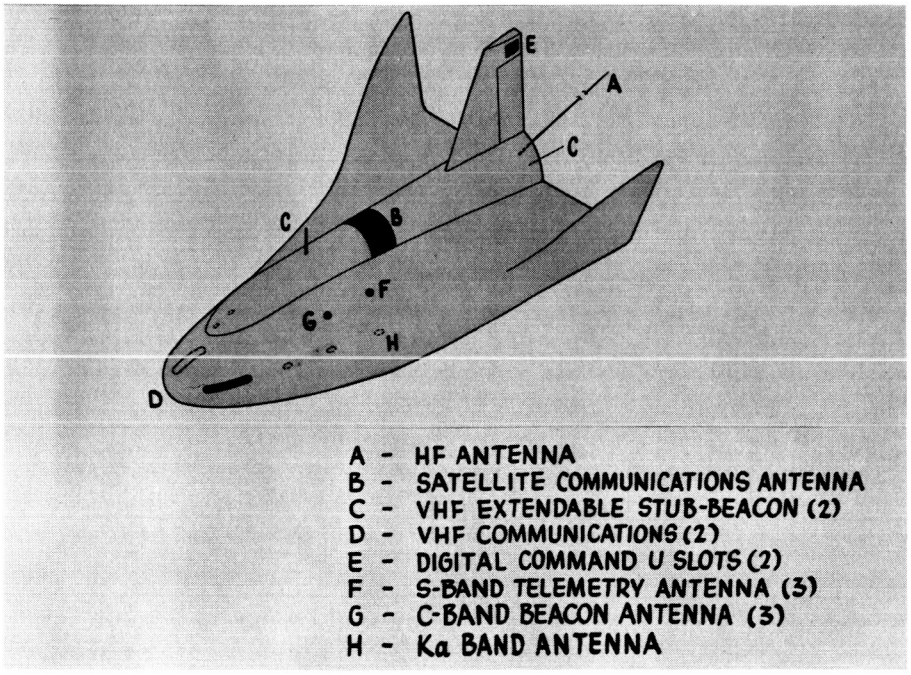

FIGURE 78. ANTENNA SYSTEM

Two recovery beacon antennas consisting of extendable stubs are employed. One of these, the primary, is extended from the rear of the vehicle and used after blackout and during the landing phase. Its location on the back of the vehicle permits its being extended early in the landing phase without being subjected to excessive airloads. A second beacon antenna is located on top of the vehicle aft of the hatch. This is an emergency antenna activated in the event of a probable landing in remote land sites. Essentially omni-azimuthal coverage is provided by this antenna.

The antennas for S-band remain, as previously, equally spaced around the body. Three radiators are employed, one at a time.

The new C-band antenna system is similar to the S-band system. These radiators are employed equally spaced around the body. However, unlike the S-band case, the individual radiators are not employed singly. A phase shifter is used to remove the deep interference nulls where the patterns of the individual radiators overlap. The phase shifter is a ferrite device operating at 400 cps.

As noted earlier, the only antenna remaining in the center fin is the command antenna. Two "U" slots of a type developed and used for ASSET are recommended. They are phased for omni-azimuthal coverage. Radio frequency transparent windows consist of teflon slabs about 8 inches square and equal to the heat shield in thickness.

The previous HL-10 communication system did not provide for communication between spacecraft and synchronous orbiting satellites. Recent revisions to the system have included this feature. The antenna proposed for this system, primarily for purposes of weight estimation, consists of a modified Dorne and Margolin design. A detailed description of the antenna cannot be given at this time because the requirement for low-frequency (about 125 MHz), circularly polarized, flush-mounted antennas designed expressly for spacecraft-to-satellite communication is a relatively new one, calling for new and possibly unique designs.

K_a-band antenna.- The antenna for the K_a-band beacon system will be a symmetrically tapered waveguide with part extended through the heat shield on the bottom centerline of the vehicle. The polarization is linear. Half-power beam widths are between 120° and 140° in roll plane and pitch plane. Ten-decibel beam widths are slightly less than twice the 3-db widths. Broad coverage in the bottom hemisphere is provided by this installation. During the glide slope approach to touchdown at low altitudes, the vehicle angle of attack is such that adequate antenna gain is achieved in the direction of the K_a-band transmitter on the ground.

Antenna and rf window mechanical details.- For purposes of mechanical integration of antennas and rf windows into the HL-10 structure, a detailed mechanical description of these components is required and given in this section.

The pancake slot antennas recommended for vhf communications require sizable rf transparent windows. The windows are necessary due to the high absorption of rf energy by the heat shield material particularly after entry. Unfortunately, window materials which are satisfactory mechanically and electrically are also good conductors of heat. This fact must be taken into account in cases where the structure temperature must be maintained at some predetermined level, say, below 800° F.

HF antenna.- The DeHavilland boom is an extendable-retractable unit similar to their Model A-32 except with a 30-foot (9.14 m) tape. The retracted dimensions are 4 by 5 by 19 inches (10.2 x 12.7 x 48.2 cm). An rf transparent window is not required.

Satellite communication antenna.- The half-cylindrical volume on top of the vehicle between stations 149 and 181 has been reserved for the satellite communication antenna. The volume and weight estimate is based on early design of antennas for similar use by aircraft by Dorne and Margolin and Electronic Communications, Incorporated. However, these antennas are not flush-mounted, and the possibility of adapting the designs for HL-10 use is probably small. An extendable mode of operation appears to be costly in terms of weight, which is the basis for the flush operation requirement.

In addition to these antennas, several conventional types, which might be developed for HL-10 use, include: the cavity-backed Archimedes spiral; cavity-backed loaded turnstile; and the small aperture hemispherical scanning (SAHS) antenna, which is a quad scimitar.

An rf transparent window for the satellite communication antenna will be provided by replacing the metallic skin with fiber glass. The fiber glass will not carry structural loads. Since the satellite communication link is used only during the orbit phase, a normal thickness of ablative heat shield material will be placed over the fiber glass. The heat shield is relatively thin on the top surface of the vehicle and, in the uncharred state, is acceptably transparent to radio frequencies planned for use in satellite communication.

Recovery beacon.- The antenna housing is cylindrical. It measures about 5 by 2 inches (12.7 x 3.08 cm). It is a one-shot device and not reusable; a window is not required.

VHF voice.- The major dimensions of the vhf cavity-backed slot are 19 inches long by 6 inches wide and 3/4 inch deep (48.2 x 15.24 x 1.91 cm). The construction is sheet metal, filled with a dielectric for electrical loading purposes. A flange is provided for attaching the antenna to the vehicle structure. The top surface (slot side) of the antenna is contoured to the vehicle skin line.

Since the antenna is in a high temperature region, a substantial rf transparent window must be provided. The design employs slip cast, fuzed silica, hollowed out to reduce weight and heat conduction. The heat shield skin line dimensions of the window are 5 by 19 inches (12.7 x 48.2 cm).

Digital command antenna.- The major dimensions of a "U" cavity-backed slot are 8 inches square by 3/4 inch deep (20.3 x 1.91 cm). Dielectric loading is used in the cavity. Two are installed in the center fin, back to back. An 8 by 8 inch (20.3 x 20.3 cm) solid teflon window, approximately 1/2 inch thick (1.27 cm), serves as the rf window.

S-band and C-band.- The radiators used for these systems are small and present no unusual installation problems. They will consist of turnstiles at S-band and either turnstiles or circularly polarized crossed slots at C-band. Figure 79 shows a typical window for use at either S-band or C-band. The heat shield line dimension is 5 inches in diameter. Again, since some of these windows are in a very hot environment, fuzed silica, hollowed out to reduce heat transfer, is used as the window material.

A summary of the HL-10 antenna system is given in table 36.

3. Radiation Patterns

This subsection contains selected principal plane radiation patterns (relative voltage versus direction) and radiation field contour maps (antenna gain versus direction).

Principal plane and conical radiation patterns of scale model HL-10 vehicle and antenna system were measured to verify the coverage provided by the recommended installations. Patterns of the hf communication antenna were measured with a 1/24-scale model. Patterns of the other system antennas tested were measured with a 1/4-scale model. Fourth-scale measurements of the C-band system required 22.4-GHz generating equipment which, at the time, was unavailable. Patterns of the S-band antennas were felt to be unnecessary because of the simplicity of the installation.

The vehicle-centered coordinate system employed is the Standard IRIG antenna pattern format. Linear polarization is expressed as E_θ or E_ϕ. The first, θ, is the angle between the positive roll axis (from nose of vehicle) to a vector from the vehicle to the field point. The second, ϕ, is the angle between the negative yaw axis (from top of vehicle) to a projection of the vector in the roll plane. It is measured in a clockwise direction looking forward.

HF communication antenna. - The antenna for this system operates in the 8- to 15-MHz frequency range. Ground-based antennas are normally linearly polarized. Horizontal polarization principal plane patterns for a full-scale frequency of 8 MHz are given in figure 80.

The wavelength at 15 MHz is about 60 feet (18.3 m). Thus, the dimensions of HL-10 are short in comparison to a wavelength over the 8- to 15-MHz band. Excitation of the 30-foot (9.14 m) boom will result in excitation of the vehicle structure. The effect in this case is an antenna/vehicle radiating system much like a "flying dipole," the predominant polarization of which is horizontal. Good coverage around the vehicle equator and poor coverage in the polar direction is characteristic. Due to the tilt of the DeHavilland boom in the extended position, however, a strong cross-polarized (vertical) field component is obtained which tends to fill in the regions of low horizontally polarized field, front and back.

Recovery beacon. - Ideal radiation patterns for the emergency (top-mounted) antenna are characterized by good coverage in the azimuth plane with moderate coverage in the vertical plane to allow for vehicle roll and pitch maneuvers during the subsonic flight regime. Figure 80 gives the principal plane patterns for right-hand circular polarization at 972 MHz which corresponds to a full-scale frequency of 243 MHz.

Pattern characteristics of the aft-mounted antenna, which is extended after communication blackout at a relatively high altitude, are optimum for signal reception by aircraft and ships below and to the sides of the vehicle.

VHF communications. - Right-hand circular principal plane patterns of the vhf communication slot antennas are given in figure 81. The slots were fed in phase. The

[redacted]

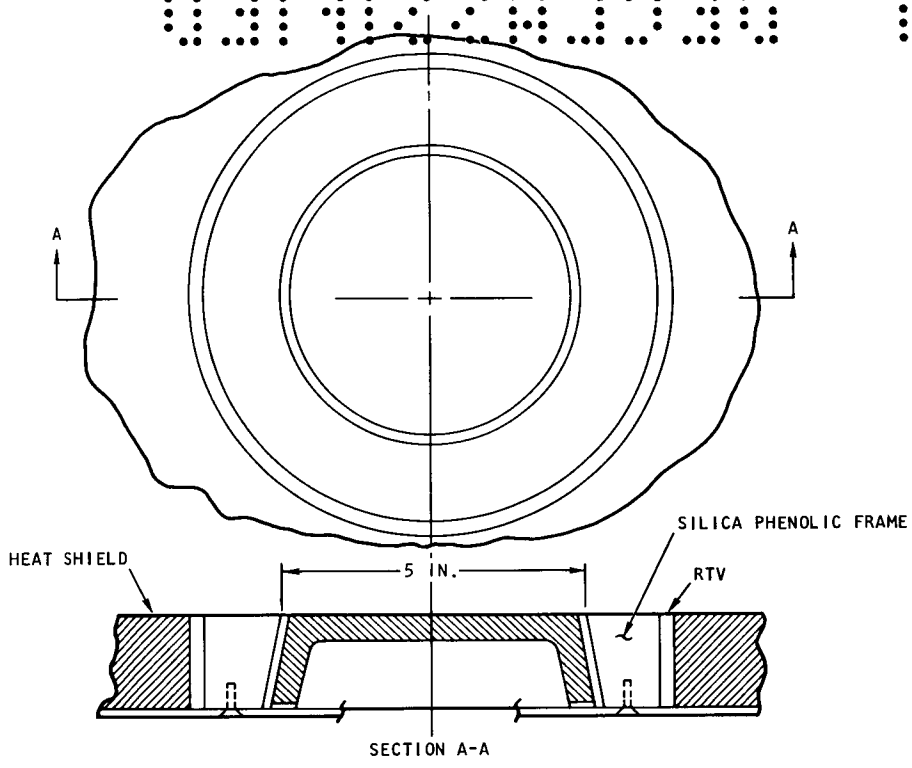

FIGURE 79. TYPICAL ANTENNA WINDOW FOR C- AND S-BANDS

TABLE 36

HL-10 ANTENNA PHYSICAL CHARACTERISTICS

System	Antenna type	Quantity	Antenna weight, lb (kg)	Window weight, lb (kg)	Total system weight, lb (kg)
1. hf communications	DeHavilland boom	1	6.7 (3.04)	--	6.7 (3.04)
2. Satellite communications	Modified Dorne and Margolin	1	40 (18.2)	--	40 (18.2)
3. Recovery beacon	Extendable stub	2	1.5 (0.68)	--	3.0 (1.36)
4. vhf voice	Cavity-backed slot	2	6.1 (2.77)	2.0 (0.91)	16.2 (7.4)
5. uhf command	"U" slots	2	3.2 (1.46)	1.4 (0.64)	9.2 (4.15)
6. S-band telemetry	Turnstile	3	0.7 (0.317)	1.0 (0.455)	5.1 (2.31)
7. C-band tracking	Turnstile or cavity-backed slots		0.5 (0.227)	0.7 (0.317)	3.6 (1.64)
Total weight			58.7 (26.7)	5.1 (2.3)	83.8 (38.1)

[redacted]

DECLASSIFIED [redacted]

(a) HF COMMUNICATIONS (b) RECOVERY BEACON

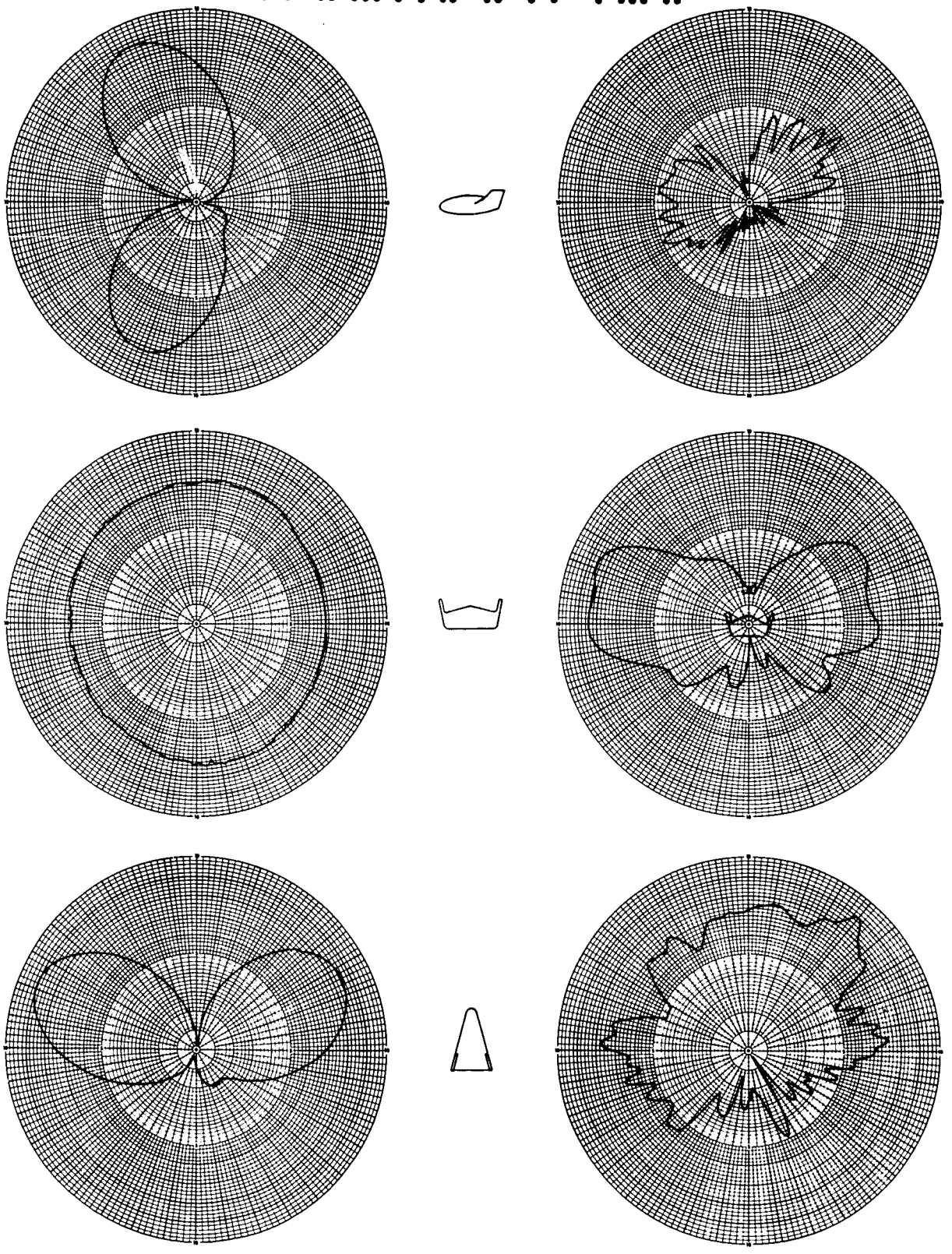

FIGURE 80. PRINCIPAL PLANE PATTERNS, HF AND BEACON

[redacted]

[redacted]

(a) VHF COMMUNICATIONS (IN-PHASE)

(b) UHF COMMAND

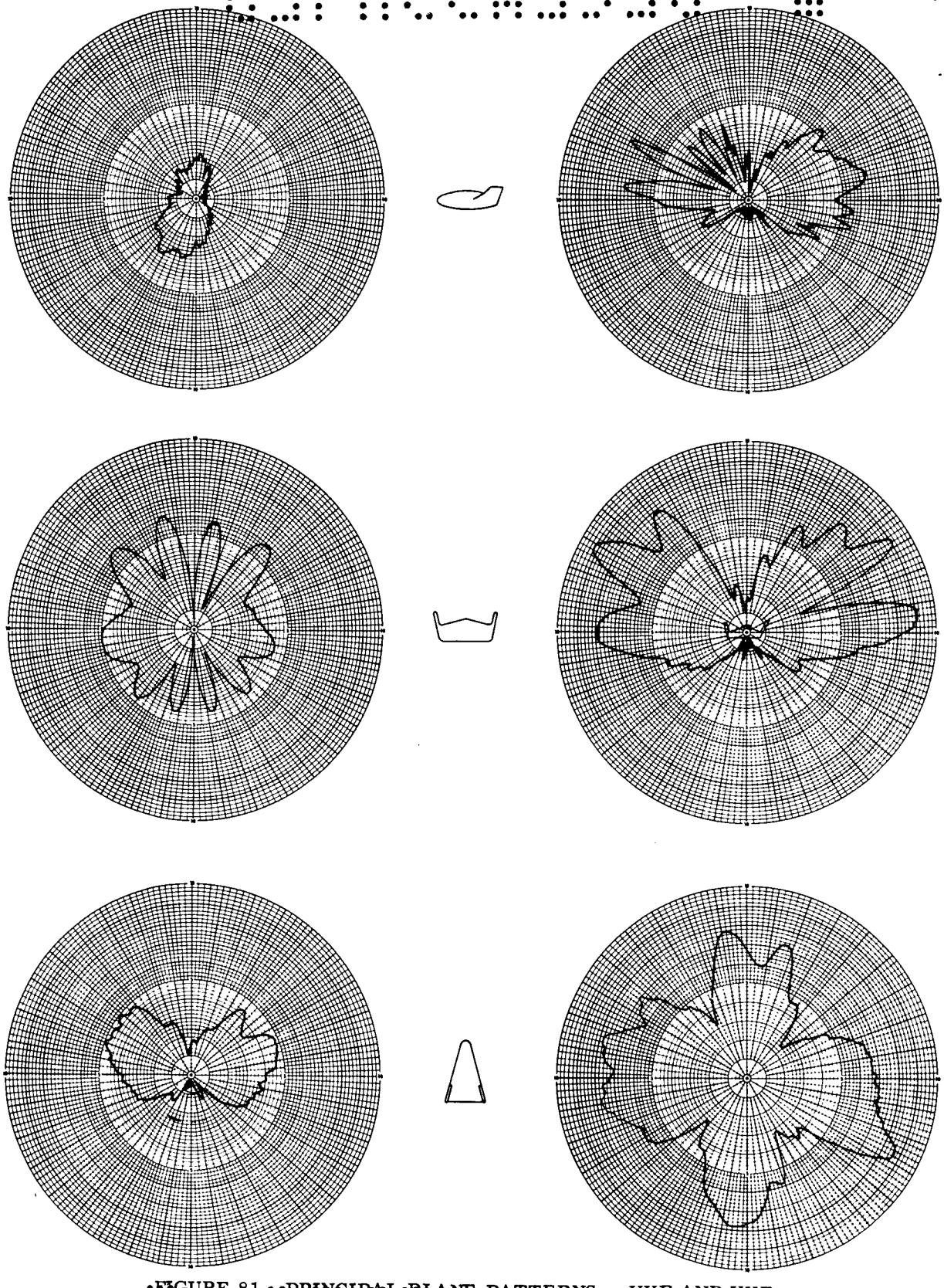

FIGURE 81. PRINCIPAL PLANE PATTERNS, VHF AND UHF

[redacted]

scale frequency is 1.2 GHz, which corresponds to a full-scale frequency of 300 MHz. A two-mode vhf antenna operation is provided on HL-10 to reduce to a minimum the "holes" that occur in any vhf antenna radiation field. Changing from one mode to the other is accomplished by a transfer switch which inserts a half wavelength line in series with one antenna. The in-phase mode tends to emphasize coverage in the forward hemisphere, which can be seen from the patterns and also from the contour map of figure 82.

UHF command. - A pair of "U" slots in the top of the center fin, fed out of phase, are used for the uhf command system. Right-hand circular principal plane patterns in figure 81 show good azimuthal coverage with acceptable coverage in the vertical plane. The region directly below the vehicle is one of low signal strength as shown in the contour map of figure 82. However, in these directions, the slant range is minimum, and reduced path loss tends to compensate for low antenna gain.

J. INSTRUMENTATION AND DATA HANDLING SUBSYSTEM

Subsystem design criteria and functional requirements are strongly influenced by the flight test measurements for the 52 research tasks. These 52 measurement lists have been defined in considerable detail in Part II, and a computer program was employed to develop complete measurement lists for particular research flights. A typical, heavily loaded research task flight (as indicated in Part IV) requires approximately 2000 measurements, even though all common measurements have been deleted by the computer program.

Figure 83 is a functional block diagram of the recommended subsystem. It is a PCM, remote multiplexed instrumentation system which can handle up to 2048 measurements.

1. Recommended Equipment Summary

The equipment selected for the D/3 vehicle configuration is based on the data submitted by potential suppliers in response to a Martin Marietta request for information and the preliminary performance specification (see Part IV).

Table 37 shows a summary of the contractor recommendations. All equipments are applicable to this program with varying degrees of modification and development required. Recommendations from the various suppliers are discussed later in this section.

Physical descriptions of units of the selected system are summarized in table 38 and the individual units are discussed in the following paragraphs.

Remote multiplex units. - Figure 84 is a block diagram of the remote multiplex unit. This unit receives a command from the central control unit to send a particular parameter. This parameter is sampled, encoded, and a serial PCM bit stream is transmitted back to the central control unit over the data bus. Estimates have been made of the size, weight, and electrical power which will be required for this unit. These estimates were based on the dimensions of the Lockheed equipment.

[redacted]

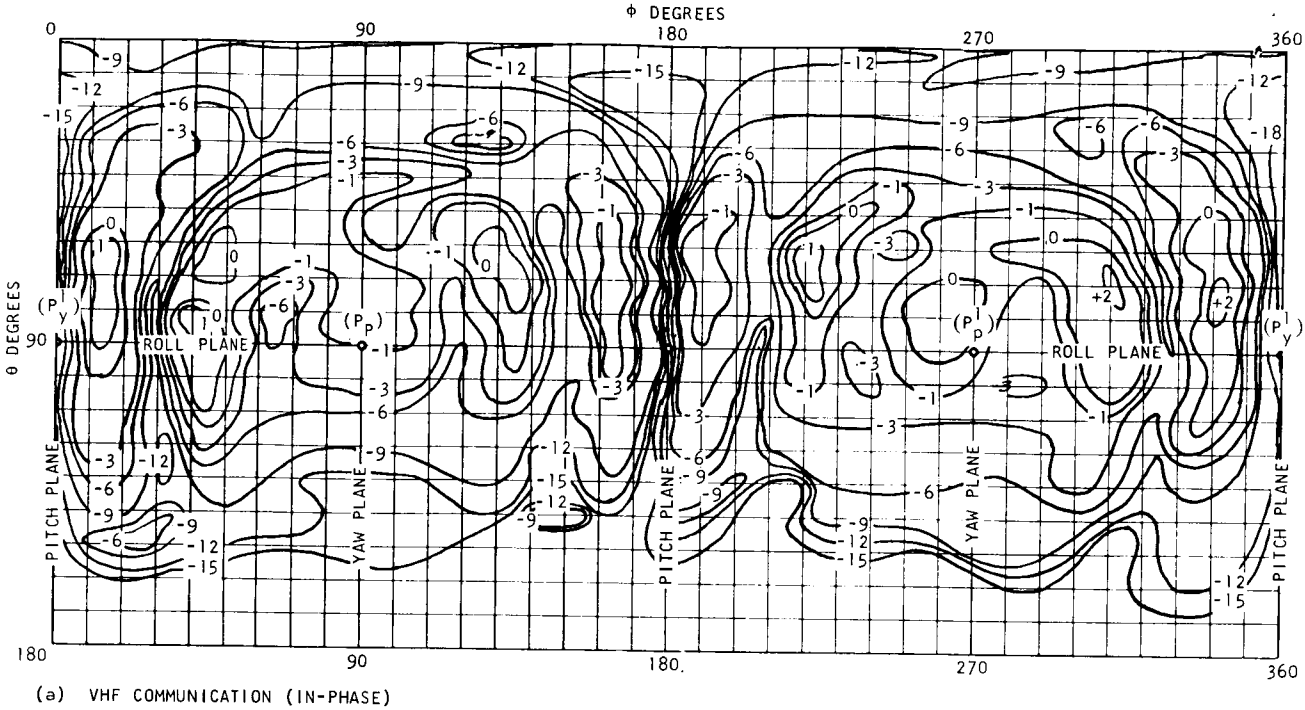

(a) VHF COMMUNICATION (IN-PHASE)

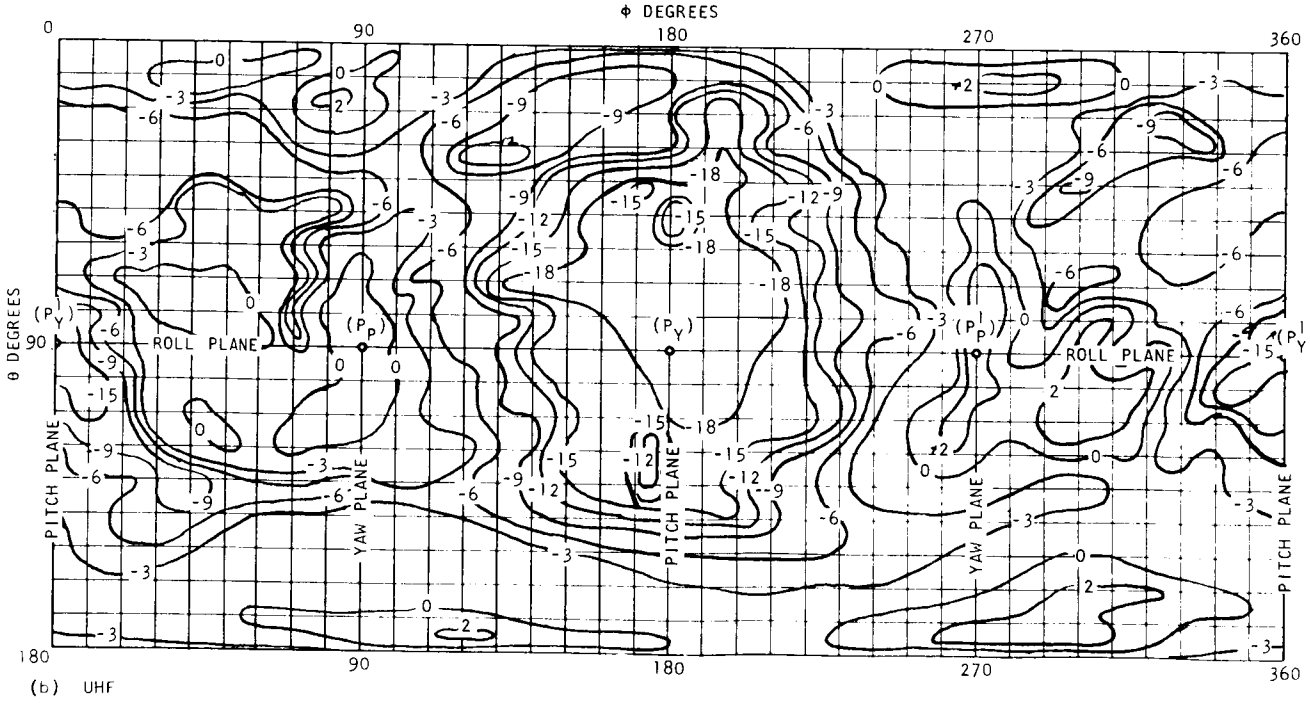

(b) UHF

FIGURE 82. ANTENNA GAIN PATTERNS

[redacted]

The estimates of equipment characteristics are:

Number of parameters:	Up to 128
Weight:	3.5 lbM (1.57 kg)
Power:	4.0 watts
Size:	3-1/8 by 4-1/2 by 6 in. (7.95 by 11.4 by 15.2 cm)

Central control unit.- Figure 85 shows a block diagram of the central control unit. The estimated characteristics of this unit are:

Weight:	36 lbM (16.3 kg)
Power:	72 watts
Size:	3-1/8 by 8 by 6 in. (7.95 by 20 by 15.2 cm) each of six modules

TABLE 37

SUPPLIER RECOMMENDATIONS

Supplier	Size, cubic inches (cc)	Weight, lbM (kg)	Power, watts	Development costs (first unit), $	Remarks
Radiation, Inc.	200 (3280)	10 (4.54)	15	300 000	Conventional approach: 1000-parameter system with central programmer
	400 (6560)	20 (9.08)	40	400 000	Integrated approach
Lockheed Missiles and Space Company	480 (7880)	20 (9.08)			Remote multiplexer units: weights and sizes refer to 6 units with 170 inputs each
	420 (6888)	18 (8.15)			Central converter unit: total system consists of remote multiplexer units shown above together with this control unit
TRW, Inc.	655 (10 750)	18 (8.15)	10		1000-parameter system: parameters shown for total system
Space Craft, Inc.	1120 (18 400)	41 (21.7)	32		1000-parameter system: these specifications are for the remote multiplexer units, 32 units with 32 inputs each
	600 (9850)	20 (9.08)	24	190 000	Central unit: development cost given for total systems
Leach Corp.	2459 (41 000)	62 (28.1)	61		Tape recorder system only

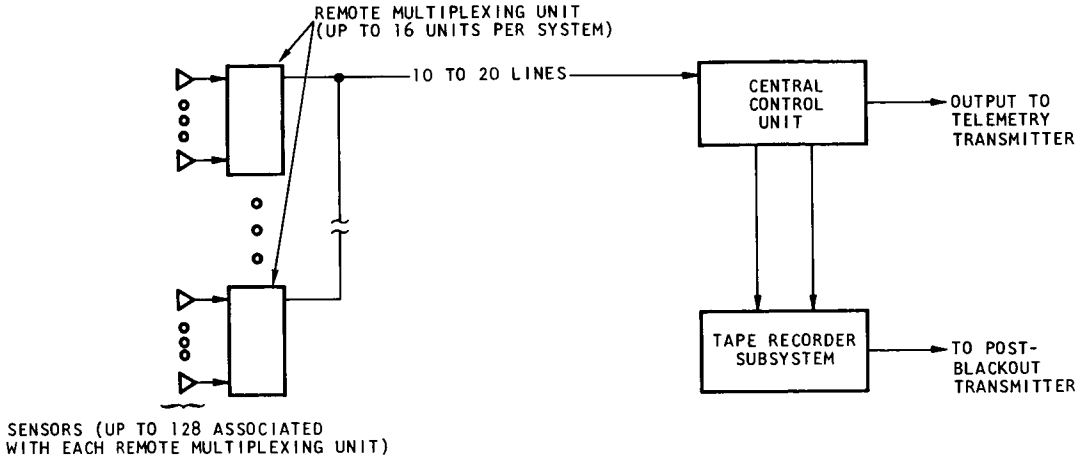

FIGURE 83. INSTRUMENTATION AND DATA HANDLING SYSTEM

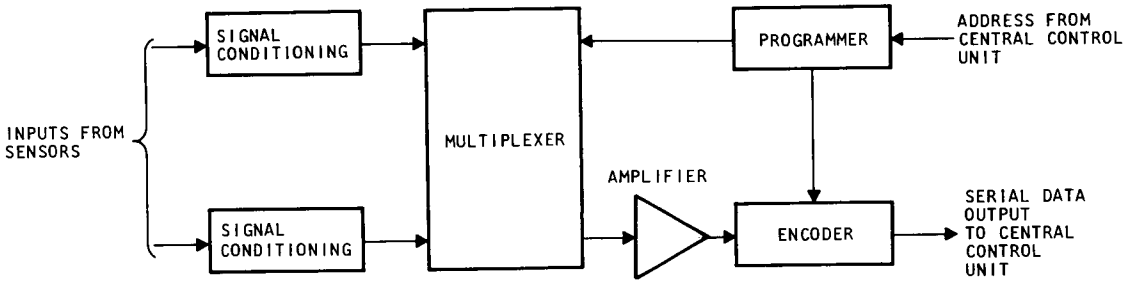

FIGURE 84. REMOTE MULTIPLEX UNIT

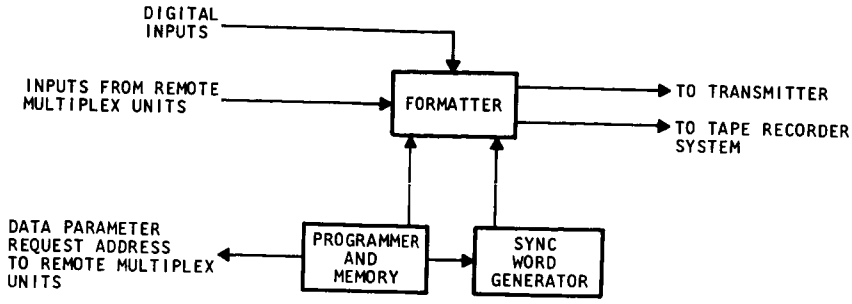

FIGURE 85. CENTRAL CONTROL UNIT

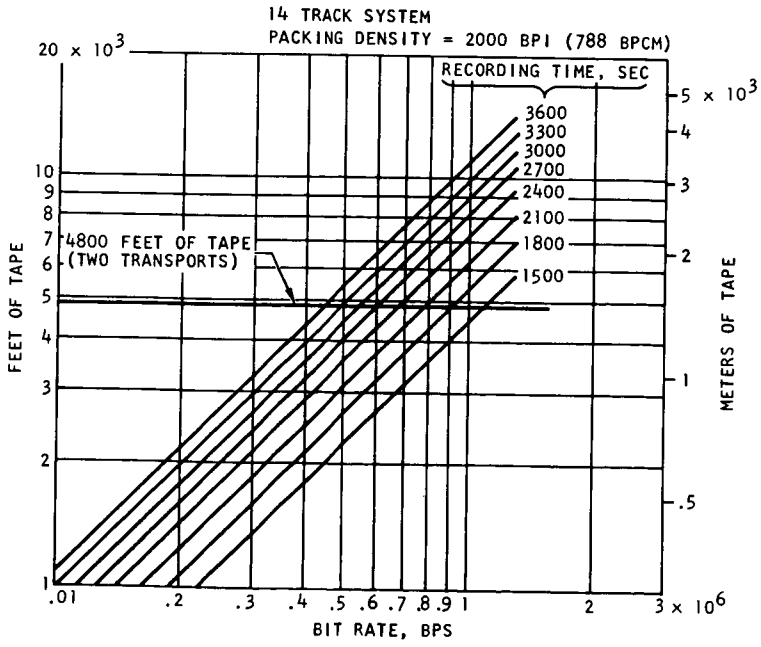

FIGURE 86. REQUIRED TAPE CAPACITY

TABLE 38

SUMMARY (2048 MEASUREMENTS)

	Size, cubic inches (cc)	Weight, lbM (kg)	Power, watts
Remote multiplex unit (16 units)	1300 (21 300)	56 (25.4)	64
Central control unit	900 (14 800)	36 (16.3)	72
Tape recorder	2495 (41 000)	62 (28.1)	61
Sensors and wiring		405 (183.5)	50
	4695 (77 100)	559 (253.0)	267

Tape recorder system.- To ensure that the data collected during the entry period is recovered, the telemetry data must be both transmitted and recorded using onboard tape recorders. The present state-of-the-art in tape recording indicates a bit packing density of about 2000 bits per inch (788 bits/cm). Figure 86 shows the number of feet of tape versus bit rate for various recording times. The magnitude of the recording problem can be readily seen from the figure. At high bit rates and for long recording times, the amount of tape required becomes completely unreasonable. However, present estimates indicate that HL-10 system parameters will lie below the 4800 feet (1465 m) of tape that would indicate the requirement for two transports.

Figure 87 shows a block diagram of the tape recorder system. Figure 88 shows a timing diagram for the recorders. The serial bit stream from the central control unit is converted to parallel bit stream and recorded on tape. On playback, the parallel tracks are again converted to a serial bit stream for transmission.

The design of this subsystem is based on equipment developed by Leach Corporation for the Apollo (Block II) program. A typical parts list for the tape recorder system is shown in table 39.

TABLE 39

TYPICAL PARTS LIST HL-10 TAPE RECORDER SYSTEM

Part	Quantity	Part number	Contractor
Tape transport	2	MTR-3200	Leach
Record amplifiers	16	32 DRA-804	Leach
Digital reproduce and slew correction amplifiers	14	32 DRA-806C	Leach
Serial-to-parallel converter	1	-	Leach

TABLE 39.--Concluded

TYPICAL PARTS LIST HL-10 TAPE RECORDER SYSTEM

Part	Quantity	Part number	Contractor
Parallel-to-serial converter	1	-	Leach
Voltage regulator	1	32 MUR-812	Leach
System preregulator	1	32 SPR-809	Leach
Motor inverter	1	-	Leach
Module housing unit	4	-	Leach
Gating circuits	1	-	Leach

2. Radiation, Inc., Recommendations

The basic approach taken by Radiation, Inc., was to develop a central multiplexed system based upon the preliminary specification. The size, weight, and electrical power requirements of this system are shown in table 37.

As an alternate approach, Radiation, Inc., suggested an integrated data system. This system includes the combined functions of timing, signal conditioning, telemetry, display outputs, and monitor and alarm within a single system. It is done at considerably decreased complexity, size, weight, power, and cost compared to the sum of each of these subsystems individually. The integrated data system, tailored to meet the anticipated HL-10 requirements, would require approximately 400 cubic inches (6550 cc), weigh 20 pounds (9.04 kg) and require a 40-watt power supply.

While the size, weight, and power estimate may be optimistic, the integrated data system as advocated by Radiation is of interest. The following discussion expands the idea of an integrated data system.

Integrated data system.- The separable functions performed by missile and spacecraft data systems have traditionally been handled as separate items. This has been wasteful because of the requirements for separate signal conditioners for each unconditioned measurement and for duplication in timing functions and in measurements of one parameter by several subsystems.

These functions may be combined into a single system at a considerable saving in hardware and, therefore, in size, weight, power, cost, and increased reliability. This combining of functions is especially compatible with even higher reliability through the addition of redundancy where high reliability is of the greatest importance.

The overall system accuracy may be enhanced through the use of more sophisticated circuitry in conditioning circuits used for a multiplicity of channels than would be feasible for individual signal conditioners where one is required for each measurement channel.

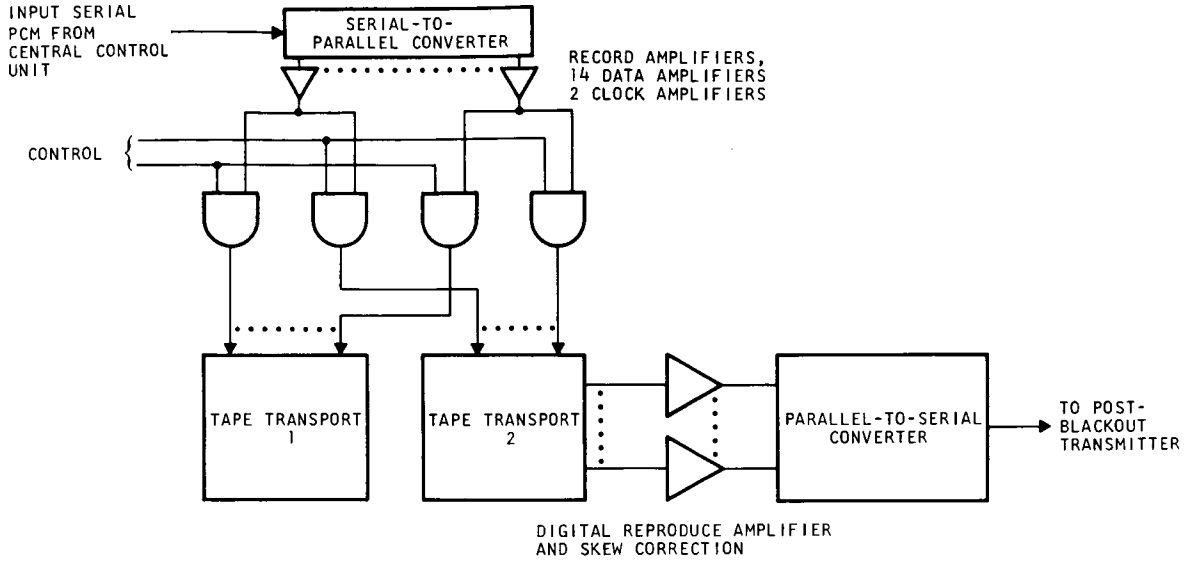

FIGURE 87. TAPE RECORDER SYSTEM

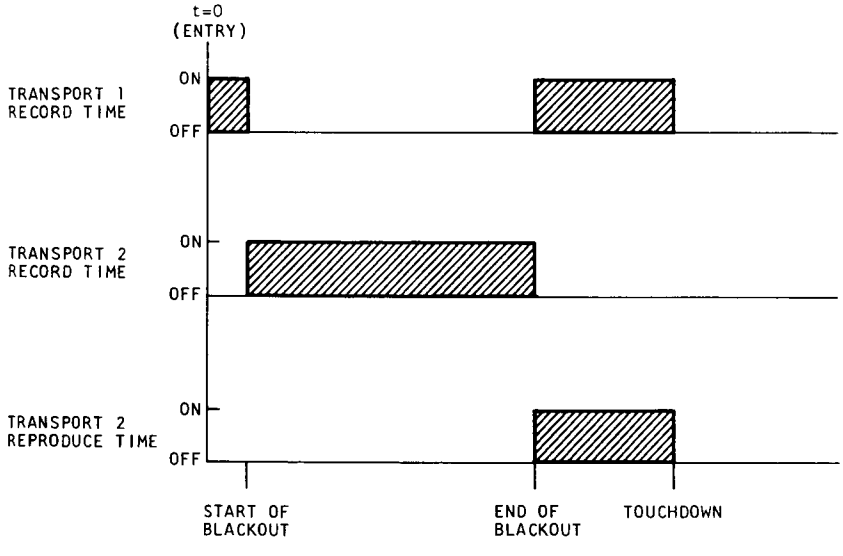

FIGURE 88. TIMING DIAGRAM FOR TAPE RECORDER SYSTEM

A high degree of flexibility may be achieved by a flexible programmer in which the number of channels of each type and the rates may be selected. Likewise, the number of channels that have conditioned outputs for display or similar circuits may be controlled by the flexible programmer.

Conventional techniques.- Signal conditioners and telemetry equipment have traditionally been treated separately in instrumentation systems. The telemetry has, at best, accepted only two or three full-scale value analog inputs. All inputs not adhering to these levels, or not in the form required (i.e., slowly varying dc), must be conditioned through a separate device. Only about one-quarter to one-half of the analog channels in a typical instrumentation system are suitable for direct connection to the telemeter without prior conditioning. The remaining channels require conditioning such as amplification, attenuation, ac (amplitude) to dc conversion, frequency to dc conversion or phase to dc conversion.

In addition, to prevent ground loops, it is desirable (if not mandatory) that each conditioner isolate the input signal, output signal, chassis ground, and vehicle power supply from each other.

The problem is further complicated when the signal is to be fed into more than one device, such as the telemeter, a display, and a malfunction warning system. This requires that the signal conditioners have three outputs, each isolated from the other, the input signal, chassis ground, and from the primary power source in order to prevent ground loops.

Integrated technique.- The techniques conventionally used in a sampled data system for slowly varying signals within predetermined voltage levels may be extended to include unconditioned signals. These signals may then be sampled prior to conditioning so that one signal conditioning device is time-shared to condition many channels of similar data.

Similar sharing of functions in the timing area may be accomplished by including the vehicle timing and programming requirements so that the programmer and timing functions may utilize common circuits.

A block diagram of this integrated approach is shown in figure 89.

The input channels that are readily available in the conventional 0- to 5-volt form are multiplexed in the conventional manner. They are handled directly, rather than through a buffer or amplifier, since it would be expected that from one-quarter to one-half of the channels may be handled through this unconditioned route.

The slowly varying dc input signals that are not already in the 0- to 5-volt range are conditioned through one of three multiplexers and amplifiers. Each of these handles a portion of the total range. This helps to prevent crosstalk of high level signals on the low level channels and permits the programmable amplifiers to be programmed over a lower range.

Each signal is sampled by a multiplexer and amplified (or attenuated) to the 0- to 5-volt range (fig. 90). Channel 1 is sampled by gate 1 while the respective gain and level settings are simultaneously switched through S_{1g} and S_{11}. This is then repeated for channel 2, etc.

If a level and gain setting were available for each input channel, each channel could have a separate setting.

The example in figure 90 assumes that a further simplification can be made by grouping the input channels into a limited number of groups with several channels per group. This permits one set of gain/level controls to be shared for several channels.

The high level channels may be single-ended, as shown in figure 89, while differential balanced inputs are considered necessary for the medium and low level channels.

The ac input channels are multiplexed in the same manner as the dc channels described above. They are gain- and level-controlled so that some channels, for example, may have spans of 0 to 32 volts while others have spans of from 105 to 125 volts. It is suggested that ac signals be attenuated to approximately 15 volts peak-to-peak near the source to prevent the mixing of low level and high level ac signals in cable bundles, either internal or external to the described system.

As shown in figure 91, the ac channels may be grouped just as were the dc channels.

The frequency input channels are multiplexed in the same method described above. They are conditioned by a linear frequency to dc converter to form a 0- to 5-volt PAM (pulse amplitude modulation) pulse train suitable for encoding. The gain and level controls may be set individually, as shown in figure 92, so that various frequency ranges and bandwidths may be converted. The number of controls may be limited by grouping similar input channels into common level/gain functions.

The ac frequency inputs could also be handled digitally by the method shown in figure 93. The signal input from the multiplexer is counted digitally and read once each time base period; that is, if the time base period is one second, the frequency is read directly in cycles per second. An eight-bit register then provides a 0- to 255-Hz readout or a 12-bit register provides a 0- to 4095-Hz readout. Longer or shorter time base periods provide handling of lower and higher frequencies, for example; a 0.1-second time base on an eight-bit register provides a frequency range of 0 to 2550 Hz. Vernier ranges may be handled through use of the least significant bits of a larger register, that is, a frequency range of 255 to 511 Hz could be accommodated through use of the eight least significant bits of a nine-bit (or larger) register with a time base of one second. This method has the advantage of accuracy in that the entire operation is digital; hence, no analog errors may appear.

As in the case of other ac devices, problems of crosstalk between these inputs and of the sensitive low-level dc inputs may be minimized by attenuating the signals to a maximum of 15 volts peak-to-peak near the source.

Phase input channels may be multiplexed and converted by a phase-to-dc converter, as shown in figure 94. These inputs are compared in phase with a common phase reference and combined into a common PAM output suitable for encoding. Similar channels may use common gain controls to limit the number of controls.

The combined outputs of each of the analog sampling devices are combined to form a single PAM signal with each pulse representing an input signal normalized in the 0- to 5-volt range. This signal is converted into a parallel digital signal by the analog-to-digital converter.

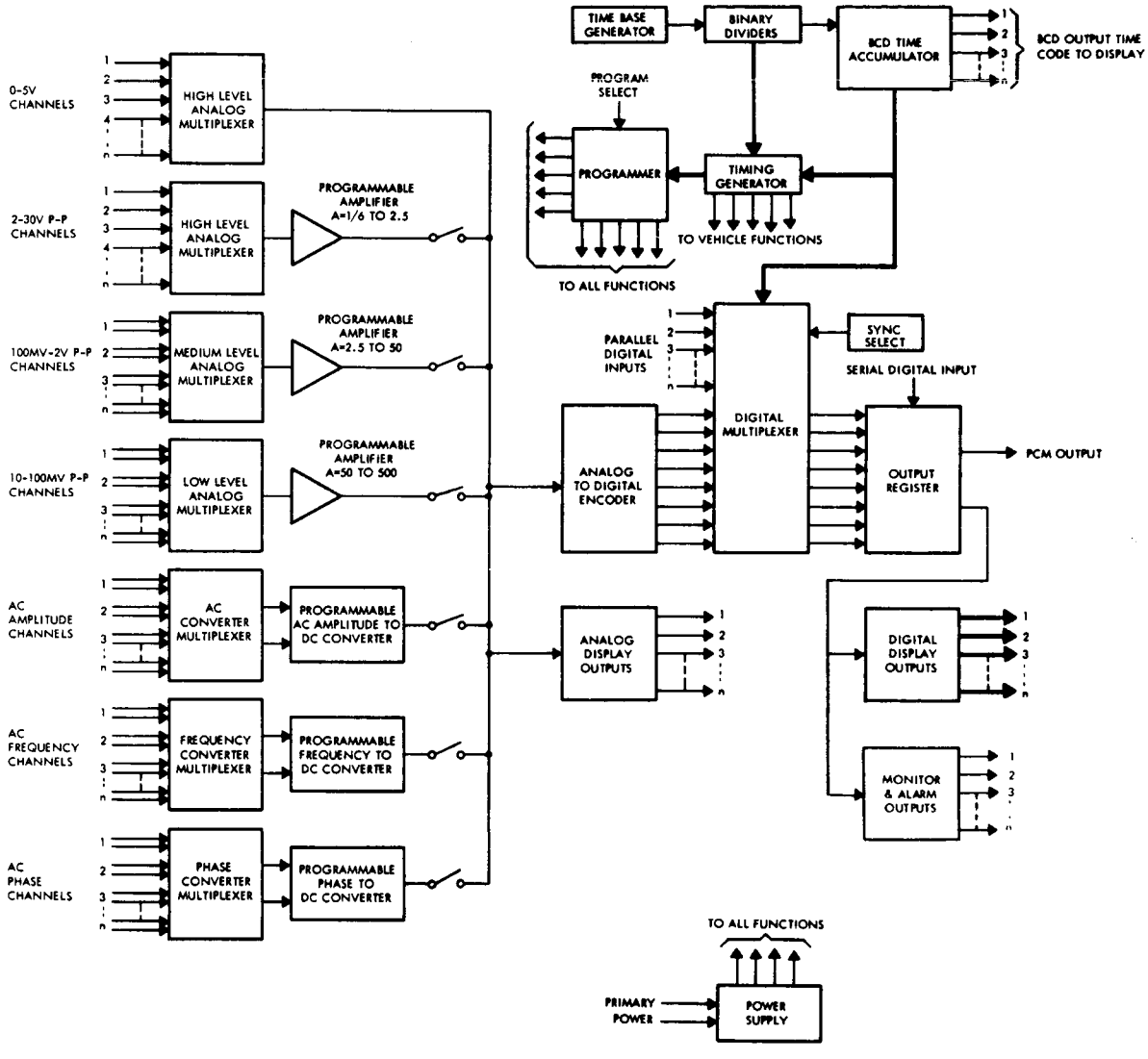

FIGURE 89. INTEGRATED DATA SYSTEM

[redacted]

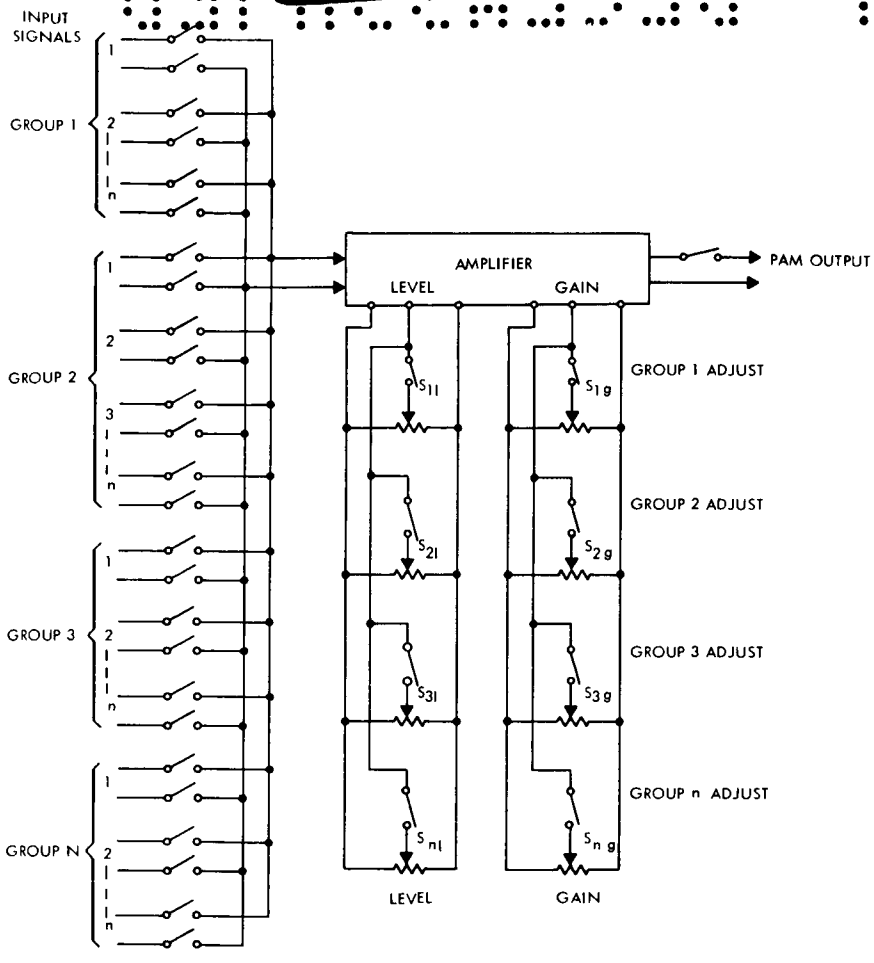

FIGURE 90. PROGRAMMABLE AMPLIFIER

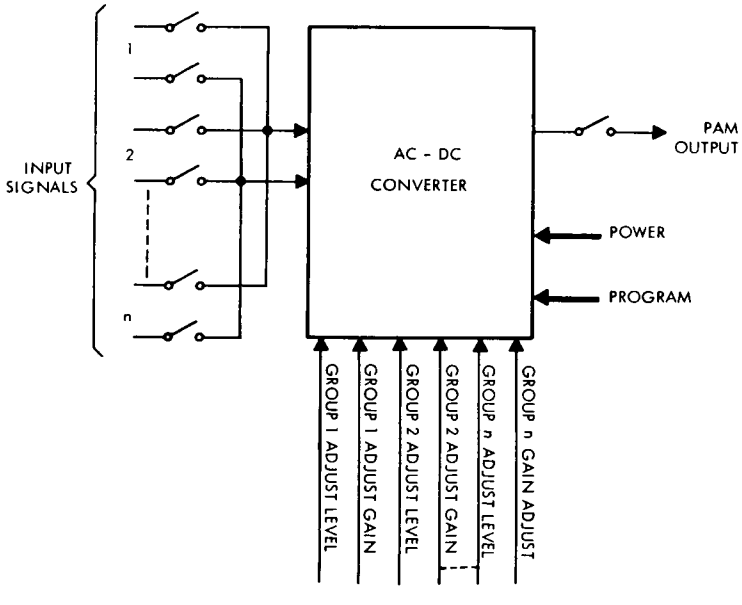

FIGURE 91. AC/DC CONVERTER

[redacted]

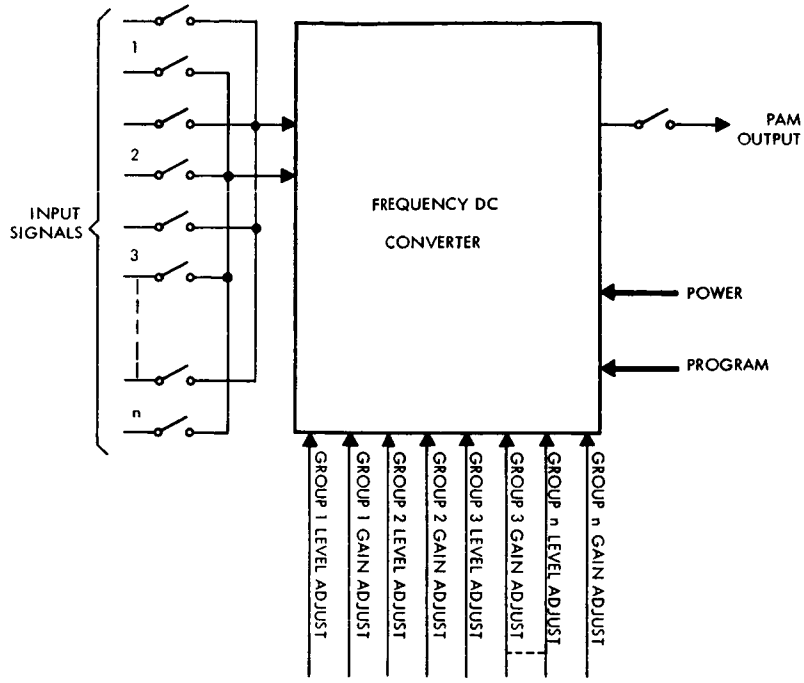

FIGURE 92. FREQUENCY/DC CONVERTER

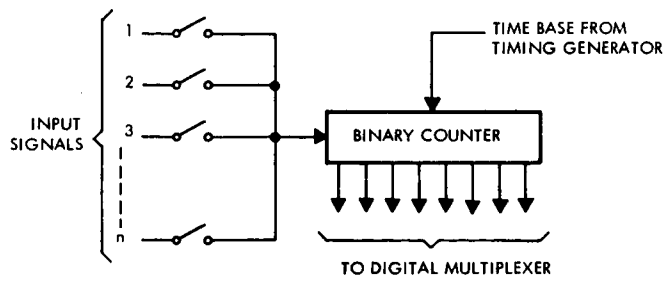

FIGURE 93. DIGITAL FREQUENCY COUNTER

Parallel digital signals are multiplexed together with the parallel outputs from the analog-to-digital encoder, the time accumulator, and the synchronization data and converted to serial NRZ (non-return to zero) form by the output register. The output register also inserts any serial digital data into the output signal.

The system time base is generated by an accurate crystal-controlled oscillator and divided to required output frequencies and finally into a second-minute-hour-day code. For convenience, this code may be in BCD (binary coded decimal) form. These timing data are combined through logic in the timing generator to provide vehicle timing functions and programming functions for the data system. The programmer utilizes these signals through further logic to provide control pulses for the entire integrated data system.

Output signals that are required for displays may be handled either by analog or digitally. The degree of isolation required by various displays can be provided through a floating power supply for each display group.

The analog display signals are generated from the normalized 0- to 5-volt PAM pulse train (fig. 95). The signals to be displayed are programmed, by time sequence, by the programmer so that each required PAM pulse is sampled by the closing of the correct switch during the particular pulse time. A buffer amplifier is inserted between the PAM signal collection point and the switches to prevent loading of the PAM and to provide a fast charging rate on the capacitor. A buffer is placed between each capacitor and the output to provide minimum loading on the capacitor and a low output impedance for displays.

Signals that are not desired to be transmitted in the PCM output train may be sampled during digital word times.

Outputs to digital displays are generated by time-selecting the particular data through programming and switching these data into the desired storage register (fig. 96). The outputs are continuously available for display or other output requirements. They may be provided in BCD form through the addition of a binary-to-BCD converter.

This method is particularly attractive as a means of providing malfunction warning. A digital code recognition unit may be added for each desired output, to recognize when preselected out-of-ordinary levels are reached, and a warning output provided.

Desired channels may be monitored to determine that they fall within preselected limits utilizing the subsystem shown in figure 97. Each channel to be monitored is digitally compared with preselected digital levels to determine that it is within a preselected range. In the event the channel is not within this range, an output is fed through a multiplexer to a bistable for outputs to a display (to show the discrepant channel) and to a second bistable to an alarm to warn the operator that an out-of-tolerance condition exists and the display should be checked.

A reset line is provided that may be triggered manually or periodically through the timing system.

The integrated data system approach can provide a degree of flexibility that is difficult to reach with conventional data systems. The programmer can include the desired amount of flexibility so that the required number of channels of each type are sampled

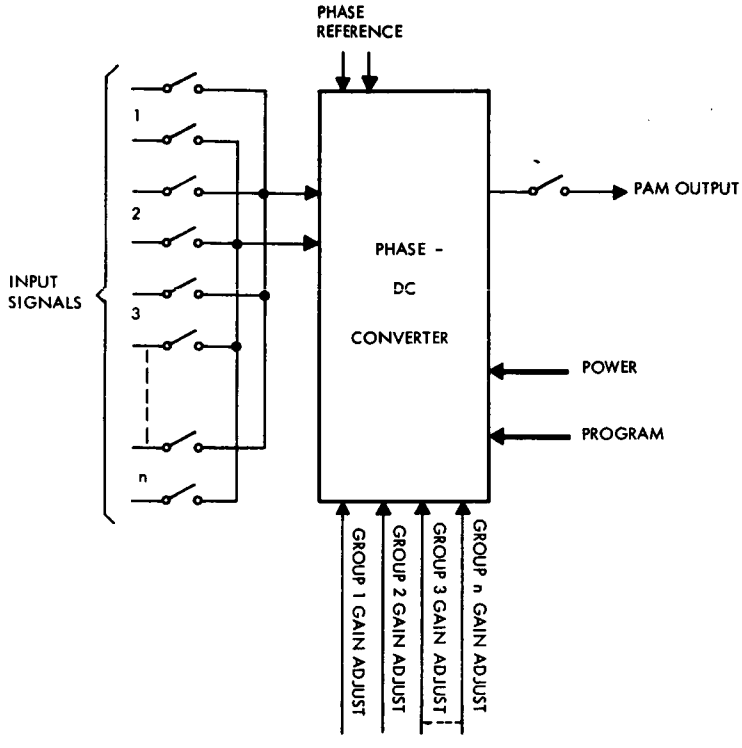

FIGURE 94. PHASE/DC CONVERTER

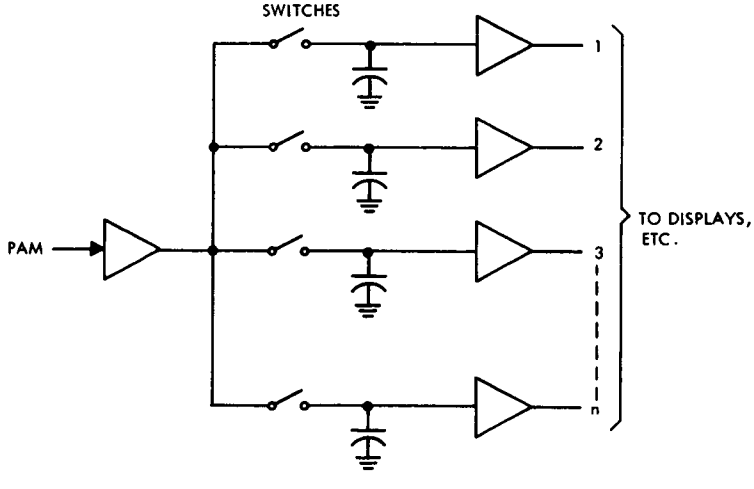

FIGURE 95. ANALOG OUTPUT BUFFERS

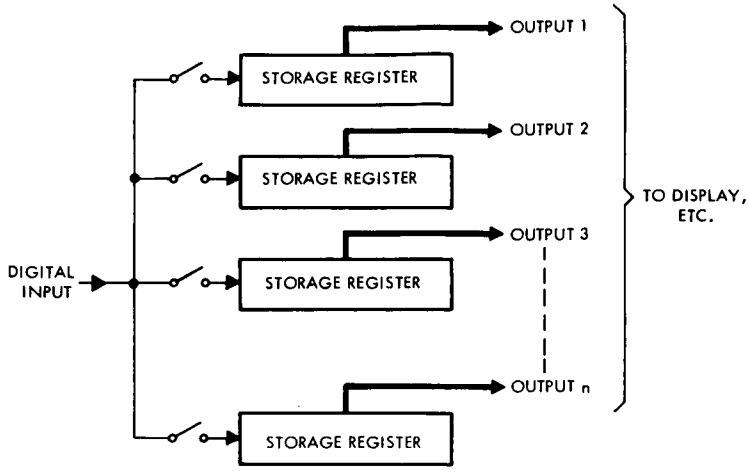

FIGURE 96. DIGITAL DISPLAY OUTPUTS

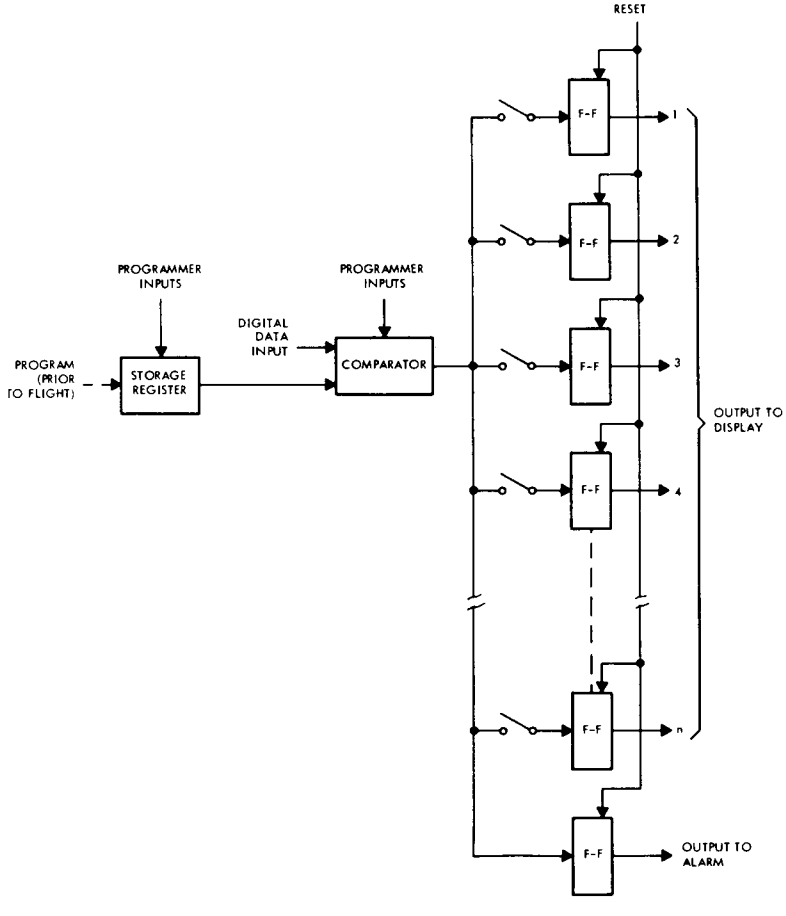

FIGURE 97. MONITOR AND ALARM SUBSYSTEM

at the required rate. The outputs selected for display or monitored alarm may also be selected so that they may be displayed on either analog or digital devices.

3. Lockheed Missiles and Space Company Recommendations

A Stored Program Telemetry System was developed by Lockheed in 1964 for application to space missions in which a high degree of data handling flexibility was required. In this system, the various data points are addressed in a random fashion under the control of a program-controlled memory. The number of channels that can be handled can be expanded by the addition of modules in blocks of 16 channels. Submultiplexers may be remotely located, and the control memory may be sized as required to control the number of channels employed.

Size and weight figures are based on the use of the modular hardware system which has been developed and the 1000 data point requirement. Several assumptions are made with respect to the mix of low-level and high-level channels because the mix affects the number of modules required. The basic multiplexing module provides either 16 differential-input low-level gates or 32 high-level single-ended gates. It is apparent that the weight and volume of the multiplexer portion of the system can vary by a factor of nearly two to one, depending on the predominance of high-level or low-level inputs.

For the purpose of the following size and weight computations, the system is assumed to consist of 750 high-level inputs and 250 low-level inputs. It is also assumed that remote multiplexing is desired and that the smaller of two modular boxes would be used to contain the multiplexing gates. The 1000-channel requirement can be met in six of the small multiplexing boxes, which have a total volume of 480 cubic inches (7880 cc) and weigh approximately 20 pounds (9.04 kg). The memory and encoder central unit occupies approximately 420 cubic inches (6880 cc) and weighs 18 pounds (8.15 kg).

Lockheed indicates that continuing development is in process which will result in substantial savings in size and weight for these functions. The foregoing descriptions are for currently available hardware, but at the time of implementation of the HL-10 program, it is expected that substantial reductions in size and weight would be possible. As a reference point, one current Lockheed project involves a microminiature multiplexer which will provide 64 single-ended channels or 32 differential channels in a volume of approximately 10 cubic inches (164 cc). In the larger system of the size envisioned for HL-10 research vehicle, it is anticipated that the volume and weight can be reduced by a factor of three or four.

Meaningful numbers are difficult to provide because power requirements are dependent on the degree of flexibility required in the format, which in turn affects the memory size. The developed modular system does include high efficiency power converter modules which operate from an unregulated 28-volt source, and they can be employed as necessary to supply the internal power required.

4. Space Craft, Inc. Recommendations

The approach recommended by Space Craft, Inc., is based on their work on the PCM equipment for the Titan III launch vehicles. Space Craft is an associate contractor to the Air Force in supplying the entire PCM telemetry for all versions of the Titan III

launch vehicles. The end product is a stored program, multichannel, highly flexible data handling system.

To implement the instrumentation and data handling system for HL-10, using the Space Craft equipment, up to two of the control units will have to be used together with the interface circuitry that may be required. This system will consist of up to 32 remote multiplexer units and four central converter units. Each remote multiplex unit contains 32 low level, differential, 0- to 40-millivolt channels. The converter controls the remote multiplex unit channels by a single digital instruction cable. A completely flexible stored program magnetic memory is employed in the converter. Channel sampling rates are controlled by the program memory. Storage for three completely different channel sampling formats is provided. Sampling rates and bit rates are changeable in flight.

Analog signals are encoded into an eight-bit binary word at either of two rates: 384 000 and 38 400 bits per second. Channel sample rates may vary from 5 to 12 000 samples per second, with data cycles adjustable from 960 to 2400 words. The system also accepts vehicle guidance computer data and up to 160 bilevel type signals.

The transmission output PCM signal is in filtered NRZ form. A landline driver output is also provided. Remote multiplex units may be located up to 140 feet (42.6 m) from the converter. Total interconnection branch cable length may be up to 500 feet (150.3 m).

The remote and converter units weigh approximately 1.5 pounds (0.68 kg) and 10 pounds (4.54 kg), respectively. Total power dissipation for the complete 1024-channel system is 56 watts.

5. TRW Systems Recommendations

The proposed data handling subsystem is based on the space-ground link subsystem. This subsystem is designed to work with the Air Force Space Systems Division satellite control facility. It is generally compatible with the NASA unified S-band subsystem.

The space-ground link subsystem handles analog data with four or eight bit quantization and digital data in any increment of four bits. The output is a serial NRZ pulse train.

The present frame length maximum is 1024 bits, with a growth potential to 2048 bits. When based on an eight-bit word, it provides a 128-word main frame, with growth to 256 words. Subcommutation can add from 16 to 1024 eight-bit words in increments of 16.

Available bit rates vary from 7.8125 bits per second to 1.024 millibits per second in 17 incremental steps. In the present space-ground link subsystem configuration, either of any two of these bit rates may be selected in flight, with the initial selection of the bit rate being made at the time of subsystem integration.

The frame synchronization word may be up to four data words, utilizing a pseudorandom code. Thus, no word synchronization words are required. The minor frame identification word is eight bits in length to properly identify the words in the 128-word subcommutations. The basic system does not include the capability for storage of a

number of telemetry formats. This requirement can be satisfied by the use of techniques developed in the spacecraft digital data processor, conceptually designed for the NASA-Manned Spacecraft Center under contract.

The spacecraft digital data processor is a general purpose multiplexer. The system is centralized in that all inputs are received and processed in one location.

Flexibility in the selection of data for processing is provided by an internal hardwired programmer, a programmable format generator, and an external computer. This flexibility makes the processor adaptable to a wide range of vehicles and missions as well as adaptable to changing requirements during missions. The one-time development and qualification costs (time and money) of the spacecraft digital data processor yields an attractive cost per mission or spacecraft.

The design features the use of a TRW proprietary technique for selecting and processing analog inputs. This concept utilizes a separate comparator for each analog input. The inputs are selected by gating on the associated comparator. Several advantages over conventional multiplexing techniques are offered.

The spacecraft digital data processor is comprised of a data acquisition unit and a flexible format generator. Salient features of the spacecraft digital data processor are:

(1) Operates in a flexible format mode in which the data acquisition unit input data are sampled in a sequence determined by data addresses stored in a core memory (in the flexible format generator). One or more word times in each telemetry frame can be assigned in this mode to allow an external computer to address the data acquisition unit and obtain output data.

(2) Operates in a fixed format mode when the sampling sequence is predetermined. While in this mode, the flexible format generator memory can be reprogrammed to alter the flexible format.

(3) Operates in a computer slave mode during which an external computer addresses the data acquisition unit to obtain data relating to any data input.

(4) Responds to onboard and ground commands to select bit rate and operating mode and to reprogram the memory.

(5) Employs a 1024-cell random access core memory with 14 bits per cell for establishing the flexible format.

(6) Utilizes the gated comparator technique in the selection and processing of analog inputs.

(7) Minimizes power consumption by power gating.

The two primary tasks performed on the spacecraft digital data processor are to:

(1) Provide the detailed paper design of a spacecraft digital data processor.

(2) Develop and fabricate special purpose integrated circuits for the system.

The weight of the present space-ground link subsystem digital telemetry unit is 6.7 pounds (3.04 kg), and the spacecraft digital data processor is estimated to be 18 pounds (8.15 kg) in its present configuration. A unit which combines the two capabilities would probably approximate the weight of the latter.

The size of the space-ground link subsystem digital telemetry unit is approximately 250 cubic inches (4100 cc); but, again, the hybrid unit would approximate the size of the spacecraft digital data processor or 655 cubic inches (10 750 cc).

Power requirements would vary between 4 and 10 watts, depending on the operating mode of the spacecraft digital data processor.

The MTBF of the space-ground link subsystem digital telemetry unit is 36 000 hours for 1100 channels. The reliability of the spacecraft digital data processor has not been examined as yet. However, there were no critical parts with low reliability identified in the conceptual design.

K. ELECTRICAL POWER

The electrical power subsystem design is based on three men operating the D/3 vehicle for up to five orbits. The electrical power system for the D/3 vehicle is composed of two separate equipment sets: the basic power supply and the flight control power supply.

1. Basic Electrical Power Supply

The load chart (table 40) shows the basic power required for all mission phases: standby, launch, orbit and entry. It does not include entry control actuation. The entry time plus 4 hours includes ground checkout time from the vehicle power supply before launch as well as time for equipment operation during orbit for test or check (such as updating the guidance equipment from ground stations). The standby condition is included as an average power integrated over an hour for all the equipment which operates on an intermittent basis during orbit. For example, the C-band beacon operates for 24 minutes per orbit at 35 watts and the balance of the time at 20 watts, for a

TABLE 40

LOAD CHART FOR D/3 VEHICLE FOR FIVE ORBITS

	Power requirement conditions, watts	
	Entry + 4 hours	Standby
Environmental control (3 men)	175	175
Guidance and control	810	300
Total	1682	760

continuous standby rating of 24 watts. The total maximum transient peak demand is well within the capability of the battery system so that voltage regulation and capacity are not adversely affected.

The D/3 electrical power system is composed of six Yardney LR-100 batteries. Two are located in the entry vehicle and four are in the adapter section. Separating the batteries in this manner results in an entry vehicle of minimum weight and volume. The batteries used for ascent and orbit power are stored in the adapter section. There are disadvantages to this practice, however. The first disadvantage is increased cost, since the batteries in the adapter section are lost and cannot be reused. Another disadvantage is the adverse effect upon the reserve of the two batteries in the entry vehicle when four batteries which have capacity remaining are thrown away. Therefore, to ensure two fully charged batteries before entry, the electrical system is manually supervised to use as much as possible of the power in the adapter section before transferring to the entry vehicle batteries.

The system can be monitored at all times from instrumentation on the flight engineer's panel. If a battery fails in the adapter section, the engineer has a choice of continuing the flight or preparing to deorbit, depending on the mission and time-to-go in orbit and the remaining battery conditions. Normal procedure on the launch pad is to close relay 1 and power all systems from the adapter batteries (fig. 98). If relay 2 is inadvertently closed, a red indicator light advises the engineer, and corrective action can be taken.

Approximately an hour before entry, the load is transferred from the adapter batteries to the entry vehicle batteries. Quick changeover is not required because the protective diodes in the adapter battery circuit will not permit charging from the entry batteries. Simultaneously, a reduction of load will increase the voltage of the adapter batteries, thereby allowing some of the load to be supplied from the adapter batteries. At any time after transfer of the load from the adapter batteries, relay 1 can be open-circuited and the adapter separated. A green signal light on the flight engineer's panel indicates that power has been transferred to the entry batteries and relay 1 is open, ready for staging of the adapter module.

The separation of the batteries makes 100 percent power reserve necessary for the entry vehicle. The adapter battery reserve is held to less than one module, since the batteries are lost and safety of return is not jeopardized by a single battery failure.

2. Flight Control Power Supply

The basic D/3 flight control system has been discussed in a previous subsection. Figure 99 is a block diagram of the electrical power system for flight controls and intermittent loads. It shows that the reaction controls, squib circuits, and other intermittent loads are assigned the flight control bus. Since these loads are large, intermittent and of short duration, they are applied to this bus to minimize radio interference from conducted noise with the other electronic systems. The large capacity of the bus makes it ideal for squib circuits with minimum disturbance on other equipment on the bus.

The capacity of the batteries for the flight control system is shown for two conditions in figure 100. The six-battery system capacity is computed on the basis that a battery fails on the launch pad at launch. A battery failure at any other time would be

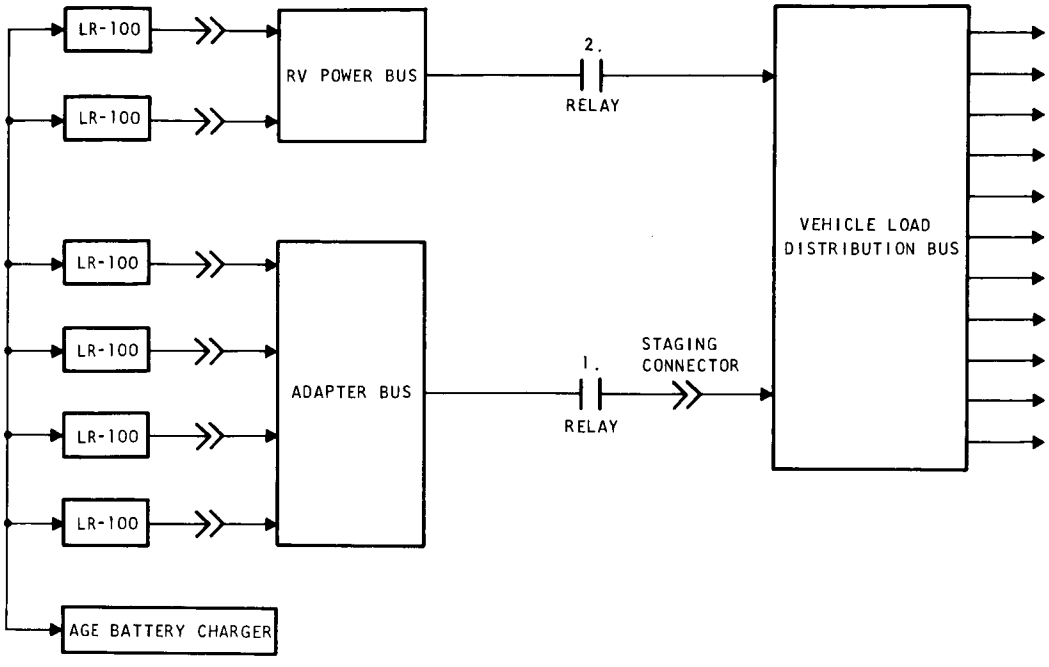

FIGURE 98. PRIMARY ELECTRICAL POWER

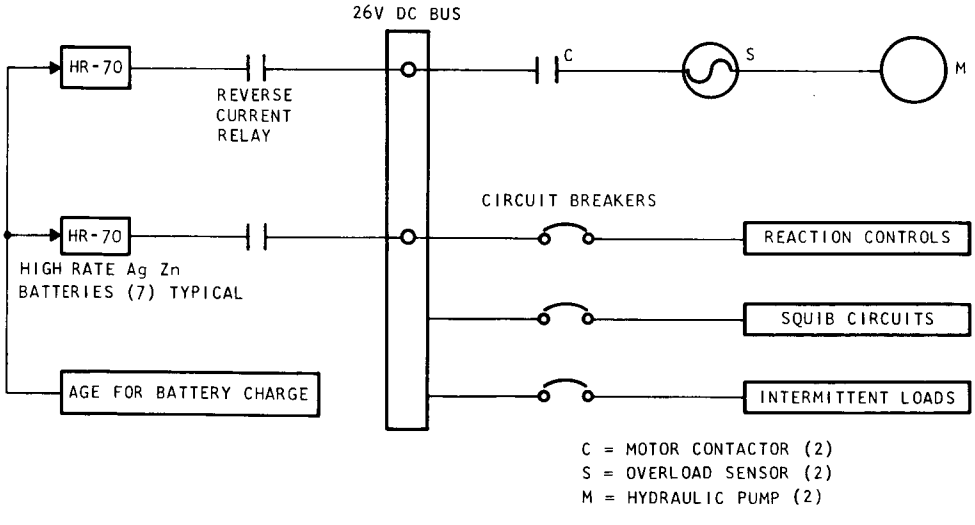

FIGURE 99. ELECTRICAL SYSTEM--FLIGHT CONTROLS AND INTERMITTENT LOADS

less significant. Based on computations defined in Part IV, the flight control power for the D/3 vehicle for the maximum duration flight is:

Mission phase	Current, amperes	Time, minutes	Discharge, ampere-minutes
Launch	298	15	4 490
Entry	356	40	14 240
Landing	465	10	4 650

$$\text{Average discharge} = \frac{23\ 380}{65} = 358\ \text{A}$$

$$\text{Percent of 7-battery system used} = \frac{65}{95} = 68.5 \text{ (from fig. 100, 358 A = 95 min)}$$

$$\text{Percent of 6-battery system used} = \frac{65}{80} = 81.2 \text{ (from fig. 100, 358 A = 80 min).}$$

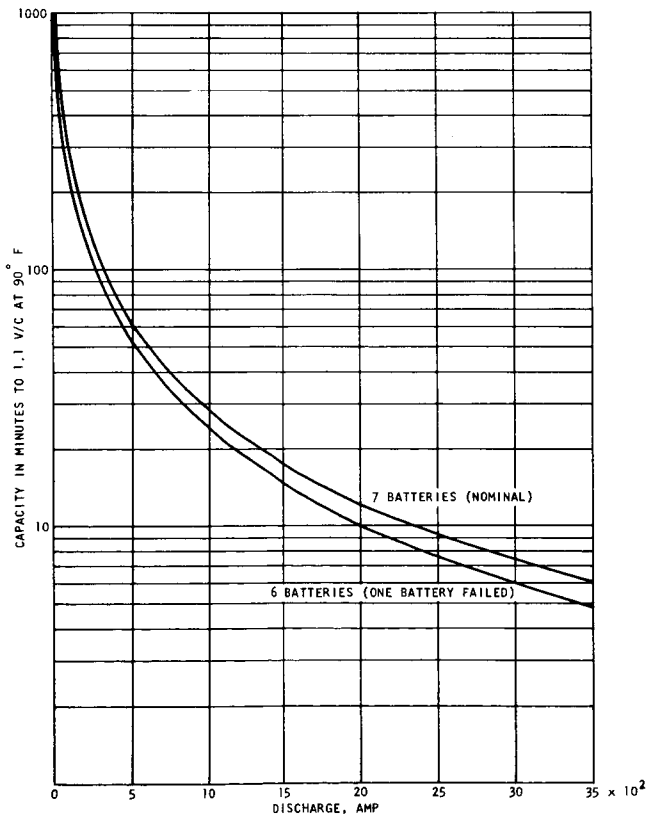

FIGURE 100. FLIGHT CONTROL POWER SUPPLY

Assuming a 10 percent derating of battery due to stand time and other variables between batteries:

$$\text{Percent of 7-battery system used} = \frac{65}{86.5} = 75$$

$$\text{Percent of 6-battery system used} = \frac{65}{72} = 90.$$

The batteries for the flight control subsystem are designed to provide power for two independent hydraulic systems, both of which are powered continuously. However, either one is sufficient to complete entry subsequent to any orbital mission of three-fourths orbit or more. For the maximum-load entry situation, which requires the use of both hydraulic systems following an ascent phase abort, the longest entry duration still results in good battery margin with one battery out. Consequently, any additional battery reserve is not recommended.

3. Subsystem Weight Summary

A total subsystem weight breakdown for the D/3 vehicle is presented in table 41. All weights are actual except the miscellaneous wire, circuit breakers, and switches, which are estimated on the basis of previous hardware programs.

TABLE 41

WEIGHT SUMMARY OF ELECTRICAL POWER SYSTEM

	Weight	
	lb	kg
Flight Control Power System		
Batteries (7)	434	197
Reverse current relays (7)	21	9.55
Motor contactors (2)	8	3.65
Miscellaneous, wire, etc.	63	28.7
	526	238.90
Basic Electrical Power System		
Batteries in entry vehicle (2)	124	56.5
Miscellaneous, wire, etc.	230	104
	354	160.6
Batteries in adapter (4)	248	113.0
Total	1128	512.4

L. ENVIRONMENTAL CONTROL AND LIFE SUPPORT

This section presents the environmental control and life support (EC/LS) system recommended for the D/3 research vehicle. The selected EC/LS system is based on current state-of-the-art concepts being utilized in the Gemini and Apollo programs. The crew is provided with a 100 percent oxygen atmosphere (5 psia, 34.4 kN/m^2) with carbon dioxide and odors removed by lithium hydroxide and activated charcoal.

The system is designed so that the crew may operate with face plate closed or open and with the space suit removed. The entire system is contained within the entry vehicle (i.e., no EC/LS equipment in the expendable adapter section). This approach was taken so that the total system is reusable except for the expendables (oxygen, water, lithium hydroxide and activated charcoal).

Design criteria for the EC/LS system are presented in table 42, and the selected system is based on tradeoffs discussed in Part IV.

The EC/LS system consists of four parts: (1) atmospheric control loop; (2) oxygen supply loop; (3) water management loop, and (4) thermal control loop. The atmospheric control subsystem controls the temperature, humidity, and pressure of the crew space suit and the vehicle cabin. The oxygen supply subsystem provides oxygen, on demand, to the crew suit loop and cabin and the pressurization gas for the water storage tanks. The water management subsystem provides drinking water for the crew and water, on demand, to the evaporative heat exchangers. The thermal control subsystem controls the temperature of the electronics and provides the heat sink required for the atmospheric control system. A schematic of the complete EC/LS system is shown in figure 101.

The atmospheric control subsystem consists of redundant suit compressors, each of which can deliver the required flow of 40 cfm (0.019 mm^3/sec), to circulate the oxygen in the suit loop. Lithium hydroxide and activated charcoal canisters remove the carbon dioxide and odors generated by the crew. Redundant canisters are provided, and each can remove the total quantity of carbon dioxide and odors generated. The crew heat exchanger controls the humidity, removes metabolic water from the suit loop, and controls the temperature of the oxygen in the suit loop. The crew temperature is controlled by adjusting the coolant flow in the heat exchanger. A debris trap is located down stream of the crew to remove particle contaminants from the suit loop.

Oxygen flows to the suit loop through redundant suit-demand regulators. These pressure regulators maintain the suit pressure between 2.5 to 3.5 inches of water (622 to 872 N/M^2) below the cabin pressure when the cabin pressure is 3.5 psia (23.8 kN/m^2) or above. The dual cabin pressure regulator maintains the cabin pressure at 5.0 psia (34.4 kN/m^2). In the event of cabin depressurization, the cabin pressure regulator closes when the cabin pressure decreases to 4.0 psia (27.6 kN/m^2), thus preventing excessive loss of oxygen. When the cabin is depressurized, the suit pressure regulator maintains the suit circuit at 3.5 psia (23.8 kN/m^2).

TABLE 42

EC/LS DESIGN CRITERIA

CONDITIONS

Prelaunch--Oxygen system capability for 4 hours of supply during a pad hold. Ground support available while vehicle is on pad.

Launch--Design for a maximum launch phase of 10 minutes. Cooling by thermal lag assumed below 100 000 feet (30.5 km).

Space--Design for 5-orbit system capability.

Entry--3080 seconds to 100 000 feet (30.5 km); 600 seconds from 100 000 feet to touchdown.

Post-landing--Oxygen supply and cooling for 15 minutes system operation after the vehicle has landed.

VEHICLE

Atmosphere--5 psia (34.4 kN/m^2), 100% oxygen normal, pressure suit face plate open; 3.5 psia (23.8 kN/m^2), 100% oxygen for emergency. Purge to 100% oxygen atmosphere prior to launch.

Repressurization--One cycle (normal), two cycles if extravehicular activity is planned.

Temperature--Suit 50° F (283° K) at inlet, 85° F (303° K) at outlet. Cabin 60° F (289° K) to 80° F (300° K), wall above 65° F (291° K) dew point during orbit.

Leakage--Cabin O_2 at 5 psia (34.4 kN/m^2), 6.1 lb (2.77 kg)/day.

CO_2 level--8 mm Hg maximum.

Humidity--30 to 70%.

METABOLIC

Heat load--Three crew members at 600 Btu/hr (176 kW). Sensible load 1/3, latent load 2/3 for pressure suit operation.

Oxygen consumption--Normal 2 lb (0.907 kg)/day/man. Entry above 100 000 feet (30.5 km), and post-landing 0.1 lb (0.0453 kg)/man/min.

Water consumption--4.6 lb (2.09 kg)/day/man.

Food consumption--1.4 lb (0.635 kg)/day/man.

CO_2 production--2.25 lb (1.02 kg)/day/man.

Urine--3.0 lb (1.36 kg)/day/man.

HEAT LOADS

Entry cooling for the hydraulic system to 125° F (325° K) above 100 000 feet (30.5 km) and 275° F (408° K) below 100 000 feet (30.5 km).

Heat rejection from the vehicle by means of boiling water in an evaporative heat exchanger.

Heat loads by mission phase, watt-hours

	Ascent and Orbit	Entry	Total
Metabolic	176	*	1 320
Electronics orbit	1134	--	6 250
2 hours prior to entry	3600	1 800	5 400
Hydraulic system	--	10 150	10 150
Entry heating	--	5 870	5 870
Total			28 990 (99 000 Btu)

* Metabolic heat is removed by high-flow O_2 during entry.

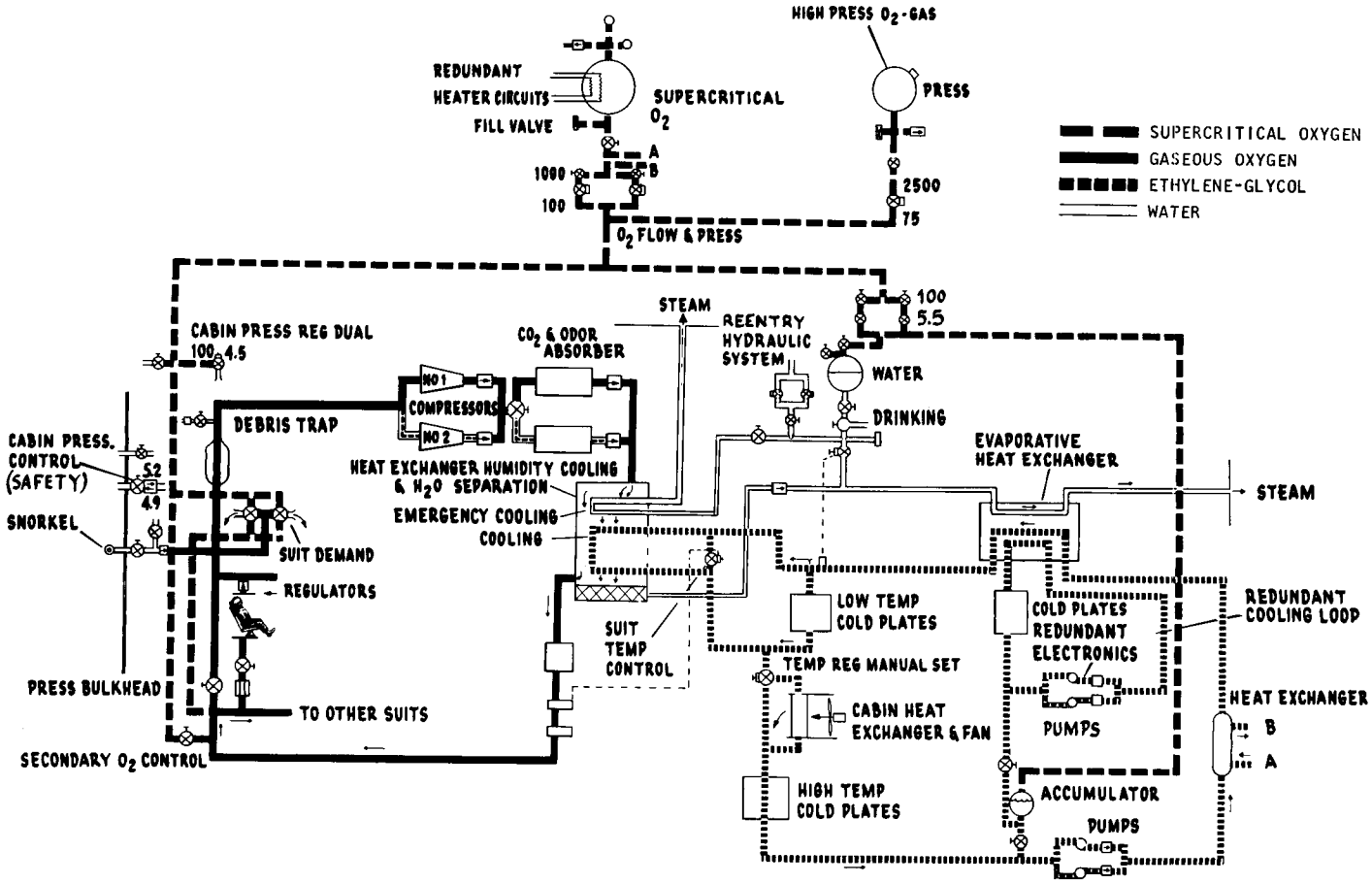

FIGURE 101. EC/LS SYSTEM

To depressurize the cabin, the manual cabin out-flow valve is opened; and to repressurize the cabin, a manual repressurization valve is provided. The cabin pressure control valve controls the differential pressure between the cabin and ambient. During ascent, the cabin pressure is relieved from the spacecraft until the pressure decreases to 5.5 psia (37.8 kN/m^2). During entry, the valve admits ambient air into the cabin, limiting the pressure differential to 20 inches of water (4.98 kN/m^2).

During entry, the secondary oxygen control is open and the compressors de-energized. The secondary oxygen control provides a flow of 0.1 pounds (0.045 kg) per minute per crewman, which satisfies both metabolic and cooling requirements during entry. During the post-landing period, the suit compressors provide ventilation as long as electrical power is available (24 hours, assuming a 50 percent duty cycle). The compressors draw ambient air into the suit circuit through the cabin in-flow valve. In the event of a water landing, a snorkel valve located on the cabin in-flow valve prevents water from entering the suit circuit.

Cabin oxygen is circulated by a fan. The temperature of the cabin atmosphere is controlled by the glycol-water flow through the cabin heat exchanger, and the temperature is manually regulated by the crew. When the crew is operating with face plates open, the cabin air circulating valve is manually adjusted to provide recirculation of the cabin oxygen through the suit circuit, thus removing carbon dioxide, odors, and moisture from the cabin atmosphere.

The oxygen supply system consists of a primary and secondary supply. The primary supply is a supercritical storage system sized for the prelaunch, ascent, and orbit phase of the mission. Redundant heaters and vent valves are incorporated to increase the reliability of the system. Redundant pressure regulators reduce the supply pressure to 110 psia (758 kN/m^2). Oxygen flows from the regulator to the dual cabin pressure regulator and to the suit circuit demand regulator.

The secondary oxygen supply is a high pressure (2500 psia, 17.2 MN/m^2) gaseous storage system. This system is sized for one orbit plus the entry period with the specified flow rate. The secondary oxygen pressure regulator reduces the supply pressure to 75 psia (512 kN/m^2). The primary oxygen pressure (110 psia, 758 kN/m^2), being greater than the secondary, retains the secondary oxygen in reserve.

The water management system supplies water for crew drinking, crew cooling (expendable heat sink), electronics cooling and hydraulic system cooling during entry. The water is stored in a positive expulsion pressure tank, with oxygen acting as the pressurant. The oxygen pressure is reduced to 10 psia (68.9 kN/m^2) through redundant pressure regulators. During orbit operations, the water is supplied, on demand, to the thermal control heat exchanger where, by boiling, it extracts heat from the glycol-water thermal control loop. The steam produced in the heat exchanger is vented overboard. If the water-glycol loop fails, a manual valve is provided to allow water to be introduced to the suit circuit heat exchanger for emergency crew cooling. The water extracted from the suit circuit by the water separator flows to the water side of the thermal control heat exchanger.

The thermal control subsystem provides temperature control for the crew and the electronics. This system consists of a water-glycol fluid loop and redundant pumps

to circulate the fluid. The water-glycol solution is used to reduce the freezing point of the solution to -40° F (233° K). The heat sources in the system are the crew heat exchanger, the cabin heat exchanger, and the electronics cold plates. The heat sinks are the thermal control heat exchanger and the oxygen supply heat exchanger. The water-glycol loop serves as a heat transfer medium between the heat sources and sinks. The major portion of the heat is dumped in the thermal control heat exchanger. During prelaunch, the ground heat exchanger controls the temperature of the water-glycol loop.

The description of the components making up the EC/LS system is presented in table 43. All components in the system, with the exception of the oxygen and water tanks, are existing qualified hardware. Table 43 also presents the weight of the EC/LS system. The dry weight is 316.9 pounds (143.5 kg), and the wet weight (dry weight plus expendables) is 473.6 pounds (214 kg).

M. MALFUNCTION DETECTION AND ALARM SUBSYSTEM

The detection of malfunctions and possible failures, plus pilot alarm or automatic correction, must be accomplished to assure crew safety and a high probability of mission success. However, the generation of pertinent subsystem functional requirements, in sufficient detail to prepare hardware design specifications, requires failure mode analyses of each subsystem. These analyses should be based on failure modes and the specific redundancies provided in each subsystem. Even though the preliminary design of the recommended D/3 vehicle details the proposed subsystem redundancies, additional reliability and redundancy optimization studies (beyond the scope of this study) are needed before it is possible to undertake the necessary failure mode analyses.

1. Recommended Approach

Recommended subsystem equipment provisions have been assumed for the D/3 vehicle configuration design. They are based on current program techniques (e.g., Titan IIIM, Gemini B, Apollo), plus limited tradeoff studies. The latter include lifting body characteristics and the related criteria for malfunction detection during critical phases of entry.

In accordance with the recommended usage of redundant equipments and/or backup modes for each potentially critical subsystem in the D/3 vehicle configuration, the additional hardware included for malfunction detection and alarm consists primarily of status sensors, programmed comparators, pilot display, and controls for initiating corrective action. For example, automatic switchover to a second of three parallel autopilot channels is accomplished within the flight control system itself, because the pilot's response time (for detection and correction) appears marginal during certain phases of entry. Conversely, where three channels are not available for mid-value type voting (e.g., the dual inertial reference units and computers), self-checking or comparative status computations are necessary. They can be accomplished within the primary guidance computer, which has adequate capability; however, a separate, small, but highly reliable computer may prove superior.

TABLE 43

EC/LS SYSTEM COMPONENTS

Schematic item no.	Component name	Unit weight lb	Unit weight kg	Number required	Status
1	Suit compressor	5.15	2.34	2	Apollo
2	CO_2 absorber package	18.0	8.16	1	Apollo
3	Cooler-condenser separator package	30.0	13.6	1	Apollo
4	Suit hose connector	1.3	0.590	3	Apollo
5	Suit flow limiter	0.4	0.181	3	Apollo
6	Suit demand regulators	1.0	0.454	1	Apollo
7	Debris trap	1.6	0.726	1	Apollo
8	Suit bypass control valve	0.6	0.272	1	Apollo
9	Secondary O_2 control valve	0.3	0.136	1	Apollo
10	Suit circuit return air valve	1.6	0.726	1	Apollo
11	Cabin pressure regulator	0.5	0.227	1	Apollo
12	Cabin O_2 flood flow control valve	0.3	0.136	1	Apollo
13	Snorkel valve	1.12	0.508	1	Gemini
14	Cabin pressure relief valve	4.8	2.18	1	Apollo
15	Suit temperature control valve	1.4	0.635	1	Apollo
16	Cabin temperature control valve	1.0	0.454	1	Similar to X-20 unit
17	Cabin heat exchanger and fan	7.8	3.54	1	Apollo
18	Water shut-off valve	0.3	0.136	2	Apollo
19	Water check valve	0.2	0.091	1	Apollo
20	Water flow control valve	0.2	0.091	1	Apollo
21	Water shut-off valve	0.3	0.136	1	Apollo
22	Water shut-off valve	0.3	0.136	1	Apollo
23	Glycol-H_2O pumps redundant cooling loop	8.6	3.90	1	Apollo
24	Glycol-H_2O pumps	8.6	3.90	1	Apollo
25	Coolant shut-off valve	0.3	0.136	1	Apollo
26	Coolant shut-off valve	0.3	0.136	1	Apollo
27	O_2 to coolant heat exchanger	0.6	0.272	1	Gemini
28	Ground cooling heat exchanger	2.19	0.993	1	Gemini
29	O_2 low pressure regulator	0.4	0.181	2	Apollo
30	O_2 shut-off valve	0.2	0.091	4	Apollo
31	O_2 high pressure regulator	1.0	0.454	2	Apollo
32	O_2 shut-off valve	0.3	0.136	2	Gemini
33	O_2 shut-off valve	0.3	0.136	1	Gemini
34	Secondary O_2 pressure regulator	0.5	0.227	1	Mercury
35	Secondary O_2 shut-off valve	0.5	0.227	1	Mercury
36	Supercritical O_2 tank assembly	16.6	7.53	1	
37	Secondary O_2 tank assembly	37.6	17.1	1	
38	Water storage tank assembly	17.6	7.98	1	
39	Evaporation heat exchanger	21.96	9.96	1	Gemini
40	Instrumentation sensors	10.8	4.90		
41	Inverters (fan and blowers)	7.3	3.31		
42	Cold plates	40.0	18.1		
43	Ducts, structures, clamps	30.0	13.6		
44	Umbilical, QDs	12.0	5.44		
45	Glycol	10.0	4.54		
	Miscellaneous (for support)	25.0	11.4		
	Total dry weight	341.97	155		
46	Primary O_2	23.8	10.8		
47	Secondary O_2	18.8	8.53		
48	Water	110.0	49.9		
49	Lithium hydroxide	4	1.81		
	Total weight	498.6	226		

The pilot display and control panel, described previously under subsection D, accomplishes the assumed malfunction detection and alarm subsystem functions throughout the mission. These functions are briefly described for the ascent, orbital and entry flight phases in the following paragraphs. Particular emphasis is placed on the ascent phase and the important boost vehicle interface provisions. Pertinent studies conducted for the Titan IIIM, Gemini B are available to serve as a guide,and the largest probability of malfunction requiring corrective action occurs during this period.

2. Ascent Phase

During ascent, launch vehicle performance is monitored to provide high crew safety and mission success probability. In the event of catastrophic failures for which there are no backups (e.g., solid rocket motors, Stage I engines, structure, etc.), an abort need is sensed and the crew is notified to initiate abort procedures.

Navigation and guidance redundancy is obtained during the ascent phase by providing backup navigation, guidance, and discrete signals. A decision-making interface exists between the launch vehicle digital computer (LVDC) and the D/3 primary digital computer (HL-10 DC). Based on functions and status inputs from both computers, it provides the necessary intelligence: (1) to drive crew displays indicating performance during the ascent phase and providing the pilot with sufficient information on which abort or guidance switchover decisions can be based, and (2) to effect an automatic switchover to the HL-10 guidance system if rapid reaction be required.

Like the LVDC, the HL-10 DC contains programs within its software routine that will monitor input performance (e.g., the IMU), output performance (e.g., steering and discrete signals) and internal (computer) performance.

The D/3 malfunction detection subsystem design is based on Martin Marietta's definition of the malfunction detection and crew displays philosophy for the Titan III, Manned Orbiting Laboratory, Gemini B program. In this effort, the following ground rules were adopted:

(1) A minimum of one primary and one confirming indication or method of detection will be provided for detecting any launch vehicle malfunction which affects mission success and requires crew decisions and action. Various combinations of cockpit displays and crew physiological sensing will be used for providing the independent methods of in-flight malfunction detection and verification. Where an indication is driven by redundant logic and sensors, that display will be considered to meet this criteria.

(2) Wherever practical, the number of cockpit displays provided will be such that any single display can malfunction and the requirements of the preceding ground rule will still be satisfied.

(3) The crew displays of any parameter and the criteria governing crew decisions will be kept simple and straightforward to permit rapid analysis and subsequent action by the crew.

(4) Autonomous malfunction detection capability will be provided for launch vehicle failures which affect mission success after handover, i.e., the loss of

ground radar tracking and the loss of real-time telemetry data. From liftoff to handover, autonomous malfunction detection will be provided to the maximum extent practical.

(5) Dependency upon ground displays as a method of malfunction detection will be applicable only in the flight period prior to handover and for slow malfunctions (warning time greater than 10 seconds). Capability will be provided in the Mission Control Center for detecting malfunctions having six seconds or more warning time.

(6) Data received by the crew from the ground SMD (Slow Malfunction Detection) monitors, relative to guidance switchover or abort decisions, will be in the form of a "guidance switchover recommended" light or an "abort recommended" light, respectively. These lights will be energized only as a result of discrete signals initiated by the ground SMD monitors. The only verbal contact with the crew will occur through the (orbiting vehicle) communicator.

(7) At the time of Stage II shutdown, a crew display will be provided to indicate successful injection into an orbit which meets the safe orbit constraints.

The possible malfunctions for the Titan III launch vehicle and end-effect cues that are used to sense the malfunction are summarized in table 44. These malfunctions and cues are based on a detailed analysis of the Titan III/MOL/Gemini B system; however, they are similar to those anticipated for the D/3 HL-10, Titan III combination.

3. Orbital Phase

The philosophy to be followed in orbit is patterned after Gemini. The HL-10 subsystem redundancy and backup modes of operation provide for crew safety and mission success. A monitor system, including an HL-10 display panel and computer programming,will assess system performance through limit comparisons. Ground support complexes will assist in the monitoring function. Continuous evaluation of spacecraft systems will provide the basis for early mission termination or backup mode operation if a malfunction occurs.

4. Entry Phase

Like the ascent and orbital modes, the entry mode utilizes computer programming as part of the monitoring system. Backup guidance is provided by a strapdown attitude reference unit. The flight control subsystem utilizes a three-channel/axis autopilot and tandem hydraulic actuators that will automatically negate the effects of a first failure.

Detailed analyses to define the malfunction detection system during entry were not conducted. This would include in-depth failure mode analyses, similar to those summarized previously for the Titan IIIM ascent phase, before hardware specifications could be prepared.

TABLE 44

SUMMARY ASCENT MALFUNCTION CONDITIONS AND DETECTION CODE

Malfunctions affecting mission success	Malfunction detection codes: Stage 0 flight	Stage I start through 0/I staging (period 08)	Stage I flight	Stage II flight
Structural failure (skirts, trusses, SRM's, TVC tanks)	U	-	-	-
Structural failure (Stage I propellant tanks)	UBPK	UPKL	UPKL	-
Structural failure (Stage II propellant tanks)	UBPK	UPKL	UPKL	UPOK
Command control receiver--inadvertent destruct output	UPKL	UPKL	UPKL	UPKL
SRM destruct charge detonates prematurely	CDM	-	-	-
Loss of vehicle control (Stage 0)				
(a) TVC loss--injectant leak	BMEF	-	-	-
(b) TVC loss--power loop failure	AMY	-	-	-
(c) One injectant valve fail open at T - 0	U	-	-	-
(d) One injectant valve fail open in flight	EF	-	-	-
Loss of vehicle control (Stage I)				
(a) Actuator control failures or hydraulic leaks	-	QMVY	QMVY	-
(b) Yaw/roll actuator null or low gain failures	-	UY	UY	-
(c) Engine loss of control failures	-	QMVY	QMVY	-
Loss of vehicle control (Stage II)				
(a) Hydraulic system leaks (including actuator leaks)	-	-	-	YQMV
(b) Actuator and engine loss of control failures	-	-	-	QMVY
(c) Pitch or yaw actuator null or low gain failures	-	-	-	UY
One SRM fails to ignite	CDM*	-	-	-
Premature thrust termination--one SRM	CDM	-	-	-
SRM burn-through				
(a) Nozzle between aft closure and throat	BDM	-	-	-
(b) Nozzle between throat and exit cone	BME	-	-	-
(c) Nozzle at and below exit cone/extension cone interface	W3	-	-	-
(d) Material or propellant defect, leaks, case rupture	CDM	-	-	-
Premature separation--one SRM				
(a) Structural failure--aft attachments	BUMP	UMP	-	-
(b) Structural failure--forward attachments	.PUPK	PUPK	-	-
(c) Premature operation--forward staging nut squib	-	PULK	-	-
(d) SRM case attachment structural failure	A	-	-	-
No start--Stage I, one or both subassemblies	-	NKL	-	-
Premature Stage 0/I staging	-	U	-	-
Pressure decay--Stage I oxidizer tank	PPW	PPNW	PPNW	-
Pressure decay--Stage I fuel tank	PPW	PPNW	PPNW	-
POGO--Stage I	-	-	U	-
Low thrust--one Stage I subassembly	-	-	NKLW	-
Total impulse low--Stage I				
(a) >10% low	-	-	WUK	-
(b) 3 to 10% low	-	-	WU	-
Premature Stage I shutdown				
(a) One subassembly shutdown	-	NKL	NKL	-
(b) Both subassemblies shutdown	-	-	NUKL	-
No Stage II start	-	-	-	OU
Delayed Stage II start	-	-	-	OU
Low thrust (>50% low)--Stage II	-	-	-	WOKL
Total impulse low--Stage II	-	-	-	RSUK
Pressure decay--Stage II oxidizer tank	PPW	PPW	PPW	POKL
Pressure decay--Stage II fuel tank	PPW	PPW	PPW	POKL
Premature Stage II shutdown	-	-	-	RSKL

* Additional cue required for detection of single SRM ignition is not yet defined.

TABLE 44.--Concluded

SUMMARY ASCENT MALFUNCTION CONDITIONS AND DETECTION CODE

Abbreviations

BIGS	Booster inertial guidance system
CTL	Control (booster not responding light)
FDI	Flight director indicator
FME	Failure modes and effects
IMP	Impulse (low thrust light)
MCC	Mission control center
RIGS	Re-entry inertial guidance system
SEC	Guidance secondary (switchover/light)
SRM	Solid rocket motor
TVC	Thrust vector control
SMD	Slow malfunction detection
OV	Orbiting vehicle

NOTE: The malfunction detection code groups, which are listed opposite the vehicle malfunction being detected, appear in their order of usage as a first cue, second cue, etc. For example, a code group such as "NKLW" indicates detection method "N" is the first cue, "K" is the second cue, etc.

A	Abort light (pitch and yaw turning rate until Stage I start)
B	Abort light (SRM hot line including TVC pressure switch)
C	Abort light (SRM chamber pressure automatic monitor)
D	SRM chamber pressure display
E*	SRM N_2O_4 pressure display
F*	SRM N_2 pressure display
G	Guidance switchover (SEC) light
H	BIGS NO-GO (PRI) light
I	RIGS NO-GO (MALF) light
J	Guidance status indicator
K	Low thrust (IMP) light
L	RIGS acceleration display
M	Overrate warning (RATE) light
N	Stage I thrust chamber pressure lights
O	Stage II thrust chamber pressure display
P	Core tank pressure displays
Q	Booster not responding (CTL) light
R	BIGS velocity-to-go display
S	RIGS velocity-to-go display
T	(Not used)
U	Crew sensory detection
V	RIGS attitude error display (FDI)
W*	MCC trajectory monitor and MCC vehicle pressurization displays
X*	MCC thrust vector position (controls) displays
Y*	MCC turning rate (controls) and Stage II hydraulic system displays
Z*	RIGS signals (slow malfunction detection displays in MCC)
1*	BIGS signals (slow malfunction detection displays in MCC)
2	Not detected
3	See analysis of failure (refers to FME tabulation)

Table 44 does not include vehicle end-effects resulting from hardware malfunctions that have probabilities of failure less than 1 ppm.

* Ground displays only.

V. CAPABILITY FOR SECONDARY OBJECTIVES

This section of this report presents the results of a study to determine the potential of the D/3 vehicle for accomplishing the following secondary objectives:

(1) The potential for research into lifting entry at supercircular velocities from near-earth orbits by the use of velocity augmentation in the deorbit phase.

(2) The potential of retrofitting the D/3 vehicle, after it has fulfilled its primary research objectives, to explore possible problems of rendezvous, docking, and transfer of men and/or equipment for applications as a ferry, logistics, or rescue vehicle in near-earth operations.

Also discussed in this section is the modification of a D/3 vehicle to accomplish an orbital experiment on a landing approach and go-around engine. A lifting body entry vehicle with such a capability would have improved operational flexibility over a simple glide vehicle, especially in adverse weather conditions.

Some of the significant subsystem modifications--such as propulsion, heat shields for the supercircular velocity entries, and environmental control and life support for the longer orbit times of the rendezvous and docking experiment--are discussed. Also presented as a conclusion to this section is a summary of the weight modification required for the secondary objectives. The slight effects of the secondary objectives, if any, on other subsystems are not discussed. An alternative guidance control logic for the supercircular velocity entries is described in Part III.

The basic D/3 vehicle was designed for the primary near-earth orbit research objectives. This vehicle is 25 feet (7.62 m) in length, has a crew of three and provides a reserved space for research equipment payloads of 74.8 cubic feet (2.12 m^3).

The purpose of this study effort was to examine the capability of the D/3 vehicle to accomplish a number of secondary research objectives after completion of the primary objectives. To accomplish this goal it will be necessary to make some modifications and alterations to the basic D/3 vehicle as well as add subsystems and/or modules to the spacecraft. The weight changes to the basic D/3 entry vehicle are summarized in the final subsection.

Brief summaries of pertinent characteristics of the two secondary missions, the supercircular velocity and the rendezvous research, are given in table 45.

A. SUPERCIRCULAR ENTRY VELOCITY MODULE

The purpose of this modification is to provide the D/3 vehicle with the propulsion and subsystems capability to allow it to explore the special problem associated with entry of this type of vehicle at velocities higher than those for near-earth orbits.

TABLE 45

SUMMARY CHARACTERISTICS OF SECONDARY MISSIONS

Supercircular velocity mission objective: Conduct research during maneuvering entry from near-earth orbit at supercircular speeds.

(1) Launch with Saturn IB: payload capability of 35 300 lb (16 000 kg). Modified D/3 with supercircular velocity module.

(2) Typical mission

(a) Launch from Cape Kennedy
(b) Inject into 35.7° (0.623 rad) inclination orbit; 80 n. mi. (148 km) perigee, 200 n. mi. (370 km) apogee
(c) Circularize at 200 n. mi. (370 km); ΔV = 210 fps (64.0 m/sec)
(d) On third orbit (over Hawaii) initiate deorbit, including acceleration to 30 000 fps (9.14 km/sec)
(e) Return to FRC (Edwards AFB)

(3) Launch to touchdown time: 295 min
Entry at γ = -6° (0.105 rad)

(4) Entry vehicle experimental weight (typical):

FM-9	25 lb	(11.3 kg)
GN-5	200	(90.7)
FM-15	15	(6.80)
SM-3	10	(4.54)
SM-6	50	(22.7)

Total allocation 300 lb (136 kg) (to be included in entry vehicle weight)

(5) Same 5-orbit design life as basic D/3 vehicle.

(6) Redefine abort system to provide Saturn safety.

(7) Same crew station setup as D/3, except one man and his seat removed. Fixed seats for the two crew.

(8) Heat shield allowance: approximately 4 in. (10 cm) on bottom and 2 in. (5 cm) on top.

Rendezvous research mission objective: Demonstrate and develop rendezvous docking and transfer systems and techniques using a modified D/3 entry vehicle and a typical orbiting docking station.

(1) Launch with Titan III-5. Payload capability of 27 400 lb (12 428 kg). Modified D/3 with tunnel egress and with rendezvous velocity and cargo module.

(2) Typical mission

(a) Launch from Cape Kennedy
(b) Inject into 35° (0.611 rad) inclination orbit; 80 n. mi. (148 km) perigee, 138 n. mi. (256 km) apogee

(c) Circularize at 138 n. mi. (256 km)	ΔV = 144 fps	(43.9 m/sec)
Plane change 0.1° (1.75 mrad)	ΔV = 45	(13.7)
Orbit change 80 ni. mi. (148 km) perigee	ΔV = 108	(32.9)
Complete orbit change 80 n. mi. (148 km) circular	ΔV = 108	(32.9)
Initiate rendezvous	ΔV = 36	(11.0)
Midcourse guidance	ΔV = 50	(15.2)
Final rendezvous 100 n. mi. (185 km) circular	ΔV = 36	(11.0)
Docking	ΔV = 20	(6.10)
Station departure	ΔV = 20	(6.10)
Margin (150 fps (45.7 m/sec) for other station altitudes plus 10% contingency)	ΔV = 221	(67.4)
Total ΔV	= 788 fps	(240)
(d) Deorbit and return to FRC (Edwards AFB)	ΔV = 520 fps	(158)

(3) Launch to touchdown time: 24 hr max.
Normal entry at γ = -1.5° (26.2 mrad)

(4) Cargo carried in adapter or velocity module. Return cargo carried in entry vehicle.

(5) Where possible, all EC/LS and electrical power supplies required for longer orbit stay times will be carried in cargo module.

(6) All docking and rendezvous avionic equipment will be built into cargo module.

(7) Relocate abort and deorbit engines to outside adapter.

(8) Velocity module provides attitude control and both high (1 g) and low acceleration (0.01 g) translation capability.

1. Design Modifications

The modified D/3 spacecraft is launched by a Saturn IB launch vehicle plus a velocity module (fig. 102). The basic D/3 vehicle has to be modified for addition of the module, and the entire spacecraft designed for the Saturn launch and abort envelop.

The basic D/3 entry vehicle is unchanged in arrangement. The required modifications are:

(1) The heat shielding is one designed for the higher pressures and heating fluxes which this type entry imposes.

(2) Structural strengthening is required at the aft end because of the mass and thrust loads imposed by the additional velocity module and because of the high abort thrust loads required to clear the Saturn overpressure envelope.

(3) Additional propellant capacity is required for the reaction control system due to the increased maneuvering and to overcome the additional perturbations from the velocity module propulsion modes--velocity increment, abort and deorbit.

The capability and systems required to accomplish the objectives of this mission are contained entirely within the adapter section; the adapter and velocity module are integrated into one and the same unit, designed specifically for this mission. This adapter differs from the standard D/3 adapter.

(1) The adapter is fabricated as a single, integrated structural unit and, in operation, separated into three sections by linear shearing devices. The overall adapter is 176 inches (452.3 cm) long and has a double taper configuration. The smaller end is the oblong shape, matching the D/3 vehicle interface. The forward section is 58 inches (147.3 cm) long and has a nominal taper of 29°--the base of this section is 106.3 inches (270 cm) in diameter. The aft section has a taper of 32° and is a right truncated cone 120 inches (305 cm) long--the base of this section matches the Saturn (S-IVB stage) 260-inch (660 cm) diameter.

(2) The double-taper configuration was derived to achieve placement of the six solid rocket motors required for Saturn pad abort with a maximum offset of 20° and have sufficient clearance from the D/3 entry vehicle when jettisoned. These abort motors are attached to the rear part of the forward section by an external framework and are jettisoned during ascent.

(3) An array of four spherical solid rocket motors is installed in the forward section for abort and/or deorbit after the external abort motors are jettisoned. This cluster of motors is identical to the motors and arrangement utilized for the standard D/3 vehicle. It is possible to add an additional separation--linear shearing type--at 23.7 inches (60.3 cm) aft of the interface to reduce weight and effects on stability from the attached adapter section after the external abort motors are no longer required.

[redacted]

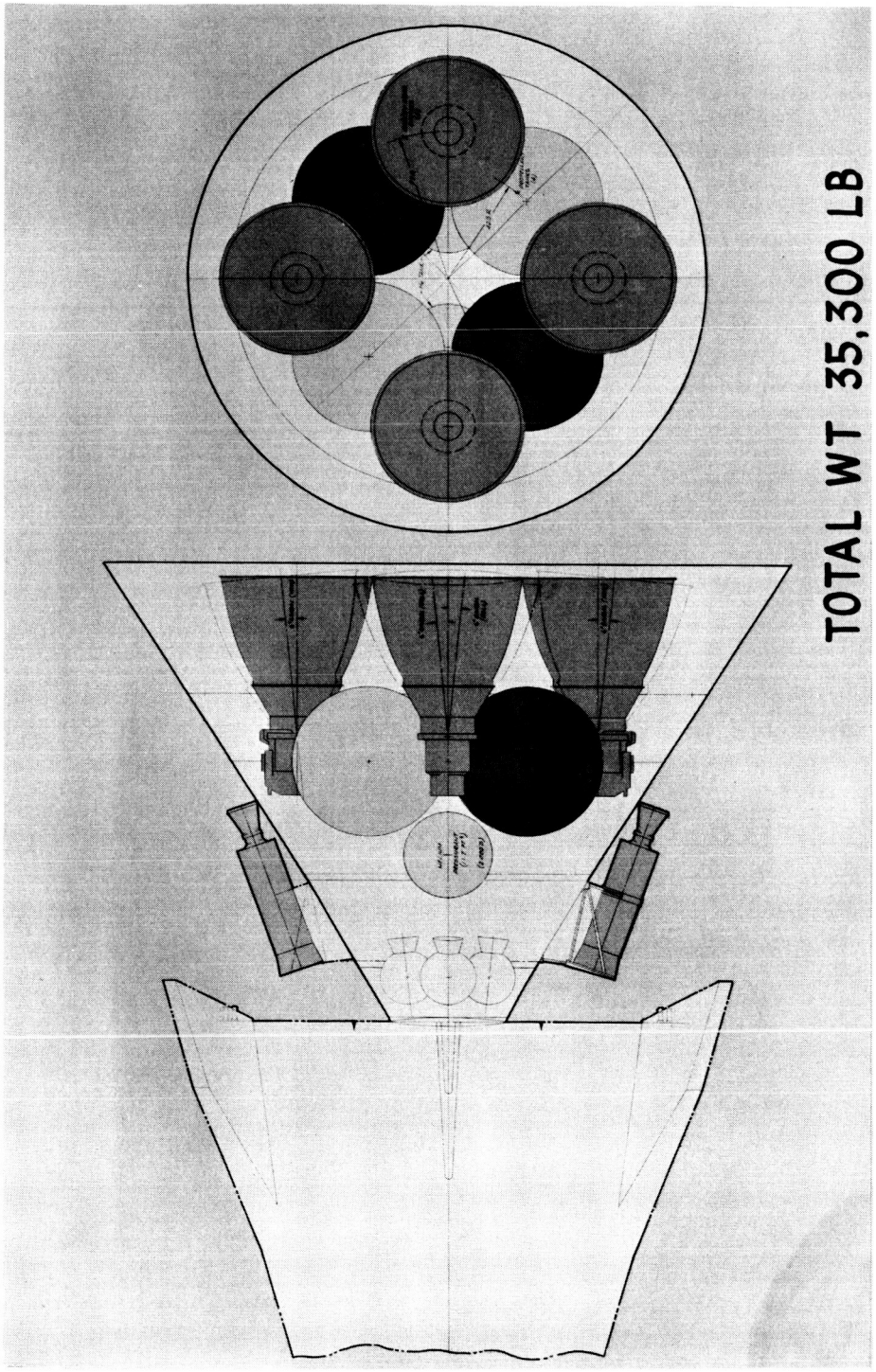

FIGURE 102. MODIFICATION FOR SUPERCIRCULAR ENTRY VELOCITY EXPERIMENT

[redacted]

(4) The aft section of the adapter is separated into two parts by a linear shearing separation. The rear part, 51 inches (129.5 cm) long, remains attached to the Saturn booster. The front part remains with the spacecraft and contains the propulsion system for maneuvering and superorbital velocity increment. The four liquid rocket motors are gimbaled for steering corrections. Storable propellants and positive expulsion are utilized in this system.

2. Velocity Module Propulsion System

The Saturn IB can boost a payload of 35 300 pounds (16.012 Mg) into a 35.7° inclination orbit having a perigee of 80 nautical miles (148.17 km) and an apogee of 200 nautical miles (370.4 km). This payload weight will consist of a modified D/3 entry vehicle and a velocity stage propulsion module to perform superorbital velocity entry experiments.

Abort system. - The abort propulsion subsystem arrangement and performance must be capable of meeting the abort environment associated with the Saturn IB launch vehicle. The abort criteria contained in reference 14 were used in this study. These criteria specified the pad abort environment to be the most severe design consideration. To limit the shock explosion overpressure to 7 psi (48.26 kN/m^2), a minimum thrust to weight ratio of 11.81 must be provided for a minimum of 1.78 seconds.

The estimated weight of the vehicle in the pad abort condition is based on a modified entry vehicle incorporating the D/3 abort/deorbit propulsion subsystem for the emergency deorbit function. The impulsive velocity increment required for deorbit from 200 nautical miles (370.4 km) is approximately 410 fps (125 m/sec). Utilization of any three of the four solid rocket motors of the D/3 abort/deorbit propulsion subsystem will supply the 410 fps requirement. This leaves the fourth motor as a backup for a single motor failure in the deorbit array. For purposes of estimating the abort condition vehicle weight, the following were assumed:

	lb	kg	
Weight of entry vehicle	= 11 342	5144.7	
Deorbit motors	= 1 148	520.7	(D/3 array)
Adapter for deorbit motors	= 220	99.8	
Weight of experiments	= 300	136.1	
W_{EV*}	= 13 010	5901.3	

The abort propulsion system required for pad abort of the entry vehicle package, $W_{EV}*$, from a Saturn IB was determined as follows:

Thrust to weight, $F/W_{IN} = 11.81$ (min.)

Thrust duration, $t_b = 1.78$ sec (min.)

Available solid rocket motors for this application will typically have a mass fraction, M. F., of 0.70 and a specific impulse, I_{sp}, of 243 seconds at sea level. The cosine of the angle between the thrust axis and entry vehicle longitudinal axis is approximately 0.94. The minimum abort propellant requirement, W_p (min.), was determined as follows:

$$\frac{W_p}{W_{IN_{min}}} = \frac{(F/W_{IN})\, t_b}{I_{sp} \cos \measuredangle}$$

$$= \frac{11.81 \times 1.78}{243 \times 0.94} = 0.092$$

For M. F. = 0.70, the abort propulsion system weight, W_{PS}, is:

$$\frac{W_{PS}}{W_{IN_{min}}} = \frac{0.092}{0.70} = 0.1314$$

The initial weight, W_{IN}, of the abort vehicle then becomes:

$$W_{IN} = W_{EV}^{*} + 0.1314\, W_{IN}$$

$$= \frac{13\,010}{1 - 0.1314} = 14\,978 \text{ lb } (6.7940 \text{ Mg})$$

For W_{IN} = 14 978 pounds (6.7940 Mg), the following are computed:

$$W_{P_{min}} = 0.092 \times 14\,978 = 1378 \text{ lb } (625 \text{ kg})$$

$$W_{PS_{min}} = 0.1314 \times 14\,978 = 1968 \text{ lb } (892.7 \text{ kg})$$

$$F_{min} = 11.81 \times 14\,978 = 176\,890 \text{ lb } (80.237 \text{ Mg})$$

A review of candidate solid rocket motors, from the CPIA catalog (ref. 13), considering also the dimensional limitations of the vehicle system, indicates the Genie (MB-1) (TU-289) closely matches the requirements. The following Genie performance is available:

F_{SL}	= 30 800 lb (13.971 Mg)
t_b	= 1.79 sec
W_{PS} (per motor)	= 478 lb (216.8 kg)
M. F.	= 0.66

Using six Genie motors for abort, the W_{IN} becomes:

$$W_{IN} = 13\,010 + (6 \times 478) = 15\,878 \text{ lb } (7.202 \text{ Mg})$$

At

$$F/W_{IN} = 11.81, \; F = 187\,519 \text{ lb } (85.059 \text{ Mg})$$

For six motors, the thrust requirement per motor is:

$$F_{req} = \frac{187\,519}{6} = 31\;\;253 \text{ lb } (14.176 \text{ Mg})$$

The Genie can be modified to provide the additional thrust to meet the requirements without significantly compromising the weight or general man-rated qualification of the motor. Six Genie motors will be incorporated on the adapter for abort system application as shown in figure 102.

Velocity system. - A ΔV of 210 fps (64 m/sec) is required to circularize the 35 300-pound (16.012 Mg) payload from the orbit established by the Saturn IB at 80 to 200 nautical miles (148.17 to 370.4 km). This ΔV will be supplied by the velocity stage located in a portion of the adapter cone. Earth storable propellant (N_2O_4/50-50) and available engine hardware were utilized in the design and sizing. Two of the four engines provided for the supercircular velocity impulse will be used. The propellant required for the 210-fps (64 m/sec) impulsive velocity addition is:

$$\Delta V = I_{sp}\, g \ln \frac{\text{Initial weight}}{\text{Initial weight} - W_P}$$

$$210 = 305\, g \ln \frac{35\,300}{35\,300 - W_P}$$

$$W_P = 746 \text{ lb } (338.4 \text{ kg})$$

Typical performance and physical characteristics of an engine suitable for application to the velocity module are those for the Lunar Module Descent Engine (LMDE).

F_{vacuum}	= 10 500 lb (4.763 Mg)
Propellant	= N_2O_4/50-50
O/F	= 1.6
Pressure fed	
Thrust vector control	= ±6° (gimbal)
I_{sp} vacuum	= 305 sec
P_c	= 110 psia (758.4 kN/m^2)
Engine dry weight (overall)	= 350 lb (159.76 kg)
Restart capability	= 20 times
t_b limit	= 1030 sec
Reliability	= 0.9991 at 90% confidence

As a result of preliminary matching studies between vehicle and propulsion system design and performance considerations, the following preliminary weights breakdown was evolved:

$W_{EV}^* = 13\ 010$ lb (5.901 Mg)

Weight of velocity module structure = 1800 lb (816.4 kg)

Weight of engines = 4 x 350 = 1400 lb (635 kg)

Weight of propellant tanks and pressure system = 2200 lb (1.905 Mg)

$\Sigma = W_E = 18\ 410$ lb (8.351 Mg)

This indicates that the quantity of propellant available for maximizing entry velocity will be:

$W_P = 35\ 300 - 18\ 410 - 746 = 16\ 144$ lb (7.323 Mg)

Assuming that 2 percent of this propellant will be unavailable, the propellant weight for impulsive velocity addition will be:

$W_{P_{useful}} = 0.98 \times 16\ 144 = 15\ 821$ lb (7.176 Mg)

The propellant tank volume required for the N_2O_4/50-50 propellant at O/F = 1.6 is determined as follows:

$N_2O_4 = 89.42$ lb/ft^3 (793.8 kg/m^3)

50-50 = 56.04 lb/ft^3 (650.2 kg/m^3)

5% ullage volume

$$V_{N_2O_4} = 16\ 890 \times \frac{1.6}{2.6} \times \frac{1.05}{89.42} = 122 \text{ ft}^3 \ (3.455 \text{ m}^3)$$

$$V_{50\text{-}50} = 16\ 890 \times \frac{1}{2.6} \times \frac{1.05}{56.04} = 122 \text{ ft}^3 \ (3.455 \text{ m}^3)$$

Total propellant tank volume = 244 ft^3 (6.91 m^3)

The tank pressurization system based on the use of helium as the pressurant will require the following weight of helium and pressurant storage tank volume:

Required propellant tank pressure = 250 psia (1.7237 MN/m^2)

Initial helium storage pressure = 3000 psia (20.684 MN/m^2)

Final helium storage pressure = 400 psia (2.7579 MN/m^2)

Pressurant will be heated to maintain storage tank temperature at room temperature.

ρ_{He} = 2 lb/ft^3 (0.0566 m^3) at 3000 psia (20.684 MN/m^2)

ρ_{He} = 0.275 lb/ft^3 (0.0078 m^3) at 400 psia (2.7579 MN/m^2)

ρ_{He} = 0.173 lb/ft^3 (0.0049 m^3) at 250 psia (1.7237 MN/m^2)

The weight of helium in the empty propellant tanks at burnout will be:

$$W_{He} = 244 \times 0.173 = 42.2 \text{ lb } (19.14 \text{ kg})$$

The helium storage tank volume and total helium weight required can now be determined as follows:

$$2\,V_{He} = 42.2 + (V_{He} \times 0.275)$$

$$V_{He} = \frac{42.2}{2 - 0.275} = 24.5 \text{ ft}^3 \ (0.694 \text{ m}^3)$$

The total helium weight requirement will then be:

$$W_{He} = 2 \times 24.5 = 49 \text{ lb } (22.23 \text{ kg})$$

The impulsive velocity equation may be written in the form of a series expansion as:

$$\frac{W_{P_{useful}}}{W_E} = \frac{(B)^2}{(g\,F)} \frac{W^2_{P_{useful}}}{2} + \frac{(B)}{(g\,F)} \frac{(1 + A)}{(g\,I_{sp})} W_P + \frac{(A)}{(g\,I_{sp})} + \frac{1}{2} \frac{(A)^2}{(g\,I_{sp})} + \text{------}$$

where

B = average centrifugal acceleration to be overcome during thrusting

F = thrust

A = impulsive velocity required to establish entry condition

The previous equation was used to develop the relation between A and W_E to determine the value of A applicable to the velocity module for this study. In consideration of the orbit conditions, weight breakdown, and propulsion performance characteristics previously discussed, the following values of the parameters of the equation are:

B = 10.6 fps^2 (3.2309 m/sec^2)

I_{sp} = 305 sec

F = 43 000 lbF (195.05 Mg)

W_P = 15 821 lbM (7.176 Mg)

The equation then becomes:

$$\frac{15.821 \times 10^3}{W_E} = 0.1208 + 1.1345 \times 10^{-4} A + 5.1838 \times 10^{-9} A^2$$

Figure 103 presents the results of solutions of the above form of the equation for a range of A values in the region of interest. For a burnout weight of 18 410 pounds (8.351 Mg), the value of A is found to be 5150 fps (1.570 km/sec).

Figure 104 presents the results of trajectory studies showing the entry velocity attainable as a function of the impulsive velocity factor A. The results of the study indicate an entry velocity of 29 000 fps (8.839 km/sec) is attainable.

3. Heat Shield Modifications for Supercircular Entry Velocities

An analysis was made of the heat shield requirements for initial entry velocities, V_i, of 30 000 fps (9.15 km/sec) and 34 000 fps (10.37 km/sec). The results are tabulated along with comparable results for orbital entry velocities in table 46.

Generally, increasing the initial entry velocity requires a higher initial entry angle, γ_i, to avoid a skipout from the atmosphere. This increase in γ_i has a twofold effect on the heating environment; the maximum convective heating rate increases by a factor of 2 to 5 over the range of V_i considered, whereas the total convective heating increases significantly only at the 34 000-fps (10.37-km/sec) point. Surface recession, as expected because of its strong dependence on heating rate, also increases with V_i.

It is significant to note that the initial entry velocity can be increased to 34 000 fps (10.37 km/sec) without increasing the total heat shield weight. However, if minimum recession is a constraint, high-density ablative materials must be used for the stagnation region and the swept leading edges, with the resulting increase in total heat shield weight (up to 47% at 34 000 fps, 10.37 km/sec).

For an operational entry vehicle system, surface recession of the ablator is not considered to be a major problem so long as the control surfaces can perform satisfactorily. However, for a research vehicle whose surface is instrumented with heating and pressure sensors, large surface recession could become a major obstacle to obtaining accurate measurements. Therefore, the higher density, lower surface recession materials are recommended for the supercircular entry velocity flight tests vehicle.

B. RENDEZVOUS AND DOCKING EXPERIMENT MODIFICATION

The purpose of this modification is to provide the spacecraft with the capabilities to explore the unique problems associated with rendezvous and docking operations with an lifting body entry vehicle.

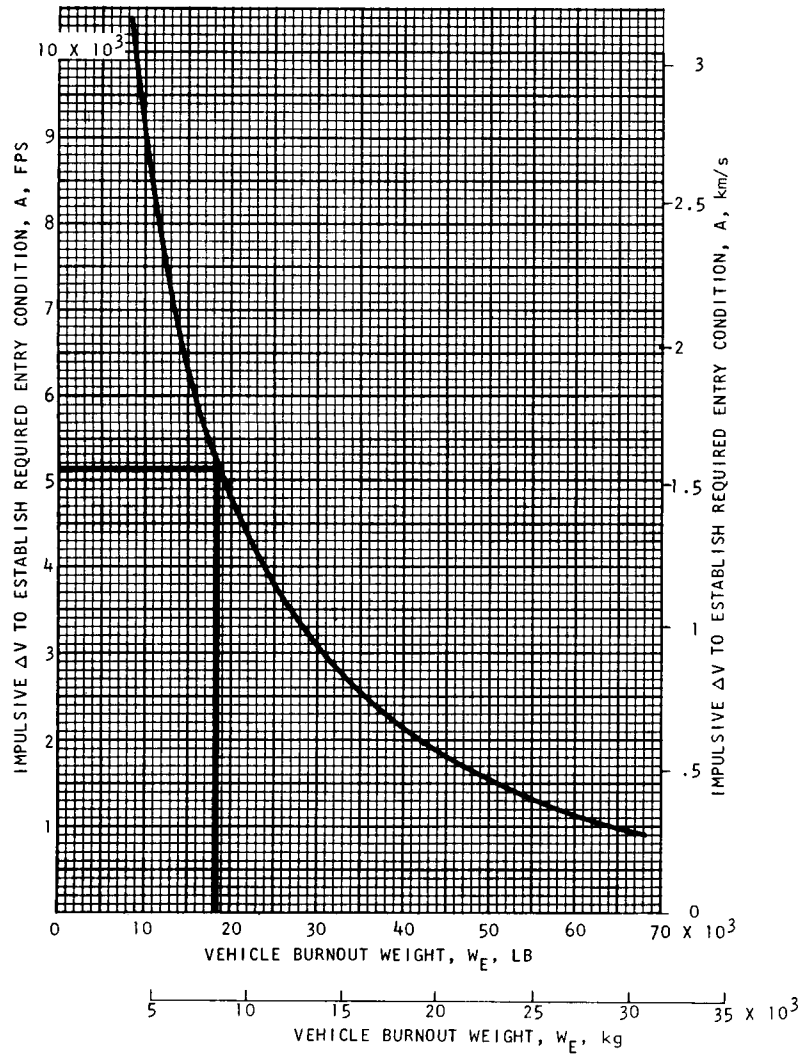

FIGURE 103. IMPULSIVE VELOCITY ADDITION--AVAILABLE VERSUS VEHICLE BURNOUT WEIGHT

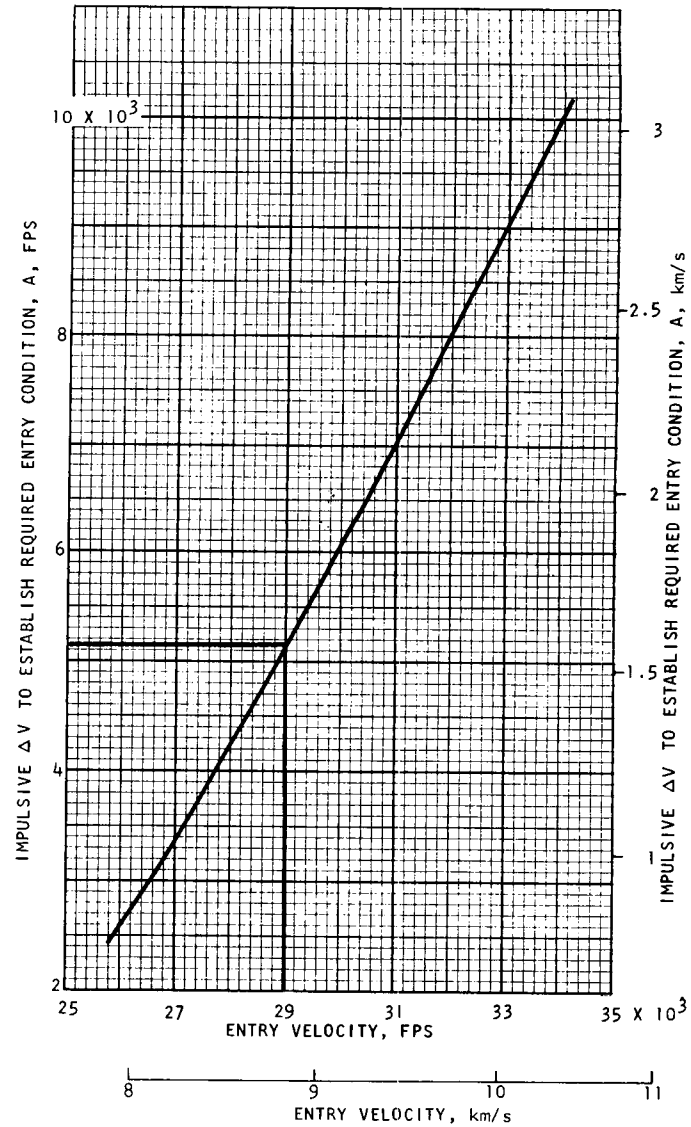

FIGURE 104. IMPULSIVE VELOCITY ADDITION REQUIRED FOR ENTRY CONDITIONS

TABLE 46

SUMMARY OF HEAT SHIELD REQUIREMENTS FOR SUPERCIRCULAR ENTRY VELOCITIES

Initial entry velocity, fps (m/sec)	Initial entry angle, deg	Maximum* heating rate	Total* heat	Stagnation area ablator material	Required** ablator thickness	Stagnation** surface recession	Vehicle body heat shield sysstem	Heat shield** weight
26 000 (7.92)	-1.5	1.0	1.0	ESA 3560 HF	1.0	1.0	ESA 3560 HF composite	1.0
26 000 (7.92)	-3.0	2.10	0.665	ESA 3560 HF LDNP	0.924 0.918	1.56 3.23	ESA 3560 HF composite	0.838
30 000 (9.15)	-5.5	4.15	0.817	LDNP	0.995	3.56	LDNP composite	0.882
34 000 (10.37)	-5.1	3.54	1.739	LDNP	1.450	5.36	LDNP plus ESA 3560 HF composite	1.150
				HDNP	1.200	3.96	HDNP plus ESA 3560 HF composite	1.210
				Carbon phenolic	1.640	1.57	Carbon phenolic plus ESA 3560 HF composite	1.370
34 000 (10.37)	-6.1	5.49	1.237	LDNP	1.190	4.16	LDNP plus ESA 3560 HF composite	0.965
				HDNP	0.930	3.10	HDNP plus ESA 3560 HF composite	1.075
				Carbon phenolic	1.490	1.28	Carbon phenolic plus ESA 3560 HF composite	1.470

*Normalized convective heating for a 1-ft (30.5-cm) nose radius.
**Normalized with respect to all-ablative heat shield for C size vehicle.

LDNP--Low density nylon phenolic HDNP--High density nylon phenolic

1. Design Modification

The spacecraft consists of the D/3 entry vehicle, adapter section, docking module and propulsion section (maneuver and rendezvous transtage--MART) (fig. 105). The docking provisions extend off the rear end of the docking module and are submerged inside a cavity provided in the MART.

The capabilities which are provided by the added sections are:

(1) Target acquisition equipment

(2) Propulsion for orbital maneuver including rendezvous

(3) Docking phase controlled by a crew member

(4) Crew transfer

(5) Cargo transfer.

This spacecraft inherently has the capabilities to conduct extravehicular operations, including rescue mission experiments, besides its stated objective. The module has been designed to be an effective airlock by closing off the pressure-tight hatches at the ends--one is at the entrance to the tunnel at the rear end of the entry vehicle and the other at the docking port on the module. Extravehicular operations are accomplished by exiting and entering through the docking port.

The basic D/3 entry vehicle is unchanged in arrangement for this mission, but some modifications are required:

(1) Access is provided through the main rear bulkhead to the exit tunnel in the body extension.

(2) A removable pressure-tight hatch cover is provided at the tunnel entrance, and locking mechanisms are included for the cover. A view port is provided in the hatch as well as a pressure relief valve for equalizing the pressure in the entry vehicle and docking module.

(3) A pressure-tight tunnel for crew passage (see fig. 106) is incorporated in the body extension,and its structure is modified to accommodate the tunnel. The tunnel has a clear inside diameter of 26.5 inches (67.3 cm) and can be used as an alternate exit after landing. The tunnel walls are wrapped with insulation to protect the body extension structure during entry.

The adapter section is the same size and configuration as the standard D/3 adapter but is designed differently to suit this mission.

(1) A pressure-tight tunnel, matching the exit tunnel in the D/3 vehicle runs through the length of the adapter and connects to the docking module. The tunnel separates at the same locations and by the same methods as the adapter section.

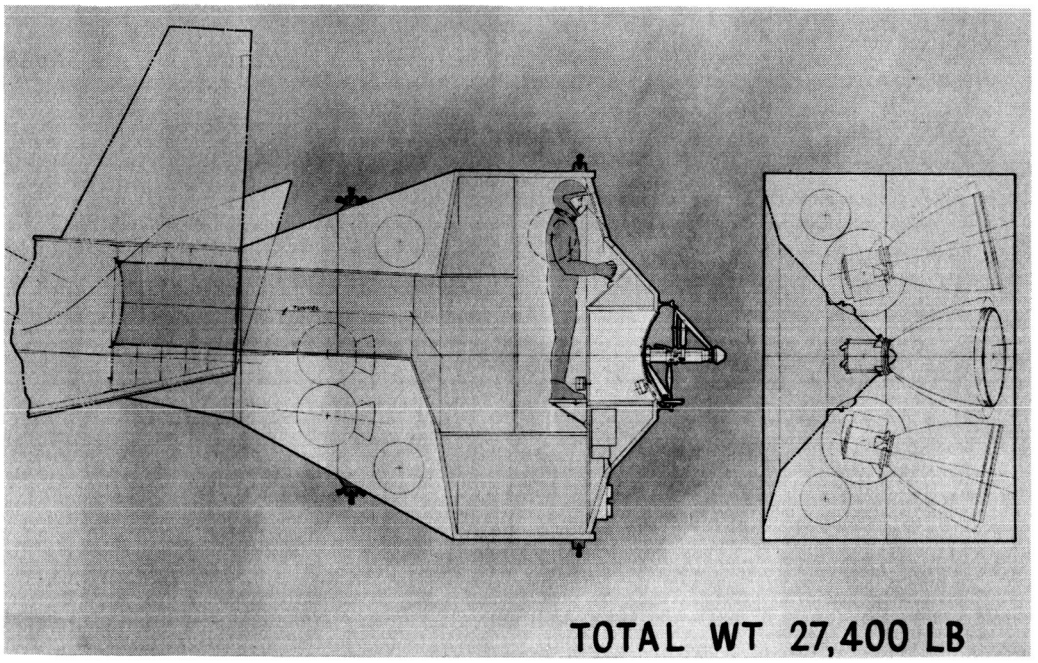

FIGURE 105. MANEUVER AND RENDEZVOUS TRANSTAGE

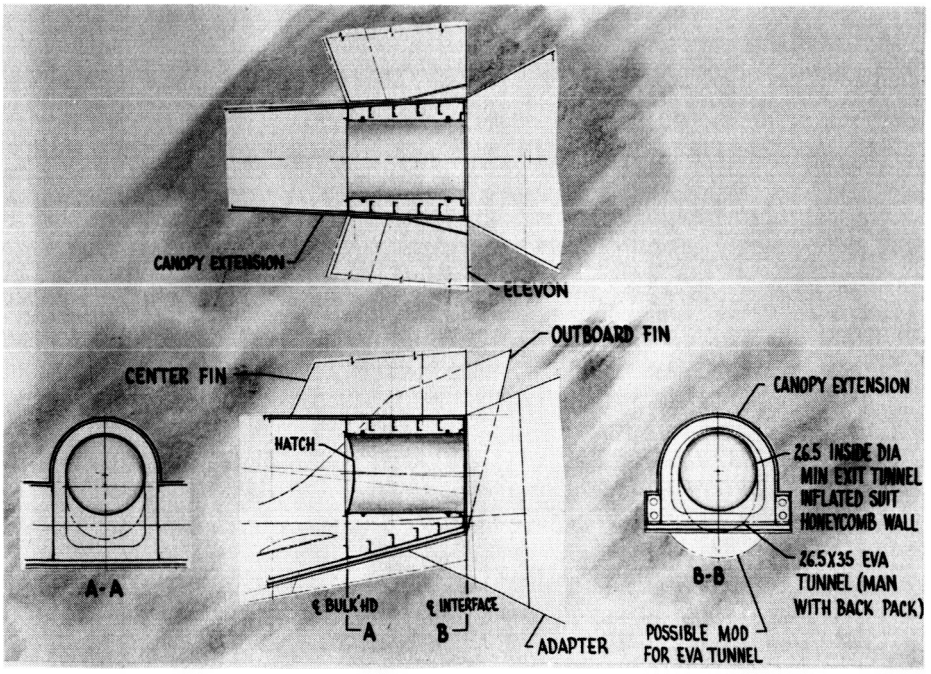

FIGURE 106. CREW PASSAGE TUNNEL LAYOUT

(2) The adapter section is separated into two parts as before; the forward part includes the same four spherical solid rocket motors as the standard D/3 for abort and deorbit, but the arrangement of the solid rocket motors is altered to clear the tunnel. This part of the adapter is 32.7 inches (88 cm) long, slightly longer than the standard D/3 section due to the relocation of the solid rocket motors.

(3) The aft part of the adapter is permanently fastened to and remains with the docking module. This part contains the propellant for docking operations (longitudinal and transverse translations) and attitude control. A pair of pillbox arrays of five thrustors each are mounted externally for the docking translations and attitude control in conjunction with a similar set on the docking module.

The docking module is a pressure-tight cylindrical section with pressure bulkheads at each end. It is 10 feet (305 cm) in diameter, matching the Titan III launch vehicle, and the cylindrical portion is 48 inches (121.9 cm) long.

(1) The internal area of the module is divided into bays by racks which support the cargo and equipment stowed in the module.

(2) A central area measuring 50 inches (127 cm) high by 26.5 inches (67.3 cm) wide is left open for crew mobility and passage.

(3) An open area in the upper rear portion of the module is reserved for the docking phase crew station. The crew member is in a standing position facing a window provided in the rear bulkhead so that he has a direct view of the entire docking operation, including the docking probe. A control and display panel is provided at this station for this phase of the operation.

(4) A pair of pillbox arrays of three thrustors each are located externally for translation and attitude control in conjunction with thrustors on the adapter. This arrangement of thrustors has been devised to preclude thrustors and exhause products from interfering with docking vision or impingement on the target vehicle and to encompass the center of gravity shifts induced by staging and propellant expenditure.

(5) The docking provisions and tunnel arrangement are exactly the same as provided by the Apollo command module, including probe, attenuation mechanism, latching and pressure-tight hatch arrangement. The docking provisions are designed as a conical projection to provide for angular and lateral misalignments without collision of any of the docking module during the docking phase. The docking port has a clear inside diameter of 28 inches (71 cm), like Apollo.

(6) Additional space has been provided in the docking module for storage of simulated cargo packages. These packages are provided for cargo transfer experiments.

The propulsion section (MART) furnishes the impulses for ascent maneuvering and rendezvous phases. It is a cylindrical section 10 feet (305 cm) in diameter and 84 inches (213.4 cm) long.

(1) The propulsion section is made as one piece but separates into two parts similar to the adapter. The aft part is a skirt section 43 inches (109.2 cm) long, permanently attached to and remaining with the launch vehicle. The forward part contains the propulsion system components. It constitutes the MART. This part separates at the aft end of the docking module; it is jettisoned after it has been expended.

(2) Storable propellants are contained in a cluster of spherical tanks, and spheres containing pressurant gas are provided for positive expulsion.

(3) An array of four liquid rocket engines are provided. These engines are gimbaled for steering (vector) control during the ascent maneuvering and rendezvous phases.

(4) As mentioned previously, the propulsion system is arranged to provide a cavity for the docking provisions which protrude from the docking module.

2. Propulsion Systems for Rendezvous and Docking Experiment

The vehicle used to accomplish the rendezvous research mission requires a number of propulsion subsystems to adequately accomplish its mission. In addition to the propulsion systems that are part of the basic D/3 entry vehicle, propulsion thrust must be supplied to perform the following functions:

	ΔV required	
	fps	m/sec
Circularize orbit at 138 n. mi. (256 km) from the injected orbit of 80 n. mi. (148 km) perigee and 138 n. mi. apogee	144	43.8
Plane change of 0.1°	45	13.7
Orbit change to 80 n. mi. perigee	108	32.9
Complete orbit change to 80 n. mi. circular	108	32.9
Initiate rendezvous	36	10.95
Midcourse guidance correction	50	15.2
Final rendezvous	36	10.95
Docking	20	6.1
Station departure	20	6.1
Margin for other station altitudes: 150 fps (45.7 m/sec) plus 10% contingency	221	67.4
Total	788	240.0

The rendezvous research mission will be accomplished by a vehicle consisting of a modified D/3 entry vehicle, rendezvous module, docking module, and an orbiting

docking station. The configuration of the vehicle to accomplish the rendezvous research mission is shown in figure 105. The vehicle (not including docking station) weighs 27 400 pounds (12.428 Mg). The object of the mission is to demonstrate and develop rendezvous, docking and crew and cargo transfer techniques. The design approach in selecting and installing propulsion subsystems in the rendezvous and docking modules to be attached to the entry vehicle involves minimum modification of the basic vehicle. It is anticipated that the entry vehicle abort/deorbit propulsion system will be similar to that of the standard D/3 vehicle; however, the motor installation must be changed to accommodate the entry vehicle tunnel egress system. The entry vehicle reaction control system will also be the same as that of the standard D/3.

The rendezvous-orbit change module will provide an impulsive ΔV capability of 688 fps (210 m/sec) at an acceleration of approximately (but no less than) 0.4 g. The cargo docking module will provide 100 fps (30.5 m/sec) impulsive ΔV at approximately 0.01 g for the docking maneuvers.

Rendezvous-orbit change module. - The rendezvous module contains the propulsion system for orbit circularization, plane change, orbit change, and initial rendezvous maneuvers. Assuming a delivered specific impulse of 306 seconds, the total propellant required for the rendezvous module is estimated by the following equation:

$$\Delta V = I_{sp} \times g \times \ln \left(\frac{1}{1 - \frac{W_P}{W_{IN}}} \right)$$

where

ΔV = impulsive velocity addition, fps

I_{sp} = propellant specific impulse, sec

g = gravitational constant, ft/sec^2

W_{IN} = initial vehicle weight, lbM

W_P = weight of propellant used, lbM

= 1870 lbM (850 kg).

Assuming a propellant expulsion efficiency of 98 percent, the total propellant required becomes

W_P = 1910 lbM (866 kg).

Four engines--Bell Aerosystems Company, Model 8258, 3500 pounds (1585 kg) thrust--operating at a propellant mixture ratio of 1.6 and utilizing N_2O_4/50-50 propellants may be utilized to supply the required thrusting time. The engines incorporate a gimbaling capability so that accurate vehicle positioning can be accomplished during the rendezvous maneuver.

The ratio of specific weights of N_2O_4/50-50 propellants is 1.6. Since the engine operates at a mixture ratio of 1.6, the propellant tank volume requirements are the same for each propellant. The equal volume tanks are the positive expulsion type. An operating pressure of 250 psi (1.72 MN/m^2) is maintained in the tank throughout the expulsion cycle.

The size of each propellant tank is 13.76 cubic feet (0.389 m^3) (including a 5% ullage allowance). The pressurant gas for propellant expulsion is helium. The helium requirements are 4.77 pounds (2.16 kg) in a storage container of 2.77-foot (84.4 cm) diameter with an initial helium storage pressure of 3000 psi (21.0 MN/m^2) and a final storage pressure of 400 psi (2.75 MN/m^2) at 70° F (21° C).

The rendezvous velocity module is jettisoned when the vehicle is in close proximity to the docking station. The remaining portion of the vehicle (entry vehicle and cargo-docking module weighing 23 000 pounds (10 450 kg)) continues with the docking maneuver.

Entry vehicle and cargo-docking module. - The entry vehicle and cargo-docking module is provided with a low-acceleration propulsion system to provide impulse for docking and station departure. The docking propulsion system is capable of providing a ΔV of 100 fps (30.48 m/sec)for translation, plus sufficient impulse for attitude control.

It is assumed that the terminal requirements for alignment and velocity during docking are similar to those reported in reference 14 for lifting entry type spacecraft. These requirements were determined by evaluation of pilot capability in performing the docking operation.

Parameter	Requirement
Translation velocity	
X axis	0.2 to 1.5 fps (0.061 to 0.45 m/sec)
Y and Z axes	0 to 0.75 fps (0 to 0.0229 m/sec)
Misalignment	±12 in. (0.303 m) linear ±10° pitch, roll, yaw
Angular rate	0 to 1.5°/sec pitch, roll, yaw

Two independent sets of reaction control systems are utilized. One is located in the cargo-docking module. This unit will supply velocity increments for the rendezvous and docking maneuvers. The second system is the Reaction Control System contained within the entry vehicle. This system would be inactive until separation of the entry vehicle from the docking module.

A preliminary evaluation of propellants for the reaction control system indicates that the storable propellant combination of N_2O_4/50-50 is the best combination based on the following:

(1) Both propellants are chemically stable and storable over a wide range of temperatures.

(2) They are hypergolic and have a short ignition delay.

(3) They have a relatively high performance over a wide range of temperatures.

(4) There is a large amount of experience in handling these propellants because of their wide use on other space programs.

A pressure-fed positive expulsion system will be used to supply propellants to the reaction control engines.

Thrust requirements for the reaction control and docking propulsion system were determined on the basis of the following moment arms and vehicle moments of inertia:

	Moment arm, ft (m)	Moment of inertia, I_{yy} slug-ft^2 (Mg-m^2)
Pitch	11.4 (3.48)	85 000 (115.2)
Yaw	11.4 (3.48)	85 000 (115.2)
Roll	5.0 (1.52)	9 000 (12.2)

The location of the translation thrustors relative to the center of gravity results in extraneous torques occurring during translation maneuvers. These torques must be canceled by simultaneous application of equal opposing torquing action. Consequently, when a pure translation maneuver is desired, there is a requirement for continuous cycling of the attitude control thrustors. This torque restoring requirement and the limit cycle operations were the considerations for sizing the reaction control system thrustors and determining the propellant requirements.

The thrust levels of the reaction control system motors are based on the requirements to nullify the corresponding torques associated with firing of the translation motors, which were sized for a vehicle acceleration of 0.01 g. The thrust and propellant requirements were calculated using the procedure outlined in Part IV, section VI. For purposes of this study, the center of gravity is assumed to be fixed in the cargo-docking module centerline, at station 280. It was determined that 18 thrustors would be required to perform the maneuvers required for docking. The thrustor locations are shown in figure 107. Thrust levels of the reaction control and docking engines are shown in table 47.

Redundancy in the reaction control system is provided by incorporating dual solenoid valves for each injector. The engines considered for use are assumed to operate at chamber pressures of approximately 100 psi (0.69 MN/m^2). A specific impulse of 280 seconds is assumed for the translation engine and 250 seconds for the reaction control engines in the pulse mode operation.

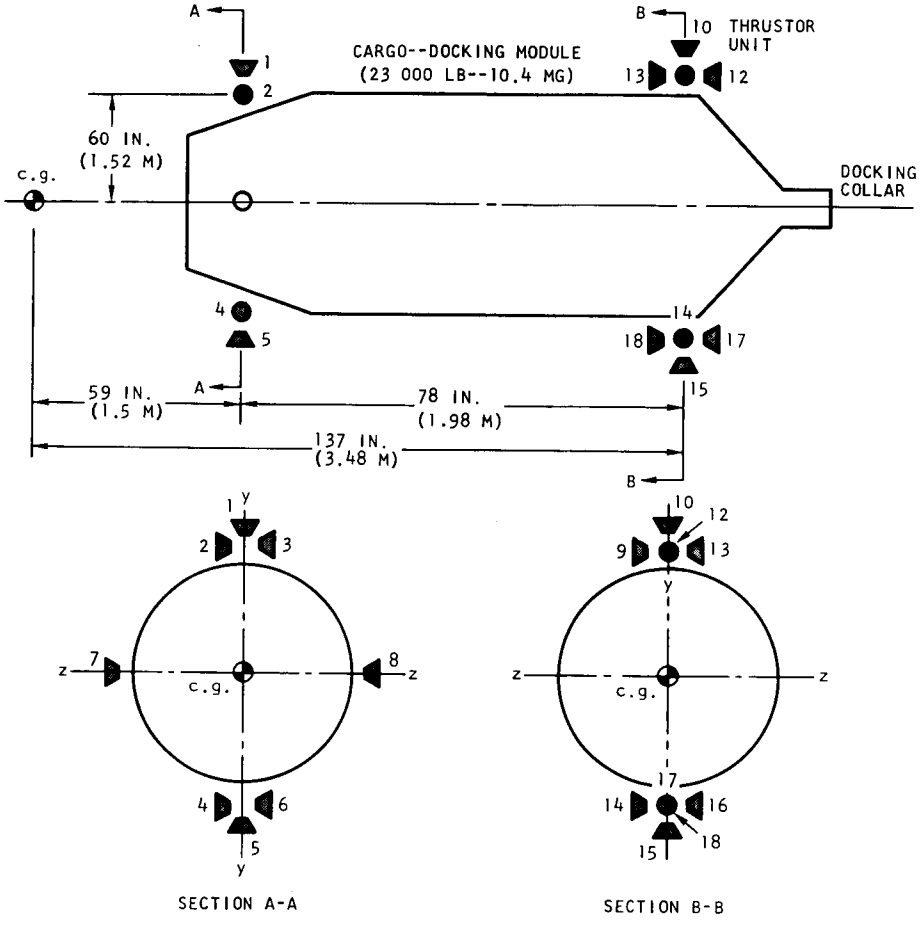

FIGURE 107. THRUSTOR LOCATIONS ON DOCKING MODULE

TABLE 47

REACTION CONTROL AND DOCKING ENGINES

Function	Thrust required per engine, lb (kg)	Total Thrust required, lb (kg)	Number of engines required	Engine location (ref. fig. 109)
Pitch	923 (133)	586 (266)	2	10, 15
Yaw	146.5 (66.5)	586 (255)	4	9, 11, 14, 16
Roll	3.53 (1.6)	7.06 (3.2)	2	2, 3, 4, 6
Vertical translation	410 (186)	820 (372)	2	1, 5
Lateral translation	410 (186)	640 (745)	4	7, 8
Longitudinal translation	115 (52.2)	460 (209)	4	12, 13, 17, 18

Assuming a specific impulse, I_{sp}, of 280 seconds for the translation engines, the total propellant required to fulfill the 100 fps (30.48 m/sec), 0.1 g requirement is 300 pounds (136 kg). Considering three-sigma tolerances on engine installation, thrust vector misalignment, and limit cycle operation, it was determined that 78.2 pounds (35.2 kg) of propellant are required for attitude control. This includes a 10 percent contingency. The total propellant required for translation and reaction control becomes:

$$W_{P_{total}} = W_{P_{translation}} + W_{P_{RCS}} = 378.2 \text{ lb } (171 \text{ kg})$$

Allowing a 98 percent propellant expulsion efficiency resulting from positive expulsion-type propellant tanks, the total requirement, $W_{P_{total}}$, is 388 pounds (176 kg).

Assuming the thrustor engines operate at a mixture ratio of 1.6, the propellant tanks are of equal volume 2.80 ft^3, (0.0792 m^3). A helium tank volume of 0.783 cubic feet (0.0221 m^3) pressurized to 1500 psi (10.5 MN/m^2) is required to maintain a helium pressure of 150 psi (10.5 MN/m^2) in the propellant tanks throughout the operating cycle.

3. Environmental Control and Life Support System

The modified configuration for the rendezvous and docking experiment mission consists of the basic D/3 HL-10 vehicle, plus a mission module which contains the equipment and controls required for rendezvous.

The environmental control and life support (EC/LS) concept for this mission was to leave the basic vehicle system unchanged and to locate any additional system components and expendables, required for the mission, to the mission module. The design

criteria for the mission module is presented in table 48, and a schematic of the EC/LS system is presented in figure 108. The mission module EC/LS system functions as follows. During ascent, the oxygen in the module is vented through the vent valve down to 5 psia (34.4 kN/m^2) where it is maintained throughout the mission by the module dual pressure regulator. The temperature of the module atmosphere is controlled by the mission module heat exchanger and fan, and the temperature of the electronics is controlled by the vehicle thermal control loop. The oxygen and water in the mission module are tied into the respective vehicle systems and are scheduled to be used before the oxygen and water located in the vehicle.

When the mission module is to be occupied by a crew member, the tunnel hatch is opened and the crew member proceeds through the tunnel. Cooling and oxygen are supplied through an umbilical connected to the vehicle suit loop. Once in the mission module, the umbilical is disconnected, and the crew member plugs his suit into the mission module suit loop system, which is part of the vehicle suit loop system.

TABLE 48

MISSION MODULE EC/LS DESIGN CRITERIA

Prelaunch	Provide electronic cooling by the HL-10 EC/LS system.
Launch	Design for a maximum launch phase of 10 minutes. Cooling by thermal lag assumed below 100 000 ft (30.5 km)
Space	Design for 24 hours. One crew member will occupy the mission module.
Vehicle	Atmosphere--5 psia (34.4 kN/m^2) 100% oxygen normal; pressure suit face plate open; 3.5 psia (24.1 kN/m^2) 100% oxygen for emergency. Purge to 100% oxygen atmosphere prior to launch. Repressurization--one cycle. Volume of mission module is 300 cubic feet (8.49 m^3) Temperature--suit 50° F at inlet, 85° F at outlet. Cabin 60° to 80° F wall above 65° F dew point during orbit. Leakage--mission module at 5 psia, 6.0 lb (2.7 kg)/day. CO_2 level--8 mm Hg maximum. Humidity--30% to 70%.
Heat load	80 watts

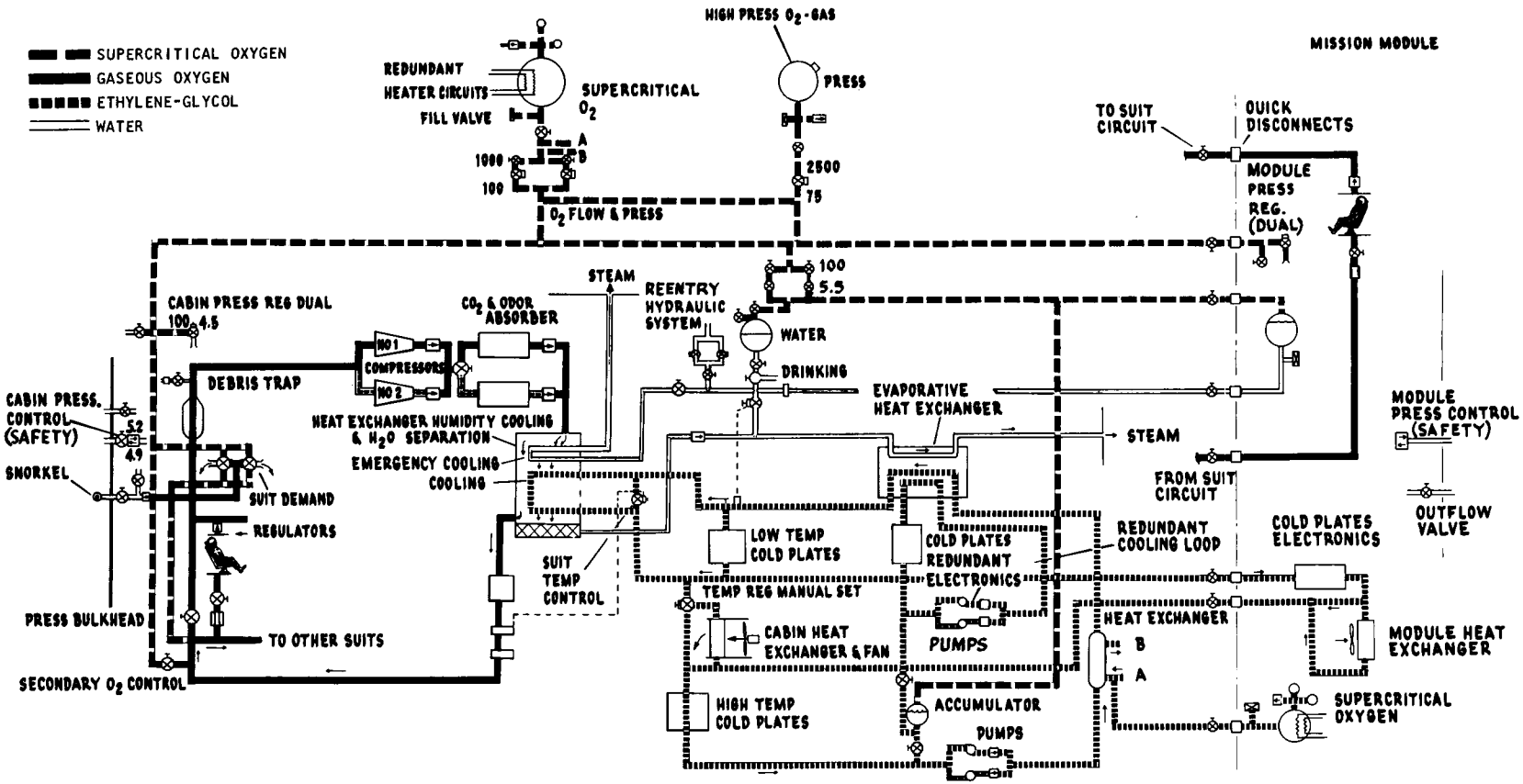

FIGURE 108. EC/LS SYSTEM FOR RENDEZVOUS AND DOCKING EXPERIMENT

ER 14471-7

C. LANDING ENGINE EXPERIMENT

The purpose of this experiment is to investigate the unique problems associated with the installation of a turbojet landing and go-around engine in an lifting body entry vehicle. The addition of an engine to a future operational entry vehicle would improve its versatility and all-weather capability. The experiment would allow an evaluation of the operational benefits and provides an indication of its value for future systems.

Additionally, the experiments will supply data to realistically define design criteria and system requirements. The included propulsion system is subjected to abnormal (as distinguished from normal engine design and installation) conditions which are, of course, imposed by an orbital and entry flight profile. Some of these conditions are: spatial environment survivability; delayed restart capability; sealing and leakage of the engine compartment; air induction and ram air efficiency; toxic and hazard effects; and launch and entry accelerations.

1. Design Modifications

In terms of entry vehicle modification, this experiment is the most involved of the secondary objectives, and also introduces additional problems and conditions affecting the vehicle design. Some of the additional problems in the vehicle design are:

(1) Installation and mounting of the turbojet engine.

(2) Loads from accelerations on engine mass during launch and entry.

(3) Incorporation of extendable air induction system.

(4) Engine cooling during operation.

(5) Exhaust system and exit port in vehicle.

(6) Fuel supply and delivery, including venting.

(7) Structural loads produced by engine weight and thrust.

(8) Inertia and torque effects from engine mass and operation.

(9) Vehicle balance.

(10) Fire hazard, fire walls and extinguishing.

The design evolved for the incorporation of the added propulsion system is significant in that the major modifications are confined entirely within the central area of the afterbody section (fig. 109). The resulting design fits the pattern of "prefab" design philosophy of the standard D/3 research vehicle.

Using the proposed fabrication technique, it is readily feasible to furnish a custom-tailored afterbody for this experiment which can be substituted in the later phases of

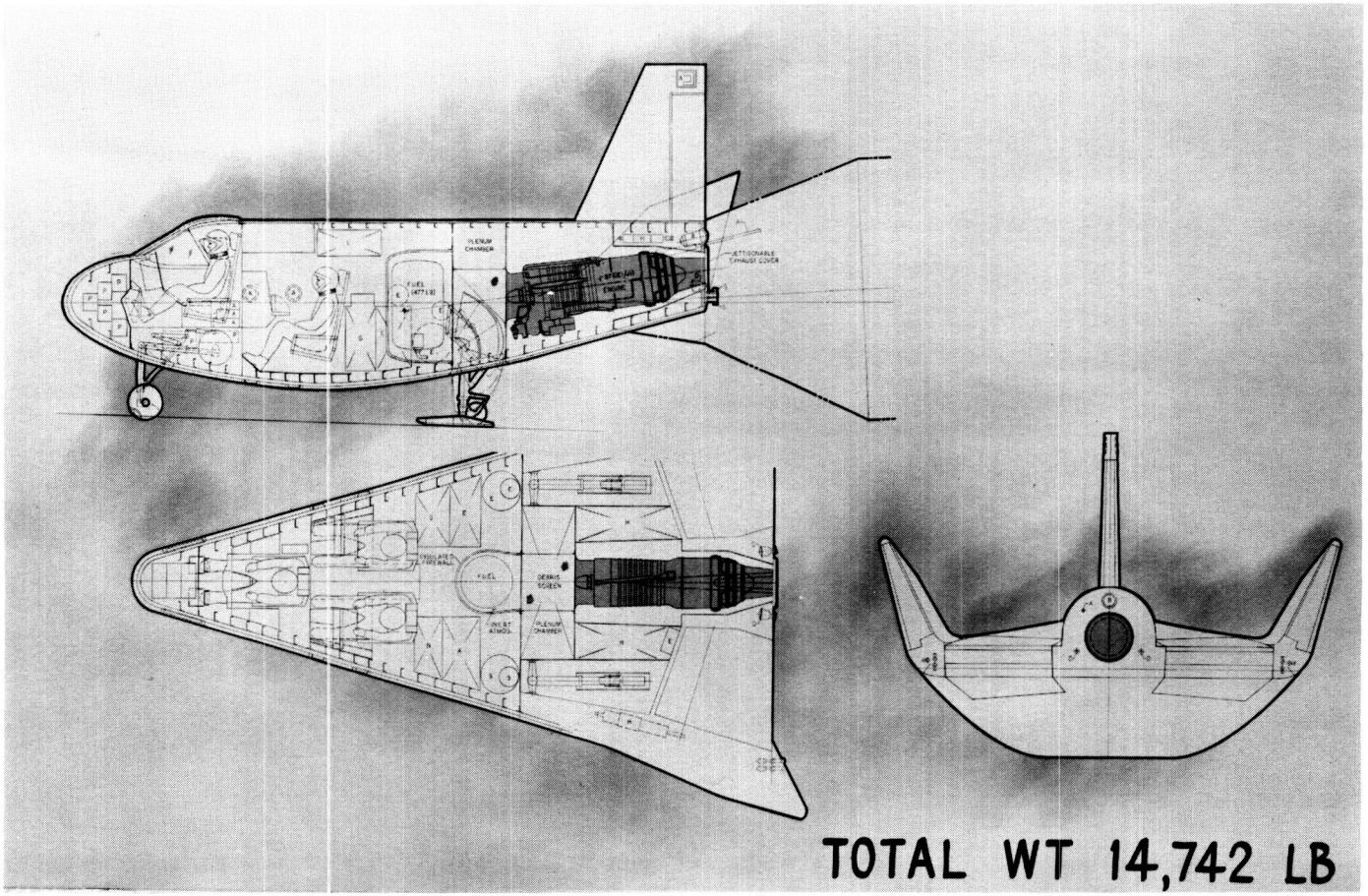

FIGURE 109. LAYOUT OF D/3 FOR TURBOJET LANDING EXPERIMENT

the program plan. With this arrangement, the program will not have to suffer long delays while the basic vehicle is being modified.

The arrangement of the D/3 vehicle remains unchanged. The only modification to the forebody is the addition of the (JP4) fuel tank and its protective shell. The tank is located here so that it is over the center of gravity, and fuel expenditure will not alter the balance or induce requirements for additional trim.

Displays and controls are added to the crew instrument panels for engine monitoring and control.

The supply tankage for the reaction control system propellant is off-loaded since the landing assist thrustors are eliminated.

The afterbody central area is modified for the addition of the turbojet engine and the engine air induction system. The outer bays of the afterbody are also modified. The vehicle recovery chute system and its canisters are deleted. The main landing gear occupies the lower halves of the outboard bays, as it does in the D/3 vehicle.

The central area of the afterbody is divided into four sections by added firewalls. A transverse firewall is located 25 inches (63.5 cm) aft of the main gear bulkhead (station 181.5) between the main gear well beams; the area between the main gear bulkhead and transverse firewall is utilized as a plenum chamber for the engine air induction system.

A pair of parallel firewalls is added between the transverse firewall and the main rear bulkhead (station 257). These firewalls are 37 inches (94 cm) apart, straddling the turbojet engine and enclosing an isolated engine compartment; the firewalls are also structural beams which pick up the engine mounts and support the engine.

The hydraulic units are located in the bays between the longitudinal (parallel) firewalls and the main gear beams. The arrangement is similar to that of the basic D/3 vehicle; however, these units are located slightly farther aft due to the addition of the plenum chamber in the forward portion of the afterbody.

The air inlet scoop is a bell-mouthed duct which is stowed inside the plenum chamber. Just prior to engine start, a knock-out panel in the lower surface is first jettisoned (this panel is located in the same place as the access panel on the basic D/3 vehicle). The inlet scoop is then rotated into place by a simple folding link and single-acting actuator and locked in proper position.

Flanges around the outside of the scoop seal the edges of the cutout when the scoop is locked in position. A debris screen is located within the plenum chamber and in line with the engine inlet duct.

Cooling air apertures are provided in the transverse firewall and engine inlet duct boundary bleeds to provide cooling air for the engine compartment during engine operation.

The body extension section is modified to provide clearance for the turbojet engine, the engine shrouding, and its exhaust system. A clearance cutout is also provided in the main rear bulkhead (station 257) for the engine.

A tailpipe and shrouding have been added to the engine so that the exhaust outlet is just aft of the base of the D/3 vehicle (station 300). The configuration of the tailpipe and shrouding provides an aspiration effect, pulling cooling air past the engine and tailpipe.

A jettisonable cover is added to the aft face of the base of the vehicle to cover the exhaust port and seal off the rear end of the pressurized engine compartment. This cover is blown off just prior to engine start.

A pair of antennas and slideout braking chute canister are relocated in the back face to clear the engine tailpipe and shrouding. The landing assist reaction thrustors, which are utilized on the standard D/3 vehicle, are deleted on the experiments which include the turbojet engine.

2. Landing Assist Engine Studies

A study was made to select an appropriate turbojet engine for use as a landing assist engine on the D/3 configuration. The purposes of the engine are to:

(1) Provide propulsion for a 25-nautical mile (46.3 km) subsonic cruise (M = 0.6) at an altitude of 8000 feet (2.44 km).

(2) Provide a capability for subsonic (M = 0.4) go-around (360° turn) at sea level.

Another requirement of the selection process is to provide an engine that can produce a vehicle rate of climb of 1000 feet per minute (5.08 m/sec) at sea level. In addition to the performance requirements, the engine must be small enough to fit within the limited installation volume available in the vehicle. The limited installation volume available eliminates fan jets and afterburning type engines from consideration because of their physical characteristics.

A study was conducted to determine landing assist engine requirements. Figures 110 and 111 show the sea level static thrust required for the specified climb rate and subsonic cruise at various vehicle gross weights. A vehicle of 13 000 pounds (5.897 Mg), including engine installation and fuel, as shown in figure 110, requires an engine rated at 3000 pounds (14.24 kN) thrust (sea level static) to accomplish a vehicle rate of climb of 1000 feet per minute (5.08 m/sec) at M = 0.4, sea level. Figure 111 indicates that the 25 nautical mile (46.3 km) cruise at 8000 feet (2.44 km) at M = 0.6 requires an engine rated at 3500 pounds (15.57 kN) (sea level static). Therefore, to successfully accomplish both missions, an engine rated at 3500 pounds (15.57 kN) (minimum) sea level static is required for use in the vehicle.

A survey of the industry to identify available engines in the 3500 pound (15.57 kN) thrust class yielded the engines listed in table 49. Although a number of engines appeared capable of fulfilling the thrust and size requirements of the D/3 vehicle, further investigation revealed that these engines were in the preliminary development test phase or "paper" stage and would not necessarily be available for application.

Based on the sea level static thrust requirement of 3500 pounds (15.57 kN), two engines were candidates (fig. 112) for the assumed 13 000-pound (5.897 Mg) vehicle.

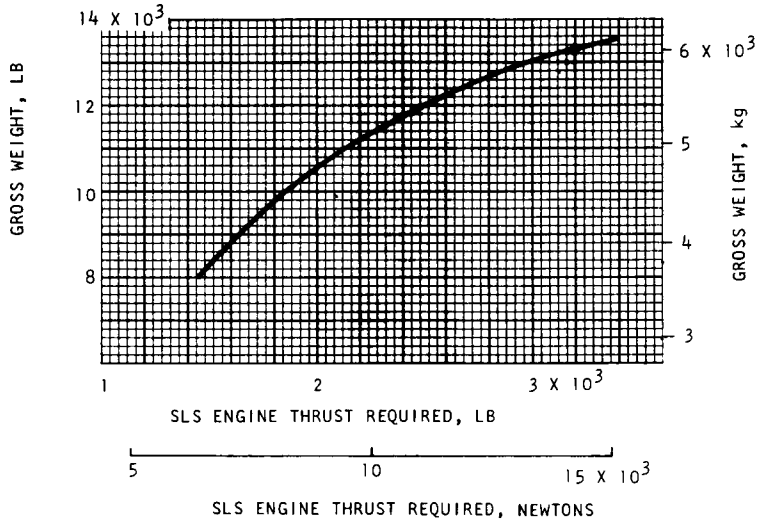

FIGURE 110. THRUST REQUIRED FOR 1000-FPM RATE OF CLIMB AT SEA LEVEL

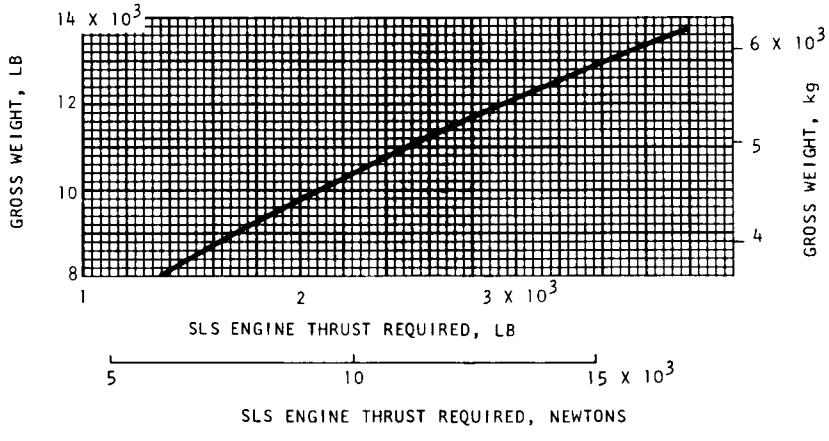

FIGURE 111. THRUST REQUIRED FOR 25 N. MI. CRUISE AT 8000 FEET

TABLE 49

ENGINE SUMMARY

Manufacturer	Engine Model	Engine Type	Dry weight, lb (kg)	Length overall, in. (cm)	Basic diameter in. max./min. (cm)	Basic frontal area, sq ft (m^2)	Thrust output takeoff military normal, lb (kN)	SFC SLS takeoff military normal, lbM/hr/lbF (kg/hr/N)	Total airflow takeoff military normal, lb/sec (kg/sec)	Remarks
Allison	615-B1	Turbojet lift engine	112 (50.8)	24.5 (62.2)	31.21/14.7 (79.3/37.3)	1.179 (0.103)	3000 (13.345)	1.30 (0.133)	39.30 (17.83)	Paper
							2700 (12.010)	1.27 (0.130)	38.30 (17.37)	
							2400 (10.676)	1.24 (0.126)	37.20 (16.87)	
Continental	LJ55A (365)	Turbojet lift engine	200 (90.7)	38.03 (96.6)	23.0/17.95 (58.4/45.6)	1.757 (0.163)	4144 (18.433)	1.068 (0.109)	56.5 (25.63)	Paper
							4000 (17.793)	1.068 (0.109)	56.5 (25.63)	
Continental	LJ55D	Lift turbojet	216 (98.0)	38.03 (96.6)	23.0/17.95 (58.4/45.6)	1.757 (0.163)	3520 (15.658)	1.145 (0.117)	56.5 (25.63)	Paper
							3853 (17.139)	1.045 (0.106)	56.5 (25.63)	
General Electric	J85/J4	Turbojet	390 (176.9)	40.6 (103.1)	17.7/16.0 (45.0/40.6)	1.396 (0.130)	2950 (13.122)	1.005 (0.102)	44.0 (19.96)	Available
							2950 (13.122)	1.005 (0.102)	44.0 (19.96)	
							2780 (12.366)	0.980 (0.100)	43.0 (19.50)	
General Electric	GE1/J1B	Turbojet	655 (297.1)	78.34 (199)	24.2/20.1 (61.5/51.1)	2.2 (0.204)	5250 (23.353)	0.886 (0.090)	66.9 (30.35)	Secret
							4885 (21.729)	0.857 (0.087)	65.0 (29.48)	Available
							4491 (19.977)	0.836 (0.085)	62.4 (28.30)	
General Electric	GE1/J4	Turbojet	645 (292.6)	--	24.2/20.1 (61.5/51.1)	2.2 (0.204)	5725 (25.466)	0.95 (0.097)	66.9 (30.35)	Uprated GE1/J1B
							5370 (23.887)	0.92 (0.094)	65.0 (29.48)	
							4970 (22.108)	0.89 (0.091)	62.4 (28.30)	
Pratt & Whitney	J60-P-6	Turbojet	495 (224.5)	70.45 (178.9)	21.9/21.9 (55.6/55.6)	2.615 (0.243)	--	--	--	Available
							3000 (13.345)	0.960 (0.098)	50.5 (22.91)	
							2570 (11.432)	0.905 (0.092)	48.2 (21.86)	
Pratt & Whitney	JT12A-9	Turbojet	470 (213.2)	76.0 (193.0)	23.4/17.82 (59.4/45.3)	1.728 (0.161)	3600 (16.014)	0.965 (0.098)	53.73 (24.37)	Paper (upgraded J-60)
							3000 (13.345)	0.913 (0.093)	51.10 (23.18)	
							2650 (11.788)	0.890 (0.091)	48.59 (22.04)	

However, the GE-1/J1B was the only engine in the hardware stage that could be available in time and, therefore, was selected as the landing assist engine. The GE-1/J1B has a sea level static thrust rating of 4885 pounds (21.73 kN) at military power and weighs 655 pounds (297 kg). A total of 442 pounds (200 kg) of fuel is required to complete both the 25 nautical mile cruise and the 360° go-around mission (fig. 113).

The inlet and induction system design for the landing assist engine is based on placing an extendable inlet on the underside of the vehicle, along the vehicle centerline, and directing the inducted air into a plenum chamber and then to the engine. The inlet has a bell mouth entrance with a capture area of 403 square inches (0.26 m^2) and a minimum area, approximately 2 inches (5.08 cm) from the lip, of 348 square inches (0.224 m^2). The total length of the induction system from the inlet lip to the plenum is 23 inches (58.4 cm) (fig. 114). The inlet configuration is in the form of a semicircle with the major axis part of the underside of the fuselage when in an unextended position (fig. 109). When the inlet is in an extended position the boundary layer effects are minimized because the circular portion exposes a minimum section of the inlet to boundary layer action. The inlet-induction system recovery factor has been estimated to be 94%. The recovery estimate is based on previous studies of similar type systems applied to lifting body vehicles.

The operation of a turbojet engine, after being exposed to a space environment, has not been part of the qualification requirements of any turbojet engine considered for application in the study. No engine companies are known to be engaged in specifically designing a turbojet engine which can be carried into a space environment and operated after entry into the atmosphere. It is deemed necessary, therefore, to encapsulate the landing assist engine and control its environment during the engine's exposure to space. The engine will be encapsulated and pressurized as indicated schematically in figure 115.

Figure 115 also shows a schematic of the propellant feed and pressurization system. A total of 486 pounds (220.4 kg) of JP-type fuel (including reserve) is required to fulfill the mission. The fuel is stored in an 11.0-cubic foot (0.3 m^3) tank and maintained at cabin temperature. A 15.0-psia (10.342 kN/m^2) pressure will be supplied in the propellant tank and maintained throughout the mission. Figure 116 shows the nitrogen tank size and pressure requirements to maintain the 15.0-psia (10.342 kN/m^2) fuel tank pressure. Vehicle installation volume limitations dictate the use of a compact, lightweight system. Consequently, a 100 cubic inch (1638 cc) aluminum nitrogen tank was selected. A redundant system which includes two regulators and two normally open solenoid valves is used to regulate pressure.

D. SUMMARY OF WEIGHT MODIFICATIONS FOR SECONDARY OBJECTIVES

The weight changes involved in modifying the basic D/3 near-earth orbit entry research vehicle to meet various research objectives are shown in table 50. The rendezvous and supercircular velocity modifications are to meet mission requirements defined as secondary objectives for this study. The go-around engine modification was conceive as a possible way to perform the experiment PP-3, landing assist engine, provided it is desired to demonstrate use of a go-around propulsion system. The vehicle design layouts for each of these three missions have been shown in the previous subsections.

The basic approach for the secondary objective has been to modify the basic D/3 vehicle as little as necessary. The weight calculations are based on the difference between the basic D/3 vehicle and the design required for the secondary objectives.

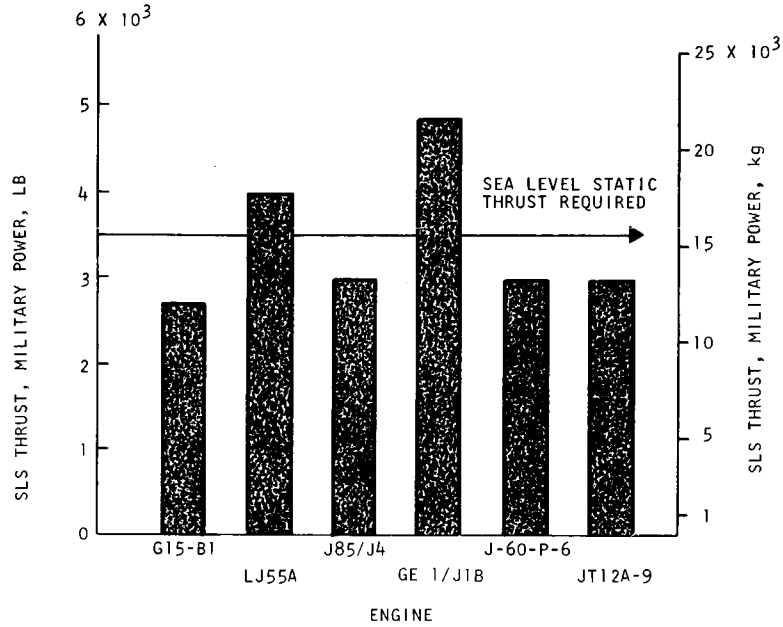

FIGURE 112. ENGINE THRUST SUMMARY

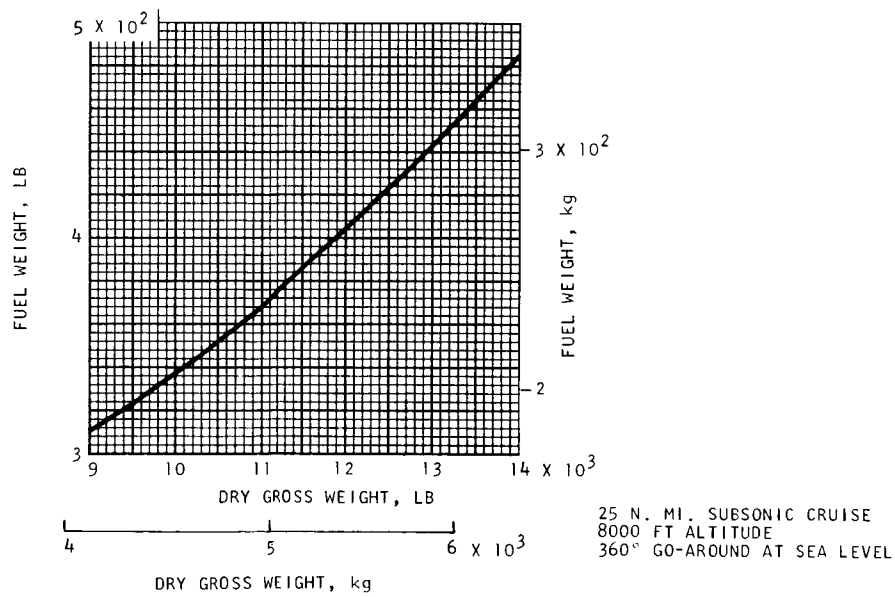

FIGURE 113. TOTAL FUEL WEIGHT

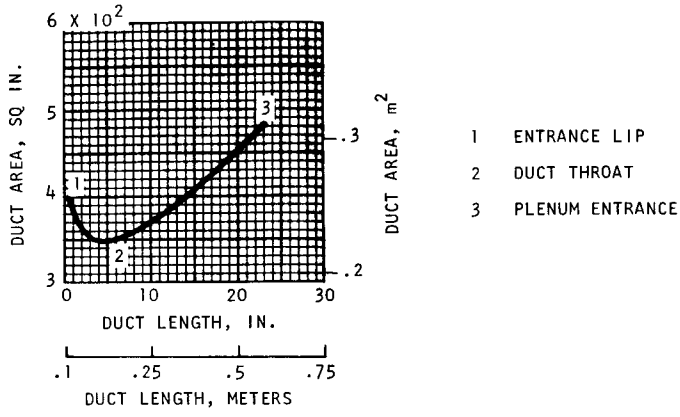

FIGURE 114. INDUCTION SYSTEM CROSS-SECTIONAL AREA DISTRIBUTION

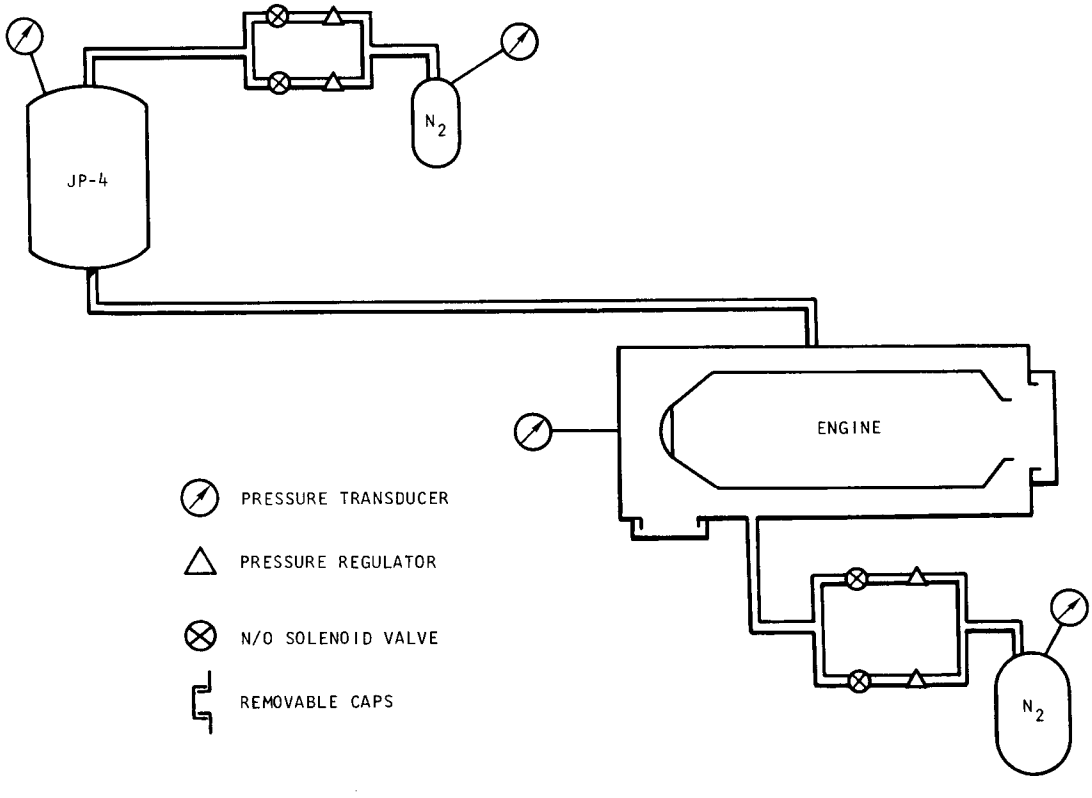

FIGURE 115. ENGINE, PROPELLANT FEED, AND PRESSURIZATION SYSTEM

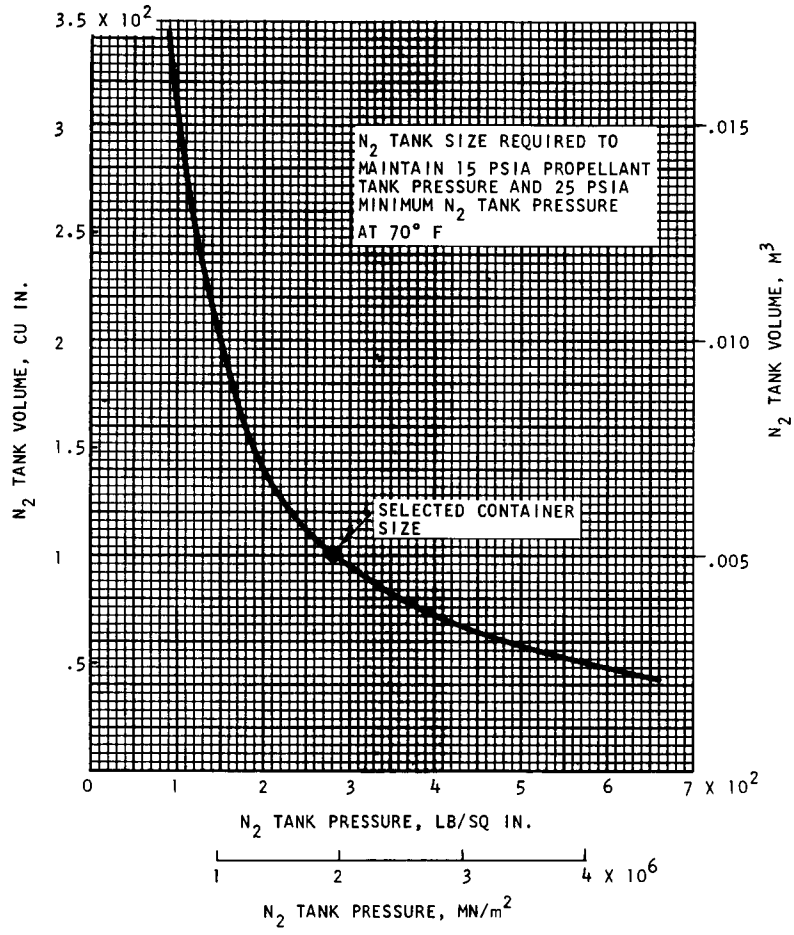

FIGURE 116. PRESSURANT TANK SIZE

TABLE 50

WEIGHT SUMMARY FOR SECONDARY OBJECTIVES

	Rendezvous		Supercircular		Go-around engine	
	lbM	kg	lbM	kg	lbM	kg
Entry vehicle	(11 263)	(5 109)	(11 819)	(5 361)	(12 779)	(5796)
D-3 entry vehicle	12 342	5 598	12 342	5 598	12 342	(5598)
Delete test equipment	-1 051	-477	-1 051	-477	-1 051	-477
Add test equipment	--	--	+300	+136	--	--
Add tunnel door	+30	+14	--	--	--	--
Remove one crewman	--	--	-252	-114	--	--
Heat shield increment	--	--	+460	+209	--	--
Delete landing assist engines	--	--	--	--	-254	-115
Add go-around engine	--	--	--	--	+1 382	+627
Ballast changes	-58	-26	+20	+9	+360	+163
Adapter	(2 360)	(1 070)	(3 443)	(1 562)	(1 963)	(890)
Structure--Titan III	510	231	--	--	510	231
--Saturn	--	--	1 990	903	--	--
Tunnel	100	45	--	--	--	--
Deorbit-abort propulsion	1 065	483	1 065	483	1 065	483
Electrical system	438	199	288	131	288	131
Environmental system	147	67	--	--	--	--
Miscellaneous	100	45	100	45	100	45
Cargo module	(10 132)	(4 595)	(--)	(--)	(--)	(--)
Structure	704	319				
Rendezvous	80	36				
Docking	150	68				
Reaction control system	150	68				
Ballast	9 048	4 104				
Propulsion module	(3 645)	(1 653)	(18 658)	(8 463)	(--)	(--)
Structure	539	245	--	--		
Propulsion	--	--	--	--		
Engines and supports	948	430	1 400	635		
Propellant system	248	112	1 210	549		
Propellants	1 910	866	16 048	7 279		
Effective weight of abort system	(--)	(--)	(430)	(195)	(--)	(--)
Aft end of Saturn adapter	(--)	(--)	(950)	(431)	(--)	(--)
Total launch weight	27 400	12 427	35 300	16 012	14 742	6686

REFERENCES

1. Stern, I.; and Rowe, W. H. Jr.: Effect of Gap Size on Pressure and Heating over the Flap of a Blunt Delta Wing in Hypersonic Flow. Journal of Spacecraft and Rockets, vol. 4, no. 1, Jan. 1967, p 109 ff.

2. Holloway, P. F.; Sterrett, J. R.; and Creekmore, H.S.: An Investigation of Separated Flow at a Mach Number of 6. NASA TND-3074, 1965.

3. Rieckmann, R. E.: Research Study to Provide Concepts of Panel Attachment Mechanisms Suitable for Refurbishable Panel Applications. Martin Marietta Corporation ER 14145, 1966.

4. Stubbs, S. M.: Landing Characteristics of a Dynamic Model of the HL-10 Manned Lifting Entry Vehicle. NASA TND 3570, 1966.

5. Solt, G. A. Jr.: Performance of and Design Criteria for Deployable Aerodynamic Decelerators. ASD TR-61-579, Dec. 1963.

6. Ladson, Charles L.: Effects of Various Canopies on the Aerodynamic Characteristics of a Manned Lifting Entry Vehicle at Mach 0.6 to 6.8 (U). NASA TMX 1321, 1966. (CONFIDENTIAL)

7. Burgess, R.T.: Technical Proposal to the Martin Co., Baltimore Division, for a Hydraulic Power Supply for the HL-10 Research Vehicle. Pesco Eng. Report no. 5132, Jan. 1967.

8. Hall, D.I.: Discussion of Redundant Servoactuator for Use on a Manned Reentry Spacecraft. Moog, Inc., Report no. MR 1162, Jan. 1967.

9. Study of Redundant Servoactuators for the MOL Launch Vehicle, Moog, Inc., Report no. MR 1051, rev. A, Oct. 1965.

10. Grimster, D.; and Hall, D.I.: Evaluation Program of Majority Voting Mechanical Feedback Servoactuator for the Saturn S-IVB. Moog, Inc., Report no. MR 1080, Vol B, Aug. 1966.

11. Lenett, S. D.: Apollo Digital Up-Data Link Description. NASA TMX 1146, 1965.

12. Study of the Influence of Size of a Manned Lifting Body Entry Vehicle on Research Potential and Cost. Martin Marietta Corporation ER 14063P-1, Vol 1, Jan. Jan. 1966.

13. Liquid Propellant Engine Manual. CPIA Publication no. 5, Dec. 1966.

14. A Lifting Reentry, Horizontal-Landing-Type Logistic Spacecraft (U), Boeing Company D2-22921, Feb. 1964.

[redacted]